Impact of the alkylphospholipid Inositol-C2-PAF on the transcription and signalling cascades in immortalized keratinocytes

Dissertation

to obtain the academic degree
Doctor rerum naturalium (Dr. rer. nat.)

Submitted to the Department of Biology, Chemistry and Pharmacy

by
Geo Semini
from Rovio (Ticino), Switzerland

Berlin, December 2010

1st Reviewer Prof. Dr. Volker Haucke

2nd Reviewer PD Dr. Kerstin Danker

Date of Defense: 31 March 2011

This work was accomplished between April 2006 and December 2010 at the Institute of Biochemistry at the University Medical Center Charité under the supervision of PD Dr. Kerstin Danker.

Affidavit

I declare that my PhD thesis “Impact of the alkylphospholipid Inositol-C2-PAF on the transcription and signalling cascades in immortalized keratinocytes” has been written independently and with no other sources and aids then quoted.

Geo Semini

TABLE OF CONTENTS

LIST OF ABBREVIATIONS

A	ampere
ab	antibody
ADP	adenosine diphosphate
APC	alkylphosphocholine
APL	alkylphospholipid
ATL	antitumour lipid
ATP	adenosine triphosphate
BCA	bicinchoninic acid
BrdU	bromodeoxyuridine
BRM	biological response modifier
BSA	bovine serum albumin
CCT	CTP:choline-phosphate cytidylyltransferase
cDNA	complementary DNA
CDP	cytidine diphosphate
CIV	collagen IV
CMP	cytidine monophosphate
CPITC	coumarin-phalloidin isothiocyanate
CTP	cytidine triphosphate
DISC	death-inducing signalling complex
DMEM	Dulbecco´s modified eagle medium
DMSO	dimethyl sulfoxid
DPBS	Dulbecco´s phosphate-buffered saline
ECM	extracellular matrix
EDTA	ethylenediaminetetraacetic acid
EGF	epidermal growth factor
ELISA	enzym-linked immunosorbent assay
ERK	extracellular signal-regulated kinase
Et-18-OCH3	1-*O*-octadecyl-2-*O*-methyl-rac-glycero-3-phosphocholine
FA	focal adhesion
FACS	fluorescence-activated cell scanning
FADD	Fas-associated death domain
FAK	focal adhesion kinase
FGF	fibroblast growth factor
FITC	fluorescein isothiocyanate
FN	fibronectin
FRET	fluorescence-resonance-energy transfer
GAP	GTPase activating protein
GDI	guanine nucleotide dissociation inhibitor
GDP	guanine diphosphate
GEF	guanine nucleotide exchange factor
GFP	green fluorescent protein
Glc-PAF	glucose-PAF
Glc-PC	glucose-PC
GO	gene ontology
GTP	guanine triphosphate
HaCaT	human adult keratinocytes kept in high calcium at low temperature
HePC	hexadecylphosphocholine
HEPES	4-(2-hydroxyethyl)-1-piperazineethanesulfonic acid
HRP	horseradish peroxidase
IC_{50}	half-maximal inhibitory concentration
ID	identification
IF	immunofluorescence

IFN-γ	interferon-γ
IGF-1	insulin-like growth factor 1
IL-1α	interleukin-1α
Ino-C2-PAF	inositol-C2-PAF
IP	immunoprecipitation
JNK	c-Jun N-terminal kinase
kDa	kilo-Dalton
LB	lysogeny broth
LC_{50}	lethal concentration, 50%
LDH	lactate dehydrogenase
LN-111	laminin-111
LPC	2-lysophosphatidylcholine
MALDI-TOF-MS	matrix-assisted laser-desorption-ionization time of light mass spectometry
MAPK	mitogen-activated protein kinase
MAPKKK	MAP kinase kinase kinase
MDCK	Madin-Darby canine kidney
MDR	multidrug resistance
MEK	MAPK/ERK kinase
MHC	major histocompatibility complex
MKK	MAP kinase kinase
MLCK	myosin light chain kinase
mRNA	messenger RNA
MTOC	microtubule-organizing center
OD	optical density
PAF	platelet-activating factor
PBS	phosphate-buffered saline
PC	phosphatidylcholine
PDK1	3´-phosphoinositide-dependent protein kinase 1
PI3K	phosphatidylinositol-3-kinase
PIC	protease inhibitor cocktail
PIP2	phosphatidylinositol-4,5-biphosphate
PIP3	phosphatidylinositol-3,4,5-triphosphate
PKB	protein kinase B
PKC	protein kinase C
PLC	phospholipase C
PLL	poly-L-lysine
PMSF	phenylmethanesulfonyl fluoride
POD	peroxidase
PPi	orthophosphate ion
PTEN	phosphatase and tensin homolog
RNA	ribonucleic acid
ROS	reactive oxygen species
rpm	revolutions per minute
rRNA	ribosomal RNA
RT	room temperature
SAPK	stress-activated protein kinase
SCC	squamous cell carcinoma
SDS	sodium dodecyl sulfate
SDS-PAGE	SDS-polyacrylamide gel electrophoresis
SFK	Src family kinase
SN	supernatant
TAE	Tris-acetate-EDTA
TBS	Tris-buffered saline
TMB	tetramethyl-benzidine
Tris	tris(hydroxymethyl)aminomethane

U	unit
UV	ultraviolet
WB	Western blotting
WM	wortmannin

1 INTRODUCTION

The development of antitumour drugs remains the most significant hurdle that modern medicine has to overcome. The first attempts to repress tumours through the use of chemotherapeutic tools were performed in the early 1940s (for overview see Chabner and Roberts, 2005). Later, researchers discovered and synthesised a pool of chemotherapeutic drugs (e.g., mercaptopurine, fluorouracil, vincristine, and cisplatin) that displayed the following similar features: 1) inhibition of tumour growth and proliferation as a consequence of the inhibition of RNA and DNA synthesis, 2) inhibition of cell division via blockade of microtubule polymerisation, and 3) induction of apoptosis (Kinsella *et al*., 1997).

However, the impact of conventional chemotherapeutic agents affected not only tumour tissues, but also rapidly dividing cells of healthy organs (e.g., bone marrow, gastrointestinal epithelial cells, and hair follicles). Furthermore, other organs, like the heart, liver, and kidney, were also observed to be injured.

One of the major hurdles of the anti-cancer therapy was represented by the multi-drug resistance (MDR), whose mechanisms include accelerated drug efflux, drug inactivation, alterations in drug targeting, and evasion of apoptosis (Wong and Goodin, 2009). Therefore, it was necessary to develop novel strategies to overcome these severe problems.

After more than half a century of cancer research, it is evident that new antitumour drugs should be metabolically stable, well adsorbed after administration, and accompanied by low toxicity at biologically effective doses while producing limited effects on non-tumour tissue.

1.1 Development of antitumour lipids

In the early 1960s, it was observed that the generation of lysolecithin (2-lysophosphatidylcholine, LPC) by phospholipase A2 induced the phagocytic activity of peritoneal macrophages *in vitro* and *in vivo* (Munder *et al.*, 1969; Munder and Modolell, 1973). Since LPC is not stable and becomes biologically inactivated either by the action of acyltransferase into lecithin (phosphatidylcholine, PC) or by lysophospholipase into glycerophosphocholine (Mulder and van Deenen, 1965), subsequent efforts have been made to synthesise metabolically stable LPC analogues for clinical research and trials. Some resultant synthetic phospholipid analogues not only worked as effective immune modulators (Munder *et al.*, 1979), but also possessed selective antineoplastic activities *in vitro* and *in vivo* (Andreesen *et al.*, 1979; Andreesen *et al.*, 1978; Modolell *et al.*, 1979; Munder, 1982; Tarnowski *et al.*, 1978). Until now, compounds like edelfosine, miltefosine, and perifosine have been tested for their antitumour activity in clinical phase I and phase II trials for a variety of tumours. Furthermore, miltefosine was the first antitumour lipid to be used clinically

for the treatment of cutaneous metastases of mammary carcinomas (Clive *et al.*, 1999; Unger and Eibl, 1988; Unger *et al.*, 1990). Finally, alkylphospholipids represent a group of compounds that are attractive for use in combination with radiotherapy, since they enhance radiation-induced apoptosis. Encouraging results have been obtained with these compounds, primarily in the treatment of leukaemic malignancies (Vink *et al.*, 2007).

1.1.1 General structure of antitumour lipids

The chemical structures of most currently used antitumour lipids (ATLs) can be divided into two main classes: 1) Alkylphospholipids (APL) and 2) Alkylphosphocholines (APC). APLs are compounds with aliphatic side-chains that are ether-linked to a glycerol backbone and are structurally derived from the platelet-activating factor (PAF; Figure 1.1), which is a naturally occurring phospholipid and a mediator of platelet aggregation and inflammation (Chignard *et al.*, 1979; Edwards and Constantinescu, 2009; Prescott *et al.*, 1990; Snyder, 1995; Wolf *et al.*, 2006). The prototype of this class is 1-*O*-octadecyl-2-*O*-methyl-rac-glycero-3-phosphocholine (Et-18-OCH_3, edelfosine, Figure 1.1), which presents an 18-C long alkyl-chain at the *sn*-1 position and a methoxy group at the *sn*-2 position of the glycerol backbone. In contrast, the glycerol backbone in APCs is absent. These molecules consist of a simple 16-C long-chain alcohol conjugated to the phosphocholine head group. Miltefosine (hexadecylphosphocholine, HePC, Figure 1.1) represents the prototype of this class. Another well studied and promising new alkylphospholipid is perifosine (D-21266, octadecyl-(1,1-dimethyl-piperidino-4-yl)-phosphate), in which the choline moiety of miltefosine is replaced by a heterocyclic piperidine group (Figure 1.1).

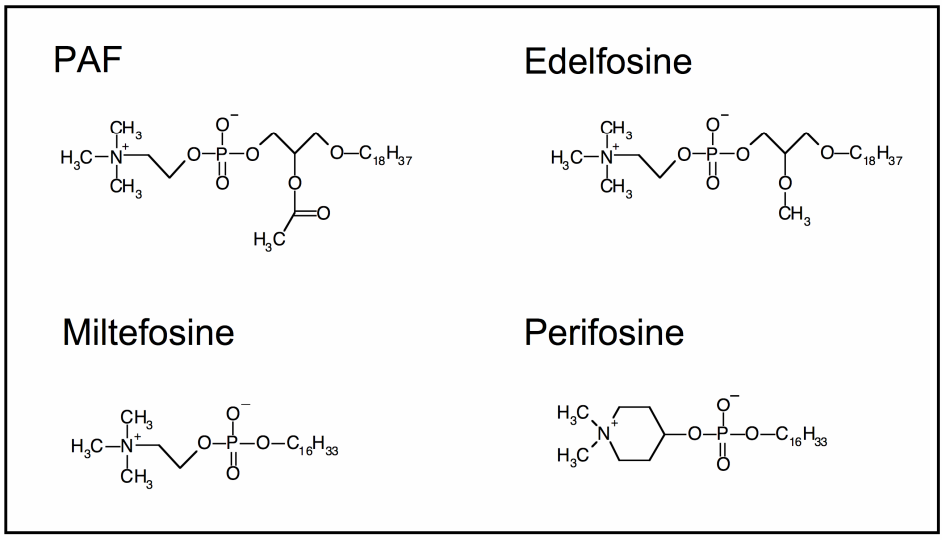

Figure 1.1. Structure of platelet-activating factor (PAF) and the common antitumour lipids edelfosine, miltefosine, and perifosine.

1.1.2 Mechanism of action of common antitumour lipids

To provide an impression of options offered by antitumour lipids (ATLs) in general, the most relevant findings regarding the influence of the known ATLs (edelfosine, perifosine, and miltefosine) on cellular morphology and signal transduction are briefly illustrated.

1.1.2.1 Uptake/absorption of antitumour lipids

In contrast to commonly used cisplatin or vincristine, ATLs do not interfere with the DNA or mitotic spindle apparatus of the cell; instead, they are incorporated into cell membranes, where they accumulate and interfere with a wide variety of key enzymes (Unger *et al.*, 1992). At high concentrations, ATLs exert a detergent-like effect and cause cell lysis. In fact, the ordered plasma membrane bilayer is destroyed after the formation of micellar clusters. Pores with a size of about 1.5 µm, which represent up to 13% of the total membrane surface, are responsible for the lytic effect of ATLs (Noseda *et al.*, 1989; Tertoolen *et al.*, 1988). However, cell lines like fibroblasts, neutrophil granulocytes, glia cells, and bone marrow precursor cells seem to be unaffected by the action of phospholipid analogues (Fleer *et al.*, 1990).

In addition to this lytic action, it has been proposed that phospholipid analogues accumulate in cellular membranes via other mechanisms. Absorption in the outer layer of the membrane (Kelley *et al.*, 1993; van Blitterswijk *et al.*, 1987; Wiese *et al.*, 2000) and subsequent uptake of ether lipids through passive diffusion has been discussed (Kelley *et al.*, 1993; Van der Veer *et al.*, 1993). Internalisation of ATLs during membrane renewal has been proposed as an alternative mechanism (Bratton *et al.*, 1992; Fleer *et al.*, 1992), but a process catalysed by phosphatidylinositol transfer proteins is also possible (Wirtz, 1991). Recent studies suggest that the cellular uptake of APLs (e.g., edelfosine and perifosine) is dependent on the integrity of lipid rafts (Ausili *et al.*, 2008; Heczkova and Slotte, 2006; Van der Luit *et al.*, 2007).

Furthemore, the similarity between the platelet-activating factor (PAF) and the ATLs might be relevant for the effects of these compounds. PAF is able to induce the programmed cell death in erythrocytes, called eryptosis, which is characterised by cell shrinkage, membrane blebbing and cell membrane phospholipid scrambling. The production of prostaglandin E2 in eryptosis results in the activation of cation channels and Ca^{2+} entry and/or release of PAF. The subsequent activation of sphingomyelinase and formation of ceramide stimulate scrambling of the cell membrane and consequently induce cell death (Foller *et al.*, 2008; Lang *et al.*, 2005).

Thus, a similar mechanism was presented for ATL as well. Treatment of leukemic and transformed cells with perifosine and miltefosine, respectively, leads to increased cellular ceramide content, mostly accompanied by reactive oxygen species (ROS) production, and causes apoptotic cell death (Rahmani *et al.*, 2005; Wieder *et al.*, 1998).

1.1.2.2 Influence of ATLs on proliferation, the cell cycle, and apoptosis

Various signalling molecules that regulate proliferation and apoptosis have been shown to be affected by ATLs. The biosynthesis of phosphatidylcholine (PC, Figure 1.2) is regarded as one of the main targets of ATLs. PC is the most abundant phospholipid in the eukaryotic plasma membrane, and its regulation has acquired new interest with the evidence that PC is involved in signal transduction processes (Daniel *et al.*, 1986; Exton, 1990). Inhibition of its biosynthesis causes stress to cells, which is sufficient to stop cell growth and to induce apoptosis. The first studies with Madin-Darby canine kidney (MDCK) cells revealed that miltefosine stopped the incorporation of choline into phosphatidylcholine (Haase *et al.*, 1991). Furthermore, it was demonstrated that miltefosine prevented the translocation of CTP:choline-phosphate cytidylyltransferase (CCT), which is the rate-limiting enzyme of PC biosynthesis, to the membrane (Geilen *et al.*, 1992; Jimenez-Lopez *et al.*, 2002). Similarly, edelfosine is able to inhibit *de novo* PC biosynthesis at the CCT step, which results in cell cycle arrest at different stages (Baburina and Jackowski, 1998; Boggs *et al.*, 1998; Boggs *et al.*, 1995a; Boggs *et al.*, 1995b; van der Luit *et al.*, 2002).

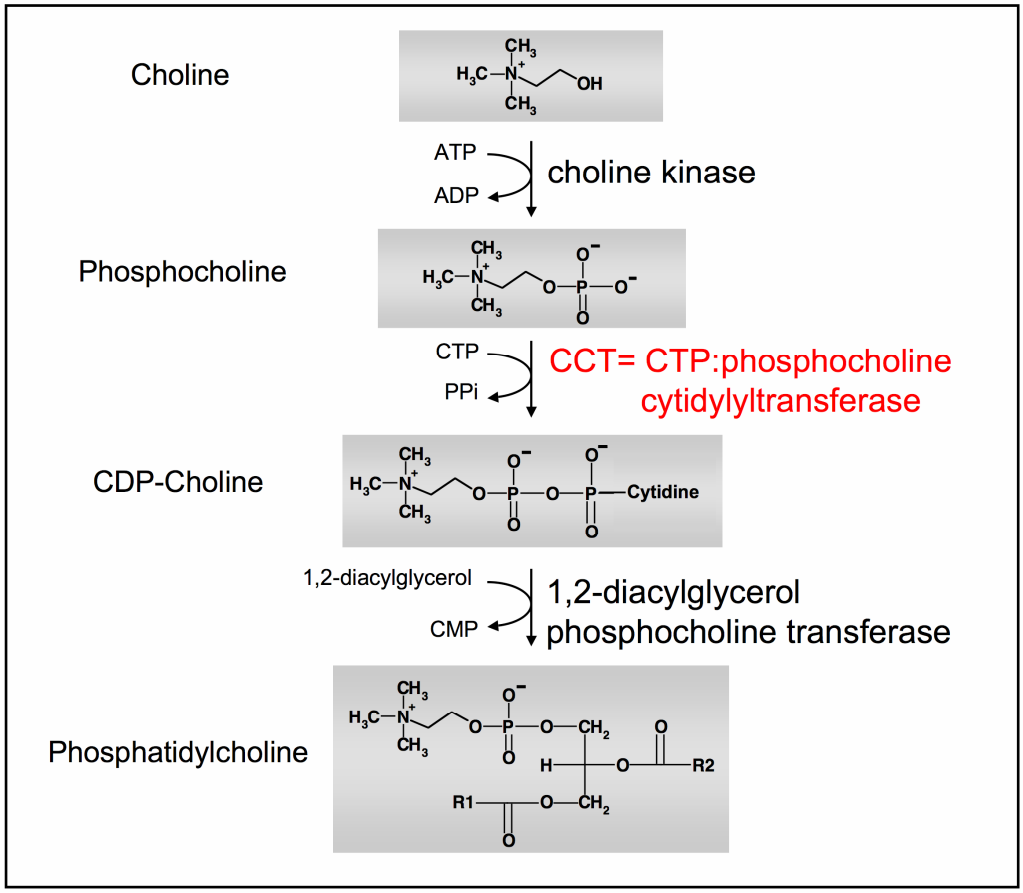

Figure 1.2. Biosynthesis of phosphatidylcholine.

In the early 1990s, edelfosine was demonstrated to trigger the apoptosis of tumour cells without affecting normal cells (Diomede *et al.*, 1993; Houlihan *et al.*, 1995; Mollinedo *et al.*,

1993; Munder and Westphal, 1990). Mollinedo and coworkers proposed that the induction of apoptosis constitutes the critical step in the cytotoxic activity of edelfosine (Figure 1.3). They demonstrated that edelfosine affected the activity of antiapoptotic proteins, such as Bcl-2 and Bcl-X_L (Mollinedo *et al.*, 1997). Moreover, the introduction of edelfosine into the cellular membrane induces 1) disruption of the mitochondrial transmembrane potential, 2) DNA-fragmentation, 3) cleavage of caspase-3 into p17 and PARP, and 4) production of ROS in human leukaemic T cell lines (e.g., Jurkat, Peer and HL-60 cells) (Cabaner *et al.*, 1999; Gajate *et al.*, 2000b). Further studies demonstrated that the loss of mitochondrial membrane potential is caused by an alteration of the phosphocholine content of the mitochondrial membrane induced by edelfosine (Vrablic *et al.*, 2001).

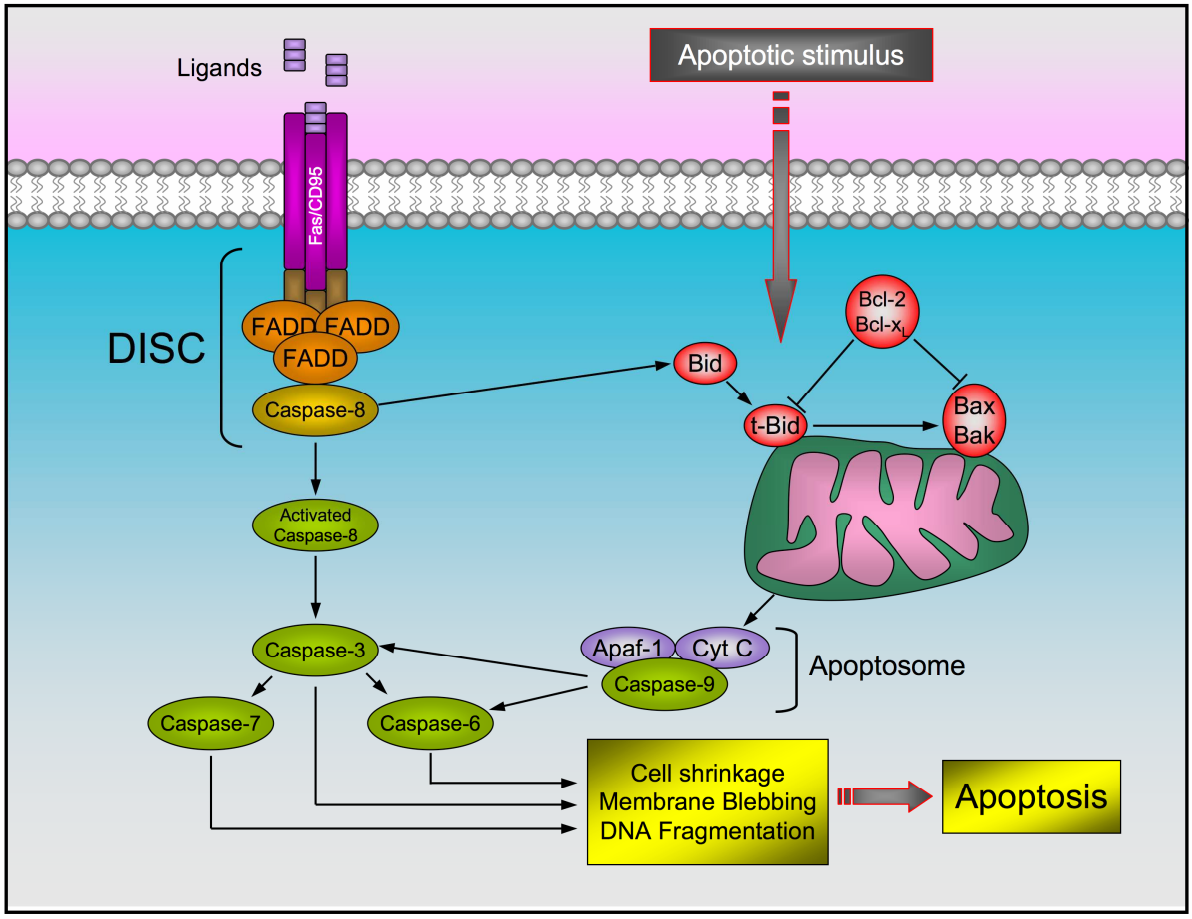

Figure 1.3. Intrinsic and extrinsic apoptotic pathways. The extrinsic pathway is initiated by binding of ligands (FasL, tumour necrosis factor, or other cytokines) to death receptors, which recruits the adaptor protein FADD and, consequently, procaspase-8. The formation of the death-inducing-signalling-complex (DISC) results in cleavage and auto-activation of caspase-8. The activated caspase-8 can then proteolytically activate downstream caspases (particularly caspase-3), which induce cell shrinkage, membrane blebbing and DNA fragmentation. Apoptosis can also be triggered by various apoptotic stimuli, which results in the activation of the intrinsic pathway. Here, caspase-8 cleaves and activates Bid. Subsequently, t-Bid translocates to the mitochondria where it can induce the oligomerization of Bax and/or Bak in the outer mitochondrial membrane leading to cytochrome c release. Afterwards, Apaf-1 binds cytochrome c and recruits caspase-9 to form a large complex, called apoptosome, which is responsible for the following avtivation of caspase-3. Anti-apoptotic Bcl-2 and Bcl-xL oppose the effecst of Bid and Bax.

Another target of ATLs appears to be the dual lipid and protein kinase phosphatidylinositol-3 kinase (PI3K, shown in Figure 1.4), which contributes to the recruitment and activation of various signalling components important for proliferation, differentiation, motility, survival, and intracellular trafficking. Alterations in the PI3K pathway are mostly correlated with cancer. Perifosine has been characterised as a potent and efficient inhibitor of the PI3K-pathway (for a review, see Gills and Dennis, 2009). This alkylphospholipid is able to inhibit the phosphorylation and membrane activation of the PI3K downstream effector Akt/PKB in a large number of tumour cells (e.g., leukaemia, prostate cancer, non-small cell lung cancer, breast cancer, human endometrial adenocarcinoma, human glioma, and epithelial carcinoma cells) (Dasmahapatra *et al.*, 2004; Elrod *et al.*, 2007; Engel *et al.*, 2008; Kondapaka *et al.*, 2003; Korkaya *et al.*, 2009; Momota *et al.*, 2005; Na and Surh, 2008; Nyakern *et al.*, 2006; Papa *et al.*, 2008; Rahmani *et al.*, 2005; Ruiter *et al.*, 2003; Tazzari *et al.*, 2008).

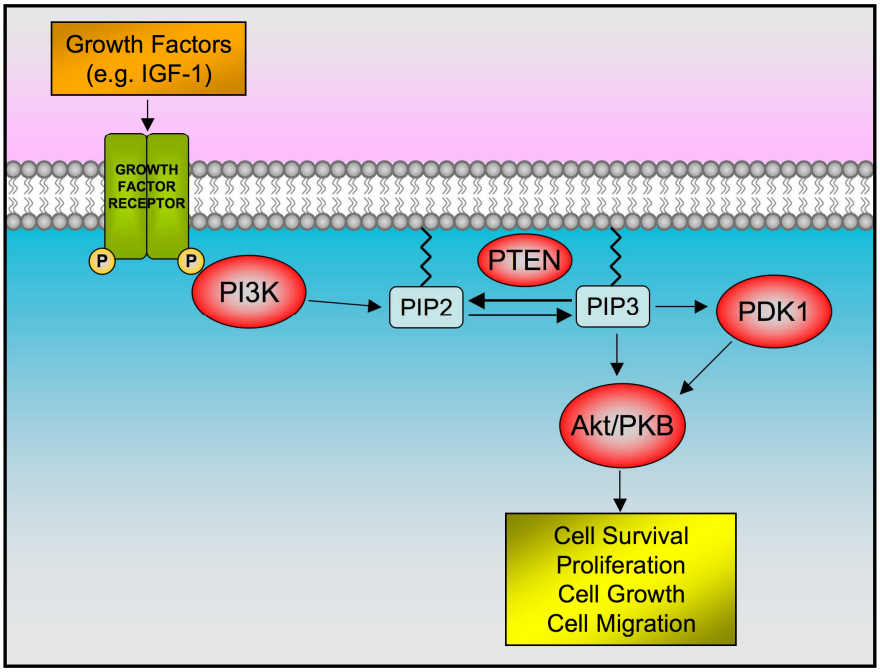

Figure 1.4. PI3K pathway regulates several cellular processes such as apoptosis, proliferation and migration. Growth factors and survival factors activate receptors that recruit PI3K to the membrane. Phosphorylation of the membrane lipid PI(4,5)P2 by PI3K produces the second messengers PI(3,4,5)P3. This lipid recruits the protein-serine/threonine kinases Akt/PKB and PDK1 to the membrane and induce a conformational change in Akt/PKB. Phosphorylation of Akt/PKB by PDK1 turns on the protein kinase activity. PTEN turns off the pathway by dephosphorylating the 3 position of PI(3,4,5)P3.

Furthermore, ATLs affect mitogen-activated protein kinase (MAPK) pathways, which in concert regulate diverse cellular activities like gene expression, mitosis, metabolism, motility, survival, apoptosis, and differentiation (for reviews see Chen *et al.*, 2001; Kyriakis and Avruch, 2001; Pearson *et al.*, 2001, Figure 1.5). Treatment of different leukemic cell lines with edelfosine constitutively activates the MAP Kinase JNK, which results in increased

mRNA levels of its substrate c-jun and induction of apoptosis (Gajate *et al.*, 1998; Hideshima *et al.*, 2006; Ruiter *et al.*, 2003). This effect is enhanced when combined with radiation (Ruiter *et al.*, 1999).

Additionally, edelfosine inhibits the ERK pathway, which is continuously activated in many cancers. Here, edelfosine is able to block the translocation of Raf-1 to the membrane, consequently inhibiting the interaction of Raf-1 with Ras and subsequently reducing ERK1/2 activity (Na and Surh, 2008; Samadder and Arthur, 1999; Samadder *et al.*, 2003). In combination with other inhibitors and chemotherapeutic agents like temozolomide, ATLs inhibit ERK activity (Momota *et al.*, 2005; Rahmani *et al.*, 2005).

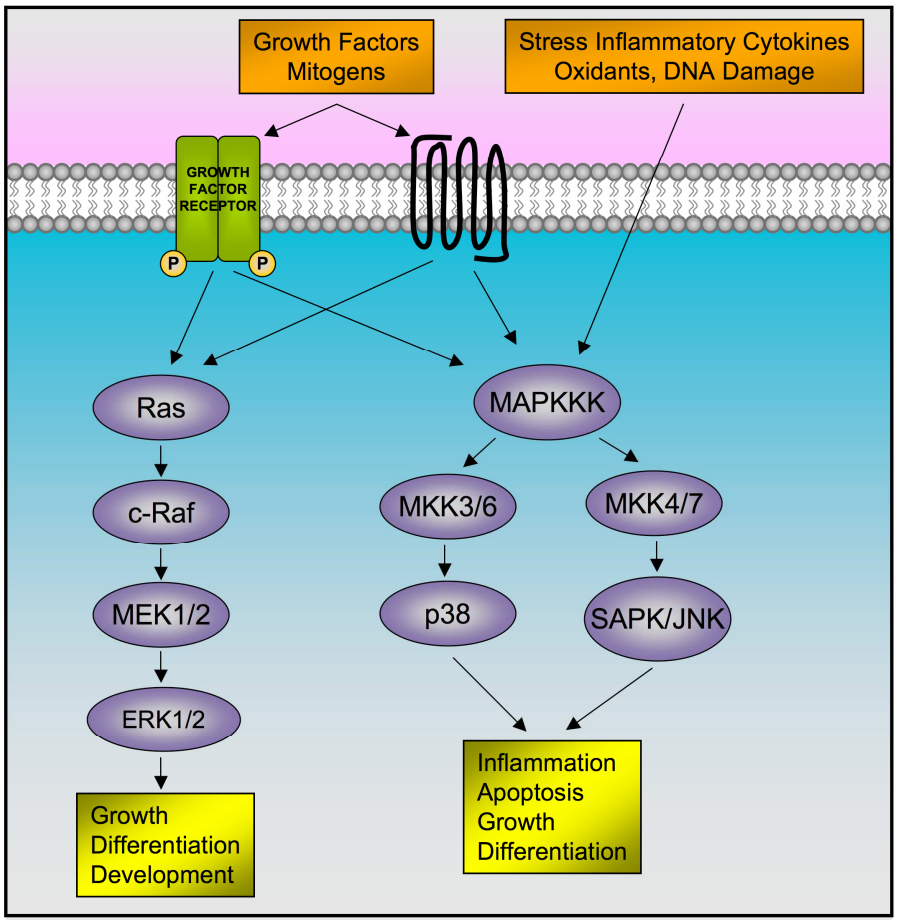

Figure 1.5. The MAPK pathways are major signalling pathways regulating cell proliferation, growth, differentiation, development and apoptosis. MAPKs are activated by receptors for growth factors, G-protein coupled receptors and stress stimuli. The 'classical' MAPK (ERK1 and 2), JNK, p38 are activated on specific threonine and tyrosine residues by a dual specificity MAPK kinase (MKK or MEK), which is in turn activated by a MAPK kinase kinase (MAPKKK or c-Raf) in response to appropriate extracellular stimuli. In contrast to ERK1/2, p38 and SAPK/JNK are additionally activated by stress inflammatory cytokines, oxidants and/or DNA damages.

Protein kinase C (PKC) isozymes play a central role in cellular signalling and are involved in the regulation of cell proliferation, differentiation, apoptosis, and angiogenesis. Therefore, dysfunction of PKC activity is associated with cancer of the prostate, breast, colon,

pancreatic, liver, and kidney (Griner and Kazanietz, 2007). Miltefosine and edelfosine inhibit phosphatidylserine-activated PKC in MDCK cells (Daniel *et al.*, 1987; Geilen *et al.*, 1991). Further studies have indicated that miltefosine and edelfosine do not interfere with PKC translocation but decrease enzyme activity at the membrane and in the cytosol of cells (Berkovic *et al.*, 1994). Finally, edelfosine is a stronger inhibitor than miltefosine.

1.2 Concept of glycosidated phospholipids analogues

In light of the severe side effects of the existing antitumour lipids, efforts have been made to synthesise phospholipid analogues with high antiproliferative capacity but less cytotoxicity.
In the late 1990s, a novel concept was developed by introducing carbohydrates or carbohydrate-related molecules to the chemical lead of alkylphospholipids (APLs), which led to the synthesis of glycosidated phospholipids. The monosaccharides (or monosaccharide-related molecules) were introduced in the *sn*-2 position of the glycerol-backbone of lysophosphocholine or lyso-platelet-activating factor (PAF). The primary idea was to increase the hydrophilic properties of these compounds in order to confer higher water-solubility without disrupting the hydrophobic character (given by the presence of the fatty acid) of the substance, thereby ensuring insertion of the substance into the plasma membrane. In subsequent studies, the use of monosaccharide-containing phospholipid analogues was also described. The group of Bittman replaced the phosphocholine head group by a carbohydrate moiety. This replacement resulted in improved efficacy in comparison to non-glycosidated, phosphocholine-containing compounds (Marino-Albernas *et al.*, 1996; Samadder *et al.*, 1998).
Based on experiences with miltefosine, which is now used for the topical treatment of skin metastases and cutaneous lymphomas (Clive *et al.*, 1999; Dummer *et al.*, 1992; Unger *et al.*, 1990), the effects of glycosidated phospholipid analogues were primarily investigated in transformed cell lines derived from skin.

1.2.1 Structure of glycosidated phospholipids

Initially, D-glucose was introduced into phosphocholine (PC) and platelet-activating factor (PAF). The resulting compounds (Glc-PC and Glc-PAF, respectively (Figure 1.6)) displayed good antiproliferative properties in HaCaT cells (Mickeleit *et al.*, 1998; Mickeleit *et al.*, 1995), a premalignant keratinocyte cell line (Boukamp *et al.*, 1988). Fluorescence-Resonance-Energy-Transfer (FRET) analysis revealed that both Glc-PAF and Glc-PC intercalated in liposomes and, moreover, were able to induce lesions in the plasma membrane of cells

(Wiese *et al.*, 2000). However, the effective concentrations of both glycosidated phospholipids were relatively close to their cytotoxic concentrations.

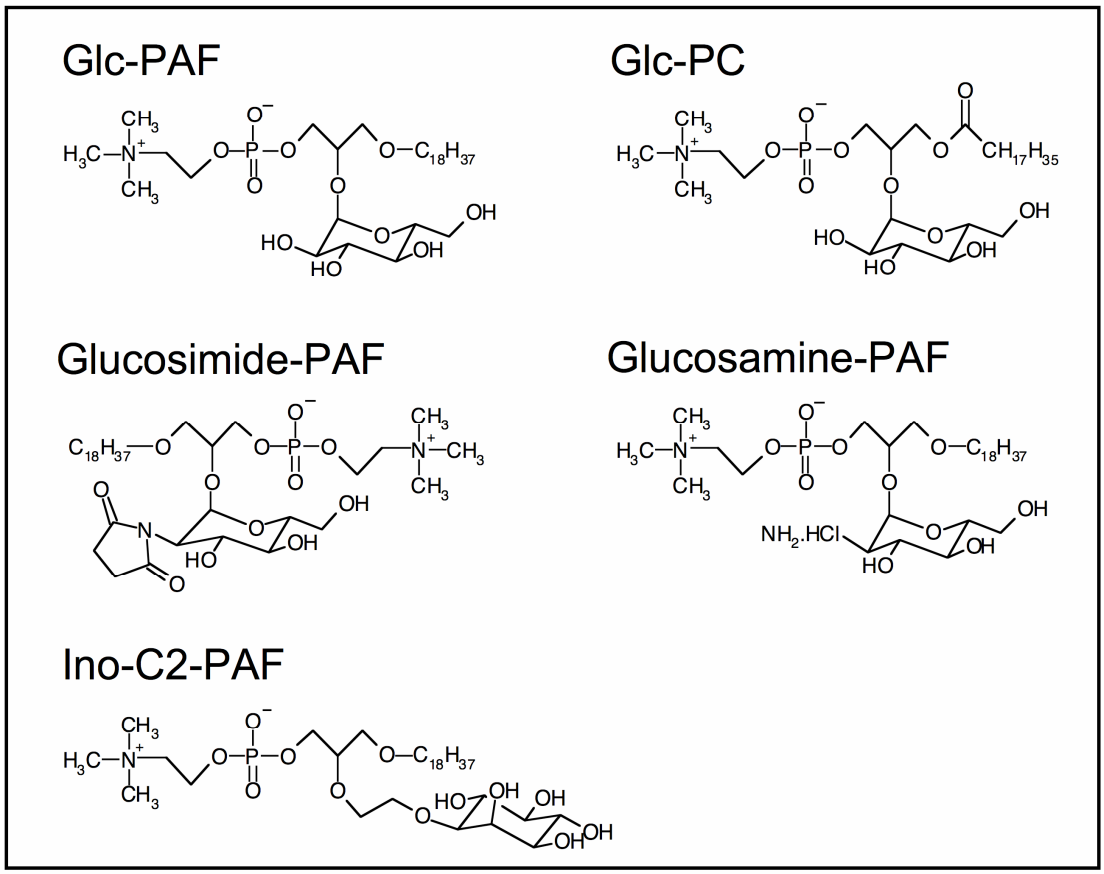

Figure 1.6. Structure of the glycosidated phospholipids Glc-PAF, Glc-PC, Glucosimide-PAF, Glucosamine-PAF, and Ino-C2-PAF

Based on the structure of Glc-PAF, a series of other glycosidated phospholipid analogues was synthesised. These included derivatives with a shorter aliphatic side-chain, other carbohydrate-substitutes, or an ether-link between the glycerol backbone and the carbohydrate-moiety, which resulted in C16-Glc-PAF, Glc-C2-PAF (not shown), Inositol-C2-PAF (Ino-C2-PAF; Fischer *et al.*, 2006; Figure 1.6), glucosimide-PAF, and glucosamine-PAF (Bartolmäs *et al.*, 2005; Figure 1.6).

1.2.2 Biological activity of glycosidated phospholipids

It is generally thought that alkylphospholipids, which are only slightly different from platelet-activating factor (PAF), are able to bind to the G protein-coupled PAF receptor. As previously shown, however, edelfosine scarcely induces platelet aggregation and exerts its biological activity via “non-specific” mechanisms (Kudo *et al.*, 1987). Additionally, glycosidated

phospholipids are not able to provoke signals that are normally induced following PAF receptor stimulation (Fischer, PhD thesis FU Berlin, 2006).

To obtain information about the uptake of glycosidated phospholipids by HaCaT cells and the stability of these compounds within cells, an analytical method based on MALDI-TOF-MS was established. With this method, it was possible to clearly distinguish synthetic phospholipids from endogenous phospholipids by their characteristic molecular weights. The resulting data revealed that the analogues were taken up by HaCaT cells during the first hour of treatment. The compounds accumulated over time in cells and their stability was demonstrated by their detection after 48 h (Fischer *et al.*, 2006).

In recent years, it has become increasingly clear that common antitumour lipids influence membrane microdomains enriched in cholesterol, which represent essential platforms for the regulation of signal transduction events, after uptake. In fact, it has been reported that modifications in the organisation of lipid rafts by edelfosine play a decisive role in the induction of apoptosis in leukaemic cells (Gajate *et al.*, 2004; Gajate *et al.*, 2009a; Gajate *et al.*, 2009b; Gajate and Mollinedo, 2001; Gajate and Mollinedo, 2007; Mollinedo *et al.*, 2004).

1.2.3 Structure-activity relationship of glycosidated phospholipids with regard to cytotoxicity and proliferation

The antiproliferative effects of these phospholipid analogues do not seem to be a simple consequence of their lytic properties because the proliferation of HaCaT cells was inhibited at non-toxic concentrations. In this regard, Ino-C2-PAF represents the most efficient glycosidated phospholipid analogue to be synthesised thus far. It inhibits the proliferation of HaCaT cells with an IC_{50} of 1.8 µM; its LC_{50} of 15 µM is clearly higher than the IC_{50} (Fischer *et al.,* 2006). Glc-PAF resulted to be less active and more cytotoxic than Ino-C2-PAF, but it exhibits a stronger inhibitory effect than the acyl-phospholipid Glc-PC (Mickeleit *et al.*, 1995). Regarding the biological activity of ATLs, metabolic stability represents a very important and crucial attribute (Eibl, 1996). In this context, alkylphospholipid analogues affect proliferation in a stronger manner than do acyl-phospholipids like Glc-PC. Ester bonds in the latter are presumably cleaved by endogenous esterases, where this confers metabolic instability and accounts for their restricted biological activity.

Proliferation assays using Ino-C2-PAF and Glc-C2-PAF indicated the importance of the cyclic alcohol inositol for the pharmacological effect of Ino-C2-PAF (Fischer, PhD thesis FU Berlin, 2006). Furthermore, it is likely that the ether bond connecting inositol to glycerol is metabolically more stable than the acetal linkage between glucose and glycerol, which can be attacked by endogenous glucosidases.

Similar to other well-studied ATLs, Ino-C2-PAF is able to inhibit the proliferation of tumour cells in a selective manner. Studies with primary fibroblasts and peripheral blood cells have demonstrated that the growth of normal cells is only marginally influenced by this compound (Fischer *et al*., 2006; Fischer, PhD thesis FU Berlin, 2006).

1.2.4. Influence of glycosidated phospholipids on cell differentiation and apoptosis

The inhibition of the proliferation by glycosidated phospholipid analogues has been proposed to be due to the concerted interference of several processes and pathways. *In vitro* differentiation assays have demonstrated that the most active glycosidated phospholipid, Ino-C2-PAF, induced to some extent the differentiation of HaCaT cells. Ino-C2-PAF increased the expression of the terminal differentiation marker involucrin and the enzyme activity of tranglutaminase (Fischer *et al.*, 2006).

While Ino-C2-PAF induces mainly differentiation in transformed keratinocytes and apoptosis only to a lesser extent, Glc-PAF and Ino-C2-PAF can induce apoptotic cell death in the leukaemia cell lines Jurkat and BJAB. Again, Ino-C2-PAF was more effective than Glc-PAF. Both Ino-C2-PAF and Glc-PAF trigger a CD95/Fas ligand- and receptor-independent atypical death-inducing-signalling-complex (DISC, for overview see Figure 1.3) that relies on the intrinsic apoptotic pathway via the endoplasmic reticulum as well as mitochondria. This is in clear contrast to studies with edelfosine and perifosine, which also induce apoptosis in lymphoid leukaemic cells but mediate their apoptotic action in the target cell via a Fas-dependent mechanism (Gajate *et al.*, 2009a; Gajate *et al.*, 2009b; Gajate *et al.*, 2007). These discrepancies in matters of apoptosis induction point to different modes of action for glycosidated phospholipid analogues and common ATLs.

1.3 Cell motility: a novel research field for APLs

As described in the previous paragraphs, many experiments investigating the effects of antitumour lipids (ATLs) on proliferation, differentiation and cell survival were performed in the last two decades. However, other important processes are also involved in the development and progression of cancer. Cell adhesion and motility represent two processes that play a crucial role during metastasis and invasion of tumour cells. Nonetheless, in the context of ATLs, cell migration and adhesion were only marginally studied (Storme et al., 1985; Schallier et al., 1991; Slaton et al., 1994). Therefore, cellular mechanisms and

signalling cascades that regulate cell movement are considered novel targets for the anticancer action of ATLs.

The cytoskeleton, a dynamic structure that maintains cell shape, is composed of three distinct elements: actin microfilaments, microtubules and intermediate filament. The actin cytoskeleton is thought to provide protrusive and contractile forces, and microtubules to form a polarized network allowing organelle and protein movement throughout the cell. Intermediate filaments are generally considered the most rigid component, responsible for the maintenance of the overall cell shape.

During cell migration, actin is organized in parallel bundles at the leading edge of the cell, which form filopodia (filopodial spikes) and in a dense meshwork that forms ruffling lamellipodia and promotes forward movement (Figure 1.7). Filopodia and lamellipodia are stabilized by adhering to the extracellular matrix (ECM) or adjacent cells via transmembrane receptors linked to the actin cytoskeleton. These adhesions serve as traction sites for migration as the cell moves forward over them, and they are disassembled at the cell rear, allowing it to detach. In the cell body and at the cell trailing edge, filamentous actin forms contractile stress fibres responsible for the contraction of the cell body and retraction of the trailing edge (Figure 1.7). The microtubule system could be directly involved in the generation of a protrusive activity, promoting membrane extension (Bretscher, 1996; Howard and Hyman, 2003).

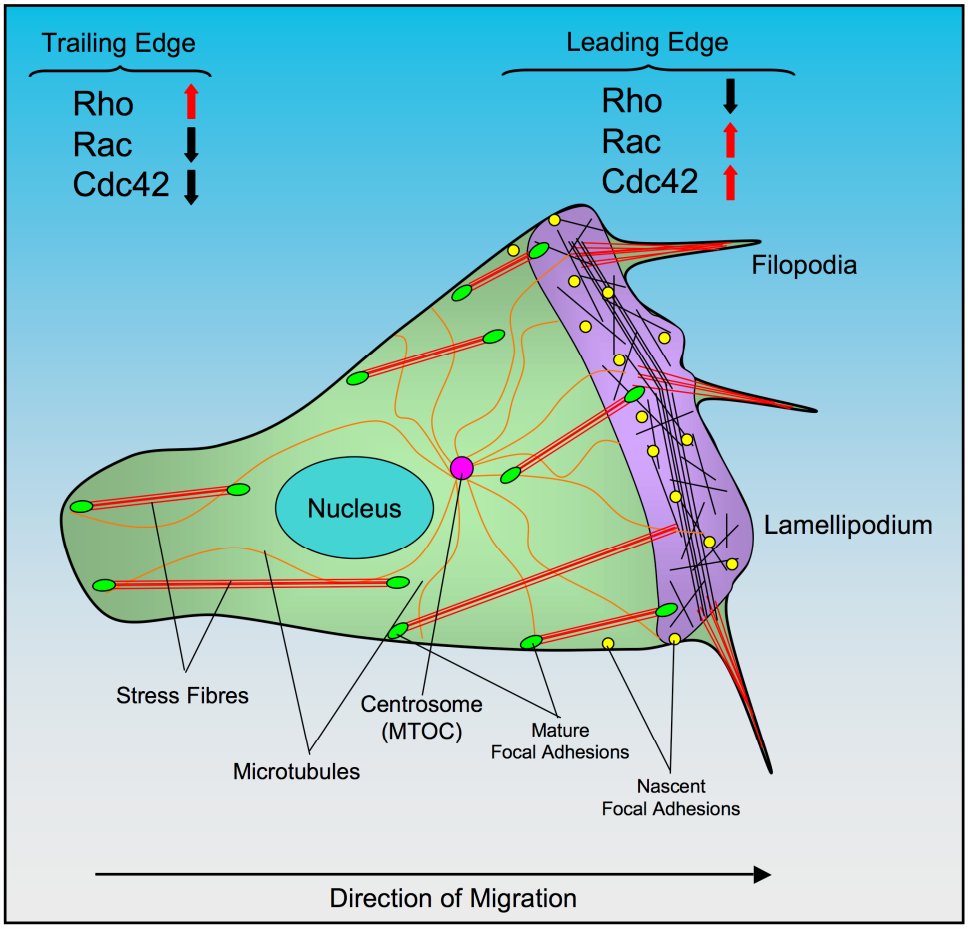

Figure 1.7. Organization of actin and microtubule cytoskeleton during cellular migration. The actin-rich region (purple) comprends actin bundles (red) organized into filopodia, a dense actin meshwork forming a ruffling lamellipodium and only a few pioneer microtubules. The lamellipodium is a region containing a high amount of nascent focal adhesions (yellow dots), whicht are not already bound to the actin cytoskeleton. Microtubules (orange) radiate from the centrosome (pink) with their plus-ends directed towards the plasma membrane. In the cell body, actin structures are essentially limited to stress fibres (red), anchored to the substrate via mature focal adhesions (dark green dots). At the leading edge active Rac and Cdc42 control cell protrusion and polarity, whereas active Rho at the trailing edge regulates cell detachment.

Like actin, microtubules organization is polarized during cell migration, with different dynamics at the leading edge and retracting edge. Furthermore, microtubules may participate in actin rearrangements and, actin and microtubules influence each other´s dynamics directly or through regulation of signalling molecules (Eddy *et al.*, 2002). Cell polarization is the result of two distinct phenomena: first, an ´intrinsic´ cell polarization enabling the cell to organize its cytoskeletal elements in a polarized manner; second, a direction-sensing mechanism, which allows a cell to orient its intrinsic polarity axis in response to extracellular cues.

1.3.1 Rho GTPases

Rho GTPases Rho, Rac and Cdc42 are pivotal regulators of actin and adhesion organization and control the formation of lamellipodia and filopodia (Figure 1.7). They are conformationally regulated by the binding of GTP and GDP: when bound to GTP, they are active and interact with their downstream target proteins, which include protein kinases, lipid-modifying enzymes, and activators of the ARP2/3 complex (Etienne-Manneville and Hall, 2002). Rho GTPases are activated by guanine nucleotide exchange factors (GEFs) and inactivated by GTPase activating proteins (GAPs) (Figure 1.8).

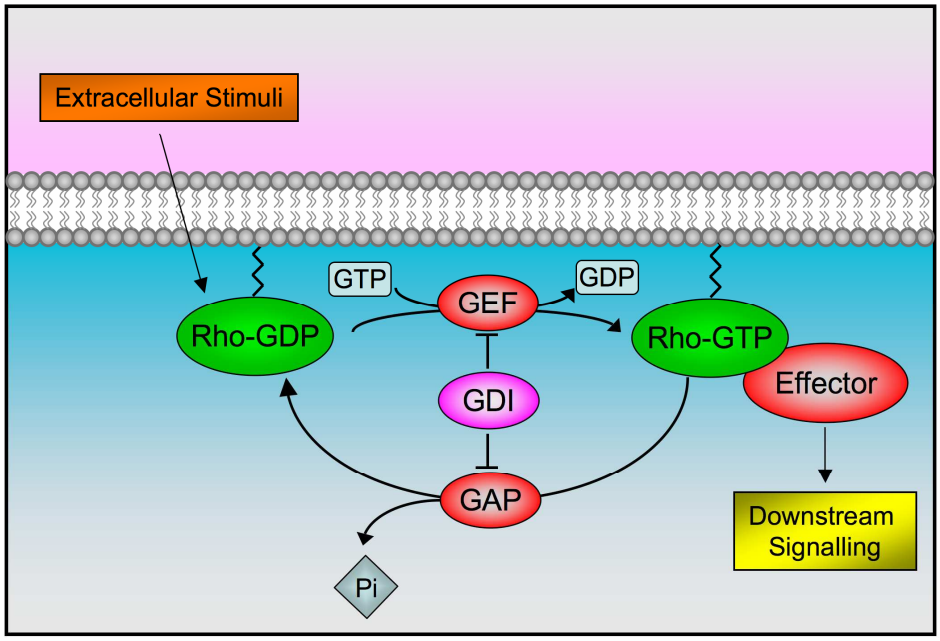

Figure 1.8. Rho GTPases are regulated molecular switches. Rho family proteins shuttle between the inactive GDP-bound and the active GTP-bound states. Activation is supported by guanine nucleotide exchange factors (GEFs), which promote exchange of GDP for GTP. Rho GTPases are down-regulated by GTPase activating proteins (GAP) and guanine nucleotide dissociation inhibitors (GDI). GAPs promote the hydrolysis of GTP to GDP, while GDIs prevent nucleotide exchange and sequester Rho from membranes. Activated GTP-bound Rho GTPases (RhoA, Rac1 and Cdc42) transmit extracellular signals by activation of effector proteins.

Rac and Cdc42 are both required at the front of migrating cells (Figure 1.7). The primary role of Rac is to generate a protrusive force through the localized polymerization of actin. Cdc42 also induces actin polymerization to generate filopodia often seen at the front of migrating cells (Nobes and Hall, 1995). Rho activity in migrating cells is associated with focal adhesion assembly and cell contractility and is responsible for cell body contraction and rear cell detachment (Figure 1.7). Cdc42 can influence polarity at the lamellipodium or by localizing the mictotubule-organizing center (MTOC) and Golgi apparatus in front of the nucleus, oriented toward the leading edge (Itoh *et al.*, 2002).

One model for how migrating cells maintain polarity is based on the fact that Rho and Rac are mutually antagonistic, each suppressing the other's activity (Evers *et al.*, 2000). Active Rac at the leading edge of cells would suppress Rho activity, whereas Rho would be more active at the sides and rear of the cell and suppress Rac activity, thereby preventing Rac-mediated protrusion at sites other than the leading edge (Figure 1.7; Worthylake and Burridge, 2003; Xu *et al.*, 2003).

Directional cell migration requires continuous spatio-temporal formation and turnover or maturation of focal adhesions (FAs) at the leading edge. Whereas, FA disassembly is best visualized at the trailing edge of cells (Webb *et al.*, 2004), nascent FAs that assemble under the lamellipodium exert tractional forces on the substrate that lead to lamellipodium growth and stability. The nascent FAs either undergo rapid turnover or mature in response to contractile forces (Zaidel-Bar *et al.*, 2003). Mature FAs facilitate increased cell contractility to pull the cell forward and are subsequently disassembled, or modified to form fibrillar adhesions that play critical role in the remodeling of ECM (Broussard *et al.*, 2008).
Focal contacts are formed at ECM–integrin junctions that bring together cytoskeletal and signalling proteins during the processes of cell adhesion, spreading and migration. Thus, integrin-mediated attachment to the ECM is a prerequisite for the controlled movement of cells (Vicente-Manzanares *et al.*, 2005). Furthermore, cell migration requires endocytosis and recycling of integrins, which is mediated by ubiquitination of integrin dimers in response to ECM binding (Lobert *et al.,* 2010). In reference to the skin, modifications of adhesive interactions with other cells and ECM components are required for the development and differentiation of keratinocytes (Kaufmann *et al.*, 1990). In both malignant and benign hyperproliferative disorders of the epidermis, integrin-dependent adhesion is often impaired (De Luca *et al.*, 1994; Schön *et al.*, 1996).

1.3.2 Focal adhesion kinase signalling pathway

Since integrins lack intrinsic enzymatic activity, their signalling function is dependent on non-receptor tyrosine kinases like the focal adhesion kinase (FAK) and Src (Figure 1.9). FAK can be activated by either ECM, upon integrin engagement, or growth factors (Chen *et al.*, 2002; Danker *et al.*, 1998; Schaller *et al.*, 1995). Tyrosine phosphorylation of FAK was a rapid event that was associated with the formation of focal contacts (Parsons, 2003). Furthermore, FAK signalling is also accompanied by the disassembly of integrin-based adhesion sites (Webb *et al.*, 2004). The loss of FAK expression also disrupts microtubule polarization within cells (Palazzo *et al.*, 2004), and this phenotype, as well as the defect in focal contact turnover, has been linked to the FAK-mediated regulation of Rho-family GTPases in cells

(Ren *et al.*, 2000). FAK protein expression is elevated in many highly malignant human cancers (Cance *et al.*, 2000), and studies have shown that FAK signalling can promote changes in cell shape (Haskell *et al.*, 2003; Ilic *et al.*, 2003) and the formation of podosomes or invadopodia (Hauck *et al.*, 2002a), which leads to an invasive cell phenotype (Hauck *et al.*, 2002b; Hsia *et al.*, 2003). Other studies have shown that FAK inhibition blocks the response to cell motility cues (Schlaepfer *et al.*, 2004).

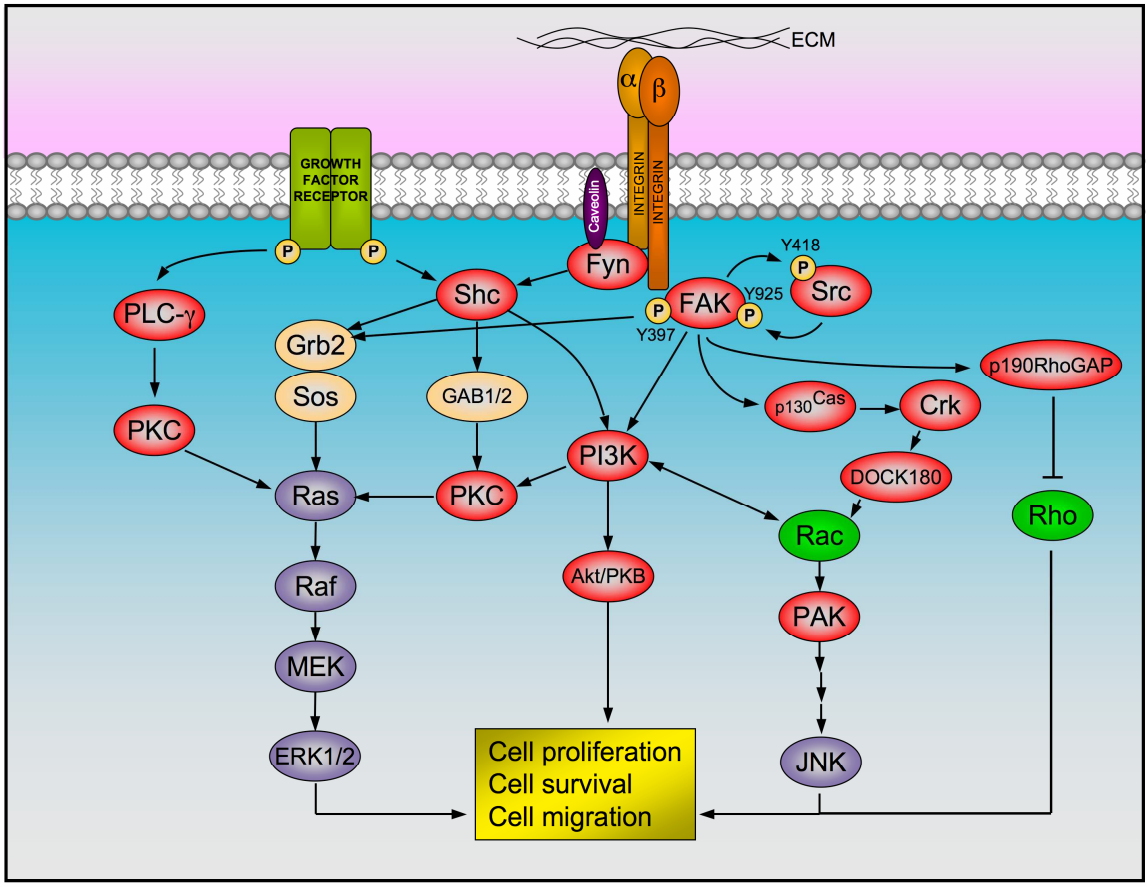

Figure 1.9. Integrin signaling at focal adhesions. After binding to the extracellular matrix (ECM), the cytoplasmic tail of integrin beta 1 recruits FAK, which is activated by auto-phosphorylation at the tyrosine 397 and thereby allow the binding and activation of Src by phosphorylation of tyrosine 418. The activated FAK/Src complex phosphorylates other kinases (i.e. p130Cas and PI3K) and GEFs/GAPs (i.e. p190RhoGAP), which in turn elicit a cascade of events that lead to cell proliferation, survival and migration. Alternatively, alpha subunits of certain integrins are able to recruit Fyn (a Src family member) via caveolin-1. This allows the activation of Shc, which combines with adaptor proteins Grb2 and SOS in order to activate the ERK/MAPK pathway. As represented, the integrin pathway has reciprocal action with other signalling cascades triggered by several growth factor receptors.

Alternatively, growth factor- and G-protein-linked stimuli that promote cell motility induce the transient recruitment of Src family kinases (SFKs) into a signalling complex with FAK and causes its activation (Schlaepfer *et al.*, 2004). FAK Tyr397 autophosphorylation promotes Src binding, which leads to the phosphorylation of Tyr418 and conformational activation of Src and results in a dual-activated FAK–Src signalling complex (Schlaepfer *et al.*, 2004).

Within this FAK–Src complex, Src phosphorylates FAK at Tyr861, which subsequently leads to an increase in SH3-domain-mediated binding of p130Cas to the FAK C-terminal proline-rich regions (Lim *et al.*, 2004). Signalling downstream of p130Cas results in increased activity of Rac, enhanced membrane ruffling or lamellipodia formation, and the promotion of cell motility or invasion (Brabek *et al.*, 2004; Cho and Klemke, 2002; Hsia *et al.*, 2003). Activated Src also phosphorylates FAK at Tyr925, which creates an SH2-binding site for the GRB2 adaptor protein. GRB2 binding to FAK is one of several connections that lead to the activation of Ras and the extracellular signal-regulated kinase-2 (ERK2)/MAPK cascade (Figure 1.9; Schlaepfer et al., 2004). ERK2 phosphorylation and the subsequent activation of myosin light chain kinase (MLCK) can modulate focal contact dynamics in motile cells (Ridley *et al.*, 2003), as well as generate both proliferative and survival signals inside cells (Hanks *et al.*, 2003).

As briefly mentioned, FAK plays also a role in the coordination of GEFs and GAPs activity that is critical for cyclic RhoGTPase regulation (Figure 1.9). Recent findings show that FAK may facilitate cycles of Rho inactivation followed by Rho activation through the selective association with p190ARhoGAP (Tomar *et al.*, 2009) and p190RhoGEF (Lim *et al.*, 2008) respectively, during cell spreading on fibronectin. In a simplistic model, FAK can generate ‘push’ at earlier stages of cell spreading by activating p190RhoGAP and inhibiting Rho, and subsequent ‘pull’, by activating p190RhoGEF and Rho at later stages of cell spreading. Additionally, the antagonism between Rho and Rac activity can also result in indirect Rac regulation via the cyclic regulation of Rho by FAK, for example through the phosphorylation of adaptor proteins such as p130Cas (Defilippi *et al.*, 2006; Schober *et al.*, 2007).
Generally, increased residency of activated FAK at FAs also enables the recruitment of effectors that lead to FA disassembly and turnover. For nascent FAs, the cyclic regulation of Rac/Rho activity may be an important determinant of FA turnover. In fact, nascent FAs mature under high contractility and turnover upon the loss of contractility (Gupton and Waterman-Storer, 2006).

2 AIM OF THE WORK

Ino-C2-PAF negatively regulates the proliferation and motility of skin cells. Nonetheless, the mechanism of action of this APL is mostly unknown. Therefore, the main focus of this study is to investigate the impact of Ino-C2-PAF on the molecular and signal transduction pathways involved in proliferation and migration of immortalized non-tumourigenic skin keratinocytes (HaCaT cells) and transformed keratinocytes derived from a squamous cell carcinoma (SCC25 cells).

To investigate the influence of Ino-C2-PAF on the transcription of the whole genome of HaCaT cells, microarray analyses will be performed. In addition, the transcriptional profile of Ino-C2-PAF will be compared with those of other two APLs, Glc-PAF and edelfosine, in order to detect potentially conserved mechanisms.

Since APLs are able to introduce and accumulate within the plasma membrane, they operate as Biological-Response-Modifier modulating several signal transduction pathways. Hence, the effects of Ino-C2-PAF on the most prominent signalling cascades that regulate proliferation and migration will be investigated. Furthermore, to characterize the role of APLs during cell movement, F-actin cytoskeleton, cell-matrix and cell-cell adhesion in the presence of Ino-C2-PAF will be analyzed.

3 MATERIALS AND METHODS

3.1 Materials

3.1.1 Devices and equipment

Agarose gel electrophoresis	Model B2	Owl Separation System, USA
Cell Counter	Coulter Z1	Coulter Electronics Ltd., UK
Centrifuges	Heraeus Biofuge pico Heraeus Biofuge fresco Heraeus Megafuge 1.0R	ThermoElectron, Langenselbold ThermoElectron, Langenselbold ThermoElectron, Langenselbold
ELISA Reader	Sunrise	Tecan, Crailsheim
FACScan		BD Biosciences, Heidelberg
Imagers	LAS-1000 Versadoc 4000 MP	Fujifilm, Düsseldorf BioRad, Munich
Magnetic stirrer	Type RH B2	IKA Werke, Staufen
Microscopes	Nikon TMS-F Diavert Axiovert 200 Fluorescence	Nikon, Japan Leica, Bensheim Zeiss, Jena
PCR	iCycler MyiQ (Single Color Real Time Detection System)	BioRad, Munich BioRad, Munich
pH meter	model 646 digital	Knick, Berlin
Power supply	Power PAC200	BioRad, Munich
Photometer	Biophotometer UV	Eppendorf, Hamburg
SDS-PAGE	Mini Protean System	BioRad, Munich
Shakers	model 3013 Stuart Orbital S150	GFL, Burgwedel Rhys International Ltd., UK
Thermomixer	Compact	Eppendorf, Hamburg
UV Transilluminator		MWG Biotech, Munich
Vortex	Mixer Genie 2	Scientific Industries, USA
Weighing machines	Adventurer (d=0,0001 g) CP622 (d=0,01 g)	Ohaus Corp., USA Sartorius AG, Göttingen

3.1.2 Chemicals and consumables

Chemicals were purchased from Carl Roth (Karlsruhe), Sigma-Aldrich (Steinheim), Merck (Darmstadt) and Applichem (Darmstadt), unless stated otherwise.
Consumables were obtained from Corning Inc. (Corning, USA), Nunc Inc. (Naperville, USA), Schott (Mainz), Carl Roth (Karlsruhe), Eppendorf (Hamburg), BD Biosciences (Franklin Lakes, USA) and Whatman (Maidstone, England).

3.1.3 Reagents

PolyMag	OZ Biosciences, France
Epidermal Growth Factor (EGF)	Biomol, Hamburg
Calcipotriol Anhydrate	Leo Pharma, Bellerup
Wortmannin	Biomol, Hamburg
Insulin Like Growth Factor-I (IGF-1)	Biomol, Hamburg
Edelfosine	Biaffin, Kassel
Collagen IV (from human placenta)	Sigma-Aldrich, Steinheim
Fibronectin (from human plasma)	Sigma-Aldrich, Steinheim
Laminin-111 (from Engelbreth-Holm-Swarm mouse sarcoma)	Roche, Mannheim
Poly-L-Lysine	Sigma-Aldrich, Steinheim
Accutase	PAA, Austria
Immersion oil	Zeiss, Jena
Gel Mounting	Sigma-Aldrich, Steinheim
Phenylmethanesulfonyl fluoride (PMSF)	Sigma-Aldrich, Steinheim
Protease Inhibitor Cocktail (PIC)	Sigma-Aldrich, Steinheim
Nocodazole	Sigma-Aldrich, Steinheim
Colchicine	Sigma-Aldrich, Steinheim
Trypsin	PAA, Austria

3.1.4 Primary antibodies

Name	Species	Source	Method	Dilution
Phospho-Akt (Ser473)	Rabbit	Cell Signaling	WB	1:1000
Phospho-Akt (Ser473)	Rabbit	R&D Systems	WB	1:1500
Phospho-Akt (Ser473)	Mouse	Cell Signaling	WB	1:1000
			IF	1:200
Phospho-Akt (Ser473)	Rabbit	BioSource	WB	1:1000

E-Cadherin	Mouse	BD Biosciences	WB	1:1000
			IF	1:200
Phospho-FAK (Tyr397)	Mouse	BD Biosciences	WB	1:1000
			IF	1:200
Phospho-FAK (Tyr397)	Rabbit	BioSource	WB	1:1000
FAK	Rabbit	BioSource	WB	1:1000
			IP	7.5 µg
β1 integrin, clone 12G10	Mouse	Abd Serotec	FACS	1:25
			IF	1:200
β1 integrin, FITC-conjugated	Mouse	Immunotech	FACS	1:25
Phospho-ERK1/2 (Thr202/Tyr204)	Rabbit	Cell Signaling	WB	1:1000
Phospho-p38 (Thr180/Tyr182)	Rabbit	Cell Signaling	WB	1:1000
Phospho-SAPK/JNK (Thr183/Tyr185)	Rabbit	Cell Signaling	WB	1:1000
Total phospho-Tyr, clone PT66	Mouse	Sigma-Aldrich	IF	1:1000
Phospho-Src (Tyr418)	Rabbit	BioSource	WB	1:1000
			IF	1:200
c-Src	Rabbit	Santa Cruz	WB	1:500
α-Tubulin	Mouse	Abcam	WB	1:5000
			IF	1:1000

3.1.5 Secondary antibodies

Name	**Source**	**Method**	**Dilution**
Goat anti-Rabbit-IgG-POD	Jackson Immunoresearch	WB	1:5000
Goat anti-Mouse-IgG-POD	Jackson Immunoresearch	WB	1:5000
Alexa Fluor® 488 Goat anti-Rabbit	Molecular Probes	IF	1:750
Alexa Fluor® 488 Goat anti-Mouse	Molecular Probes	IF	1:750
		FACS	1:750
Alexa Fluor® 594 Goat anti-Rabbit	Molecular Probes	IF	1:750
Alexa Fluor® 594 Goat anti-Mouse	Molecular Probes	IF	1:750
Phalloidin-CPITC	Sigma	IF	1:100
Phalloidin-Texas Red	Invitrogen	IF	1:100
Goat anti-Mouse-IgG FITC	Sigma	FACS	1:25
Anti-Biotin, HRP-linked	Cell Signaling	WB	1:2500

3.1.6 Protein markers

Biotinylated Protein Ladder	Cell Signaling, USA
Precision Plus Protein Standards	BioRad, Munich

3.1.7 Antibiotics

Kanamycin	(Working conc.: 30 µg/ml)
Neomycin	(Working conc.: 25 µg/ml)

3.1.8 Plasmids

GFP-FAK	(Gift of Prof. Jun-Li Guan; Li et al., 2002)
Src-Y527F-GFP	(Gift of Prof. Margaret Frame; Sandilands et al, 2004)
CD2-FAK	(Gift of Prof. Shuang Huang; Chan et al., 1994)

3.1.9 Bacterial strains

E. coli TOP10	Invitrogen, Karlsruhe
E. coli MC1061/P3	Invitrogen, Karlsruhe

3.1.10 Kits

Transcriptor High Fidelity cDNA Synthesis Kit	Roche, Mannheim
Cell Proliferation ELISA, BrdU (colorimetric)	Roche, Mannheim
RNeasy Mini Kit	Qiagen, Hilden
Plasmid Mini Kit	Qiagen, Hilden
HiSpeed Plasmid Maxi-Kit	Qiagen, Hilden
PureYield™ Plasmid Midiprep System	Promega, USA

3.1.11 Buffers, solutions and media

Commonly used media, buffers, and solutions were prepared using deionized or double destilled water. If necessary, solutions were autoclaved at 121℃ for 20 min at 1 bar. Thermolabile components were filter-sterilized (0.22 µm) and added after autoclaving. The pH was adjusted using HCl or NaOH. Buffers, solutions and media are listed at the end of each method.

3.1.12 Software and databases

Database for Annotation, Visualization and Integrated Discovery (DAVID) of the National Institute of Allergy and Infectious Diseases (NIAID)
(http://david.abcc.ncifcrf.gov/)

GeneVenn supplied by the Bioinformatics Organization, Inc Hudson, USA
(http://www.bioinformatics.org/gvenn/).

Axiovision (Zeiss, Jena)

GeneSpring GX 10 (Agilent Technologies, USA)

NCBI homepage
(http://www.ncbi.nlm.nih.gov/)

3.2 Methods

3.2.1 Cell Biology

3.2.1.1 Cell culture

SCC25 cells were grown in Ham's F12/DMEM medium supplemented with penicillin (100 U/ml), streptomycin (0.1 mg/ml), L-glutamine (440 mg/l), hydrocortisone (0.4 µg/ml), and heat-inactivated fetal bovine serum (10%). HaCaT cells were grown in RPMI medium supplemented with heat-inactivated fetal bovine serum (10%), penicillin (100 U/ml), streptomycin (0.1 mg/ml), and L-glutamine (440 mg/l). Cells were disaggregated with trypsin and 0.02 mM EDTA. Two days prior to experimentation, cells were adapted to defined keratinocyte serum-free medium with growth supplements (pituitary extract including insulin, EGF, and FGF) (Gibco/BRL). Experiments were performed in defined keratinocyte serum-free medium.

Growth-medium for HaCaT cells
BioWhittaker RPMI 1640
Fetal bovine serum (10%)
Penicillin (100U/ml)
Streptomycin (0.1 mg/ml)
L-glutamine (440 mg/l)

Keratinocytes growth-medium
Defined Keratinocyte SFM
Supplement factor (1 vial)
Penicillin (100U/ml)
Streptomycin (0.1 mg/ml)
L-glutamine (440 mg/l)

Phosphate-buffered saline (PBS, 1X)
150 mM NaCl
3 mM KCl Fetal bovine serum (10%)
8 mM $Na_2HPO_4.2H_2O$
1 mM KH2PO4
in ddH_2O
adjust to pH 7.2

Growth-medium for SCC25 cells
DMEM:F12 1:1
Streptomycin (0.1 mg/ml)
Penicillin (100U/ml)
L-glutamine (440 mg/l)
Hydrocortisone (0.4 µg/ml)

PBS-EDTA solution
0.05% EDTA
in PBS

3.2.1.2 Cell proliferation assay

A colorimetric immunoassay (cell proliferation ELISA with bromodeoxyuridine (BrdU); Roche Diagnostics, Mannheim, Germany) was used to detect replicating cells. Cells were seeded in a 96-well microtiter plate at 1,5 x 10^4 cells per well and incubated with varying concentrations of Ino-C2-PAF for 6 h. Simultaneously, BrdU labeling solution (100 µM) was added to give a final concentration of BrdU of 10 µM per well. Further steps were performed according to the manufacturer's instructions. The colorimetric reaction was determined photometrically at 405 nm and subsequently quantified. The untreated cells were set at 100%.

3.2.1.3 Cell migration assay

Haptotactic transwell migration assays were performed using transwell plates (Costar, Corning, NY, USA) with a pore size of 8 µm. The bottom side of the filter was coated with 50 µl collagen IV (20 µg/ml) for 30 min at room temperature followed by blocking of non-specific binding sites for 30 min at room temperature. A total of 600 µl serum-free medium was added per well. The upper compartment was filled with 100 µl of a cell suspension containing 5.5 x 10^4 cells. Cells were then allowed to migrate for 6 h at 37°C. For migration experiments with transfected cells migration time was elongated to 16 h. Afterward, cells were removed

from the upper surface with cotton swabs, and the filters were washed in PBS. Migrated cells were fixed in 4% paraformaldehyde in PBS containing 0.025% saponin for 30 min, stained for 35 min with 0.1% crystal violet, and counted using a 20x objective and a 10x10 grid.

Migration assay staining solution	Blocking solution
0.1% (w/v) crystal violet	1% BSA
in PBS	in PBS

3.2.1.4 Transfection of cells

GFP-FAK, Src-WT-GFP, CD2-FAK, EGFP were transfected into cells using the MagnetofectionTM transfection reagent PolyMag (OZ Bioscience, Marseille, France). The day before transfection, 6 x 10^5 cells were plated on a 35 mm dish in complete culture medium. 2 µg DNA were diluted in 200 µl serum and culture medium free of antibiotics, and subsequently mixed with 2 µl of PolyMag. After 20 min of incubation, the complex was added to the cells and the dish was placed upon the magnetic plate for 20 min. In order to eliminate untransfected cells, the medium was changed 2 h after transfection and the dishes were incubated for further 24 h at 37°C. Subsequently, cells were used for migration assays or live imaging. Transfection efficiency was between 50 and 80 % depending on the respective cDNA construct.

3.2.1.5 Cell attachment assay

For attachment assays, HaCaT cells were incubated for 48 h in the presence or absence of Ino-C2-PAF. At the same time, 96-well plates were coated with extracellular matrix components as indicated (20 µg/ml PBS; Sigma, Munich, Germany) and incubated for 16 h at 4°C. Non-specific binding was blocked for 4 h at 4°C. A total of 5 x 10^4 HaCaT cells in 100 µl medium per well were plated onto the indicated matrix proteins. After 2 h of incubation at 37°C, non-attached cells were removed by washing with PBS. Attached cells were fixed and stained with 0.1% crystal violet. Plates were photometrically measured at 570 nm after Triton X-100 dye solubilization.

Adhesion assay staining solution	Blocking solution
0.1% (w/v) crystal violet	1% BSA
in PBS	in PBS

Permeabilisation solution
0.5% Triton X-100
in H_2O

Fixation solution
1% glutardialdehyde
in H_2O

3.2.1.6 Wound healing assay (scratch)

Confluent cells were serum-starved overnight. After washing in DPBS, a wound was applied to the confluent monolayer with a yellow tip. Floating cells were rinsed off twice with DPBS and the adherent cells were incubated an additional hour at 37℃ in keratinocyte serum-free medium. Treatment with or without Ino-C2-PAF occurred for the indicated periods of time.

3.2.1.7 Flow cytometry

HaCaT and SCC25 cells were incubated with Ino-C2-PAF or left untreated. Cells were detached with accutase and 5 x 10^5 cells were transferred to a FACS-tube, and washed twice with 3 ml PBS. The pellet was then resuspended in 500 µl FACS-Flow and unspecific binding sites were blocked with 1% BSA in FACS-Flow for 30 min on ice. The blocking solution was washed off and the cells were resuspendend in 500 µl FACS-Flow containing the respective concentration of primary antibody for 45 min on ice. Afterwards, cells were washed twice and incubated in the dark with the secondary antibody for another 45 min on ice. Each centrifugation step was performed at 900 rpm for 3 min. Surface integrin expression was measured using a FACScan. For the controls, cells were incubated with the respective secondary antibody only.

FACS-Flow (BD Biosciences, Heidelberg)
0.1% (w/v) BSA
0.03% (w/v) NaN_3
in PBS

3.2.1.8 Immunofluorescence studies

A total of 3 x 10^4 (subconfluent state) or 1 x 10^5 (confluent state) HaCaT or SCC25 cells were seeded onto 8-well Permanox® slides (Nunc, Wiesbaden, Germany) coated with collagen IV (20 µg/ml in PBS) and cultivated overnight with the respective culture medium. The cells were washed with PBS and incubated with serum-free medium for further 16 h, before being incubated with or without Ino-C2-PAF. After the indicated incubation periods, cells were washed with PBS, fixed, and permeabilized for 20 min at room temperature. After blocking for 10 min with 1% BSA in PBS, cells were incubated with the respective antibody at 4℃

overnight. For detection of phosphorylated proteins, cells were blocked with a solution of 1% BSA in TBS, incubated first with the respective primary antibody diluted in TBS at 4℃ overnight. The cells were then accurately washed with PBS (or TBS) and PBS/Triton X-100 (or TBS/Triton X-100). Afterwards, cells were incubated in the dark with the secondary antibody for 2 h and accurately washed again.
Slides were analyzed on a Zeiss Axiovert 200 microscope with an Axiocam and Axiovision software (AxioVs40V; Zeiss, Jena, Germany). Images were further processed using Adobe Photoshop (version 8.0.1). Images that are meant to be compared one with another were acquired using identical settings of exposure and processing.

PBS
137 mM NaCl
2.7 mM KCl
8 mM $Na_2HPO_4.2H_2O$
1.8 mM KH2PO4
in ddH_2O
adjust to pH 7.6

TBS
20 mM Tris pH 7.6
150 mM NaCl
in ddH_2O

PBS/Triton X-100
0.1% Triton X-100
in PBS

TBS/Triton X-100
0.1% Triton X-100
in TBS

IF fixation and permeabilization buffer
4% (w/v) paraformalaldehyd (PFA)
0.025% (w/v) saponin
in PBS

3.2.2 Biochemistry

3.2.2.1 Solubilisation

To analyse or quantify proteins cells solubilised. After stimulation, cells were washed twice with ice-cold PBS, scraped into 100 µl solubilisation buffer and incubated on ice for 30 min. The soluble cell lysates were spun for 15 min at 13.000 rpm at 4℃. Supernatant was transfered in an new tube, quantified using the BCA Protein Assay and boiled in the presence of Laemmli sample buffer at 95℃ for 5 min .

Solubilisation buffer
20 mM Hepes/NaOH pH 7.5
150 mM NaCl
1 mM $MgCl_2$
1 mM $CaCl_2$
1% (v/v) Triton X-100
0.1 mM $NaVO_4$
1 mM PMSF
0.2% (v/v) PIC
25 mM NaF
in ddH_2O

Laemmli´s sample buffer (5X)
250 mM Tris
25% (v/v) glycerol
7.5% (w/v) SDS
0.25 mg/ml bromphenol blue
12.5% β-mercaptoethanol
in ddH_2O

3.2.2.2 Protein quantification

The BCA Protein Assay is a detergent-compatible formulation based on bicinchoninic acid (BCA) for the colorimetric detection and quantification of total protein. A fresh protein standard was prepared by diluting the 2 mg/ml BSA stock standard (Pierce, USA) with water in serial dilution in a 96-well plate, reaching a volume of 20 µl. The samples were diluted 10 x in water. Reagent A and B were mixed together in a ratio of 1:50 and 180 µl of reagent´s mixture were added to standard and samples. The samples were shortly mixed and the plate was subsequently incubated for 30 min at RT. The absorptions were determined at 570 nm in an ELISA reader. A standard curve was prepared and the protein concentrations were determined using this standard curve.

3.2.2.3 SDS-polyacrylamide gelelectrophoresis

Denaturing sodium dodecylsulfate polyacrylamide gel electrophoresis (SDS-PAGE) is a commonly used method to separate proteins on polyacrylamide gels according to their size (Laemmli, 1970).
Solutions A, B and C were used to prepare separating and stacking gels. Protein samples, which were supplemented and boiled with Laemmli sample buffer, were loaded on to the gels. Gelelectrophoresis was performed in SDS-PAGE running buffer until the bromphenol blue band exits the gel. Gels were then applied to Western Blot.

Solution A (Rotiphorese Gel 30)
30% (w/v) acrylamide
0.8% (w/v) bis-acrylamide

Solution B
1.5 M Tris pH 8.8
0.4% (w/v) SDS

Solution C
0.5 M Tris pH 6.8
0.4% (w/v) SDS

SDS-PAGE running buffer (10X)

192 mM Tris pH 7.3

25 mM glycine

0.1% (w/v) SDS

in ddH_2O

Separating gel	**7.5%**	**10%**	**15%**
Solution A	2.25 ml	3 ml	4.50 ml
Solution B	2.25 ml	2.25 ml	2.25 ml
dd H_2O	4.50 ml	3.75 ml	2.25 ml
APS (10% w/v)	45 µl	45 µl	45 µl
TEMED	4.5 µl	4.5 µl	4.5 µl

Stacking gel	**4%**
Solution A	0.40 ml
Solution C	0.75 ml
dd H_2O	1.85 ml
APS (10% w/v)	18 µl
TEMED	5 µl

3.2.2.4 Western Blotting

For western blotting, cells were lysed in solubilisation buffer and supernatants were denatured by boiling with Laemmli's sample buffer (see point 3.2.2.1). Samples were separated by 7.5 or 10% SDS-PAGE under reducing conditions. Separated proteins were transferred in blotting buffer to nitrocellulose membranes for 1h at 4℃ with a constant amperage of 25 mA. The protein transfer on the membrane was verified by staining with Ponceau S solution, followed by the decoloration with 0.1% acetic acid solution and PBS or TBS. Membranes were subsequently blocked for 1 h. The blots were incubated overnight at 4℃ with suitable primary antibody. After incubatio n with the appropriate horseradish peroxidase-conjugated secondary antibody, proteins were detected with Supersignal West Pico or Femto reagents (Pierce, Thermo Fischer Scientific, Bonn) and signals were visualized using a Digital Imaging System (LAS-100) by Fuji (Raytest, Straubenhardt, Germany) or with Versadoc 4000 MP (BioRad, Munich).

Phosphate-buffered saline (PBS, 1X)
137 mM NaCl
2.7 mM KCl
8 mM $Na_2HPO_4.2H_2O$
1.8 mM KH2PO4
in ddH_2O
adjust to pH 7.6

Tris-buffered saline (TBS, 1X)
20 mM Tris pH 7.6
150 mM NaCl
in ddH_2O

PBS with Tween-20 (PBS-T, 1X)
0.1% (v/v) Tween-20
in PBS

TBS with Tween -20 (TBS-T, 1X)
0.1% (v/v) Tween-20
in TBS

Blocking buffer for anti-phospho-antibodies
5% (w/v) BSA
in TBS-T

Blocking buffer
5% (w/v) skim milk powder
in PBS-T

Ponceau S staining solution (5X)
2% (w/v) Ponceau S
30% (v/v) trichloroacetic acid
30% (v/v) sulfosalicylic acid
in ddH_2O

Blotting buffer (10X)
1 M Tris pH 8.3
1.92 M glycine
10% (v/v) Ethanol
in ddH_2O

3.2.2.5 Co-immunoprecipitation

2.5 x 10^6 cells were incubated with 5 µM Ino-C2-PAF for 3 h. Cells were subsequently washed twice with cold TBS and lysed in 200 µl Tris/CHAPS buffer. After an incubation for 30 min on ice, the cell lysates were spun for 15 min at 4 ℃ at 6000 x g. For co-immunoprecipitation, Protein A-Sepharose (Amersham Biosciences, Uppsala, Sweden) was blocked with ovalbumin-containing IP buffer. Cell lysates were precleared with 50 µl of 10% (w/v) protein A-Sepharose to remove unspecific binding. Protein A-Sepharose was pelleted and the supernatants were incubated with 7.5 µg of panFAK (BioSource) for 1 h at 4℃. Immunocomplexes were recovered after a 30 min at 4°C incubation with 50 µl of 10% (w/v) protein A-Sepharose and subsequently washed four times with IP buffer. Bound proteins were eluted in 30 µl of 2 x sample buffer and boiled at 95℃ for 5 min. Precipitated proteins were further analyzed by Western blottting.

Tris/CHAPS lysis buffer
20 mM Tris/HCl pH 7.4
150 mM NaCl
10% glycerol
1% (w/v) CHAPS
0.2% (v/v) PIC
0.4 mM PMSF
1 mM sodium vanadate
25 mM NaF
in ddH_2O

IP buffer
50 mM Tris/HCl pH 8.5
150 mM NaCl
2 mM CaCl2
0.05% NP-40
0.02% NaN_3
1 mg/ml ovalbumin
in ddH_2O

Sample buffer (2X)
250 mM Tris/HCl pH 6.8
0.025% (w/v) bromphenol blue
10% (w/v) SDS
25% (v/v) glycerol
10 mM dithiothreitol

3.2.3 Molecular Biology

3.2.3.1 Preparation of competent bacteria

Stretches of Top10 frozen stocks were placed on LB agar plates and incubated overnight at 37℃. One colony was picked into 3 ml antibiotic-fr ee LB medium and incubated overnight at 37℃ with shaking. One ml of the overnight culture was transferred to 100 ml antibiotic-free LB medium and incubated at 37℃ with shaking (160 r pm) until the culture reached a OD_{600} of 0.6. The cells were cooled down on ice before being centrifuged at 3000 rpm for 15 min at 4℃. The cell pellet was resuspendend in 25 ml cold $CaCl_2$-solution, centrifuged, resuspended and centrifuged again. The resulting cell pellet was resuspended in 2.5 ml $CaCl_2$-solution, aliquoted in 50 µl samples, immediately put in liquid nitrogen and finally stored at -80℃.

$CaCl_2$-solution
10 mM PIPES pH 7
60 mM $CaCl_2$
15% (v/v) glycerol
in ddH_2O

3.2.3.2 Transformation of bacteria with plasmid DNA

Competent cells were transformed with plasmid DNA using the heat shock procedure. About 1-2 µl of plasmid DNA was added to 50 µl thawed competent bacteria and incubated on ice for 30 min. Then, bacteria were heat shocked for 45 sec at 42°C and subsequently put on ice for 2 min. Thereafter, 250 µl pre-warmed SOC medium (Invitrogen, Karlsruhe) was added and bacteria were incubated at 37°C for 1 h with shaking at 300 rpm. Transformed bacteria were grown overnight at 37°C on LB plates containing the appropriate antibiotic.

LB medium (1X)
1% (w/v) tryptone
0.5% (w/v) yeast extract
0.5% (w/v) NaCl
in ddH_2O
(supplemented with 1.5% (w/v) agar for agar plates)

3.2.3.3 Glycerol culture

5 ml of LB medium containing the transformed bacterium and the appropriate antibiotic was incubated overnight at 37°C with shaking at 160 rpm. The cell culture were then centrifuged at 3000 rpm for 5 min. The resulting cell pellet was washed with 5 ml antibiotic-free LB medium and finally resuspended in 1.5 ml antibiotic-free LB medium. 750 µl of the suspension were mixed with the same volume of glycerol and stored at -80°C.

3.2.3.4 Agarose gel electrophoresis

Agarose gel electrophoresis was used to separate DNA fragments after PCR or restriction enzyme digestion. Samples were supplemented with 6x loading dye and loaded on 1-2% agarose gels, which were prepared with 0.5 µg/ml ethidium bromide in TAE buffer. The Gene Ruler™ 1 kb or 100 bp DNA ladder (Fermentas, St. Leon-Rot) were used as size standards. Gels were run in agarose gel electrophoresis chambers at 100 V for approximately 1 hour in TAE buffer before images were taken for the photographic documentation under an

ultraviolet transluminator.

TAE-Buffer (1X)	DNA loading buffer (6x)
40 mM Tris	0.05% (w/v) bromophenol blue
1 mM EDTA	0.05% (w/v) xylene cyanol
40 mM Acetic acid	30% (v/v) glycerol
in ddH_2O	in ddH_2O

3.2.3.5 Plasmid-DNA purification

Plasmid-DNA was extracted with Plasmid Mini Kit in accordance to the manufacturer instructions (Qiagen, Hilden, Germany). After purification, plasmid-DNA was mixed with water in a ratio of 1:30 and the concentration was measured using a UV biophotometer.

3.2.3.6 RNA preparation

Total RNA was extracted with RNeasy Mini Kit in accordance to the manufacturer instructions (Qiagen, Hilden, Germany). The integrity of RNA was verified by the presence of the 28S and 18S rRNA on agarose gels and an OD260/280 ratio in the range of 1.9–2.1.

3.2.3.7 Microarray analysis

Microarray analysis was performed by Atlas Biolabs GmbH, Berlin, Germany. 200 ng of total RNA were used for production of fluorescent cRNA as described in the Agilent analysis instruction manual for One-Color Microarray-Based Gene Expression Analysis (Agilent Technologies, Palo Alto, USA). All samples were hybridized to Agilent whole human genome microarray kit 44K. Arrays were scanned with the use of a GenePix 4000A Scanner (Axon Instruments-Molecular Devices, Sunnyvale, USA). The signal values were extracted using the Agilent Feature Extracting Software version 9.5.3.

3.2.3.8 Data analysis

The GeneSpring GX 10 software (Agilent Technologies, Palo Alto, USA) was used to identify differentially expressed genes. Up-regulation and down-regulation between the three control experiments and each of the three phospholipid analogues experiments (Ino-C2-PAF, Glc-PAF, edelfosine) were defined whenever each expression value was higher or lower by factor two (p-value $< 0,05$).

Alternatively, gene expression data were reanalyzed with CorrXpression-Software (Klein *et al.*, 2009; Wessel *et al.*, 2006). Over- and under-expression were defined whenever a transcript expression value for each experiment of the 3 control experiments was higher or lower by at least a factor of two compared to each transcript expression value of the respective APL stimulation experiment. Therefore, for each transcript and for each APL stimulation experiment nine comparisons were calculated. Only those genes were considered as significant with at least one P-value < 0.05.

To classify up- or down-regulated genes into statistically significant biological processes Gene Ontology analysis was performed using the Database for Annotation, Visualization and Integrated Discovery (DAVID) of the National Institute of Allergy and Infectious Diseases (NIAID) (http://david.abcc.ncifcrf.gov/) (Dennis *et al.*, 2003; Huang *et al.*, 2009).

Venn diagrams were generated using the web software GeneVenn supplied by the Bioinformatics Organization, Inc Hudson, USA (http://www.bioinformatics.org/gvenn/).

4 RESULTS

4.1 Ino-C2-PAF inhibited proliferation of HaCaT and SCC25 cells

Previous investigations determined the cytotoxic potential of Ino-C2-PAF using an assay based on the release of lactate dehydrogenase (LDH) in the cell culture supernatant. It turned out that Ino-C2-PAF is non-toxic in the range of 0.6-5 µM for exposure times of 4 and 48 h in HaCaT cells (Fischer *et al*., 2006). At higher concentrations, necrotic cell death could be observed, with an LC_{50} value of about 15 µM. In SCC25 cells, Ino-C2-PAF displays a similar effect.

In this work, the anti-proliferative efficacy of Ino-C2-PAF on transformed keratinocyte cell lines, HaCaT and SCC25, was measured using a colorimetric immunoassay that monitors the incorporation of the thymidine analogue 5-bromo-2´-deoxyuridine (BrdU) into DNA of proliferating cells.

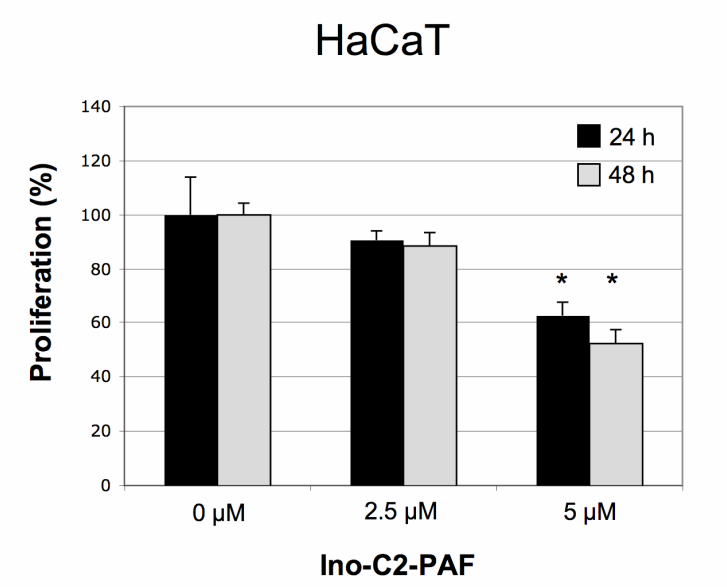

Figure 4.1. Influence of Ino-C2-PAF on HaCaT cells proliferation. 1.5 x 10^4 HaCaT cells/well in keratinocyte serum-free medium were treated for 24 h and 48 h with the indicated concentrations of Ino-C2-PAF, or left untreated. Untreated cell were set at 100%. All experiments were performed in quadruplicate and repeated at least three times. Data that are significantly (P-value < 0.05) different from control cells are indicated by a star (*).

Figure 4.1 shows the influence of Ino-C2-PAF on the proliferation of HaCaT cells. Ino-C2-PAF decreased cell proliferation in a dose-dependent manner. 5 µM Ino-C2-PAF significantly inhibited the proliferation by about 40%. However, no relevant differences between cells that were incubated for 24 or 48 h with Ino-C2-PAF were detected.

Similarly to HaCaT cells, the anti-proliferative activity of Ino-C2-PAF was also detectable on the highly invasive keratinocyte cell line SCC25 (Figure 4.2). In fact, 5 µM Ino-C2-PAF inhibited significantly the cell growth of about 40%.

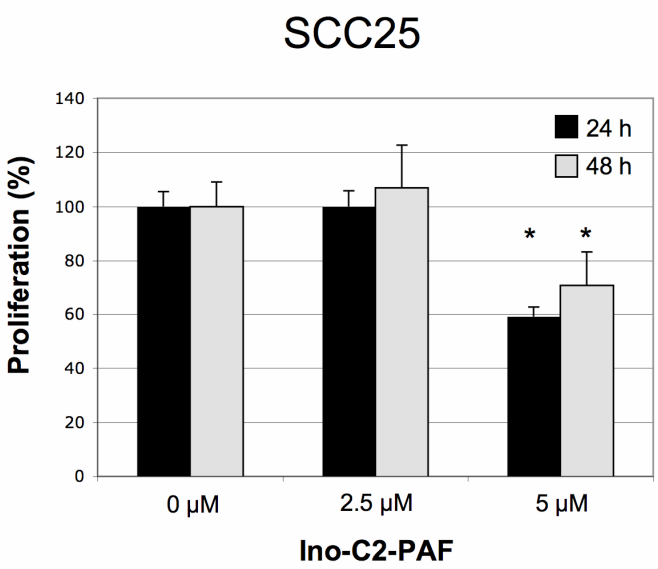

Figure 4.2. Influence of Ino-C2-PAF on SCC25 cells proliferation. 1.5 x 10^4 SCC25 cells/well in keratinocyte serum-free medium were treated for 24 h and 48 h with the indicated concentrations of Ino-C2-PAF, or left untreated. Untreated cell were set at 100%. All experiments were performed in quadruplicate and repeated at least three times. Data that are significantly (P-value < 0.05) different from control cells are indicated by a star (*).

As already mentioned in the introduction, phosphatidylinositol 3-kinase (PI3K) regulates a multitude of cellular processes associated with cell survival, gene expression, cell metabolism, and cytoskeletal rearrangement. Cell growth and proliferation are among the most prominent pathways that are coordinated by PI3K. Moreover, previous studies demonstrated that APLs, such as edelfosine and perifosine, are able to modulate the function of the PI3K. To investigate the influence of Ino-C2-PAF on PI3K activity in keratinocytes, BrdU incorporation in HaCaT cells was monitored in the presence of Ino-C2-PAF and the PI3K inhibitor wortmannin, respectively. Wortmannin, in contrast to 5 µM Ino-C2-PAF, was not able to significantly decrease the keratinocyte proliferation (Figure 4.3). In combination with Ino-C2-PAF it has no further influence on cell growth.

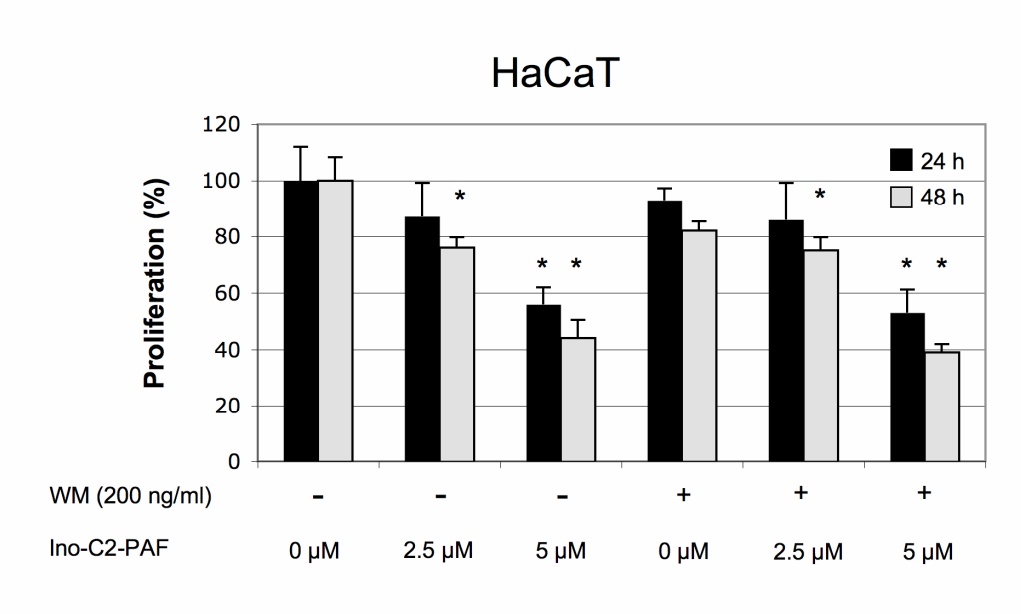

Figure 4.3. Influence of Ino-C2-PAF or wortmannin on HaCaT cells proliferation. 1.5 x 10^4 HaCaT cells/well in keratinocyte serum-free medium were treated for 24 h and 48 h with the indicated concentrations of Ino-C2-PAF or wortmannin (WM), or left untreated. Untreated cell were set at 100%. All experiments were performed in quadruplicate and repeated at least three times. Data that are significantly (P-value < 0.05) different from control cells are indicated by an asterisk (*).

4.2 Ino-C2-PAF reduces migration of SCC25 and HaCaT cells

Migration of epithelial cells is an important step in metastasis. *In vitro* cell motility can be studied by monitoring haptotactic migration towards a collagen IV gradient. To assess whether the motility of SCC25 and HaCaT cells is influenced by non-toxic concentrations of Ino-C2-PAF, cells were treated with 5 µM Ino-C2-PAF or left untreated for 48h and then allowed to migrate toward a collagen IV gradient for 6h at 37℃ (Figure 4.4, panel A). Ino-C2-PAF significantly reduced migration by 50% in both cell lines. To be sure that the reduction of migrated cells was not due to an effect on proliferation a proliferation assay with SCC25 cells was performed in parallel (Figure 4.4, panel B). It turned out that Ino-C2-PAF did not significantly influence proliferation of SCC25 cells after 6h. This had also been shown for HaCaT cells in an earlier study (Fischer *et al*., 2006).

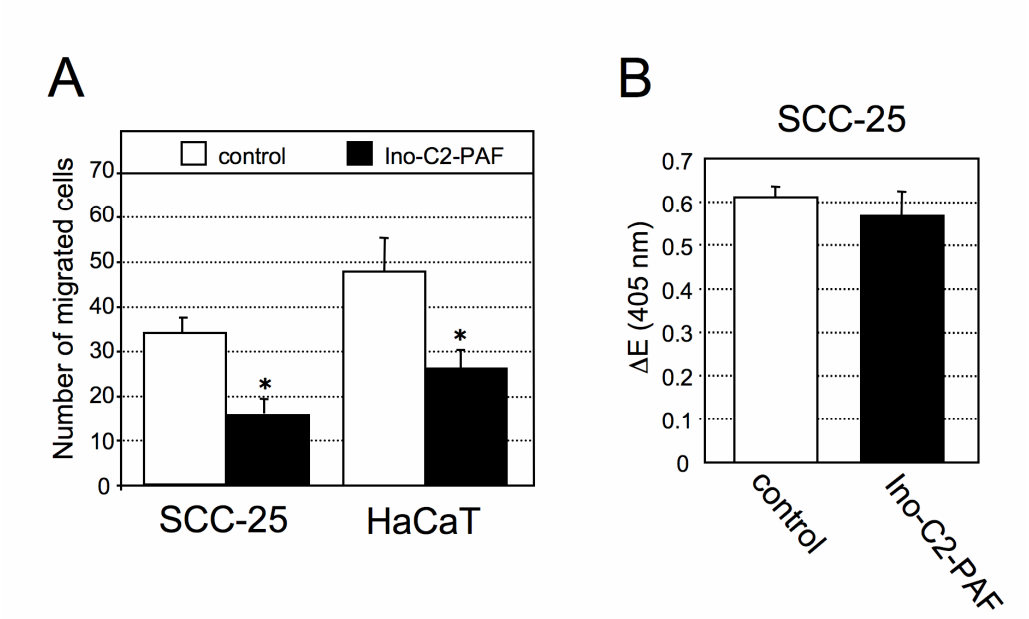

Figure 4.4. Influence of Ino-C2-PAF on the migration of SCC25 and HaCaT cells. (A) SCC25 or HaCaT cells (5.5 x 10^4) were incubated in serum-free medium in the presence or absence of 5 µM Ino-C2-PAF for 48h. Cells were allowed to migrate toward a collagenIV gradient for 6h in haptotactic transwell chamber assays. Three independent experiments have been performed. (*) indicates a significant difference (P-value < 0.05) from the control cells. (B) To determine the influence of Ino-C2-PAF on proliferation of SCC25 cells, 1.5 x 10^4 cells per well were treated as described in (A) and were further incubated for 6h in the presence of bromodeoxyuridine (BrdU). The colorimetric reaction was detected photometrically at 405 nm.

4.3 Impact of APLs on the gene expression profile of HaCaT cells

The previous investigations demonstrated that Ino-C2-PAF inhibits proliferation and migration of HaCaT and SCC25 cells. However, the exact mechanism that regulates these cellular processes is still unknown. Presumably, APLs control cell-growth and cell motility at the transcriptional level. Furthermore, whereas numerous studies describe the influence of each single antitumour lipid on various biological effects as well as their effects on signalling pathways, little is known whether they have an impact on gene expression.

Therefore, to understand the basis of these differential responses and the mechanism of action of Ino-C2-PAF, and APLs in general, genome-wide gene expression analyses were performed by the use of cDNA microarrays (Agilent´s 44K Whole Human Genome Oligo microarray) with the keratinocyte-derived HaCaT cells, which were treated either with Ino-C2-PAF, Glc-PAF or edelfosine or left untreated. Additionally, expression data were compared.

4.3.1 Differential gene expression changes induced by Ino-C2-PAF, Glc-PAF and edelfosine

To determine the influence of APLs on the transcriptome of immortalized keratinocytes, HaCaT cells were incubated with 5 µM of Ino-C2-PAF, Glc-PAF or edelfosine for 24h. By the use of the Agilent GeneSpring GX 10 software we compared the data obtained in the presence of APLs with the data of untreated cells. Genes were defined as differentially expressed when the gene expression values changed at least twofold (each experiment of the control group was compared to each experiment of the APL-treated group, P-value < 0.05), as summarized in Table 4.1.

Probes	Number of Differentially expressed transcripts	Up-regulated transcripts	Down-regulated transcripts
Controls vs. Ino-C2-PAF	592	336	256
Controls vs. Glc-PAF	132	95	37
Controls vs. Edelfosine	250	184	66

Table 4.1. Differentially expressed transcripts. Differentially expressed genes between untreated cells and cells incubated with Ino-C2-PAF, Glc-PAF or edelfosine, respectively. The values represent the number of all differentially expressed transcripts, only up-regulated or only down-regulated transcripts.

Ino-C2-PAF had the strongest influence on the gene expression profile of HaCaT cells in comparison to edelfosine and Glc-PAF. 592 transcripts were differentially expressed with Ino-C2-PAF, whereas edelfosine regulated 250 genes. Glc-PAF had the weakest influence on the transcription, affecting only a set of 132 transcripts (Table 4.1). In addition, differentially expressed genes were mainly up-regulated by APLs, although this effect for edelfosine and Glc-PAF (74% and 72%, respectively) was markedly stronger than for Ino-C2-PAF (60%, Table 4.1). The complete list of the differentially expressed transcripts by Ino-C2-PAF, Glc-PAF and edelfosine is shown in Tables A1-3, respectively (see Appendix A).

We compared the three sets of transcripts regulated by Ino-C2-PAF, Glc-PAF and edelfosine using Venn diagrams. In order to include the total number of differentially expressed transcripts, the list containing Agilent ID annotations (see Table S1) was employed, even though associated gene information was not available for every Agilent ID. In general, it was found that a subset of 48 regulated transcripts was common to all three groups: 71% of these transcripts were up-regulated, whereas 29% of them were down-regulated. The number of differentially expressed genes between and specific to the APLs is depicted in Figure 4.5.

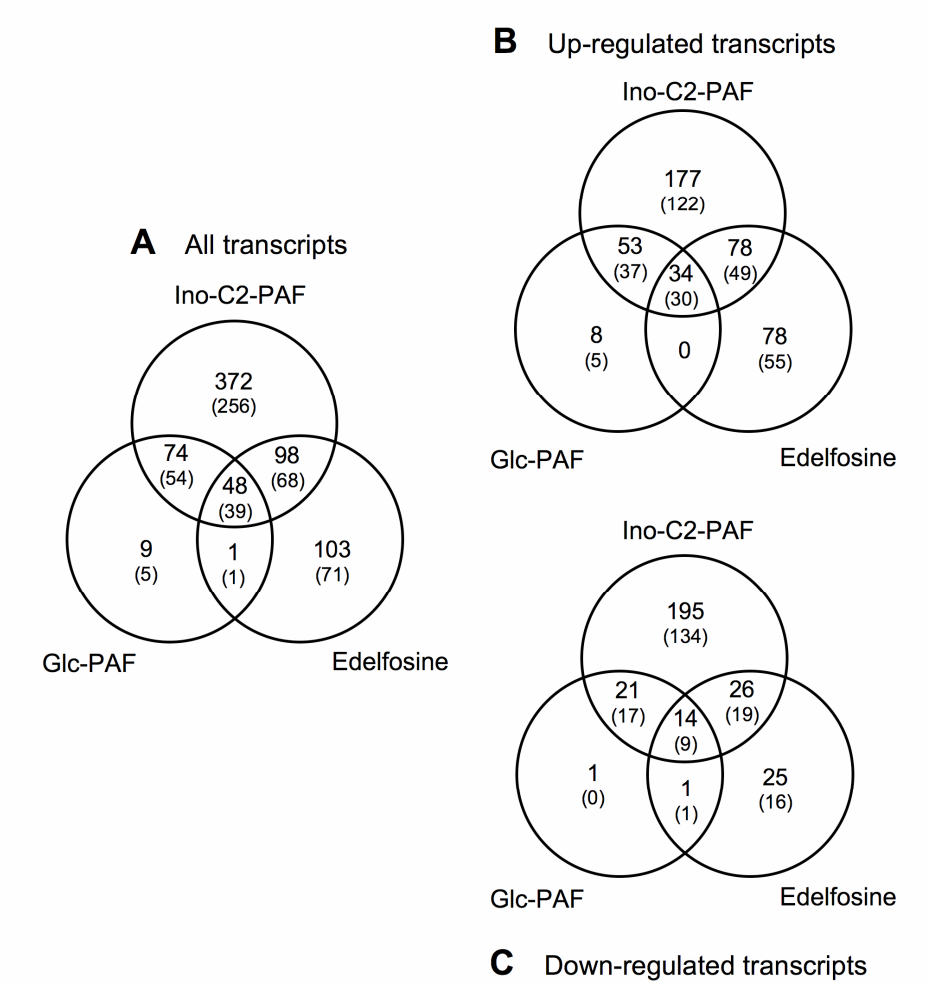

Figure 4.5. Venn diagrams representing differences and similarities among differentially expressed transcripts after treatment with Ino-C2-PAF, Glc-PAF or edelfosine. In (A) all differentially expressed transcripts, in (B) only the up-regulated and in (C) only the down-regulated transcripts are considered. The numbers indicate differentially expressed transcripts with Agilent ID. Numbers in brackets designate differentially expressed transcripts with official gene symbol.

Most of the genes that were up-regulated by all three synthetic phospholipids encode components of the membrane and the cytoplasm (e.g. *KRT34*, *IL21R*, *SPRR1A*), and proteins involved in cell differentiation or developmental processes (e.g. *ETV4*, *ETV5*, *HEY1*). The down-regulated transcripts common to all three APLs mostly encode membrane and extracellular components (e.g. *ALPP*, *DCN*, *FOLR1*) or proteins involved in the regulation of processes like defence response, development and ion homeostasis (e.g. *APOL3*, *IGFBP3*, *TRPV5*).

This analysis revealed that the targets of Glc-PAF were mostly common with those of Ino-C2-PAF; genes encoding components of the extracellular region and plasma membrane as well as genes encoding proteins that regulate response to external stimuli, defence response and ion homeostasis were principally repressed (e.g. *CCL28*, *CCRL1*, *CTSB*, *MMP1*), whereas transcripts that express components of the cytoplasm and regulate lipid

metabolism were increased (e.g. *ACLY*, *FDPS*, *LSS*). Surprisingly, only one gene, which encode a membrane component (*TMPRSS11E*), was commonly regulated by both Glc-PAF and edelfosine. In contrast, the intersection between edelfosine and Ino-C2-PAF encompassed a greater number of transcripts (98), suggesting a mutual mode of action. Edelfosine and Ino-C2-PAF induced expression of genes that encode proteins associated with cell differentiation and cell development, as well as plasma membrane, cytoskeletal and extracellular elements (e.g. *COL13A1*, *DST*, *VEGFA*). However, the expression of several genes encoding components of the plasma membrane and extracellular region, besides genes that regulate cell development and differentiation, were also inhibited by both Ino-C2-PAF and edelfosine (e.g. *CXCR7*, *RAB26*, *TNFAIP2*, *TSPAN8*). Tables B1 and B2 (see Appendix B), respectively, show the list of up- and down-regulated transcripts having an official gene name for each group of the Venn diagrams.

A selection of up-regulated genes uniquely expressed in HaCaT cells treated with Ino-C2-PAF is constituted by *SPRR2D*, *CNN1* and *CD6*, which encode proteins involved in cell differentiation and adhesion. Among the down-regulated transcripts it was possible to distinguish genes encoding several members of the major histocompatibility complex (MHC) class II (*HLA* transcripts, *CIITA*, *CD74*), peptidase inhibitors (*PI3*, *SERPINA3* and *SERPINB1*), components of proteasome (PSMB9 and PSMB10), keratins (*KRT4*, *13*, *15* and *77*), matrix metalloproteinases (*MMP7*, *10* and *12*), defensins (*DEFB1* and *DEFB4*), differentiation markers (*TGM1*), besides other genes encoding proteins involved in immunological processes as *CTSS*, *CXCL2*, *IL32* and *TLR5*.
A selection of transcripts induced exclusively by edelfosine is represented by the cytokine IL1-β (*IL1B*), matrix metalloproteinase *MMP9*, peptidase inhibitors *SERPINE1* and *SERPINE2*, and tropomyosin *TMP4*, whereas edelfosine repressed genes involved in system and multicellular organismal development like *TLR3* and *SEMAD6*.
The best characterized genes uniquely up-regulated by Glc-PAF were *BBC3*, *COL21A1* and *LIPE*.

The above mentioned genes, with the exception of approximately ten transcripts (*CXCL2*, *IL1R1*, *DCN*, *COL21A1*, *KRT34*, *KRT77*, *SERPINE1*, *TMPRSS11E*, *TSPAN8* and *TLR5*), showed relatively high processed signal values. As represented in Table 4.2, the mean value of the signal, which is indicated in arbitrary units, varied between about 50 and 250000.

Probe ID	Gene ID	Definition	Control	Ino	Glc	Edel
A_23_P66787	***ACLY***	ATP citrate lyase	1713	7222	5434	3314
A_23_P210900	***ACSS2***	acyl-CoA synthetase short-chain family member 2	7293	38181	27050	18140
A_24_P156295	***ACSS2***	acyl-CoA synthetase short-chain family member 2	772	4353	2848	2085
A_23_P79587	***ALPP***	alkaline phosphatase, placental (Regan isozyme)"	13764	2982	4905	3131
A_24_P416997	***APOL3***	apolipoprotein L, 3	222	81	121	127
A_23_P29237	***APOL3***	apolipoprotein L, 3	1848	616	881	852
A_23_P382775	***BBC3***	BCL2 binding component 3	4509	9814	9118	8436
A_23_P503072	***CCL28***	chemokine (C-C motif) ligand 28	96	28	46	49
A_23_P6909	***CCRL1***	chemokine (C-C motif) receptor-like 1	88	22	35	37
A_23_P311875	***CD6***	CD6 molecule	3	13	13	16
A_23_P70095	***CD74***	CD74 molecule, MHC, class II, invariant chain"	224	74	124	150
A_23_P59210	***CDKN1A***	cyclin-dependent kinase inhibitor 1A (p21, Cip1)	3241	6477	5338	5447
A_24_P89457	***CDKN1A***	cyclin-dependent kinase inhibitor 1A (p21, Cip1)	173	337	284	314
A_23_P33384	***CIITA***	MHC, class II, transactivator"	85	22	38	46
A_23_P353478	***CIITA***	class II, major histocompatibility complex, transactivator"	403	117	204	204
A_23_P125233	***CNN1***	calponin 1, basic, smooth muscle	4	46	22	28
A_24_P90005	***COL13A1***	collagen, type XIII, alpha 1"	116	249	184	280
A_23_P1331	***COL13A1***	collagen, type XIII, alpha 1"	69	143	104	171
A_23_P31124	***COL21A1***	collagen, type XXI, alpha 1"	4	9	10	5
A_24_P303770	***CTSB***	cathepsin B	4718	2103	2337	3146
A_24_P397928	***CTSB***	cathepsin B	1605	579	716	977
A_24_P242646	***CTSS***	cathepsin S	16	4	7	10
A_23_P46141	***CTSS***	cathepsin S	500	212	292	321
A_24_P257416	***CXCL2***	chemokine (C-X-C motif) ligand 2	76	29	39	55
A_23_P315364	***CXCL2***	chemokine (C-X-C motif) ligand 2	81	27	34	56
A_23_P131676	***CXCR7***	chemokine (C-X-C motif) receptor 7	15240	7525	9462	6022
A_23_P64873	***DCN***	decorin	81	14	19	13
A_23_P71480	***DEFB1***	defensin, beta 1	434	133	185	213
A_23_P157628	***DEFB4***	defensin, beta 4	107	39	60	82
A_23_P59388	***DST***	dystonin	667	2430	1918	1410
A_23_P431776	***ETV4***	ets variant 4	124	751	469	688
A_24_P416346	***ETV4***	ets variant 4	89	501	309	466
A_23_P9836	***ETV5***	ets variant 5	4	76	42	55
A_32_P30649	***ETV5***	ets variant 5	8	116	65	83
A_23_P44132	***FASN***	fatty acid synthase	1041	2459	1751	2333
A_24_P114183	***FDPS***	farnesyl diphosphate synthase	53021	144064	120443	92382
A_23_P53176	***FOLR1***	folate receptor 1	666	236	309	217
A_32_P83845	***HEY1***	hairy/enhancer-of-split related with YRPW motif 1	40	152	117	162
A_23_P42306	***HLA-DMA***	MHC, class II, DM alpha"	826	370	524	505
A_24_P50245	***HLA-DMA***	MHC, class II, DM alpha"	767	339	471	456
A_32_P351968	***HLA-DMB***	MHC, class II, DM beta"	516	103	217	311
A_24_P354800	***HLA-DOA***	MHC, class II, DO alpha"	584	273	362	380
A_23_P30913	***HLA-DPA1***	MHC, class II, DP alpha 1"	399	136	233	271
A_23_P258769	***HLA-DPB1***	MHC, class II, DP beta 1"	186	50	100	138
A_24_P166443	***HLA-DPB1***	MHC, class II, DP beta 1"	396	169	252	300
A_24_P196827	***HLA-DQA1***	MHC, class II, DQ alpha 1"	24	8	13	19
A_24_P326084	***HLA-DQA1***	MHC, class II, DQ alpha 1"	148	39	82	100
A_32_P87697	***HLA-DRA***	MHC, class II, DR alpha"	809	241	421	510
A_24_P343233	***HLA-DRB1***	MHC, class II, DR beta 1"	2811	1000	1534	1866
A_23_P145336	***HLA-DRB3***	MHC, class II, DR beta 3"	462	146	251	299
A_24_P402222	***HLA-DRB3***	MHC, class II, DR beta 3"	841	305	477	624
A_24_P370472	***HLA-DRB4***	MHC, class II, DR beta 4"	611	218	343	414
A_23_P31006	***HLA-DRB5***	MHC, class II, DR beta 5"	2251	699	1220	1531
A_23_P45099	***HLA-DRB5***	MHC, class II, DR beta 5"	1295	400	660	809
A_23_P215634	***IGFBP3***	insulin-like growth factor binding protein 3	7795	1360	2307	3212
A_24_P320699	***IGFBP3***	insulin-like growth factor binding protein 3	720	148	227	341
A_23_P79518	***IL1B***	interleukin 1, beta"	876	1712	1341	3248
A_24_P227927	***IL21R***	interleukin 21 receptor	183	2257	1710	902
A_23_P15146	***IL32***	interleukin 32	310	144	185	263
A_32_P87013	***IL8***	interleukin 8	29	9	12	27
A_24_P228149	***KRT13***	keratin 13	20139	5920	9565	9361

Probe ID	Gene ID	Definition	Control	Ino	Glc	Edel
A_23_P27133	***KRT15***	keratin 15	263272	124896	179153	149286
A_23_P101054	***KRT34***	keratin 34	3	22	10	25
A_23_P2674	***KRT4***	keratin 4	4300	476	863	1021
A_24_P666035	***KRT77***	keratin 77	54	13	20	33
A_23_P38876	***LIPE***	lipase, hormone-sensitive"	1240	2874	2648	2130
A_24_P162211	***LSS***	lanosterol synthase	197	617	549	259
A_24_P384839	***LSS***	lanosterol synthase	11522	23109	20082	13584
A_23_P211252	***LSS***	lanosterol synthase	285	897	770	389
A_24_P110799	***LSS***	lanosterol synthase	5802	11856	10348	6670
A_23_P1691	***MMP1***	matrix metallopeptidase 1 (interstitial collagenase)	1567	521	700	1324
A_23_P13094	***MMP10***	matrix metallopeptidase 10 (stromelysin 2)	947	411	460	569
A_23_P340698	***MMP12***	matrix metallopeptidase 12 (macrophage elastase)	274	52	86	118
A_23_P52761	***MMP7***	matrix metallopeptidase 7 (matrilysin, uterine)"	3052	978	1291	1911
A_23_P40174	***MMP9***	matrix metallopeptidase 9 (gelatinase B)	188	193	165	675
A_23_P160920	***PDZK1IP1***	PDZK1 interacting protein 1	1415	299	558	888
A_23_P394304	***PDZK1IP1***	PDZK1 interacting protein 1	665	145	261	428
A_23_P210465	***PI3***	peptidase inhibitor 3, skin-derived"	1091	261	325	925
A_23_P140807	***PSMB10***	proteasome (prosome, macropain) subunit, beta type, 10"	27000	12109	15680	15517
A_23_P111000	***PSMB9***	proteasome (prosome, macropain) subunit, beta type, 9	16315	7273	9437	9821
A_23_P54709	***RAB26***	RAB26, member RAS oncogene family"	1029	468	669	371
A_23_P103310	***S100A7***	S100 calcium binding protein A7	831	178	320	551
A_23_P434809	***S100A8***	S100 calcium binding protein A8	1813	527	1097	1545
A_23_P23048	***S100A9***	S100 calcium binding protein A9	354	99	178	297
A_23_P63618	***SCD***	stearoyl-CoA desaturase (delta-9-desaturase)	3354	11857	8642	6791
A_24_P626920	***SCD***	stearoyl-CoA desaturase (delta-9-desaturase)	410	936	794	614
A_23_P162918	***SERPINA3***	serpin peptidase inhibitor, clade A member 3"	636	239	289	547
A_23_P2920	***SERPINA3***	serpin peptidase inhibitor, clade A member 3"	2103	807	983	1790
A_23_P214330	***SERPINB1***	serpin peptidase inhibitor, clade B (ovalbumin), member 1	11890	5410	5997	9900
A_24_P158089	***SERPINE1***	serpin peptidase inhibitor, clade E (nexin, plasminogen activator inhibitor type 1), member 1"	16	29	19	61
A_23_P50919	***SERPINE2***	serpin peptidase inhibitor, clade E (nexin, plasminogen activator inhibitor type 1), member 2"	16	55	58	75
A_23_P348208	***SPRR1A***	small proline-rich protein 1A	2231	3368	2560	3655
A_23_P74012	***SPRR1A***	small proline-rich protein 1A	1709	7114	3821	7400
A_23_P11644	***SPRR2D***	small proline-rich protein 2D	84	207	66	191
A_23_P65618	***TGM1***	transglutaminase 1	4950	2234	2726	3985
A_23_P29922	***TLR3***	toll-like receptor 3	335	147	192	166
A_23_P85903	***TLR5***	toll-like receptor 5	48	19	30	35
A_23_P18751	***TMPRSS11E***	transmembrane protease, serine 11E"	48	11	17	19
A_23_P421423	***TNFAIP2***	tumor necrosis factor, alpha-induced protein 2	76186	16723	28433	31759
A_23_P93973	***TRPV5***	transient receptor potential cation channel, subfamily V, member 5"	227	84	100	105
A_23_P36531	***TSPAN8***	tetraspanin 8	58	15	21	12
A_23_P70398	***VEGFA***	vascular endothelial growth factor A	240	550	484	571
A_24_P12401	***VEGFA***	vascular endothelial growth factor A	223	500	412	466
A_24_P179400	***VEGFA***	vascular endothelial growth factor A	69	163	141	174

Table 4.2. Processed signals of a subjective selection of differentially expressed transcripts. Processed signals are represented as mean value of three independent analyses for untreated (control) or by Ino-C2-PAF (Ino), Glc-PAF (Glc) and edelfosine (Edel) treated cells, respectively.

4.3.2 Ino-C2-PAF, Glc-PAF and edelfosine show markedly different gene expression profiles compared with unstimulated HaCaT cells

Principal component analysis was used to examine the relationship between different data sets. In order to reduce the dimensionality, this method transforms a number of possibly correlated variables into a smaller number of uncorrelated variables called principal components. Samples can be plotted, making it possible to visually assess similarities and differences. Data sets based on all probes and conditions revealed a clear separation of the APL samples from the control (untreated cells) samples. Moreover, it was possible to observe a subtle but significant difference between samples of cells treated with Ino-C2-PAF, Glc-PAF or edelfosine (Figure 4.6, panel A). These results indicated that all APLs induced a nearly common pattern of gene expression changes, which differed from the control pattern.
Two transcripts (selected from the pool of 9083 expressed genes), *TNFAIP2* and *ACSS2*, represented two examples of markedly down- and up-regulated transcripts, respectively, which are differentially expressed between untreated cells and cells treated with the phospholipid analogues (Figure 4.6, panels B and C).

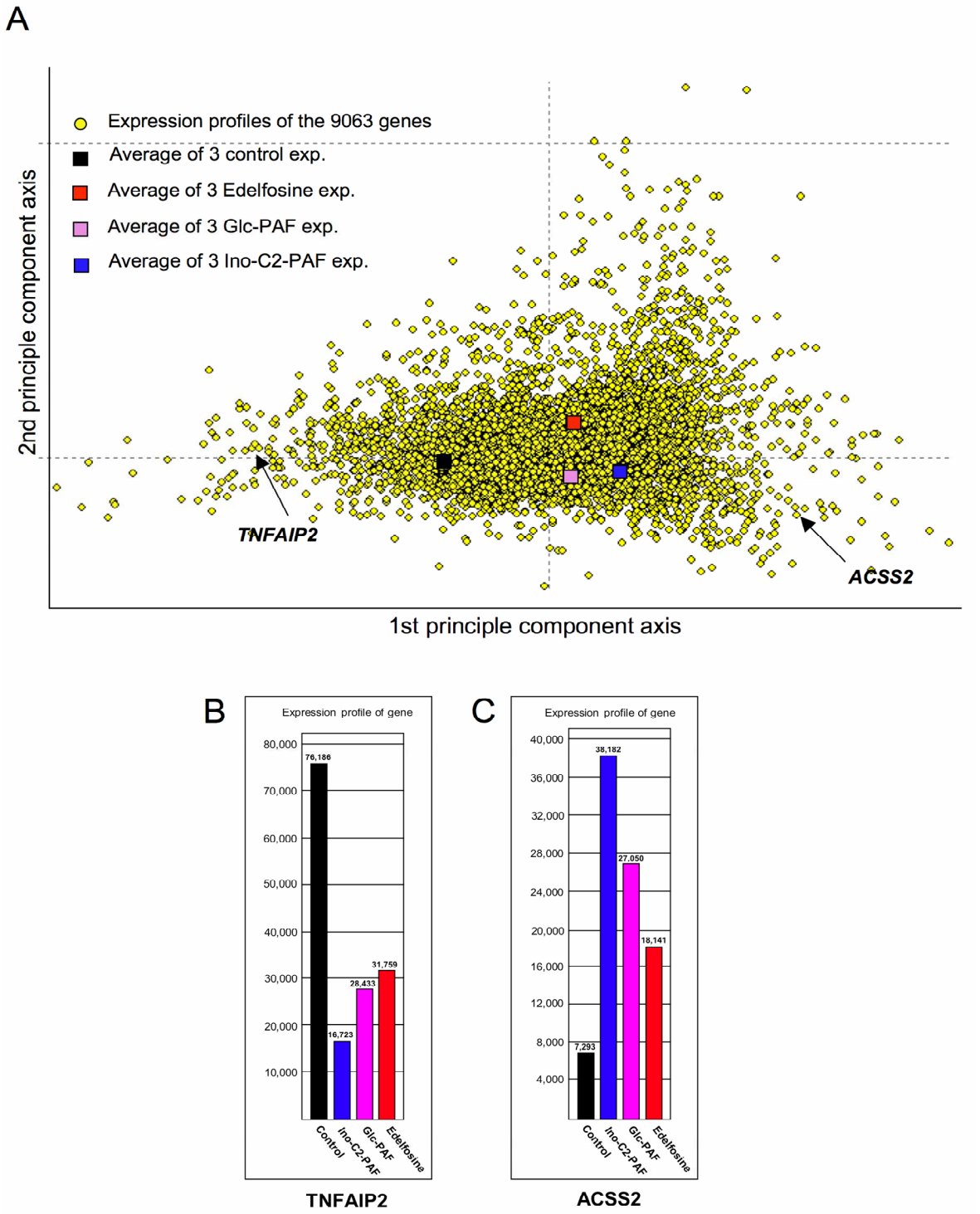

Figure 4.6. Expression profile of genes. (A) Presentation of 9083 expressed genes (yellow circles) and the position of the analyzed experiments with the help of correspondence analysis (see Materials and Methods). The control cells (black: average of three control experiments) are located on the left side, whereas the experiments with phospholipid analogues are clearly distributed on the right side of the diagram (pink: average of three Glc-PAF experiments, blue: average of three Ino-C2-PAF experiments, red: average of three edelfosine experiments). (B) and (C) are two selected examples of differentially expressed genes between untreated cells and cells treated with the phospholipid analogues: TNFAIP2 (down-regulated) and ACSS2 (up-regulated).

4.3.3 Gene Ontology classification for Ino-C2-PAF, Glc-PAF and edelfosine

To characterize the differentially expressed genes from untreated and APLs-treated HaCaT cells, the transcripts of each tested phospholipid analogue were subjected to functional clustering according to Gene Ontology (GO) classification for biological processes, molecular function and cellular components. For this purpose we used the web-accessible program DAVID (Database for Annotation, Visualization and Integrated Discovery), considering only categories with a P-value less than 0.05.
In general, due to the functional information actually available, the GO classification was only possible for about 60% of the genes. For the biological functions, which represent probably the most interesting group, we performed a classification with the total number of available differential expressed genes and we obtained 132 categories for Ino-C2-PAF, 106 for edelfosine and 24 for Glc-PAF (data not shown).
In our study we investigated up- and down-regulated genes separately (Table 4.1, or see complete list in Table A1-3, Appendix A).

Top-ranked GO categories regarding biological processes significantly enriched for up-regulated transcripts in Ino-C2-PAF versus untreated cells included mainly categories associated with lipid biosynthesis and metabolism (Figure 4.7), whereas processes significantly enriched for down-regulated transcripts were predominantly related with the immune response (Figure 4.8).
Similarly to Ino-C2-PAF, most of the genes, which were up-regulated by Glc-PAF, are basically involved in lipid biosynthetic and metabolic pathways (Figure 4.7). However, down-regulated genes were associated with processes regulating taxis, cellular calcium and metal ion homeostasis (Figure 4.8). The analysis of differentially expressed genes by edelfosine revealed that this phospholipid analogue positively regulated pathways that are involved in cell differentiation, development and motility (Figure 4.7). Controversially, genes that regulate similar processes, such as system and multicellular organismal development, were inhibited by edelfosine as well (Figure 4.8).

DAVID permits also to identify GO terms for molecular functions. The most significant category was observed for MHC class II receptor activity, which was down-regulated by Ino-C2-PAF with a P-value of 7.17E-11 (data not shown).

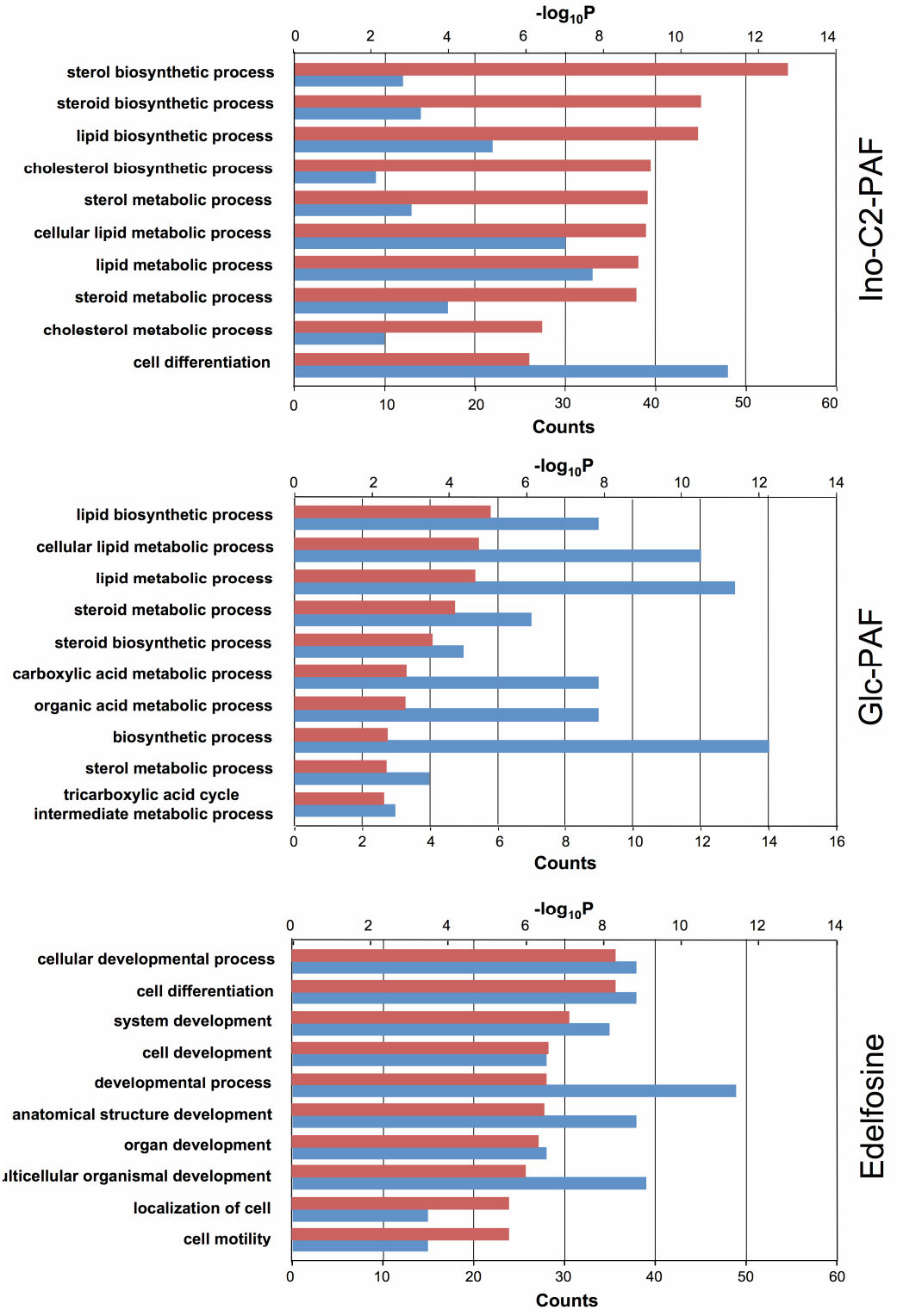

Figure 4.7. Comparison of Gene Ontology categories. Significant enrichments ($P < 0.05$) of Gene Ontology categories of differentially expressed genes concerning Biological Processes for **UP**-regulated transcripts in HaCaT cells treated with Ino-C2-PAF, Glc-PAF or Edelfosine, respectively. Red bars represent P-values (expressed as the negative logarithm [base 10]) for the 10 top-ranked GO categories over-represented in the differentially expressed transcripts. Blue bars represent the number of differentially expressed genes (counts) involved in each category.

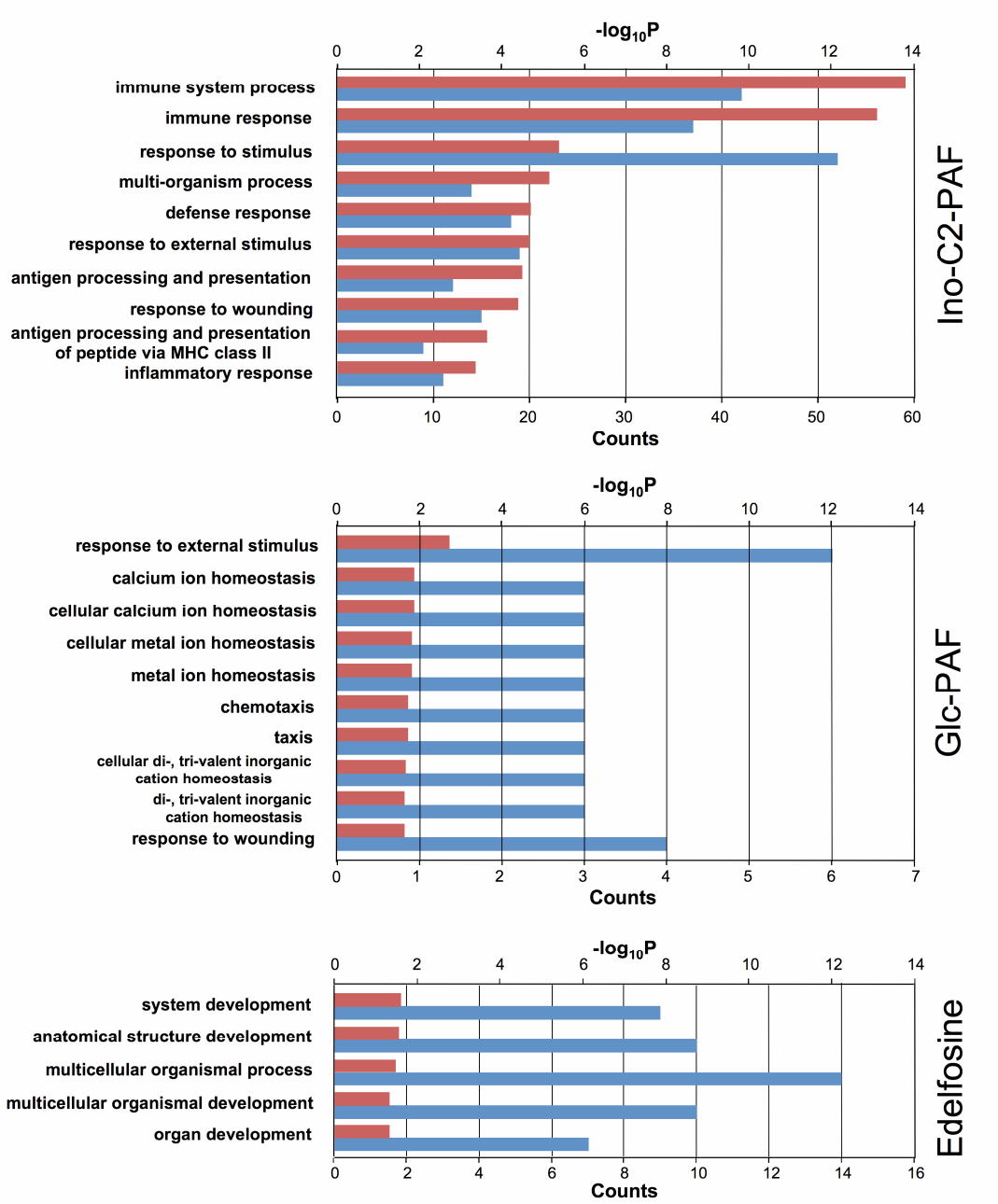

Figure 4.8. Comparison of Gene Ontology categories. Significant enrichments ($P < 0.05$) of Gene Ontology categories of differentially expressed genes concerning Biological Processes for **DOWN**-regulated transcripts in HaCaT cells treated with Ino-C2-PAF, Glc-PAF or Edelfosine, respectively. Red bars represent P-values (expressed as the negative logarithm [base 10]) for the 10 top-ranked GO categories over-represented in the differentially expressed transcripts. Blue bars represent the number of differentially expressed genes (Counts) involved in each category. Edelfosine, in comparison to the other APLs, presents only 5 significant down-regulated GO categories.

These microarray analyses revealed that Ino-C2-PAF, and APLs in general, does not or only marginally control cell proliferation and migration at the transcriptional level. However, a large number of genes implicated in other cellular processes are differentially expressed in HaCaT cells treated with APLs.

4.4 Ino-C2-PAF influences the activity of Akt/PKB and MAPKs

Beside transcriptional regulation, cell growth and proliferation are processes that can be also controlled at the post-translational level by different signalling pathways, which then eventually might modulate the gene expression. The phosphatidylinositol 3-kinase (PI3K)-regulated Akt/PKB pathway, as well as mitogen-activated protein kinase (MAPK) pathways, which are activated by several mitogens and growth factors, are among the most important signalling cascades for the regulation of proliferation.

In order to ascertain whether Ino-C2-PAF inhibited keratinocyte proliferation by decreasing the activity of components of the PI3K and MAPK signalling pathways, the phosphorylation level of several protein kinases was examined.

For this purpose, HaCaT cells were cultivated in the presence or absence of 5 µM Ino-C2-PAF for different periods of time and subsequently, the phosphorylation level of Akt/PKB, ERK1/2, p38 and JNK/SAPK was analysed by Western blotting with phosphorylation site-specific antibodies.

In order to elucidate the effect of Ino-C2-PAF on the PI3K signalling cascade, HaCaT cells were treated with the PI3K inhibitor wortmannin and the insulin growth factor-1 (IGF-1), which is one of the most potent natural activators of the PI3K pathway after binding to its specific receptor IGF-1R. Subsequently, Akt/PKB phosphorylation was measured.

Surprisingly, Ino-C2-PAF led to an increase in Akt/PKB phosphorylation compared to control cells, but this rise was much lower than elicited by IGF-1 (Figure 4.9). However, pre-treatment with Ino-C2-PAF and subsequent stimulation with IGF-1 exhibited similar Akt/PKB phosphorylation levels to cells uniquely incubated with Ino-C2-PAF. Moreover, inhibition of PI3K by wortmannin remained unaltered, since further addition of IGF-1 or Ino-C2-PAF led not to an increase in Akt/PKB phosphorylation. These results suggest that Ino-C2-PAF-dependent Akt/PKB activation is due to the upstream activation of PI3K, but without the participation of receptors.

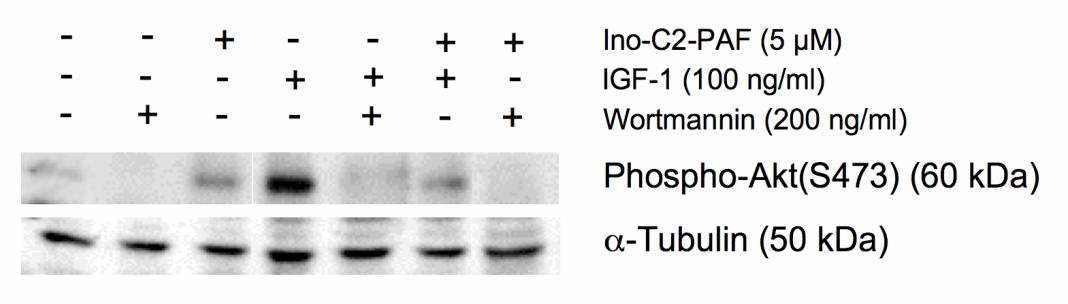

Figure 4.9. Detection of Akt/PKB phosphorylation after stimulation with Ino-C2-PAF, IGF-1 and wortmannin in HaCaT cells. HaCaT cells were incubated with defined keratinocyte serum-free medium overnight and treated with Ino-C2-PAF (5 µM) for 30 min, IGF-1 (100 ng/ml) for 10 min or wortmannin (200 ng/ml) for 20 min at the indicated concentrations, respectively. With two substances together, cells were pre-treated with wortmannin (20 min) and then stimulated with Ino-C2-PAF (20 min) or IGF-1 (10 min). Otherwise, cells were pre-treated with Ino-C2-PAF for 20 min and then stimulated with IGF-1 for 10 min. Whole-cell lysates (40 µg) were separated on a 7.5% SDS-PAGE and subjected to Western blotting using anti-phospho-Akt/PKB antibody. α-tubulin was used as a loading control.

The analysis of ERK1/2 phosphorylation revealed that physiologically, untreated cells displayed a biphasic ERK1/2 activation with a first peak after 10 min and the second peak after about 60 min (Figure 4.10, left part). Nonetheless, this course of phosphorylation is markedly affected by Ino-C2-PAF, which strongly enhanced phosphorylation of ERK1/2 already after 10 min of exposure. Subsequently, ERK1/2 phosphorylation decreased by 60 min after exposure to return at higher levels after 360 min (Figure 4.10).

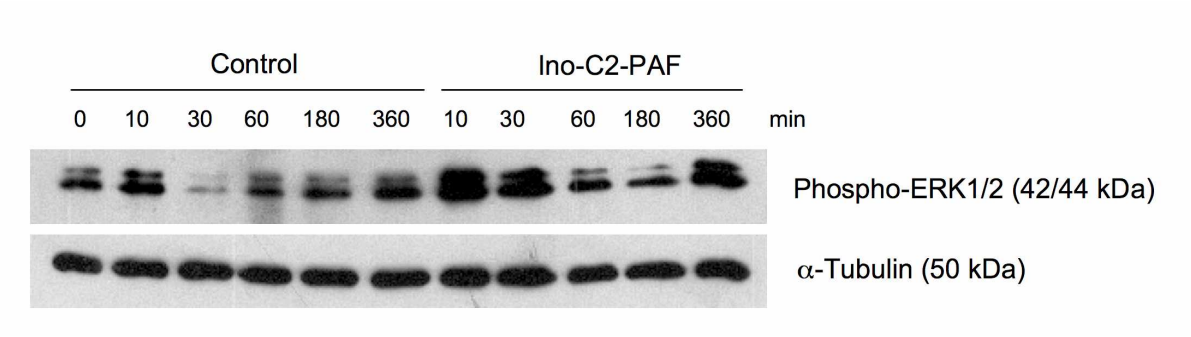

Figure 4.10. Time-dependent effect of Ino-C2-PAF on ERK1/2 activity in HaCaT cells. HaCaT cells were incubated with defined keratinocyte serum-free medium overnight, treated with or without 5 µM Ino-C2-PAF for the indicated periods. Whole-cell lysates (40 µg) were separated on a 10% SDS-PAGE and subjected to Western blotting using an anti-phospho-ERK1/2 antibody. α-tubulin was used as a loading control.

Furthermore, HaCaT cells were treated with the epidermal growth factor (EGF) in order to study the influence of Ino-C2-PAF on ERK1/2 activation in more detail (Figure 4.11). As shown in Figure 4.10, Ino-C2-PAF increased ERK1/2 phosphorylation after 30 min of exposure. This induction was even stronger evoked by EGF stimulation for 5 min, and this

high activation level did not change if cells were treated with both EGF and Ino-C2-PAF simultaneously.

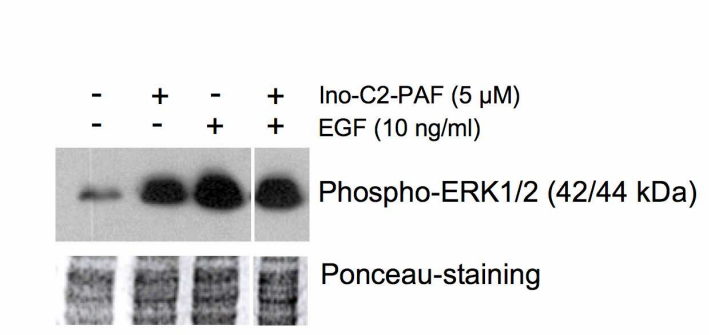

Figure 4.11. Detection of ERK1/2 phosphorylation after co-stimulation of Ino-C2-PAF with EGF in HaCaT cells. HaCaT cells were incubated with defined keratinocyte serum-free medium overnight, and treated with Ino-C2-PAF for 30 min or EGF for 5 min at the indicated concetrations. With two substances together, cells were pretreated with Ino-C2-PAF for 20 min and then stimulated with EGF for 5 min. Whole-cell lysates (40 µg) were separated on a 10% SDS-PAGE and subjected to Western blotting using anti-phospho-ERK1/2 antibody. Ponceau S staining was used as a loading control.

Since proliferation assays revealed that Ino-C2-PAF inhibited the proliferation of highly invasive keratinocytes SCC25 (Figure 4.2), also SCC25 cells were incubated in the presence of 5 µM Ino-C2-PAF up to 48 h and activated ERK1/2 was analyzed. Whereas the time course of phosphorylation of ERK1/2 in untreated SCC25 cells was characterized by a biphasic activation with a first peak in the first hour and a second peak after 24 h, Ino-C2-PAF increased phosphorylation of ERK1/2 mainly in the first phase. (Figure 4.12).

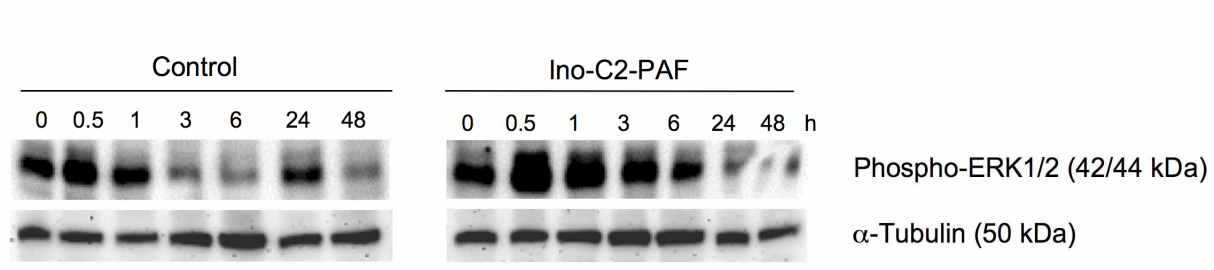

Figure 4.12. Time-dependent effect of Ino-C2-PAF on ERK1/2 activity in SCC25 cells. SCC25 cells were kept in serum-free medium overnight, treated with or without 5 µM Ino-C2-PAF for the indicated periods. Whole-cell lysates (40 µg) were separated on a 10% SDS-PAGE and subjected to Western blotting using an anti-phospho-ERK1/2 antibody. α-tubulin was used as a loading control.

The strong initial phosphorylation increase of ERK1/2 was also detected for the other two MAPKs, p38 and JNK/SAPK (Figure 4.13). Indeed, in the presence of Ino-C2-PAF, phosphorylation of all three MAP kinases was maximal after 1 h of exposure and decreased with longer incubation times. However, HaCaT cells treated with Ino-C2-PAF for 48 h showed a second perceptible rise in JNK/SAPK phosphorylation but a pronounced inactivation of ERK1/2. p38 phosphorylation instead remained unaffected.

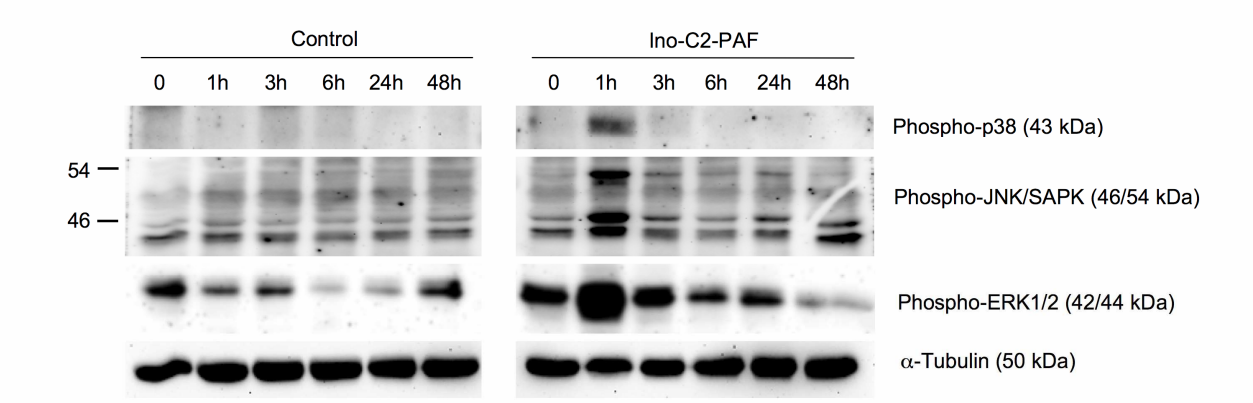

Figure 4.13. Time-dependent effect of Ino-C2-PAF on MAP Kinases activity in HaCaT cells. HaCaT cells were incubated with defined keratinocyte serum-free medium overnight, treated with or without 5 µM Ino-C2-PAF for the indicated periods. Whole-cell lysates (40 µg) were separated on a 10% SDS-PAGE and subjected to Western blotting using anti-phospho-ERK1/2, anti-phospho-p38 and anti-phospho-JNK/SAPK antibodies. α-tubulin was used as a loading control.

4.5 Ino-C2-PAF induces the redistribution of the F-actin cytoskeleton

Cell migration is a complex process that results from the coordinated changes in the F-actin cytoskeleton and the controlled formation and dispersal of cell-substrate adhesion sites. During cell migration, the F-actin cytoskeleton provides the driving force at the cell front, where F-actin is organized in parallel bundles that form filopodia and in a dense meshwork that generates ruffling lamellipodia and promotes forward movement

The F-actin cytoskeleton of subconfluent monolayer of HaCaT and SCC25 cells in absence or presence of 5 µM Ino-C2-PAF was analyzed after 3 and 24 h using CPITC-conjugated phalloidin. In order to visualize very thin F-actin-containing cell protrusions, black and white images were imported into Adobe Photoshop and inverted. Once inverted, F-actin appeared in black.

In untreated HaCaT cells, the F-actin was organized into filopodia and ruffling lamellipodia. Stress fibres were oriented to the front of the cell (Figure 4.14, panel A; arrowheads). In Ino-C2-PAF-treated HaCaT cells F-actin was predominantly localized in filopodia, which were increased in number and mostly directed to adjacent cells (Figure 4.14, panel A; thick arrows). An 24 h incubation with Ino-C2-PAF disrupted the existing disorganized stress fibres and augmented cell ruffles and the number of cell-cell contacts (Figure 4.14, panel A; thin arrows).

Furthermore, untreated subconfluent HaCaT cells displayed an intact actin dynamics at the front and at the rear of the cell, characterized by lamellipodia (Figure 4.14, panel B; arrowheads) and F-actin bundles (Figure 4.14, panel B; thick arrows) at the leading edge. In

contrast, HaCaT cells treated with Ino-C2-PAF were mostly unpolarized, exhibiting a round shape, and possessed disorganized stress fibres (Figure 4.14, panel B).
At the wound edge, which was induced by mechanical scratch wounding, untreated cells migrated into the wound bed and displayed a polarized F-actin cytoskeleton, while Ino-C2-PAF-treated cells demonstrated a reduced migration accompanied by an increased concentration of cortical F-actin at the cell periphery (Figure 4.14, panel B; thin arrows).

Generally, untreated HaCaT cells that migrated into the wound bed or towards a chemoattractant displayed a polarized cytoskeleton with F-actin bundles oriented perpendicularly to the leading edge. Nonetheless, HaCaT cells kept under subconfluent conditions and stimulated with Ino-C2-PAF demonstrated three distinct actin phenotypes that diverged from those of untreated cells (for control cells see Figure 4.14, panel A). First, Ino-C2-PAF treated cells exhibited a strong cortical F-actin at the cell periphery (Figure 4.14, panel C´; arrowheads). Second, an inexistent or totally disrupted cytoskeleton (Figure 4.14, panel C´´; arrow) was visible in some cells near other cells presenting non-polarized stress fibres (Figure 4.14, panel C´´; arrowheads). Third, Ino-C2-PAF lead to the formation of a cytoskeletal structure characterized by F-actin stress fibres connected to peripheral focal contacts and that cross each other at the cell centre. Moreover, these F-actin stress fibres are associated with large and stable focal adhesions at the cell periphery (Figure 4.14, panel C´´´; arrowheads).

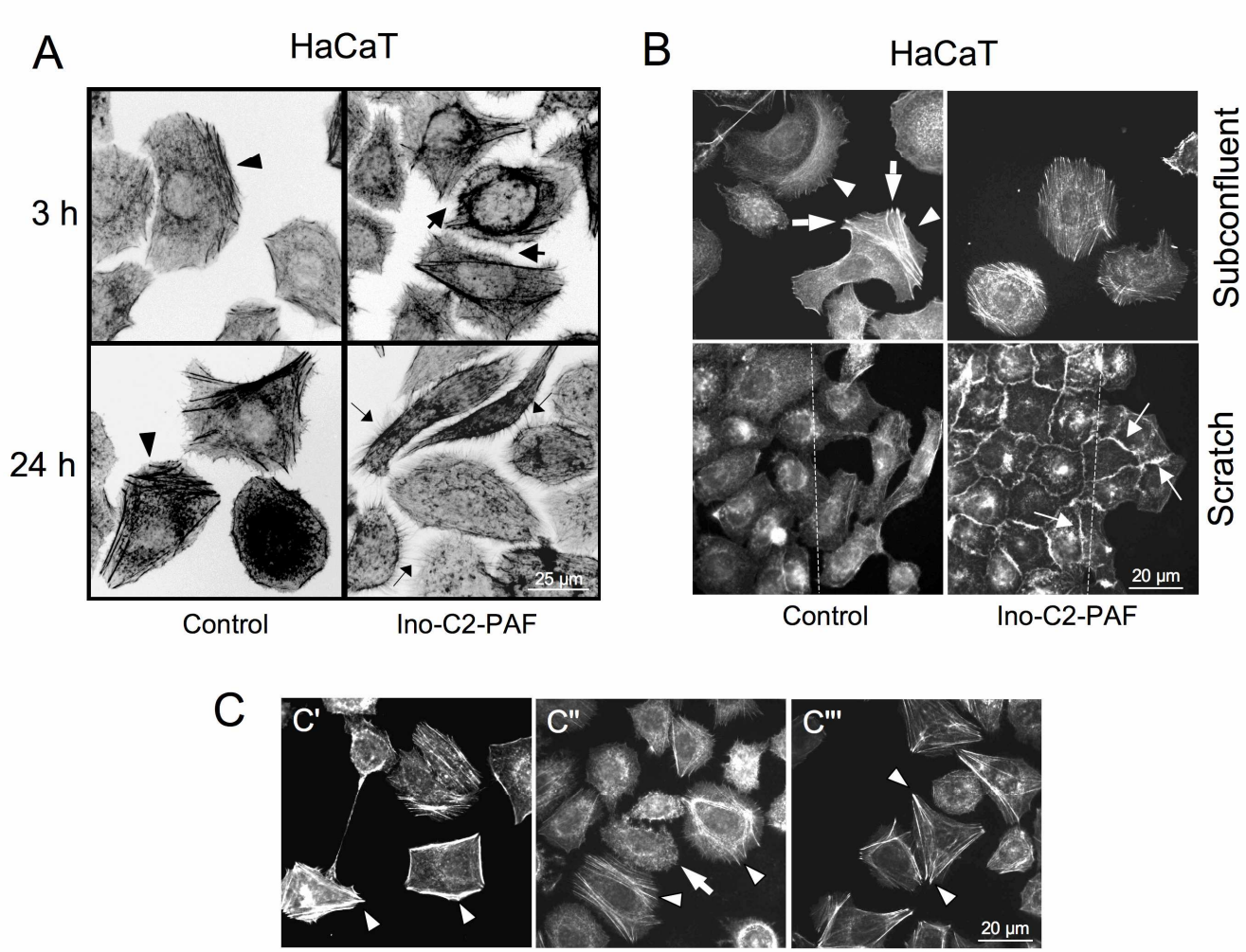

Figure 4.14. Ino-C2-PAF-dependent redistribution of the F-actin cytoskeleton. To analyze the F-actin cytoskeletons of motile cells, subconfluent or scratched HaCaT cells on collagen IV were treated with or without 5 µM Ino-C2-PAF and were allowed to migrate for (A) the indicated times or for (B,C) 3 h. Cells were then fixed with para-formaldehyde, blocked with BSA and incubated with CPITC-conjugated phalloidin. Images were taken on a Zeiss Axiovert 200 microscope. (A) To visualize very thin F-actin containing protrusions, black and white images were imported into Adobe Photoshop and inverted. F-actin appears in black. Arrowheads indicate F-actin at the lamellipodium, thick and thin arrows point to F-actin in filopodia between adjacent cells. (B) Arrowheads indicate F-actin at the lamellipodium, thick arrows point to F-actin bundles at the leading edge and thin arrows point to cortical F-actin. Dotted lines indicate the wound edge at the origin. (C) Three different actin phenotypes in the presence of 5 µM Ino-C2-PAF. Arrowheads in C´ indicate cortical F-actin at the cell periphery. Arrowheads in C´´ show non-polarized stress fibres, arrow points to disrupted cytoskeleton. Arrowheads in C´´´ indicate F-actin stress fibres connected to peripheral focal contacts. The figures are representative for at least three independent experiments.

SCC25 cells showed a phenotype similar to that of HaCaT cells: in untreated cells filopodia, lamellipodia and stress fibres were oriented to the front of the cell (Figure 4.15, panel A; arrowheads), whereas F-actin was localized in filopodia (Figure 4.15, panel A; thick arrow) accompanied by an increasing number of cell ruffles after 24 h incubation with Ino-C2-PAF (Figure 4.15, panel A; thin arrows).

Moreover, Ino-C2-PAF induced a concentration of cortical F-actin at the wound edge (Figure 4.15, panel B; thin arrows). However, cortical F-actin at the cell periphery was observed

under subconfluent conditions as well. Furthermore, in contrast to HaCaT cells, SCC25 cells generally showed stronger cell-cell adhesion, characterized by scratches that presented clumps of not completely detached cells at the wound edge, and by few single cells. Otherwise, untreated SCC25 cells demonstrated well-organized actin cytoskeleton with the typical stress fibres and lamellipodia (Figure 4.15, panel B; arrowheads).

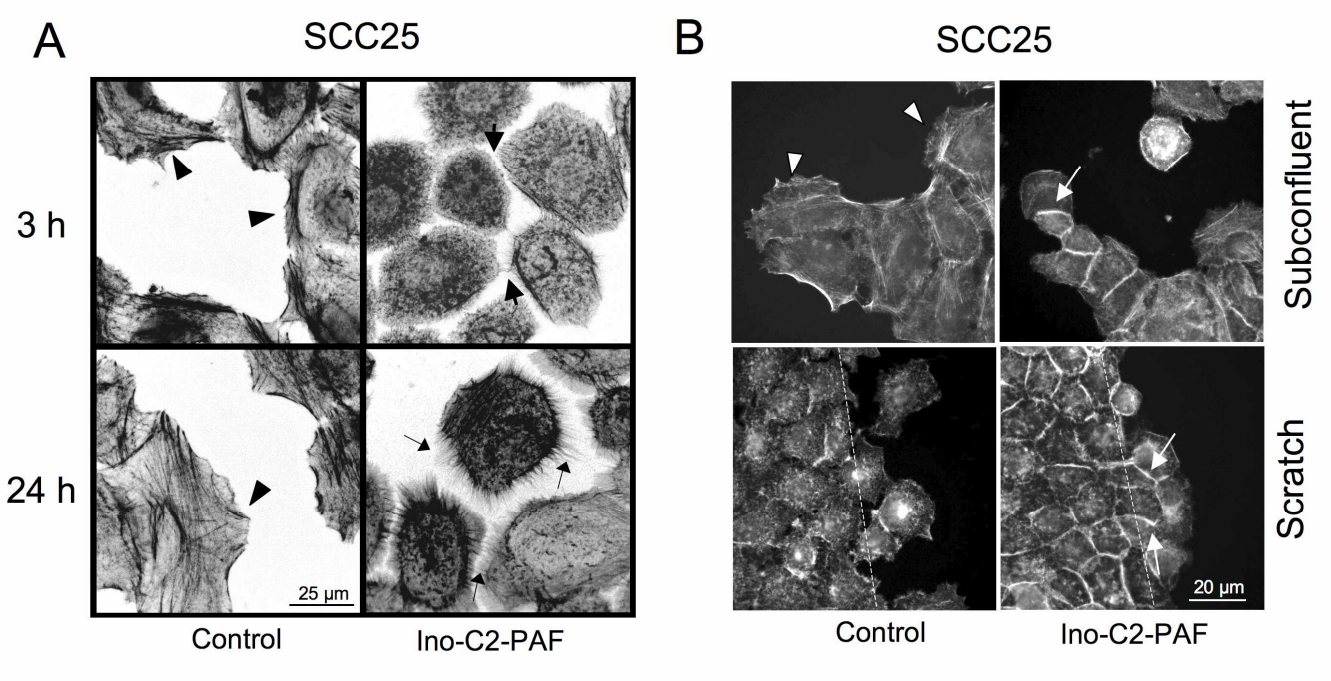

Figure 4.15. Impact of Ino-C2-PAF on the polarized migration of SCC25 cells. To analyze the F-actin cytoskeletons of motile cells, subconfluent or scratched SCC25 cells on collagen IV were treated with or without 5 µM Ino-C2-PAF and were allowed to migrate for (A) the indicated times or for (B) 3 h. Cells were then fixed with para-formaldehyde, blocked with BSA and incubated with CPITC-conjugated phalloidin. Images were taken on a Zeiss Axiovert 200 microscope. (A) To visualize very thin F-actin containing protrusions, black and white images were imported into Adobe Photoshop and inverted. F-actin appears in black. Arrowheads indicate F-actin at the lamellipodium, thick and thin arrows point to F-actin in filopodia between adjacent cells. (B) Arrowheads indicate F-actin at the lamellipodium and thin arrows point to cortical F-actin. Dotted lines indicate the wound edge at the origin. The figures are representative for at least three independent experiments.

4.6 The F-actin cytoskeleton of Ino-C2-PAF-treated cells resembles the F-actin cytoskeleton of cells stimulated with nocodazole and colchicine

In order to investigate the role of Ino-C2-PAF on the activity of Rho small GTPases, which among others control signalling pathways regulating actin and focal adhesion assembly or disassembly (Hall, 2005), HaCaT cells were stimulated with the anti-neoplastic agents nocodazole and colchicine. Nocodazole affects the cytoskeleton by interfering with the polymerization of microtubules and causes similar effects as some dominant negative Rho GTPases (Wittmann and Waterman-Storer, 2001). Colchicine inhibits microtubule

polymerization by binding to tubulin and consequently prevents mitosis (Margolis and Wilson, 1977).

Untreated cells and cell incubated with a small amount of dimethylsulfoxid (DMSO), which was used as vehicle for both microtubule disruption agents, exhibited a normal microtubule cytoskeleton (Figure 4.16, panel A).
As expected, after 3 h, it was possible to observe that nocodazole and colchicine induced the collapse of microtubules almost completely (Figure 4.16, panel B and C, respectively). Moreover, the effect of nocodazole was concentration-dependent (Figure 4.16, panel B). Disruption of microtubule in HaCaT cells also induced strong actin polymerization, characterized by non-polarized F-actin fibres associated with enlarged focal adhesions. This F-actin phenotype is comparable to that of Ino-C2-PAF-treated cells (Figure 4.14, panel C).
In contrast, whereas F-actin cytoskeleton was markedly affected by Ino-C2-PAF, microtubules remained intact (Figure 4.16, panel D). This finding suggests that Ino-C2-PAF might control cell migration in part affecting the activity of Rho GTPases, but an alternative mechanism is certainly required.

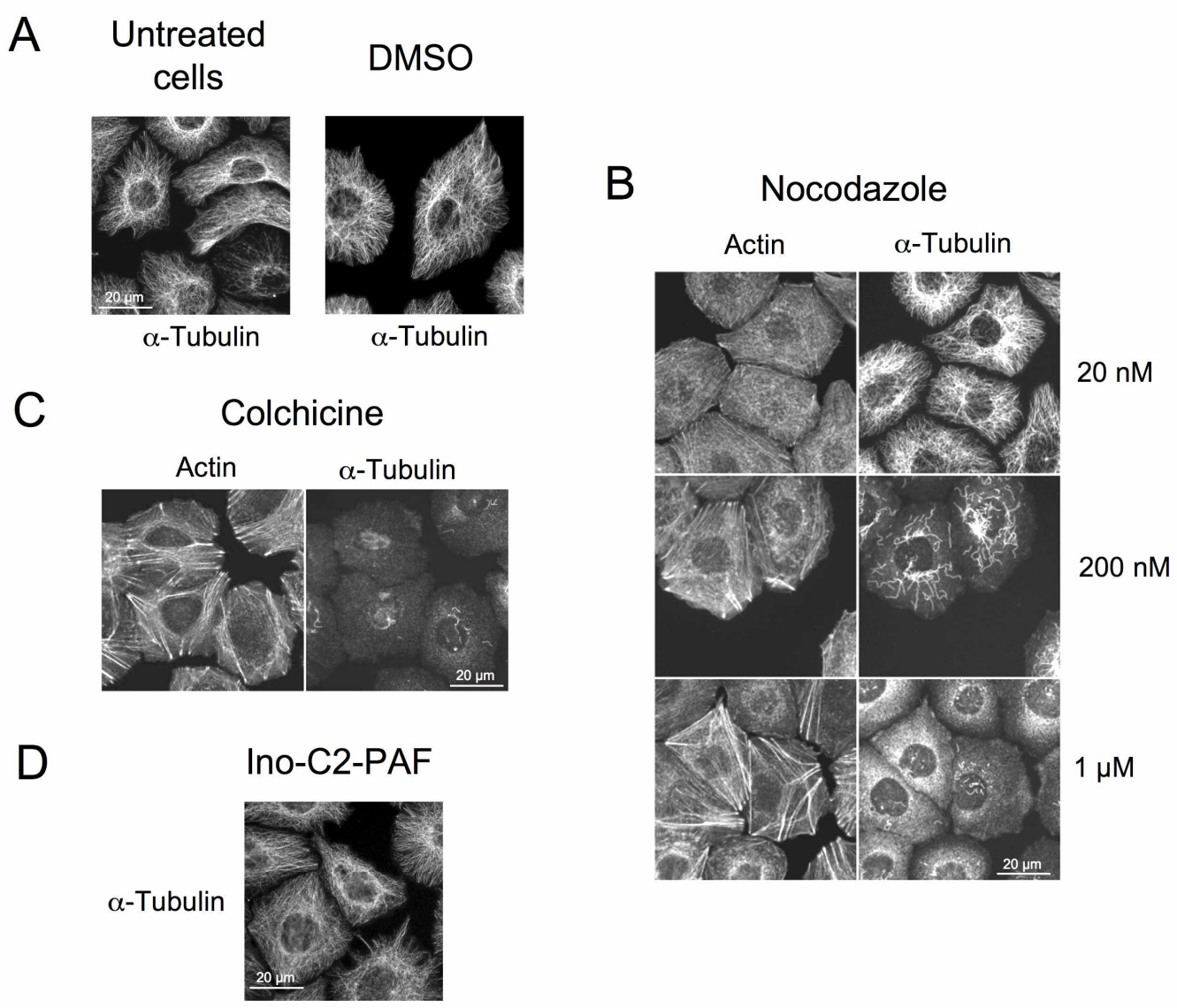

Figure 4.16. Effect of nocodazole and colchicines on microtubule and actin cytoskeleton. To analyze the F-actin and microtubule cytoskeleton of subconfluent cells, HaCaT cells on collagen IV were treated with (A) a small amount of DMSO, (B) indicated concentrations of nocodazole, (C) 1 µM of colchicine, (D) 5 µM Ino-C2-PAF for 3 h or (A) left untreated. Cells were then fixed with para-formaldehyde, blocked with BSA and incubated with CPITC-conjugated phalloidin and an anti-α-tubulin antibody. Images were taken on a Zeiss Axiovert 200 microscope. One representative of three independent experiments is shown.

4.7 Ino-C2-PAF affects total tyrosine phosphorylation

Since many focal adhesion components are substrates of tyrosine kinases, and several are tyrosine kinase themselves, tyrosine phosphorylation is necessary for the assembly of focal adhesions (Miyamoto *et al.*, 1995). Furthermore, the final composition of the mature focal complex is distinct from that of early focal adhesions (Zaidel-Bar *et al*., 2003).

In order to understand the role of glycosidated phospholipids on cell migration, the impact of

Ino-C2-PAF on the activity of several tyrosine kinases present in focal adhesions was investigated.

The total tyrosine phosphorylation in focal adhesions could be demonstrated by indirect immunofluorescence using the anti-phosphotyrosine antibody PT-66. HaCaT and SCC25 cells treated with Ino-C2-PAF clearly exhibited a reduction in total tyrosine phosphorylation in focal adhesions in comparison to untreated cells, where the phosphorylation state remain constant for the indicated time points (Figure 4.17).

Total tyrosine phosphorylation was also monitored in cells at an artificial wound edge. Untreated HaCaT and SCC25 cells at the front row of the wound edge contained total phosphorylated tyrosine in focal adhesions at the leading edge of the cells (Figure 4.18). In Ino-C2-PAF treated cells only small PT-66 signals could be detected in cells facing the wound bed. However, in the presence of Ino-C2-PAF, the residual phosphorylation signals obtained by the antibody PT-66 were primarily localized in the cell-cell junctions in both cell lines, HaCaT and SCC25.

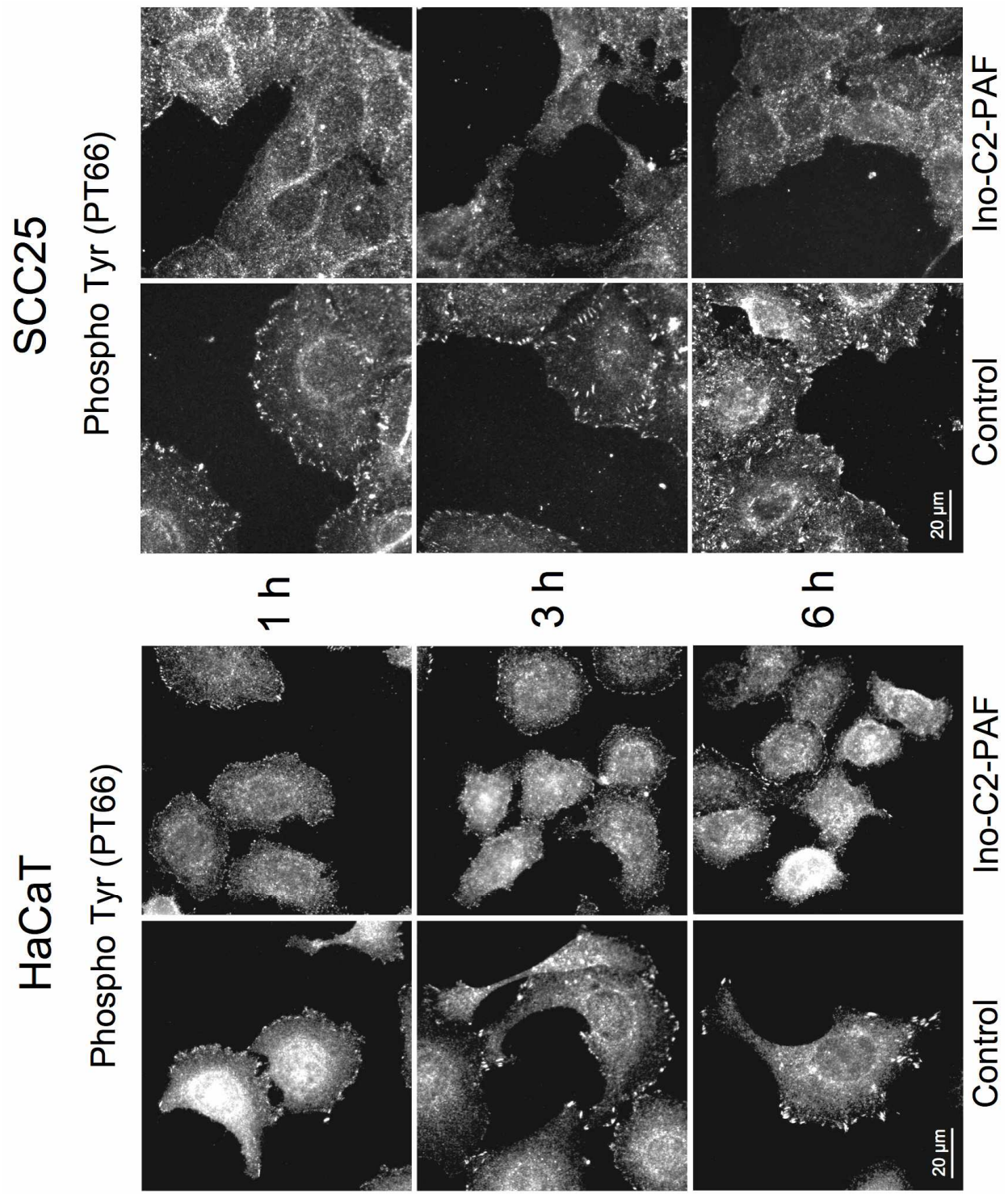

Figure 4.17. Effect of Ino-C2-PAF on tyrosine phophorylation in focal adhesions of subconfluent cells. Subconfluent HaCaT (left panel) and SCC25 cells (right panel) were cultivated on collagen IV and treated with 5 µM of Ino-C2-PAF or left untreated for the indicated periods. Cells were then fixed with para-formaldehyde, blocked with BSA and incubated with a monoclonal anti-phosphotyrosine (clone PT66) antibody. Images were taken on a Zeiss Axiovert 200 microscope. One representative of at least three independent experiments is shown.

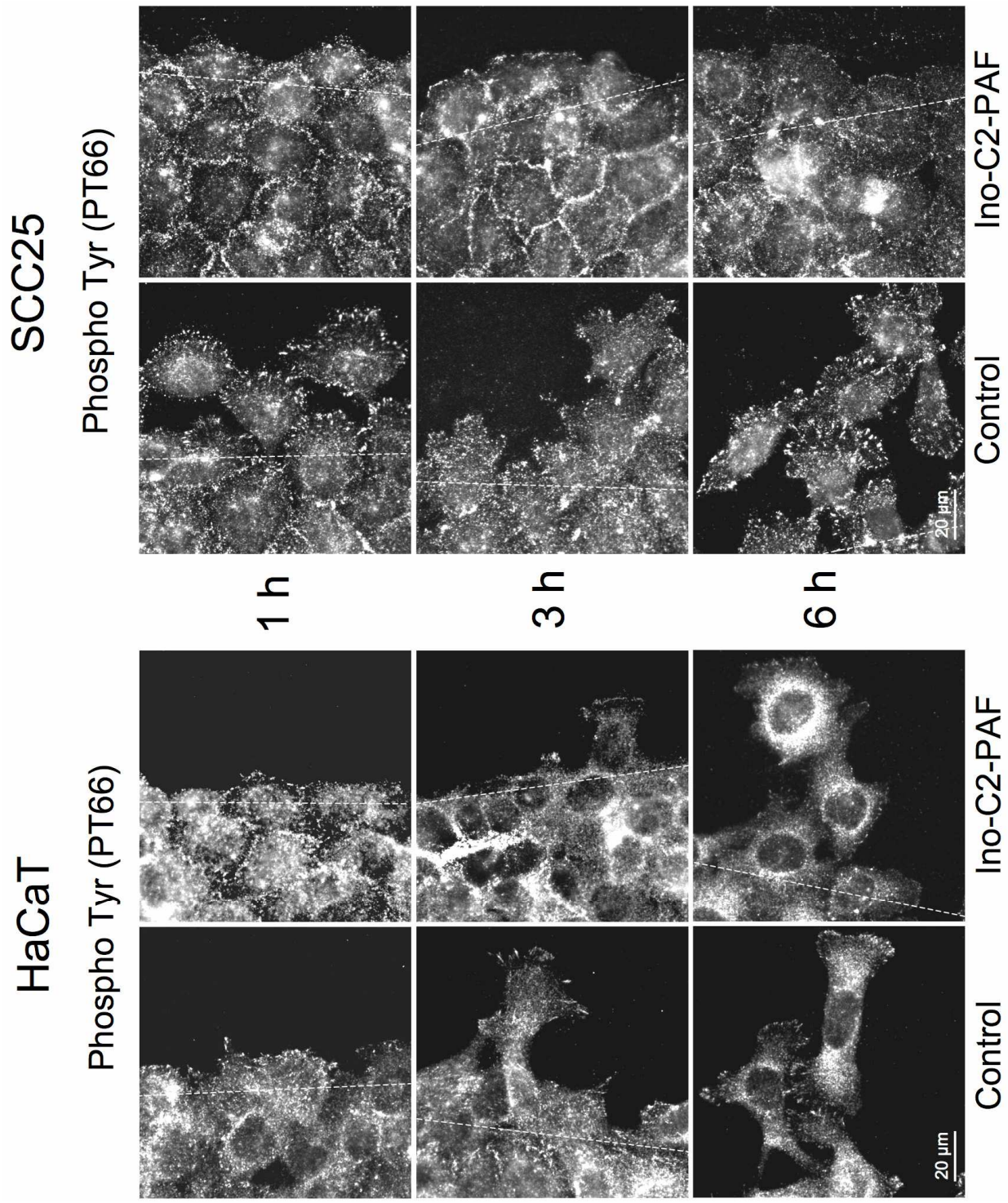

Figure 4.18. Effect of Ino-C2-PAF on tyrosine phophorylation in focal adhesions of cells at wound edge. Confluent HaCaT (left panel) and SCC25 cells (right panel) were cultivated on collagen IV and an *in vitro* wound with an average width of 475 µm was introduced as described in Material and Methods section. Cells were then treated with 5 µM of Ino-C2-PAF or left untreated for the indicated periods. Cells were fixed with para-formaldehyde, blocked with BSA and incubated with a monoclonal anti-phosphotyrosine (clone PT66) antibody. Images were taken on a Zeiss Axiovert 200 microscope. Dotted lines indicate the wound edge at the origin. One representative of at least three independent experiments is shown.

4.8 Ino-C2-PAF modulates phosphorylation of cytoplasmic tyrosine kinases FAK and Src

The cytoplasmic tyrosine kinases FAK and Src are key regulators of focal adhesion turnover and cell motility. Furthermore, FAK promotes cell migration by influencing the remodelling of the actin cytoskeleton through regulation of the Rho family of small GTPases (Hsia *et al*., 2003). Upon adhesion, FAK is activated by autophosphorylation on tyrosine residue 397 (Y397), which creates a binding site for Src, which in turn is also phosphorylated on the tyrosine residue 418 (Y418). The FAK/Src complex regulates a variety of signalling cascades that modulate focal contact dynamics in motile cells (Mitra *et al.*, 2005).

Accordingly to the total tyrosine phosphorylation, in the presence of Ino-C2-PAF indirect immunofluorescence revealed an inhibition of Src(Y418) and FAK(Y397) phosphorylation in both HaCaT (Figures 4.19 and 4.21) and SCC25 cells (Figures 4.20 and 4.22). Moreover, in wound healing analysis with Ino-C2-PAF, also Src(Y418) phosphorylation-site specific antibody mainly displayed residual phosphorylation signals localized in the cell-cell junctions. This effect was not detected for FAK(Y397) phosphorylation-site specific antibody.

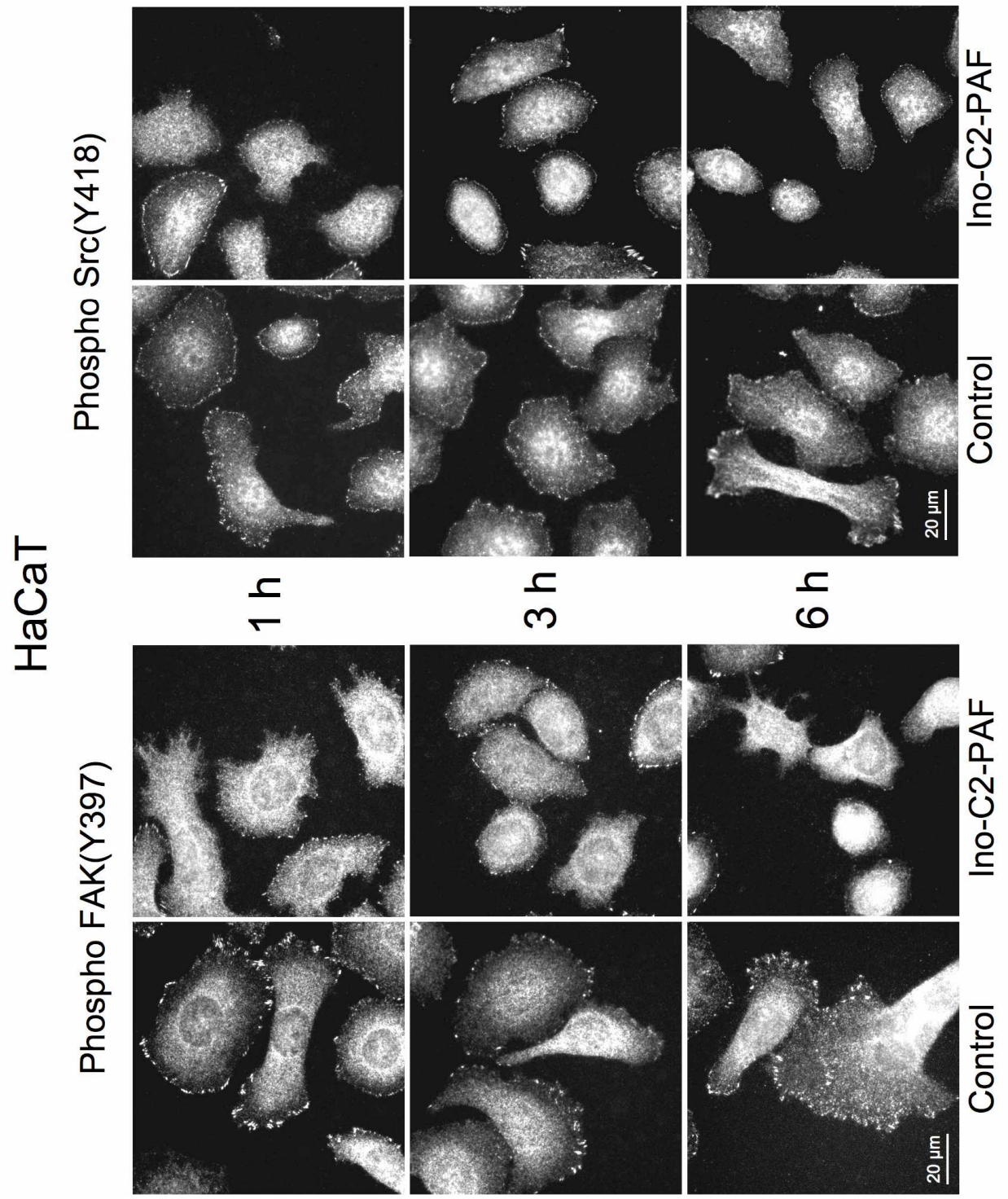

Figure 4.19. Effect of Ino-C2-PAF on FAK(Y397) and Src(Y418) phosphorylation in subconfluent HaCaT cells. Subconfluent HaCaT were cultivated on collagen IV and treated with 5 µM of Ino-C2-PAF or left untreated for the indicated periods. Cells were then fixed with para-formaldehyde, blocked with BSA and incubated with anti-phospho-FAK(Y397) (left panel) or anti-phospho-Src(Y418) (right panel) antibodies. Images were taken on a Zeiss Axiovert 200 microscope. One representative of at least three independent experiments is shown.

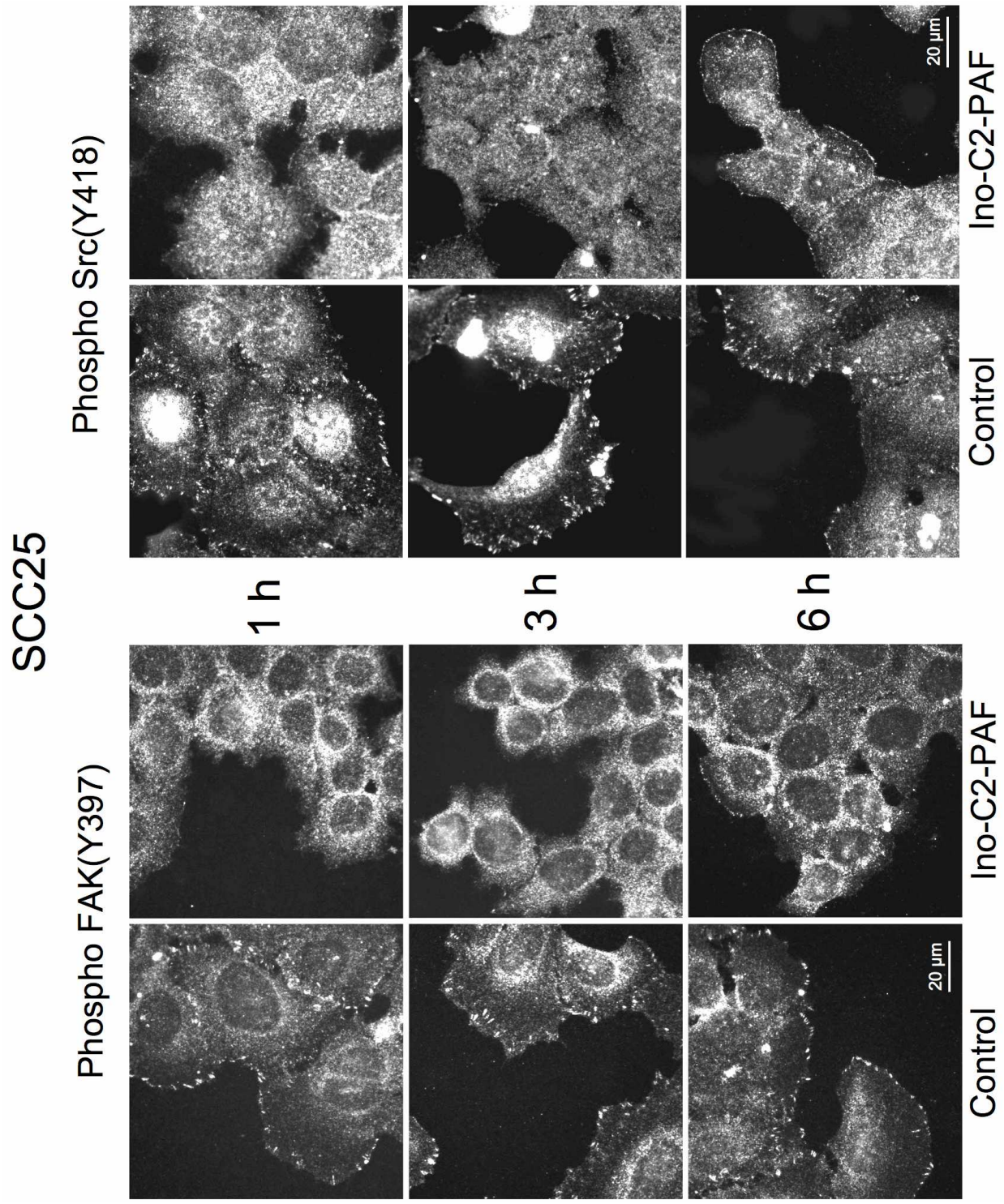

Figure 4.20. Effect of Ino-C2-PAF on FAK(Y397) and Src(Y418) phosphorylation in subconfluent SCC25 cells. Subconfluent SCC25 were cultivated on collagen IV and treated with 5 µM of Ino-C2-PAF or left untreated for the indicated periods. Cells were then fixed with para-formaldehyde, blocked with BSA and incubated with anti-phospho-FAK(Y397) (left panel) or anti-phospho-Src(Y418) (right panel) antibodies. Images were taken on a Zeiss Axiovert 200 microscope. One representative of at least three independent experiments is shown.

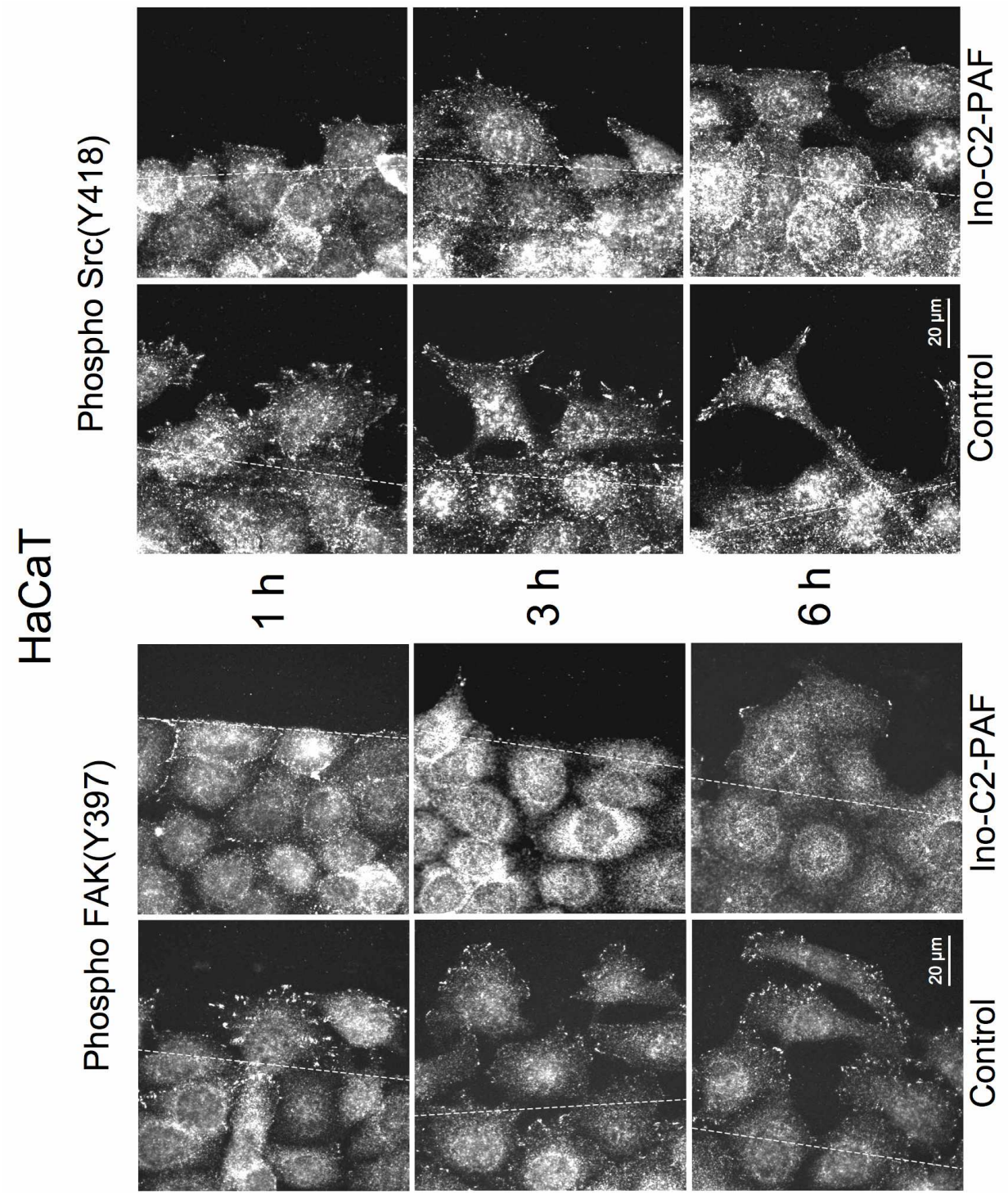

Figure 4.21. Effect of Ino-C2-PAF on FAK(Y397) and Src(Y418) phosphorylation in HaCaT cells at wound edge. Confluent HaCaT cells were cultivated on collagen IV and an *in vitro* wound with an average width of 475 µm was introduced as described in Material and Methods section. Cells were then treated with 5 µM of Ino-C2-PAF or left untreated for the indicated periods. Cells were fixed with para-formaldehyde, blocked with BSA and incubated with anti-phospho-FAK(Y397) (left panel) or anti-phospho-Src(Y418) (right panel) antibodies. Images were taken on a Zeiss Axiovert 200 microscope. Dotted lines indicate the wound edge at the origin. One representative of at least three independent experiments is shown.

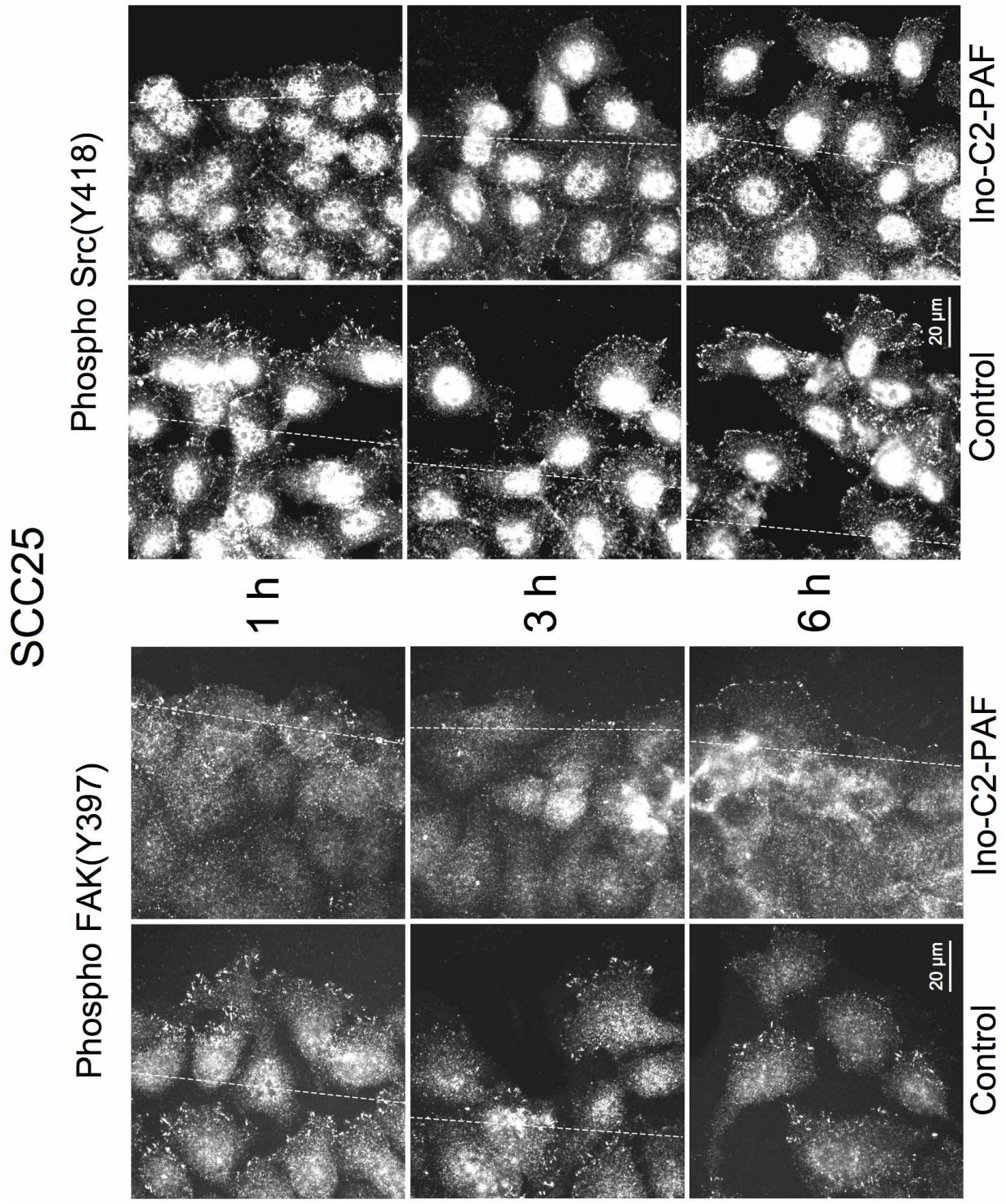

Figure 4.22. Effect of Ino-C2-PAF on FAK(Y397) and Src(Y418) phosphorylation in SCC25 cells at wound edge. Confluent SCC25 cells were cultivated on collagen IV and an *in vitro* wound with an average width of 475 µm was introduced as described in Material and Methods section. Cells were then treated with 5 µM of Ino-C2-PAF or left untreated for the indicated periods. Cells were fixed with para-formaldehyde, blocked with BSA and incubated with anti-phospho-FAK(Y397) (left panel) or anti-phospho-Src(Y418) (right panel) antibodies. Images were taken on a Zeiss Axiovert 200 microscope. Dotted lines indicate the wound edge at the origin. One representative of at least three independent experiments is shown.

Phosphorylation of Src at position 418 and FAK at position 397 in cell lysates of HaCaT and SCC25 cells after treatment with Ino-C2-PAF was additionally studied using Western blotting with phosphorylation site-specific antibodies.

In subconfluent HaCaT cells, phosphorylation of Src(Y418) was initially increased and then clearly reduced after treatment with 5 µM Ino-C2-PAF in comparison to untreated cells. Phosphorylation of FAK at tyrosine residue 397 was also attenuated under these conditions (Figure 4.23, panel A). Furthermore, the microarray analysis revealed that expression of FAK and Src is not significantly affected by Ino-C2-PAF-treatment (Figure 4.23, panel B).

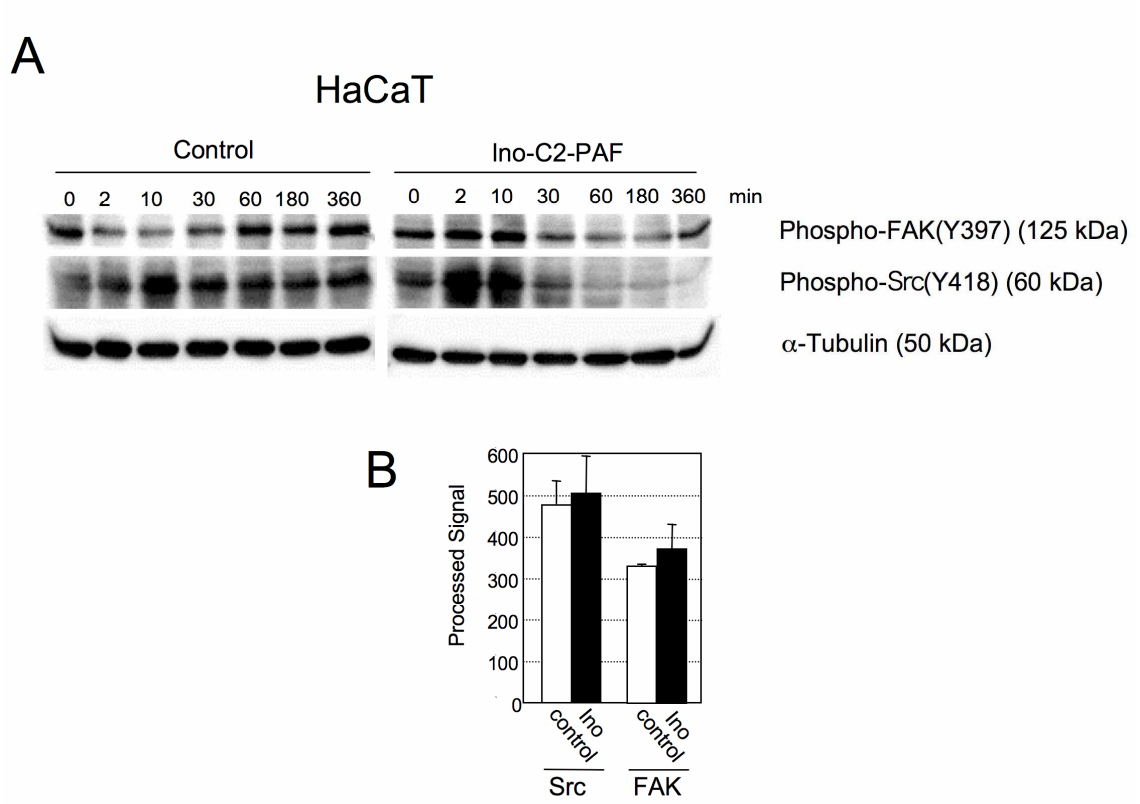

Figure 4.23. Time-dependent effect of Ino-C2-PAF on FAK(Y397) and Src(Y418) phosphorylation in HaCaT cells. (A) HaCaT cells were incubated with defined keratinocyte serum-free medium overnight, treated with or without 5 µM Ino-C2-PAF for the indicated periods. Whole-cell lysates (40 µg) were separated on a 7.5% SDS-PAGE and subjected to Western blotting using anti-phospho-FAK(Y397) and anti-phospho-Src(Y418) antibodies. α-tubulin was used as a loading control. (B) Expression of FAK and Src mRNA using microarray analysis. Subconfluent HaCaT cells were treated with 5 µM Ino-C2-PAF for 24 h, mRNA was isolated and cDNA was synthesized as described in Material and Methods section. Processed signal are the mean value of three independent experiments.

A similar pattern for both Src(Y418) and FAK(Y397) could be observed also in SCC25 cells (Figure 4.24).

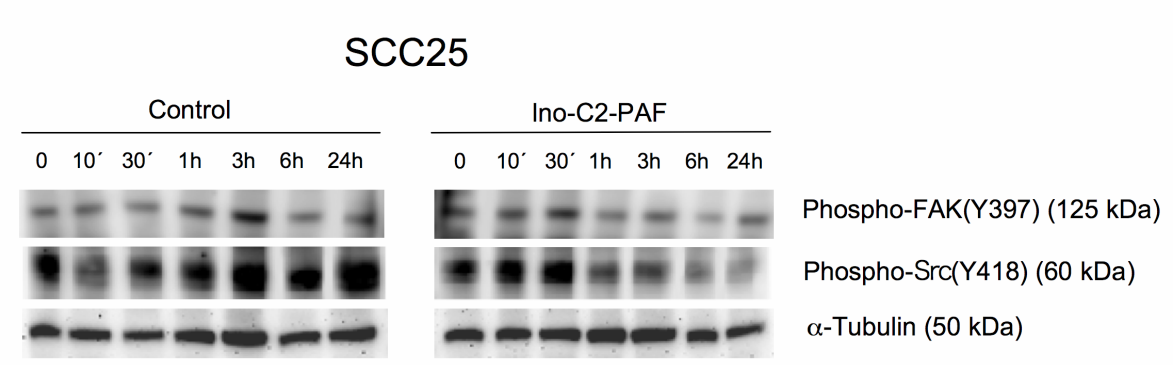

Figure 4.24. Time-dependent effect of Ino-C2-PAF on FAK(Y397) and Src(Y418) phosphorylation in SCC25 cells. (A) SCC25 cells were incubated with serum-free medium overnight, treated with or without 5 µM Ino-C2-PAF for the indicated periods. Whole-cell lysates (40 µg) were separated on a 7.5% SDS-PAGE and subjected to Western blotting using anti-phospho-FAK(Y397) and anti-phospho-Src(Y418) antibodies. α-tubulin was used as a loading control.

4.9 Ino-C2-PAF does not influence the formation of the FAK/Src-complex

FAK(Y397) is known to serve as a docking site for the recruitment of Src, which in turn can further phosphorylate remaining sites of tyrosine phosphorylation in FAK (reviewed by Schlaepfer *et al.*, 1998). To obtain evidence whether inhibition of the autophosphorylation site on FAK by Ino-C2-PAF leads to a reduced complex formation with Src, co-immunoprecipitation experiments were carried out. Immunoprecipitates were formed by using anti-FAK antibody. The presence of Src in the precipitate was determined by Western blotting using anti-Src antibody. Treatment with Ino-C2-PAF for 3 h, had no influence on the FAK/Src complex. In precipitates of HaCaT cells the same amount of Src was detected compared to immunoprecipitates from untreated cells (Figure 4.25).

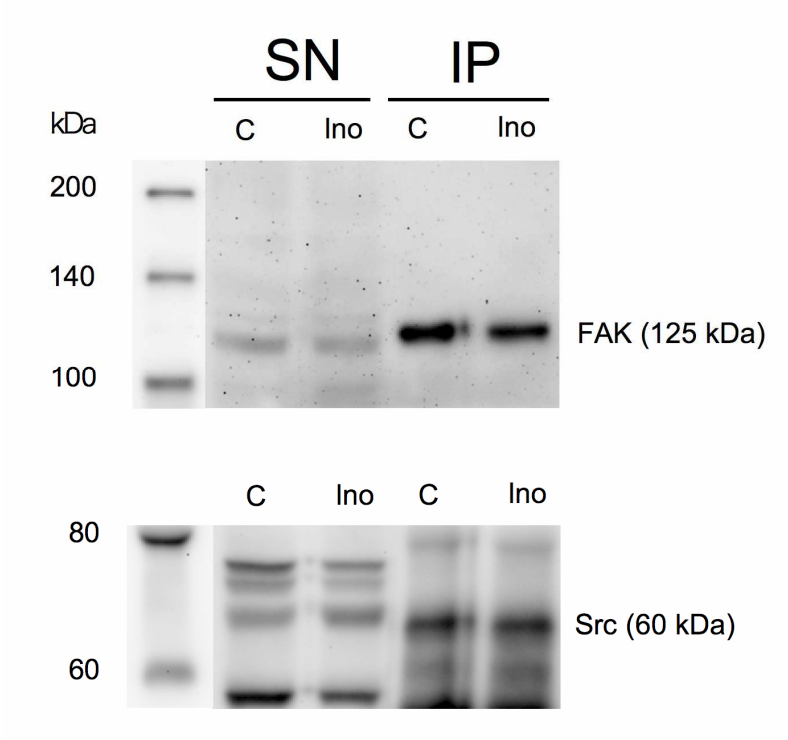

Figure 4.25. Effect of Ino-C2-PAF on the FAK/Src complex in HaCaT cells. HaCaT cells were plated on collagen IV in serum-free medium and incubated with 5 µM Ino-C2-PAF for 3 h. Cells were lysed and FAK was immunoprecipitated from cell extracts using an anti-FAK antibody. The immunoprecipitate was then separated by SDS-PAGE and transferred to nitrocellulose by Western blotting before being analyzed with anti-Src antibody. IP: immunoprecipitate; SN: supernatant after precipitation; C: untreated, control cells; Ino: Ino-C2-PAF.

4.10 Constitutively active variants of Src and FAK can in part rescue the inhibition of migration caused by Ino-C2-PAF

To evaluate whether the inhibition of migration caused by Ino-C2-PAF could be rescued migration assays were performed in the absence or presence of Ino-C2-PAF with cells that were transiently transfected with constitutively active Src (Src-Y527F) and FAK (CD2-FAK) or empty GFP plasmid (EGFP) as control, respectively. It turned out that in HaCaT cells transfection of Src-Y527F could partially bypass the effect of Ino-C2-PAF while the transfection of CD2-FAK completely compensated for the inhibitory effect caused by Ino-C2-PAF. In SCC25 cells, transfection of the cDNAs has a slight impact on the inhibitory effect of Ino-C2-PAF but it is less pronounced than in HaCaT cells (Figure 4.26).

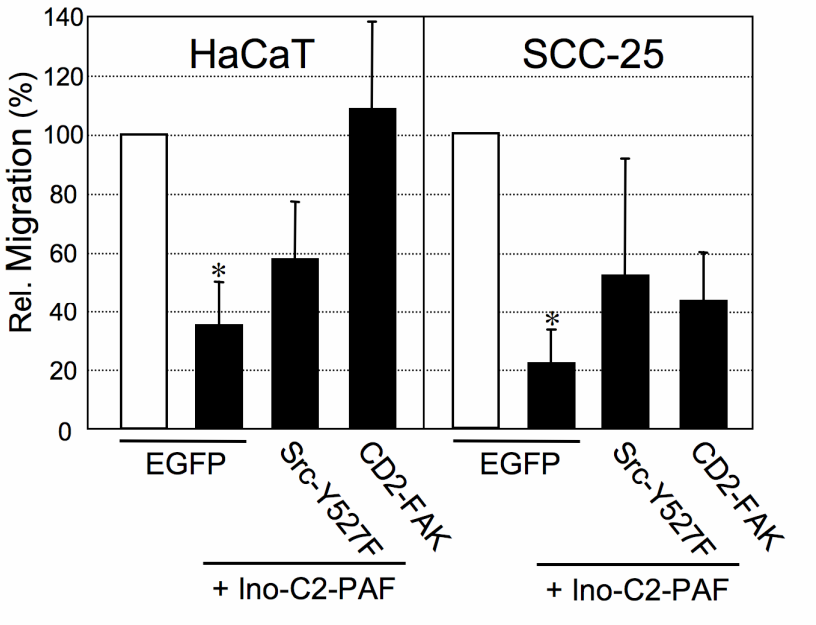

Figure 4.26. Influence of constitutively active variants of Src and FAK on the inhibition of migration caused by Ino-C2-PAF. HaCaT and SCC25 cells were transiently transfected with plasmids expressing constitutively form of Src (Src-Y527F) and FAK (CD2-FAK) or empty GFP plasmid (EGFP) as control. Cells were then incubated in the presence or absence of Ino-C2-PAF for 24h. Subsequently, cells were allowed to migrate in haptotactic transwell chamber assays as described in the Material and Methods section. (*) indicates a significant difference ($P < 0.05$) from the control cells.

4.11 Ino-C2-PAF inhibits Akt/PKB activation in migrating cells

Besides cell growth, proliferation, and survival the signalling cascade regulated by PI3K controls cell migration as well. Following the same experimental design conducted for the FAK/Src signalling pathway, a scratch was introduced in confluent HaCaT cells and the phosphorylation state of Akt/PKB was analyzed by indirect immunofluorescence. In untreated cells active Akt/PKB was detected at the leading edge of motile cells facing the wound bed (Figure 4.27; arrowheads). This Akt/PKB activation was minimal or absent in cells treated with 5 µM Ino-C2-PAF.

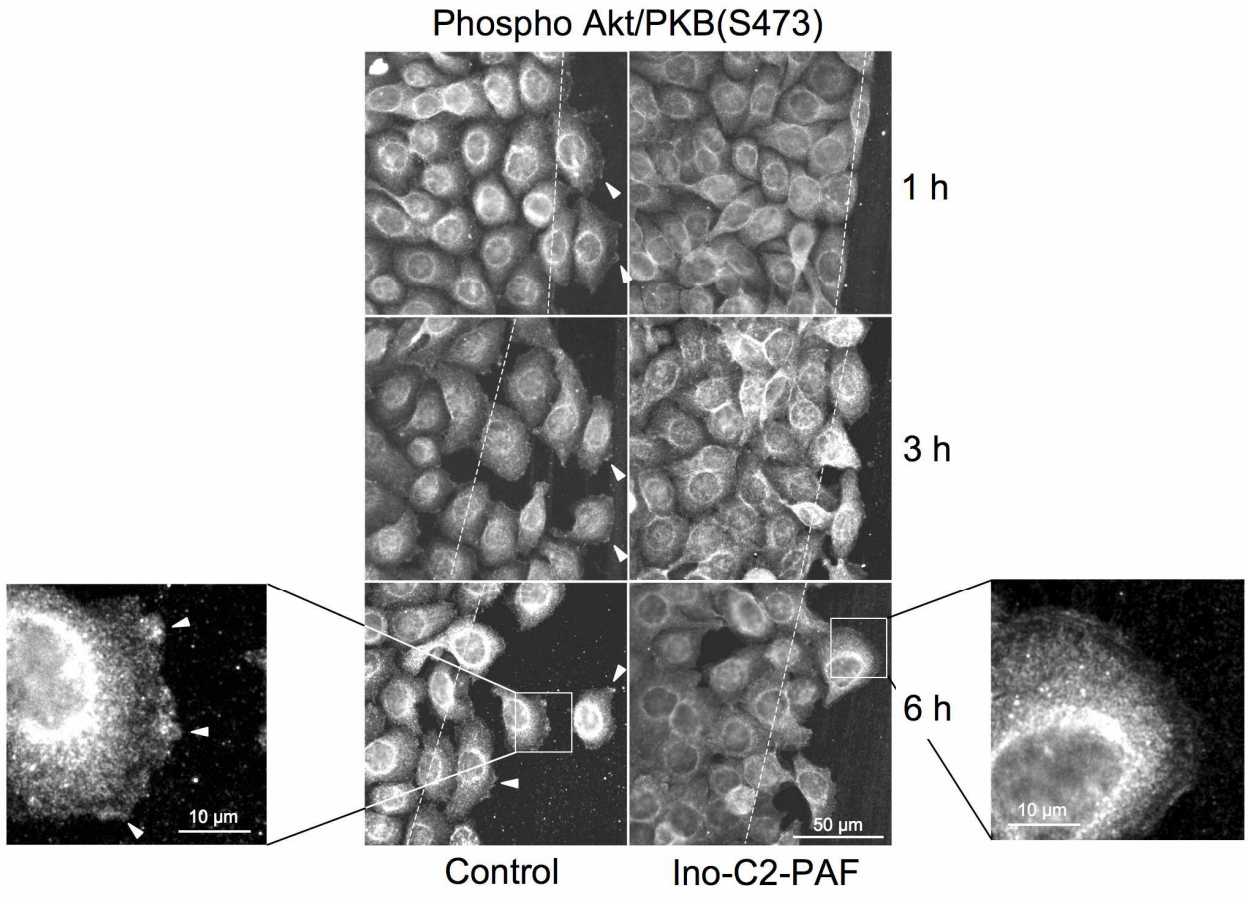

Figure 4.27. Effect of Ino-C2-PAF on Akt/PKB(S473) phosphorylation in HaCaT cells at the wound edge. Confluent HaCaT cells were cultivated on collagen IV. An *in vitro* wound with an average width of 475 µm was introduced as described in the Material and Methods section. Cells were then treated with 5 µM of Ino-C2-PAF or left untreated for the indicated periods. Cells were fixed with para-formaldehyde, blocked with BSA and incubated with anti-phospho-Akt/PKB(S473) antibody. Images were taken on a Zeiss Axiovert 200 microscope. Dotted lines indicate the wound edge at the origin. Arrowheads show active Akt/PKB at the leading edge of motile cells. One representative of at least three independent experiments is shown.

4.12 Ino-C2-PAF increases attachment to extracellular matrix components

Integrin-mediated cell attachment to extracellular matrix components (ECMs) is a fundamental requirement for migration. Former studies revealed that Ino-C2-PAF significantly increases attachment of HaCaT cells to collagen IV, fibronectin, and laminin-111 in a concentration-dependent manner (Fischer, PhD thesis FU Berlin, 2006). Since no data were available for SCC25 cells, adhesion assay with this highly invasive cell line was performed following the same protocol and using the same ECM components (Figure 4.28). SCC25 cells exhibited a similar adhesion behaviour as seen for HaCaT cells. The most pronounced effect could be observed on collagen IV, on which adhesion was enhanced by 43% relative to untreated cells. After incubation with 5 µM Ino-C2-PAF, attachment to fibronectin and laminin-111 was increased by 23 and 15%, respectively. This increase in adhesion was clearly integrin-dependent, as background attachment to poly-L-lysine was unaffected.

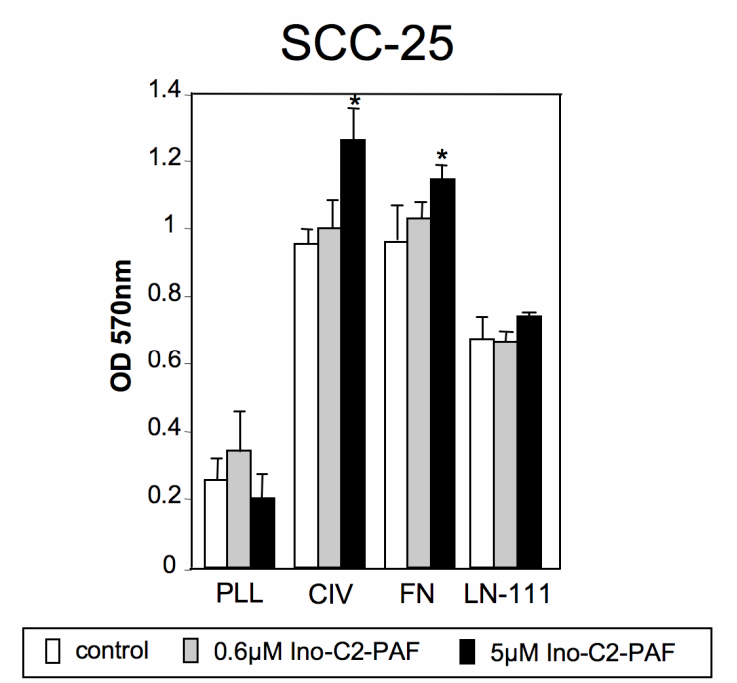

Figure 4.28. Ino-C2-PAF-dependent cell-matrix attachment in SCC25 cells. For monitoring cell-matrix attachment, cells were incubated with 0.6 or 5µM Ino-C2-PAF or were untreated for 48h. Cells were then plated onto matrix proteins as indicated for 2h, washed, fixed, and stained with crystal violet. Plates were measured photometrically at 570 nm after TritonX-100 dye solubilisation. (*) indicates a significant difference ($P < 0.05$) from the control cells. PLL: poly-L-lysine; CIV: collagen IV; FN: fibronectin; LN-111: laminin111.

To ascertain whether expression of integrin subunits accounts for the differences observed we used the integrin-specific data obtained by the microarray experiments with mRNA of Ino-C2-PAF-treated and control HaCaT cells already presented in chapter 4.3.1. It turned out

that expression of none of the integrin subunits present in HaCaT cells was altered significantly by Ino-C2-PAF (Figure 4.29). Furthermore, this finding was partly consistent with earlier investigations obtained by flow cytometry. Here, surface expression of the integrin subunits, α3, α6, β1 and β4 of cells was quantified in the presence and in the absence of Ino-C2-PAF (Fischer, PhD thesis FU Berlin, 2006). Surface expression of the α3 and β1 integrin subunit remained unaltered after incubation with Ino-C2-PAF in both cell lines. However, in HaCaT cells surface expression of the α6 and β4 subunits, which assemble into the integrin α6β4, was significantly elevated. In SCC25 cells surface expression of both subunits was slightly but not significantly increased. Thus, the observed rise in matrix attachment determined in both SCC25 and HaCaT cells could not directly be due to the over-expression of the α6β4 integrin since the surface expression of the α6β4 integrin was only elevated in one of both cell lines and binding to β1 integrin ligands was mainly affected. Nonetheless, these results show that Ino-C2-PAF controls the expression of integrins mainly at the post-translational level.

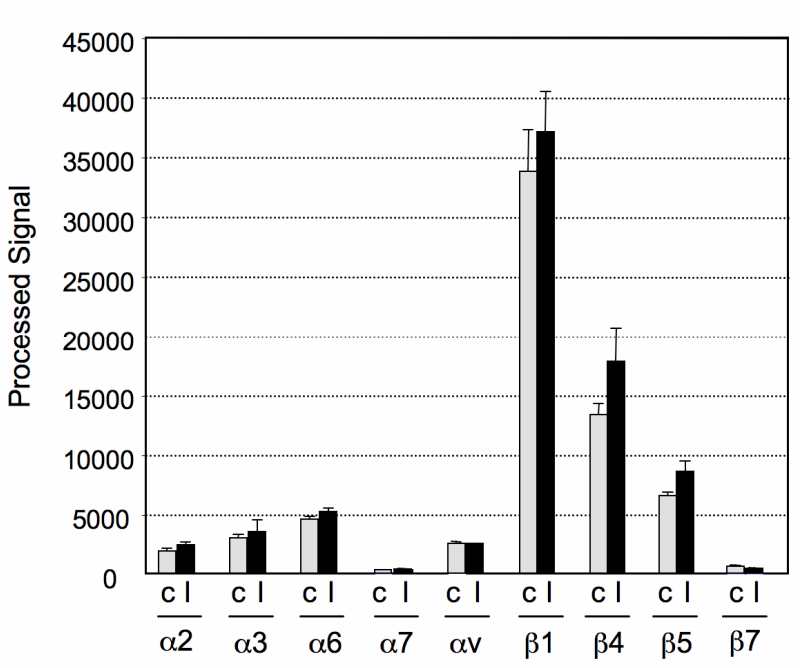

Figure 4.29. Effect of Ino-C2-PAF on the integrin expression. mRNA expression of several integrin subunits was performed using microarray analysis. HaCaT cells were treated with 5 µM Ino-C2-PAF for 24 h or left untreated, mRNA was isolated and cDNA was synthesized as described in Material and Methods section. Processed signal are the mean value of three independent experiments. C: control; I: Ino-C2-PAF.

To investigate whether the rise in attachment is due to increased avidity or increased affinity of β1 integrins, first of all the activation state of the β1 integrin was examined by the use of the antibody 12G10, which recognizes the high-affinity state of β1 integrins. As shown by flow cytometry, neither 0.6 µM nor 5 µM Ino-C2-PAF are capable of changing the activation

state of β1 integrins in both cell lines (Figure 4.30, upper panel). As a positive control $MnCl_2$ was used as a known positive regulator of integrin affinity (Mould *et al.*, 2002; Figure 4.30, lower panel). While the amount of β1 integrin remained unaltered, Mn^{2+} increased the amount of 12G10 binding.

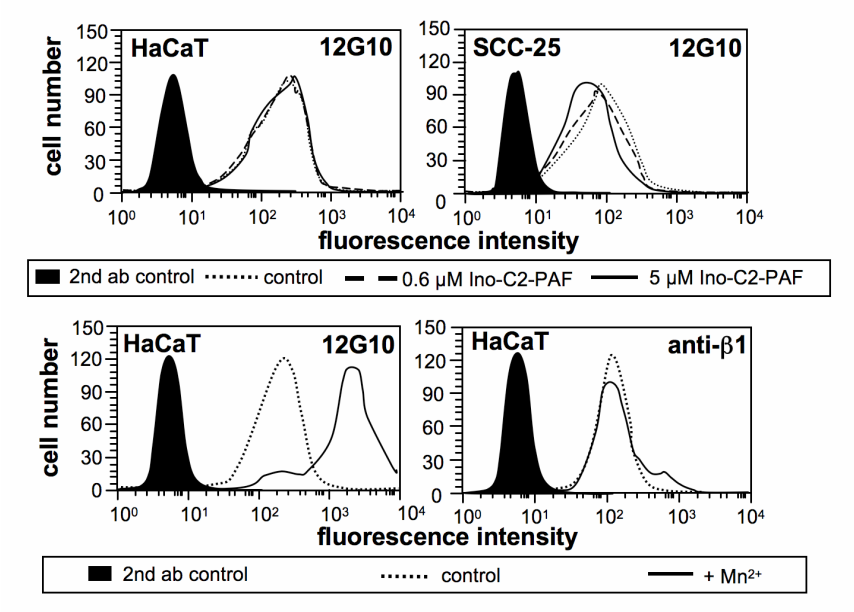

Figure 4.30. Effect of Ino-C2-PAF on the activity of β1 integrin. To assess the activity of β1 integrins, HaCaT and SCC25 cells were treated with Ino-C2-PAF or left untreated for 24 h and analyzed by flow cytometry using the 12G10 antibody. Total expression of β1 integrin was examined using a FITC-conjugated anti-CD29 antibody. Cells incubated with the respective secondary antibody only (2nd ab control) served as negative controls. As a positive control cells were stimulated with 5mM $MnCl_2$ in TBS.

The increase in size of focal complexes, which is mostly correlated with reduced motility (Ren *et al.*, 2000) could also be visualized in HaCaT cells transiently transfected with GFP-FAK (Figure 4.31). Control cells transfected with GFP-FAK reveal a normal turnover of focal complexes with detachment of focal complexes in some cell protrusions (arrowhead) and the subsequent formation of new focal adhesions in other regions of the cell (upper panel; arrow). In cells treated with Ino-C2-PAF some of the focal complexes increased in size (arrowheads) but the formation of new focal complexes could not be observed.

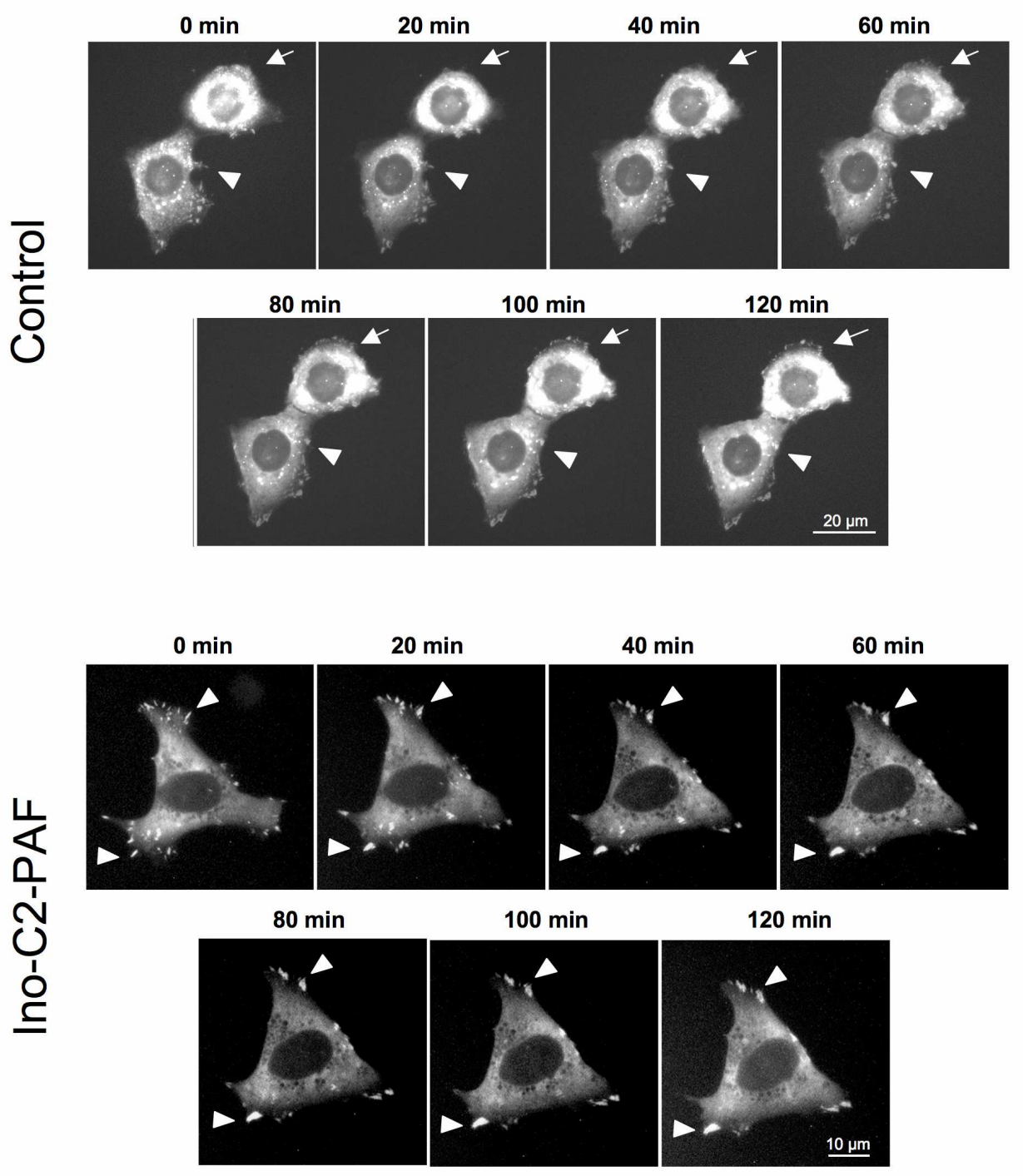

Figure 4.31. Time-dependent influence of Ino-C2-PAF on focal adhesion dynamics. HaCaT cells transiently transfected with GFP-FAK plasmid using magnetofection were replated on collagen IV-coated glass coverslips. Analysis was performed in serum- and phenol red free medium containing 20 mM Hepes. Cells were incubated in the presence or absence of 5 µM Ino-C2-PAF for the indicated periods. In the control cells, arrowhead indicates disappearing focal adhesions whereas arrow shows new focal adhesions. In Ino-C2-PAF-treated cells arrowheads indicate focal adhesion that persists over the time. Images were taken on a Zeiss Axiovert 200 microscope. The data are representative for three independent experiments.

4.13 Ino-C2-PAF increases cell-cell adhesion in HaCaT cells

Reduced migration is often accompanied by an increased cell-matrix and cell-cell adhesion. These processes are regulated by a dynamical change in cell matrix attachment and detachment, which is facilitated by integrins. It has long been recognized that the cell-cell adhesion receptor, E-cadherin, is an important determinant of tumor progression, serving as a suppressor of invasion and metastasis in many contexts (for review see Jeanes *et al.*, 2008). To investigate whether Ino-C2-PAF has an impact on adherent junctions, HaCaT cells were cultured at 90% confluency, treated with Ino-C2-PAF and E-cadherin localization was detected by indirect immunofluorescence analysis. After 6 h exposure no significant difference in localization of E-cadherin was observed. Cells stimulated with 5 µM Ino-C2-PAF for 24 h show an increased amount of E-cadherin at cell-cell contacts (Figure 4.32; arrowheads).

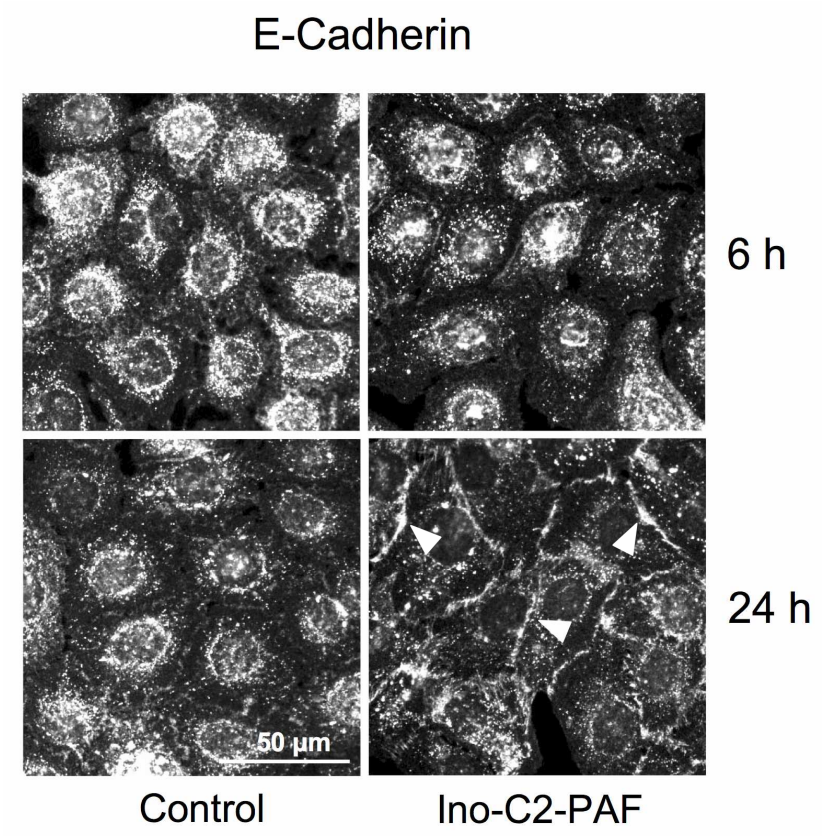

Figure 4.32. Effect of Ino-C2-PAF on E-cadherin localization in HaCaT cells. To observe the role of E-cadherin during the formation of cell-cell contacts, subconfluent HaCaT cells (90% density) on collagen IV were treated with or without 5 µM Ino-C2-PAF for the indicated periods. Cells were then fixed with para-formaldehyde, blocked with BSA and incubated with an anti-E-cadherin antibody. Images were taken on a Zeiss Axiovert 200 microscope. Arrowheads indicate E-cadherin at the cell-cell contacts. The data are representative for three independent experiments.

However, neither Western blot analysis (Figure 4.33, panel A) nor microarray studies (Figure 4.33, panel B) showed an increase of E-cadherin expression in Ino-C2-PAF-treated cells. These results suggest that Ino-C2-PAF treatment leads to E-cadherin redistribution within the cell.

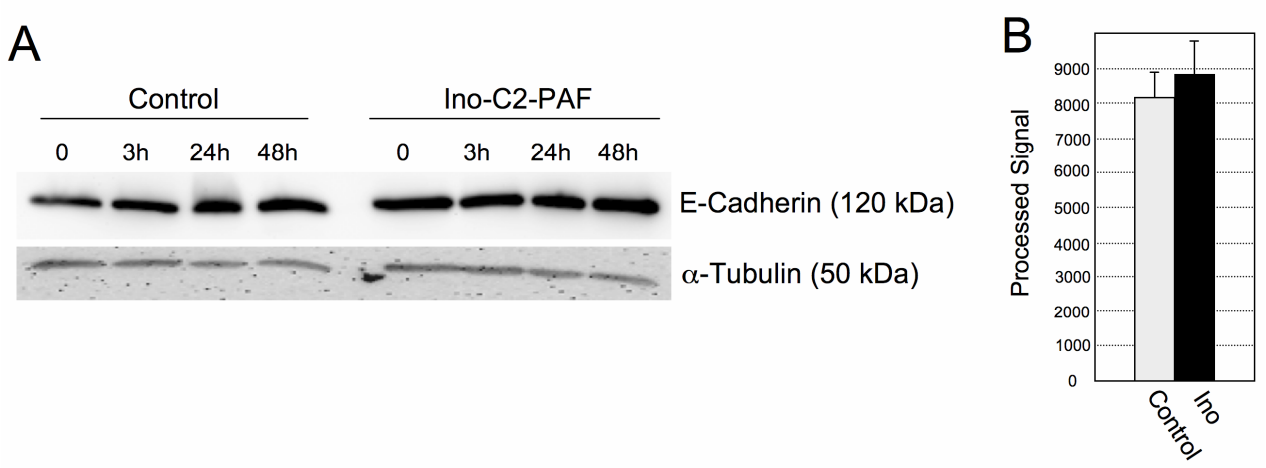

Figure 4.33. E-cadherin expression in HaCaT cells. (A) HaCaT cells were incubated with defined keratinocyte serum-free medium overnight, treated with 5 µM Ino-C2-PAF or left untreated for the indicated periods. Whole-cell lysates (40 µg) were separated on a 7.5% SDS-PAGE and subjected to Western blotting using an anti-E-Cadherin antibody. α-tubulin was used as a loading control. (B) Expression of E-Cadherin mRNA using cDNA microarray analysis. HaCaT cells were treated with 5 µM Ino-C2-PAF (Ino) for 24 h or left untreated (Control), mRNA was isolated and cDNA was synthesized as described in Material and Methods section. Processed signal are the mean value of three independent experiments. Control: untreated cells; Ino: Ino-C2-PAF.

5 DISCUSSION

In the present work, the mechanism of action of the glycosidated phospholipid Ino-C2-PAF has been investigated. For the first time, the influence of APLs on the transcription of the whole genome was studied. Using Agilent cDNA microarray technology, global gene expression profiles of HaCaT cells treated with Ino-C2-PAF, Glc-PAF, or edelfosine were compared with the profile of untreated control cells. Furthermore, the effects of Ino-C2-PAF on the cytoskeleton and on signalling pathways regulating important cellular processes such as cell proliferation, adhesion and migration of immortalized keratinocytes were analyzed.

5.1 Influence of Ino-C2-PAF on cell proliferation and migration

The proliferation assay represents a basic and essential experiment that is normally performed to test the efficacy of a new substance with anti-cancer properties in normal and tumour cell lines.

Although previous studies allowed to define the LC_{50} and IC_{50} values for Ino-C2-PAF in HaCaT and SCC25 cells already (Fischer, PhD thesis FU Berlin, 2006; Fischer *et al.*, 2006), a new series of proliferation assays in HaCaT and SCC25 cells was performed in order to verify the efficacy of Ino-C2-PAF and the experimental procedure with previous data. Moreover, the impact of the PI3K inhibitor wortmannin on cell proliferation was also investigated. Similar to the work of Fischer, Ino-C2-PAF, at a concentration of 5 µM, showed a clear anti-proliferative activity in both HaCaT and SCC25 cell lines.

Comparing the results for Ino-C2-PAF with those for other antitumour lipids (ATLs) that were described in the literature, it is possible to assess that the anti-proliferative activity of ATLs depends on their structure as well as on the cell type that was treated. In keratinocytes, Ino-C2-PAF shows the strongest anti-proliferative effect compared to other ATLs. In fact, the half inhibitory concentration (IC_{50}) of Ino-C2-PAF in HaCaT cells is 1.8 µM, whereas miltefosine and

Glc-PAF have an IC_{50} of 3 µM and 4.8 µM, respectively (Mickeleit *et al.*, 1998; Wieder *et al.*, 1998).

Although micro-molar concentrations of ATLs are already sufficient to inhibit the proliferation of epithelial cells, ATLs can display relatively high IC_{50}-values and, consequently, a reduced efficacy. In Madin-Darby canine kidney (MDCK) cells, edelfosine and miltefosine inhibited cell proliferation with an IC_{50} of 75 µM and 135 µM, respectively (Wieder *et al.*, 1995a). Even in related cell lines the activity of ATLs can vary drastically. Among malignant lung tumours,

small cell lung carcinoma (SCLC; IC_{50} of about 4 µM) exhibits greater edelfosine resistance compared with non-small cell lung carcinoma (NSCLC; IC_{50} between 7 and 67 µM) (Strassheim *et al.*, 2000). However, with an IC_{50} of 2 µM, edelfosine efficiently inhibits the proliferation of breast cancer cell line MCF-7 (Samadder and Arthur, 1999), whereas Ino-C2-PAF, as demonstrated in recently performed studies, shows a reduced activity (IC_{50} of about 5 µM) in comparison to edelfosine or to Ino-C2-PAF in keratinocytes. In general, such discrepancies have been found also in leukemic cell lines (Berkovic *et al.*, 1994; Mollinedo *et al.*, 2010).

The anticancer activity of Ino-C2-PAF regards also cell migration. Ino-C2-PAF drastically inhibits haptotactic migration of both HaCaT and SCC25 cells towards a collagen IV gradient. Moreover, this effect is proliferation-independent, because Ino-C2-PAF does not show any significant impact on the proliferation during the time course of the experiment.
Similarly, other ether lipids with antitumour properties, such as miltefosine and edelfosine, have previously been reported to influence cellular motility. Both miltefosine and edelfosine reduce the capacity of malignant murine MO4 cells to invade pre-cultured heart fragments, an *in vitro* model for cancer cell invasion (Schallier *et al.*, 1991). At high concentrations, edelfosine reduces both invasion and haptotactic migration of transitional cell carcinoma cells (Slaton *et al.*, 1994). However, other studies have reported conflicting results, describing edelfosine-stimulated invasion of human MCF-7 breast and human HCT-8/S11 colon cancer cells (Steelant *et al.*, 2001, Van Slambrouck *et al.*, 2007).

The different influence of ATLs on the proliferation and migration of various cell lines could be partly relied on factors like plasma membrane structure and multidrug resistance.
Since ATLs mainly exert their function through their incorporation in the cellular membrane, a slightly different plasma membrane composition between normal and malignant cells might affect their activity. Indeed, it has been found that malignant transformations are associated with changes in the dynamic properties of cellular membrane (Inbar *et al.*, 1977).
In the context of ATLs, several biophysical studies using synthetic membranes in the presence of edelfosine were performed in the last decade (Ausili *et al.*, 2008; Hac-Wydro and Dynarowicz-Latka, 2010; Torrecillas *et al.*, 2006). The results suggest that ATLs associate with cholesterol-sphingomyelin enriched membrane microdomains, also known as lipid rafts, and change their properties drastically. Therefore, lipid rafts may be considered a new potential target in anticancer therapy, such as in multiple myeloma (Heczkova and Slotte, 2006; Mollinedo *et al.,* 2010).

The multidrug resistance (MDR), which represents an important obstacle in the development of anticancer drugs, is a well-studied phenomenon responsible for the acquired drug resistance. After selection for resistance to a single cytotoxic drug, cells may become cross-resistant to a whole range of drugs with different structures and targets (Kool *et al.*, 1997). In human cancer cells, MDR can be caused by enhanced drug efflux mediated by transporter proteins such as ATP-binding cassette (ABC) transporters and P-glycoproteins (Borst *et al.*, 1997; Endicott and Ling, 1989; Ling, 1997). Furthermore, malignant melanoma show high levels of intrinsic drug resistance associated with a highly invasive phenotype. However, expression of P-glycoprotein has been also found in normal epithelia, such as those of the gastrointestinal tract, liver, pancreas, kidney, and reproductive organs (Hunter *et al.*, 1993).

Proliferation and migration are also controlled by numerous signalling cascades that will be discussed in the next paragraphs.

5.2 Influence of APLS on gene expression

Signalling pathways can be regulated at different levels through transcriptional and translational control, as well as post-translational modifications. Most studies with alkyl-phospholipids (APLs) deal with mechanisms of post-translational modulation, such as phosphorylation of key enzymes of the PI3K/AKT and MAPK pathways, cleavage of pro-enzymes like caspases in apoptosis, and conformational modifications that permit the activation and/or translocation of specific proteins to define sub-cellular regions (for reviews see Danker *et al.*, 2010; Gajate and Mollinedo, 2002). Until now, only a few publications have presented data obtained from expression studies after treatment with APLs. Furthermore, these data result from a targeted search that considers only a group of genes (e.g. genes correlated with perifosine cytotoxicity) (Zhang *et al.*, 2008). This study considers for the first time the effects of APLs on the expression of the whole human genome. In addition, it was important not to restrict this analysis just to Ino-C2-PAF, but to extend the knowledge to other APLs, namely edelfosine and Glc-PAF. Therefore, the transcriptional activities of these compounds are compared in order to confer new insights about the role of the respective structural modifications and to identify a possible common mechanism of action.

Here, it is shown that 592 transcripts are differentially regulated in HaCaT cells treated with Ino-C2-PAF, 250 trascripts are regulated by edelfosine and 132 transcripts by Glc-PAF. In general, most differentially expressed genes are up-regulated. Moreover, the main finding is given by the Gene Ontology (GO) analysis, which reveals an important role of APLs in lipid metabolism, immune and inflammatory response.

Although previous investigations demonstrated that APLs are able to inhibit the proliferation of several transformed cell lines (Fischer *et al.*, 2006; Hochhuth *et al.*, 1990; Roos and Berdel, 1986; Wieder *et al.*, 1995b; Wiese *et al.*, 2000), this gene expression analysis shows that Gene Ontology categories concerning cell proliferation are not significantly regulated. It was nevertheless possible to detect differentially expressed genes implicated in the regulation of cell proliferation. Among these genes, *CDKN1A* and *IGFBP3* represent putative targets which might contribute to the anti-proliferative activity of APLs (Edmondson *et al.*, 2005; Hager *et al.*, 2001; Hauser *et al.*, 2004; Massoner *et al.*, 2009). Otherwise, due to the restricted number of regulated genes for such important biological processes, one can suggest that APLs control these pathways basically upon post-translational modifications.

Comparison of the differentially expressed genes using Venn diagrams evidences that most targets of Glc-PAF are regulated by Ino-C2-PAF as well. The structural similarity between the two glycosidated APLs does not seem to be the main reason for this phenomenon. In contrast to Glc-PAF, Ino-C2-PAF shows a relative high number of genes in the intersection with edelfosine (Figure 4.5). Moreover, it has been previously shown that Ino-C2-PAF has an enhanced anti-proliferative capacity and a reduced cytotoxicity relative to Glc-PAF (Fischer *et al.*, 2006). Edelfosine and Ino-C2-PAF have similar effects on cell differentiation and cellular development. Additionally, Ino-C2-PAF modulates genes involved in the process of inflammation (see below).

Thus, it may be supposed that the different ability of alkylphospholipids to intercalate into the plasma membrane is correlated with their specific biological activity. In fact, stability and rigidity of ether lipid represent crucial factors for the insertion efficiency (Eibl, 1996). And, since the three tested APLs display the same alkyl chain length (18 carbon atoms), which is required for the entry of the drugs into the membrane (Geilen *et al.*, 1994; Wiese *et al.*, 2000), it was supposed that the slightly different hydrophilic character of the respective ether linked residues is responsible for their different penetration and, subsequently, biological activity. Indeed, previous investigations demonstrated that Ino-C2-PAF accumulates over a longer time in HaCaT cells compared to Glc-C2-PAF, which is related to Glc-PAF and has the same antiproliferative properties, and displays an enhanced metabolic stability (Fischer *et al.*, 2006).

5.2.1 APLs affect lipid biosynthesis and metabolism

GO analyses reveal significant enrichment for genes involved in lipid metabolism in transcripts that are up-regulated by Ino-C2-PAF and Glc-PAF. This is consistent with previous studies showing an up-regulated sterol biosynthesis in cells cultured in the

presence of amphiphiles, (Lange and Steck, 1994). This effect is produced by inhibiting the internalization of plasma membrane cholesterol, thereby reducing the pool of sterol in the endoplasmic reticulum, which regulates sterol responsive elements binding protein (SREBP) maturation (Lange *et al.*, 1999). Alkylphospholipids (APLs) might penetrate in the plasma membrane and interact with "sensor" proteins, such as multidrug-resistant (MDR) P-glycoproteins (Debry *et al.*, 1997; Luker *et al.*, 1999). Furthermore, this hypothesis is supported by the role of SREBP in the transcriptional regulation of genes encoding farnesyl diphosphate synthase (*FDPS*), fatty acid synthase (*FASN*) and stearoyl CoA desaturase-1 (*SCD*) (Guan *et al.*, 1995; Kim and Spiegelman, 1996; Lopez *et al.*, 1996), which are de-regulated by APLs as well. A similar regulatory mechanism was recently demonstrated in HepG2 cells. Edelfosine and miltefosine, even if in much higher concentrations (25 μM), increase indeed the level of genes expressing cholesterol-synthesizing enzymes, such as HMG-CoA synthase (*HMGCS1*), HMG-CoA reductase (*HMGCR*), farnesyl diphosphate synthase (*FDPS*) and farnesyl diphosphate farnesyltransferase-1 (*FDFT1*) (Carrasco *et al.,* 2010).

Surprisingly, edelfosine, which has been shown to insert into the plasma membrane and interact with lipids *in vivo* and *in vitro* (Ausili *et al.*, 2008; Busto *et al.*, 2007; Cabaner *et al.*, 1999; Dymond *et al.*, 2008; Gajate *et al.*, 2000a; Gajate and Mollinedo, 2001; Hac-Wydro *et al.*, 2009; Heczkova and Slotte, 2006; Zaremberg *et al.*, 2005), seems to have a reduced impact on the transcription of genes encoding elements of the lipid metabolism and biosynthesis.

5.2.2 APLs influence the immune and inflammatory response

In this work it is reported for the first time that glycosidated phospholipids negatively influence the immune and inflammatory response. Moreover, previous DNA microarray studies on inflammatory skin diseases suggest that APLs might exhibit an inhibitory/therapeutic activity on psoriasis, lupus erythematosus and systemic sclerosis.

Ino-C2-PAF demonstrates the strongest anti-inflammatory activity, inhibiting the expression of *PI3* (protease inhibitor 3, elafin), *SERPINA3*, *SERPINB1* and *DEFB4*. *PI3* is highly and specifically expressed in keratinocytes of psoriatic epidermis (Kamsteeg *et al.*, 2009; Schalkwijk *et al.*, 1993; Wiedow *et al.*, 1990), and in epidermal skin tumours (Pfundt *et al.*, 2001). High *SERPINA3* expression is associated with HLA-positive tumors, which are characterized by higher expression of genes associated with an inflammatory profile (Kloth *et al.*, 2008), whereas *SERPINB1* is over-expressed in invasive oral squamous cell carcinoma and promotes the migration of oral cancer cells (Tseng *et al.*, 2009). DEFB4 (Human β-defensin-2, hBD-2) is a peptide, mainly produced by the epithelium, that exhibits its killing

activity against bacteria, fungi and certain viruses. *DEFB4* plays a crucial role in host defense under infectious and inflammatory conditions, and its expression is increased in certain skin diseases such as psoriasis and atopic dermatitis (Weinberg *et al.*, 1998).

Furthermore, the anti-inflammatory activity of Ino-C2-PAF is confirmed by the down-regulation of several genes encoding members of class II of the major histocompatibility complex (*HLA-DM*, *HLA-DO*, *HLA-DP*, *HLA-DQ*, *HLA-DR*, *CD74*).
MHC class II products (HLA-DR, -DP, -DQ) are mainly restricted to the surface of B lymphocytes, macrophages and dendritic cells (Bryant and Ploegh, 2004). However, cytokine stimulation *in vitro* or the state of inflammation *in vivo* results in the induction of MHC class II expression on a variety of endothelial and epithelial cells, including keratinocytes (Gottlieb *et al.*, 1986), which represent non-professional antigen-presenting cells (Kim *et al.*, 2009; Nickoloff and Turka, 1994). Besides, the up-regulation of the MHC class II complex by keratinocytes in several dermatoses including psoriasis, allergic contact dermatitis, and atopic dermatitis has also been reported (Day, 1996; Gottlieb *et al.*, 1986; Krueger *et al.*, 1990; Lampert, 1984).
Enhanced expression of the class II major histocompatibility complex molecules is often used as marker of keratinocyte activation and they are also considered to have pathophysiologic importance. (Friedrich *et al.*, 2003; Gonzalez-Gay *et al.*, 1994; Krueger *et al.*, 1990). Importantly, Ino-C2-PAF, in addition to MHC class II genes, inhibits the expression of their regulator CIITA (MHC class II transactivator), which is a transcriptional coactivator and can only be detected in MHC class II-positive cells (Takagi *et al.*, 2006). Although previous immunohistochemical analyses showed that no or only few HaCaT cells expressed HLA-DR (class II MHC) at the cell surface under non-stimulated conditions or in resting keratinocytes (Middel *et al.*, 2000), these microarray analyses displayed significant processed signals (Table 4.2).
Further evidence of the influence of glycosidated phospholipids on the inflammatory response is represented by the down-regulation of *CTSB* and *CTSS* transcripts. In the skin, as well as in cultured HaCaT cells, MHC class II-mediated antigen presentation is regulated by cathepsins, which represents a group of 11 human cysteine proteases (among them CTSB and CTSS) (Deussing *et al.*, 2002; Schwarz *et al.*, 2002; Turk *et al.*, 2000).

5.2.3 APLs regulate expression of genes associated with migration and invasion

Unlike glycosidated phospholipids, edelfosine does not display significant anti-inflammatory potential, but rather induces the expression of genes implicated in cell differentiation, development, migration and invasion. Members of the family of matrix metalloproteinases are proteins involved in these processes and represent therapeutic targets for preventing tumor

initiation and progression.
Unfortunately, it is rather difficult to compare these results with other studies performed in skin models and keratinocytes cell cultures directly, because most of the experiments reported in the literature studied exclusively the post-translational regulation of these proteases on the basis of immunohistochemical analysis, Western blots and zymography.

MMP9 (gelatinase B), which is clearly up-regulated by edelfosine, exhibits proteolytic activity and plays a key role in tumour invasion and metastasis (Chambers and Matrisian, 1997; Sauter *et al.*, 2008) through degradation of extracellular matrices (Fidler *et al.*, 2007; Nelson *et al.*, 2000). The findings of this work are in agreement with previous investigations that reported also an increased invasion of colon cancer cells upon induction and activation of MMP9 after stimulation with edelfosine (Van Slambrouck *et al.*, 2007).
Beside *MMP9*, induced expression of *SERPINE1* and *SERPINE2* emphasizes the tumour-promoting role of edelfosine in HaCaT cells. In fact, SERPINE1 (plasminogen activator inhibitor-1) operates in the early stages of human skin carcinoma progression (Maillard *et al.*, 2005) and it is required for epithelial cell migration during wound repair (Providence and Higgins, 2004). Analogously, it was reported that SERPINE2 (protease nexin-1) mRNA is significantly elevated in several tumours, e.g. oral squamous cell carcinomas, mammary and colorectal cancers (Fayard *et al.*, 2009; Gao *et al.*, 2008; Selzer-Plon *et al.*, 2009).

Whereas expression of *MMP9* remaines unaltered, in cells treated with glycosidated phospholipids, particularly with Ino-C2-PAF, expression of other MMPs is down-regulated, namely *MMP1*, *MMP7*, *MMP10* and *MMP12*. MMP1 (collagenase 1) cleaves fibrillar type I collagen and is needed to initiate keratinocyte migration. The inhibition of MMP1 completely blocks the movement of keratinocytes (Pilcher *et al.*, 1997). Gene expression analysis has shown an enhanced transcription of *MMP1* in psoriasis (Wolk *et al.*, 2006). Furthermore, MMP1 plays also an important role in the mobility of skin cancer cell, such as tongue squamous cell carcinoma (Cao *et al.*, 2009). MMP7 (matrilysin) was significantly up-regulated in squamous cell carcinoma tissues (Kuivanen *et al.*, 2006; Weber *et al.*, 2007), and represents a marker of malignant transformation of epithelial cells (Karelina *et al.*, 1994). Similarly, epithelial expression of MMP12 (metalloelastase) in chronic wounds and skin cancers provides a diagnostic marker for distinguishing squamous cell carcinomas from non-malignant wounds and keratinocytes (Impola *et al.*, 2004; Kerkelä *et al.*, 2000). In addition, MMP12 may induce the inflammatory response in psoriatic lesions (Chandler *et al.*, 1996). Finally, a significant correlation between metastatic tumour spread and over-expression of matrix metalloproteinases MMP10 (stromelysin 2), as shown for MMP7, can be considered an unfavorable prognostic factor in many cutaneous neoplasms (Fernandez-Figueras *et al.*,

2007; Kren *et al.*, 2006).

5.2.4 APLs and inflammatory skin diseases

Interestingly, gene expression profiles of HaCaT cells treated with alkylphospholipids (APLs) show some analogies with the transcriptome of psoriatic lesional skin and other inflammatory skin diseases. Genes like *DEFB1*, *SPRR1A*, *SPRR2D*, *PDZK1IP1*, *CXCL2*, *IL-1*, *TGM1* which are up-regulated in psoriatic lesional skin and other inflammatory skin diseases (Bowcock *et al.*, 2001; Gudjonsson *et al.*, 2009; Kulski *et al.*, 2005; Nomura *et al.*, 2003) exhibit a significant down-regulation in HaCaT cells stimulated with Ino-C2-PAF. Moreover, the transcriptome of psoriatic tissue can be compared with the data from cultured keratinocytes exposed to the pro-inflammatory cytokine interleukin-1α (IL-1α) and the Th1 cytokine interferon-γ (IFN-γ) (Mee *et al.*, 2007).

A hypothetical anti-psoriatic role of Ino-C2-PAF is supported by an alternative analysis of the microarray data. Reanalyzing the processed signals revealed a new set of genes (i.e. *S100A7-9* and *IL-8*, Table 4.2), which are distinctly down-regulated by APLs. These transcripts represent gene markers in several auto-inflammatory diseases and they are clearly up-regulated in psoriatic keratinocytes (Bowcock *et al.*, 2001; Oestreicher *et al.*, 2001; Quekenborn-Trinquet *et al.*, 2005).

5.3 Influence of Ino-C2-PAF on PI3K signalling cascade

Proliferation assays and detection of the phosphorylation state of Akt/PKB, a serine/threonine protein kinase activated by phosphatidylinositol 3-kinase (PI3K), demonstrated that Ino-C2-PAF affects the PI3K signalling cascade.

Wortmannin, a potent inhibitor of PI3K, only marginally inhibits the proliferation of HaCaT cells. In addition, the effect of wortmannin is comparable to the impact of 2.5 µM of Ino-C2-PAF. However, when incubated together, wortmannin does not increment the inhibitory effect of Ino-C2-PAF (Figure 4.3). These results suggest that Ino-C2-PAF either directly affects the PI3K activity and inhibits its translocation to the plasma membrane, or exert a drastic change in the membrane composition that prevents the interaction of PI3K to PIP2, and the subsequent phosphorylation to PIP3.

Immunoblotting analysis with Insulin-Growth Factor-1 (IGF-1; Figure 4.9), an activator of PI3K upon binding to IGF-1 receptor at the cell membrane (Frasca *et al.*, 2008), and wortmannin confers further evidence on the inhibitory role of Ino-C2-PAF on the PI3K pathway, but an alternative mechanism is proposed. Ino-C2-PAF might act at the plasma

membrane interfering with the function of receptor tyrosine kinases (RTKs), which is then necessary for PI3K activation. In fact, Ino-C2-PAF is able to reduce the effect of IGF-1, but it is not capable to induce Akt/PKB activation in the presence of wortmannin.

Nonetheless, the PI3K pathway does not seem to be the unique pathway controlled by Ino-C2-PAF since 5 µM Ino-C2-PAF causes a much stronger inhibition of HaCaT cells proliferation than wortmannin and 2.5 µM Ino-C2-PAF together. This outcome indicates that a higher amount of Ino-C2-PAF may interact also with components of other signalling pathways controlling proliferation and cell-growth, such as MAPK pathways.

5.4 Influence of Ino-C2-PAF on MAPK signalling cascades

Mitogen-activated protein kinase (MAPK) pathways are kinase modules that link extracellular signals to the machinery that controls fundamental cellular processes such as growth, proliferation, differentiation, migration and apoptosis (Dhillon *et al.*, 2007; see Introduction for pathway description). Moreover, MAPKs play a critical role in the development and progression of cancer. For these reasons, MAPK pathways are other well-studied signalling cascades in context of antitumour lipids (Gajate *et al.*, 1998; Hideshima *et al.*, 2006; Na and Surh, 2008; Ruiter *et al.*, 2002; Samadder *et al.*, 2003). Whereas edelfosine inhibits the phosphorylation state of ERK1/2 (Na and Surh, 2008; Ruiter *et al.*, 2002; Zhou *et al.*, 1996), Ino-C2-PAF, similarly to perifosine in multiple myeloma cells (Hideshima *et al*., 2006), induces the ERK1/2 activation. Nonetheless, the phosphorylation of ERK1/2 appears to be biphasic in both Ino-C2-PAF-treated and untreated control cells. Although normally induced by mitogens, this biphasic activation of ERK1/2 consists of a rapid and strong burst of kinase activity peaking at 5-10 min followed by a second wave of lower but sustained activity that persists throughout the G1-phase (Kahan *et al.*, 1992; Meloche, 1995; Meloche *et al.*, 1992). Interestingly, the activation peak in the first 10 min after incubation with APL was also observed for edelfosine in A431 epidermoid carcinoma cells (Ruiter *et al*., 2002). Hence, the first peak could be interpreted as an unspecific activation that is not exclusively triggered by mitogens but also by a slight change in the cellular environment (e.g. fresh medium or washing steps).

The simultaneous activation of JNK/SAPK, p38 and ERK1/2 displays the strong effect of Ino-C2-PAF on this family of kinases, although the three MAPK pathways participate in separated cellular processes and are activated by distinct molecules. In cancer therapy, the stress-activated JNK/SAPK pathway plays an important role in promoting apoptosis (Kennedy *et al*., 2003), and JNK/SAPK activation represents a crucial step in the pro-

apoptotic process induced by APLs in tumour cells (Gajate *et al.*, 1998; Hideshima *et al.*, 2006; Nieto-Miguel *et al.*, 2006; Ruiter *et al.*, 1999). However, as already shown for edelfosine in non-small and small cell lung carcinoma cell lines, APL-induced changes in JNK/SAPK, ERK1/2, or p38, could not be good predictors of cell susceptibility to APL-induced cytotoxicity (Shafer and Williams, 2003).

Surprisingly, the induction of ERK1/2 phosphorylation by Ino-C2-PAF or by ERK1/2-activator EGF was almost identical. Moreover, whereas edelfosine represses EGF-induced ERK1/2 activation after 10 min incubation (Zhou *et al*., 1996), Ino-C2-PAF does not exhibit any influence on ERK1/2 phosphorylation in combination with EGF. These results suggest that Ino-C2-PAF might directly interact with EGFR (epidermal growth-factor receptor) and induce its ligand-independent activation. Alternatively, Ino-C2-PAF might activate the membrane-associated Ras through the recruitment of SOS (son of sevenless), a Ras-activating guanine nucleotide exchange factor. However, experiments with specific inhibitors in order to verify this statement are required.

A ligand-independent activation of plasma membrane receptors in the presence of ATLs does not represent a novel mechanism. In fact, Mollinedo and coworkers have proposed that apoptosis induction in lymphoid tumour cells by edelfosine proceed via engagement of the Fas/CD95 death receptor independent from its natural ligand (Gajate *et al.*, 2004; Gajate *et al.*, 2000; Gajate and Mollinedo, 2007). Therefore, after translocation into lipid raft clusters, Fas/CD95 mediates apoptosis through its intracellular activation by edelfosine (Mollinedo and Gajate, 2006; Nieto-Miguel *et al.*, 2006).

5.5 Influence of Ino-C2-PAF on cell migration and actin cytoskeleton

Cell migration is an essential process in all multicellular organisms and is not only important during development, but also throughout life such as in wound repair and during immune surveillance. Moreover, cell migration plays a fundamental role in angiogenesis, tumour invasion and metastasis. Dynamic polarization of cells in response to growth factors and extracellular matrix interactions, formation of cell protrusions and focal adhesions at the leading edge, reorientation of the Golgi and microtubule organizing center, and coordination of focal adhesion disassembly at trailing cell regions are required for cell motility (for review see Vicente-Manzanares *et al.*, 2005).

Cell locomotion can be triggered by signals generated by receptors that participate in adhesion and receptors for cytokines and growth factors. The former mode of motility is

referred to as haptokinesis and haptotaxis, while the latter is constituted by chemokinesis and chemotaxis (Wells, 2000).

As already pointed out at the beginning of the discussion, Ino-C2-PAF inhibits the migration of both HaCaT and SCC25 cells. Moreover, Ino-C2-PAF-treated subconfluent keratinocytes, which were stained with phalloidin-CPITC, exhibit a failed polarized migration that is characterized by the absence of defined lamellipodia and by the presence of F-actin stress bundles. This phenomenon could be caused by alteration of the Rho GTPases activation and localization within the cell. Indeed, Rac and Cdc42 control the formation of the lamellipodium at the leading edge, generating a protrusive force through the localized polymerization of actin. Furthermore, Cdc42 is required for the establishment of cell polarity. Therefore, Ino-C2-PAF might inactivate the GTPase Rac directly or by inhibiting the function of their specific GEFs and GAPs. Alternatively, Ino-C2-PAF may affect other proteins that regulate actin dynamics and organization, such as vasodilator-stimulator phosphoprotein (VASP), Wiskott-Aldrich syndrome protein (WASP), profiling and the Arp2/3 complex, which are localized to the periphery of protruding lamellipodia (Castellano *et al.*, 2001; Machesky *et al.*, 1997; Reinhard *et al.*, 1992; Rottner *et al.*, 2001).
Further evidence on the possible role of Ino-C2-PAF on the activity of Rho GTPases is provided by former investigations. In haptotactic migration assays, it has been demonstrated that the inhibition of migration induced by Ino-C2-PAF could be rescued by transfection of a constitutively-active variant of Rac1 or partially rescued by inhibition of the RhoA signalling pathway (Fischer, PhD thesis FU Berlin, 2006).

Although APLs negatively affect keratinocyte polarization, they might induce the activity of Cdc42 as well. Indeed, Ino-C2-PAF-treated cells exhibit long filopodia (Figures 4.14 and 4.15). In epithelial cells, filopodia, which are generated by Cdc42 at the front of migrating cells (Nobes and Hall, 1995), seem to play a direct role in establishing intimate contacts between neighbouring cells to drive cell-cell junction assembly. Normally, these cell-cell contacts lead to cell polarization (Vasioukhin *et al.*, 2000), but in the presence of Ino-C2-PAF, subconfluent cells still display a round shape and adherens junctions assembly is prevented.

In vitro, haptotactic migration can be simply generated by scratching (wounding) a cell monolayer, which induces the coordinated movement of sheets of cells. Ino-C2-PAF-treated cells at the wound edge show neither a defined lamellipodiium nor filopodia. Nonetheless, adherent cells exhibit an increased cortical actin. It is well established that members of the WASP family serve as effector proteins for Cdc42 and Rac-mediated cortical actin

polymerization by directly binding to and activating the actin nucleation activity of the actin related protein Arp2/3 complex (Higgs and Pollard, 1999). Furthermore, activated Rac is necessary for actin recruitment and anchoring to clustered cadherin receptors (Braga *et al.*, 1999; Lambert *et al.*, 2002), whereas Cdc42 induces actin accumulation at junctions without the participation of E-cadherin (Kodama *et al.*, 1999; Stoffler *et al.*, 1998; Takaishi *et al.*, 1997). The effect of this process is an increased cell-cell adhesion and diminished migration. Thus, in particular for Rac and Cdc42 regulation, these findings suggest that Ino-C2-PAF possess a dual mechanism that controls the function of Rho GTPases: inhibition at the cell front and activation at the cell-cell contacts.

Interestingly, SCC25 cells, which are highly invasive, display a greater “innate” cell-cell adhesion that caused several complications during wound insertion in the cell-monolayer. Subsequently, under subconfluent conditions, SCC25 cells exhibit an elevated presence of cortical actin between neighbouring cells that are freshly adherent and only few single cells.

Comparative studies using nocodazole and colchicine revealed that Ino-C2-PAF might induce the activity of Rho. It is well known that nocodazole and colchicine disrupt microtubules and activate Rho, which is then responsible for a general increase in cell contractility and for the formation of stress fibres and focal adhesion (Bershadsky *et al.*, 1996; Liu *et al.*, 1998; Palazzo and Gundersen, 2002). Although Ino-C2-PAF does not seem to interfere with the microtubular network, it exhibits a very similar effect on the actin cytoskeleton. However, a reversible interplay between actin and microtubule cytoskeletons is not strictly necessary. Actually, disruption of microtubules perturbs the polarity of the actin cytoskeleton (Omelchenko *et al.*, 2002; Palazzo and Gundersen, 2002), whereas actin depolymerization does not affect the polarization of the microtubule cytoskeleton (Etienne-Manneville and Hall, 2001; Magdalena *et al.*, 2003; Palazzo *et al.*, 2001).

HaCaT cells treated with Ino-C2-PAF exhibit three different phenotypes: strong cortical F-actin at the cell periphery, an inexistent or totally disrupted cytoskeleton and, F-actin stress fibres that cross each other at the cell centre and connect cell contacts (Figure 4.14, panel C). A plausible explanation is the cell cycle-dependent insertion of APL into the plasma membrane. Lipid composition at the plasma membrane undergoes a remodelling during cell cycle and might temporarily and spatially control the course of several signalling cascades that regulate the most prominent cellular function. For example, changes in cholesterol and sphingomyelin content in early G1 can alter the membrane fluidity (Kojima, 1993). Analogously, variations in the composition of the plasma membrane could explain the different effects of APLs between malignant neoplastic cells and their normal counterparts.

Finally, beside increased cortical actin and unpolarized F-actin bundles, HaCaT cells display F-actin stress fibres with large tips that cross each other. This “star-like” organization of F-actin fibres show similarities with the actin cytoskeleton of integrin β1 null keratinocytes (Raghavan *et al.*, 2003).

5.6 Influence of Ino-C2-PAF on FAK/Src signalling cascade

Integrin-linked focal adhesion complexes provide the main sites of cell adhesion to extracellular matrix (ECM) and associate with the actin cytoskeleton to control cell movement. These functions are primarily regulated by non-receptor tyrosine kinases like the focal adhesion kinase (FAK) and Src. In skin cells, FAK controls cytoskeletal dynamics and focal adhesion disassembly. Therefore, the reduction in cellular motility caused by Ino-C2-PAF may be due to the inhibition of FAK autophosphorylation on tyrosine residue 397. In turn, the consequent reduction in Src activation negatively affects the disassembly of focal complexes and results in enlarged focal adhesions. Accordingly, FAK-null keratinocytes display perturbed motility and fail to emigrate out of skin explants (Schober *et al.*, 2007). Ino-C2-PAF appears to exclusively down-regulate the activation state of FAK and Src without affecting their complex.
The effect of Ino-C2-PAF on the activity of FAK and Src was confirmed by the transient transfection of keratinocytes with constitutive activated forms of FAK and Src, where the migration is partially recovered. However, differences between HaCaT and SCC25 cells are detectable, which allude to a distinct efficiency of Ino-C2-PAF in both cell lines.

Controversely, other studies with APLs, such as edelfosine, reported an induction of migration and invasion of human HCT-8/S11f colon cancer cells. This effect appears to be linked to β1-integrin and is characterized by increased phosphorylation of Src and FAK (Van Slambrouck *et al.*, 2007). Moreover, the pro-invasive and pro-migratory activity of edelfosine is also supported by microarray analyses in HaCaT cells. The evaluation of significantly up-regulated transcripts by edelfosine revealed that this phospholipid analogue positively regulates pathways that are involved in cell differentiation, development and motility (Figure 4.7).

Data obtained by Western blotting and immunofluorescence analysis are fundamental to identify how Ino-C2-PAF acts on phosphorylated focal adhesions. Primarily, Ino-C2-PAF reduces the turnover (i.e. assembly/disassembly of focal complexes and adhesions) of focal

adhesion contacts through the inhibition of FAK autophosphorylation at the wound edge during wounding closure. Although FAK recruitment to focal adhesion contacts is associated with increased FAK tyrosine phosphorylation (Zaidel-Bar *et al*., 2003), focal adhesion contacts are also formed in FAK null fibroblasts, which indicates that FAK activity is not essential for the process of focal adhesion formation (Ilic *et al.*, 1995). However, focal adhesion contacts in FAK-/- cells are formed primarily around the cell periphery, enmeshed in a cortical actin ring, and do not undergo a normal maturation cycle (Sieg *et al.*, 1999). FAK re-expression in FAK-/- cells promotes the reorganization of the immature focal adhesion contacts, which allows for their connection to actin stress fibres, therefore mediating cell contractility and cell polarization (Sieg *et al*., 1999). In addition, as seen in squamous cell carcinoma and lung carcinoma, FAK over-expression and activity within invadopodia, which are cell extensions enriched with integrins and matrix metalloproteinases (MMPs), is associated with an invasive cell phenotype (Hauck *et al.*, 2001; Hsia *et al.*, 2003; Schneider *et al.*, 2002). Therefore, the inhibition of FAK activity appears to be essential in the anti-migratory action of Ino-C2-PAF.

Even though Ino-C2-PAF inhibits Src activation at the focal adhesions, it increases total tyrosine and Src phosphorylation between neighbouring cells. It is known that Src plays an important role in regulation of adherens junction integrity and function through its ability to modulate cadherin-catenin complexes needed for these cell-cell connections (Wadhawan *et al.*, 2010). There is evidence that Src can modulate the expression of cadherin at the cell membrane. Moreover, Src can alter turnover and degradation of E-cadherin as well as phosphorylation (particularly on tyrosine) of catenin proteins, which facilitate the association of cadherins with the actin cytoskeleton. However, it was demonstrated that in endothelial cells Src-induced tyrosine phosphorylation of VE-cadherin is not sufficient to promote junctional disassembly (Adam *et al.*, 2009). Besides, Src is involved in the formation of adherens junctions induced by nectin, a cell adhesion molecule that forms cell-cell contact cooperatively with cadherins (Fukuyama *et al.*, 2005). In fact, also in HaCaT and SCC25 cells, induction of Src phosphorylation at cell-cell contacts by Ino-C2-PAF is accompanied by an increased localization of E-cadherin and cortical actin.

As indicated above, in FAK-null fibroblasts or cells expressing inactive FAK mutants severe focal adhesion turnover defects could be observed (Lim *et al.*, 2008; Webb *et al.*, 2004). Moreover, FAK-null fibroblasts exhibit motility defects in part as a result of elevated Rho activity, which subsequently leads to increased focal contact formation, and the inability to remodel contact sites in response to various motility stimuli (Chen *et al.*, 2002; Ren *et al.*, 2000; Schlaepfer *et al.*, 2004). Thus, increased activity of Rho results in increased focal

adhesion lifetime. Accordingly, in FAK+/+ cells co-transfected with activated Rho (V14Rho), focal adhesion turnover was dramatically reduced which leads to the formation of enlarged focal complexes (Ren et al., 2000). In live imaging assays a very similar phenotype is obtained in HaCaT cells transiently transfected with GFP-FAK that were concomitantly incubated with Ino-C2-PAF. These results support the hypothesis that glycosidated phospholipids influence the function of Rho.
In this context, the GTPase activating protein p190RhoGAP could play an essential role. Inhibition of FAK activity by Ino-C2-PAF might result in reduced tyrosine phosphorylation of p190RhoGAP, which in turn is necessary for inactivation of Rho and formation of new focal contacts that are needed for lamellipodia formation. Moreover, it has been shown that the FAK-p190RhoGAP interaction is important in promoting cell polarity (Tomar *et al.*, 2009).

Also the inhibition of Akt/PKB phosphorylation by Ino-C2-PAF at the leading edge of migrating HaCaT cells could be a direct consequence of reduced activity of FAK. In fact, FAK is also implicated in the activation of PI3K and its localization at the cell front. It was demonstrated that FAK Tyr397 represents the binding site for the p85 subunit of PI3K (Chen *et al.*, 1996). Subsequently, PI3K association with FAK plays a positive role in cell migration and might be involved in cell proliferation and survival as well (Cary and Guan, 1999). However, PI3K might be alternatively activated in a FAK-independent manner. Cell migration stimulated by Rac or Cdc42 is also dependent on PI3K, and a constitutively active PI3K construct promotes migration on collagen (Keely *et al.*, 1997). Rac itself can stimulate the recruitment and/or activation of PI3K at the plasma membrane, which then acts upstream of Rac by PI(3,4,5)P3-sensitive Rac GEFs (Srinivasan *et al.*, 2003; Welch *et al.*, 2003).

5.7 Influence of Ino-C2-PAF on cell adhesion

Generally, in comparison to cell proliferation and apoptosis, the influence of APLs on cell adhesion, and consequently cell migration, was only marginally investigated. Whereas the impact of Ino-C2-PAF on cell adhesion and integrin expression in HaCaT cells was basically analyzed in previous studies (Fischer, PhD thesis FU Berlin, 2006), little was known about the effect of this glycosidated phospholipid on cell adhesion of malignant SCC25 cells.

As already demonstrated in HaCaT cells, Ino-C2-PAF increases the adhesion of SCC25 cells to several extra-cellular matrices. Nonetheless, adhesion of Ino-C2-PAF-treated HaCaT cells to collagen IV (70% relative to untreated cells versus a 43% increase exhibited by SCC25 cells), fibronectin (40% versus 23%) and laminin (40% versus 15%) is markedly stronger than of SCC25 cells.

Cell-matrix adhesion is principally mediated by integrins, which are members of a glycoprotein family. Integrins are heterodimeric cell-surface receptors generated by selective pairing between α and β subunits that are non-covalently linked. Generally, each subunit has a large extracellular domain, a transmembrane strech and a short, non-catalytic cytoplasmic tail. The distinct integrin receptors bind extracellular matrix ligands with different affinities (Hynes, 2002; Luo *et al.*, 2007).
The dynamic regulation of cell-matrix adhesion mainly depends on affinity, avidity and valency. The overall strength of cellular adhesiveness (i.e. avidity) is governed by the intrinsic affinity of the individual receptor-ligand bonds, and the number of these bonds (valency). Valency is governed by the density of receptor and ligand on the adhesive surfaces, the geometric arrangement of those surfaces, and the ability of the receptor and ligand to move, either passively or actively, from other parts of the cell into the zone of cell adhesion (Carman and Springer, 2003).

In HaCaT cells, Ino-C2-PAF induces cell-matrix adhesion without significantly affecting the transcriptional expression of genes related with integrin-subunits. However, former FACS experiments showed that Ino-C2-PAF increases the expression of α6 and β4 subunits at cell-surface of HaCaT cells, while expression of α3 and β1 subunits, as well as all tested integrin subunits in SCC25 cells, remain unchanged (Fischer, PhD thesis FU Berlin, 2006).

Ino-C2-PAF-treated HaCaT and SCC25 cells exhibit a stronger adhesion to collagen IV, which is mainly mediated by integrin heterodimers containing the β1 subunit (Humphries, 1990). Increased adhesion is further confirmed in HaCaT cells transfected with GFP-FAK and consequently treated with Ino-C2-PAF, which build stable focal adhesions and provide evidence of a defective focal complex turnover. Nevertheless, the 12G10 antibody that recognizes the high-affinity state of β1 integrin subunit could not demonstrate an increased affinity of the integrin β1, and it indicates that a rise in avidity in Ino-C2-PAF-treated cells seems to be responsible for increased cell-matrix adhesion. This hypothesis is also supported by previous investigations. Immunofluorescence analyses showed that Ino-C2-PAF induces clustering of integrin β1 subunits on the cell surface of both HaCaT and SCC25 cells (Fischer, PhD thesis FU Berlin, 2006). Although clustering is often taken as positive evidence for valency regulation, it might be accompanied by an increased affinity of β1 or other subunits.

Beside the interaction between cell and extracellular matrix, epithelial cells are characterized by a strong intercellular cell-cell adhesion mediated by particular junctions. These

interactions are implicated in numerous cellular processes such as tumour progression and invasiveness (Makrilia *et al.*, 2009). Classical cadherins are versatile cell–cell adhesion receptors. As type 1 membrane glycoproteins, they function as dynamic calcium-dependent membrane-spanning macromolecular complexes (Goodwin and Yap, 2004). The extracellular regions are responsible for adhesive recognition, binding to the ectodomains of other cadherins presented on neighbouring cells (Leckband and Prakasam, 2006). On the other side of the plasma membrane, the cadherin cytoplasmic tails interact with a range of proteins that link the cadherin receptor to fundamental intracellular processes, including the actin cytoskeleton, cell signalling and trafficking (Bryant and Stow, 2004; Mege *et al.*, 2006; Yap and Kovacs, 2003).

Normal E-cadherin (epithelial) expression and function is of paramount importance in the maintenance of epithelial integrity and polarity (Larue *et al.*, 1994). Loss of expression and/or abnormal function of E-cadherin lead(s) to loss of cell polarity and disarrangement of normal tissue architecture (Karayiannakis *et al.*, 1998; Karayiannakis *et al.*, 2002). Studies have established that in most cancers of epithelial origin, E-cadherin-mediated cell–cell adhesion is lost concomitantly with the acquisition of an invasive and aggressive phenotype (Cavallaro and Christofori, 2004).

Therefore, in HaCaT cells, the anti-cancer activity of Ino-C2-PAF is further proved by its capacity to increase the localization of E-cadherin at cell-cell contacts, which is supported by accumulation of cortical actin. This process is not correlated to an effect of E-cadherin gene expression.

Cell-cell adhesion is influenced by other APLs as well. On the one hand, edelfosine is able to restore the E-cadherin function in the adhesion-deficient MCF-7/6 cells (Steelant *et al.*, 1999). On the other hand, edelfosine induces a loss of cell-cell adhesion and stimulates the invasion of MCF-7 breast cancer cells into collagen type I, which results in the inhibition of E-cadherin-mediated adhesion by episialin in membrane microdomains (Steelant *et al.*, 2001; Van Slambrouck *et al.*, 2008). Moreover, the trans-epithelial electrical resistance of human colorectal cancer cell layers T84 revealed that edelfosine reversibly opens epithelial tight junctions (Leroy *et al.*, 2003).

Finally, the formation of cadherin-based cell-cell junctions has been associated with FAK signalling, and the activity of the FAK/Src complex promotes the disruption of colon carcinoma cell homotypic adhesions (Irby and Yeatman, 2002). Therefore, E-cadherin-mediated cell-cell adhesion induced by Ino-C2-PAF may be partly associated with its effect on FAK and Src activation.

5.8 Model for the mechanism of action of Ino-C2-PAF during cellular motility

The data obtained in this work permit to develop a model describing the inhibitory activity of antitumour lipids on cell motility.

Under normal conditions, haptotactic cell migration is characterized by dynamic focal adhesion turnover and the formation of a lamellipodium (Figure 5.1; Panel A). After binding to the extracellular matrix (ECM), integrin beta 1 recruits FAK, which is activated by auto-phosphorylation at the tyrosine 397 (Y397) and thereby allows the binding and activation of Src by phosphorylation of tyrosine 418 (Y418). The activated FAK/Src complex phosphorylates other kinases and GEFs/GAPs (for a more detailed description see Figure 1.9), which in turn elicit a cascade of events that lead to the activation of Rac and Cdc42, and to the inhibition of RhoA.

In the presence of Ino-C2-PAF, the cell movement is markedly reduced displaying persistent, enlarged focal adhesions, defective membrane protrusions and impaired cell polarity (Figure 5.1; Panel B). Ino-C2-PAF, due to its amphiphilic character, is incorporated into the plasma membrane, where it is accumulated. The accumulation leads to a changed lipid environment, which is accompanied by an increased avidity (cellular adhesiveness) and valency (number of receptor-ligand bonds) of integrin molecules. In addition, Ino-C2-PAF accumulation presumably affects also membrane targeting of crucial signalling components such as Src and small GTPases. Subsequently, downstream events like tyrosine phosphorylation of the FAK/Src complex and other signalling pathway components are disturbed. The effect might a destabilization of the balance between the three Rho GTPases, which could be characterized by RhoA activation and inhibition of Rac and Cdc42.

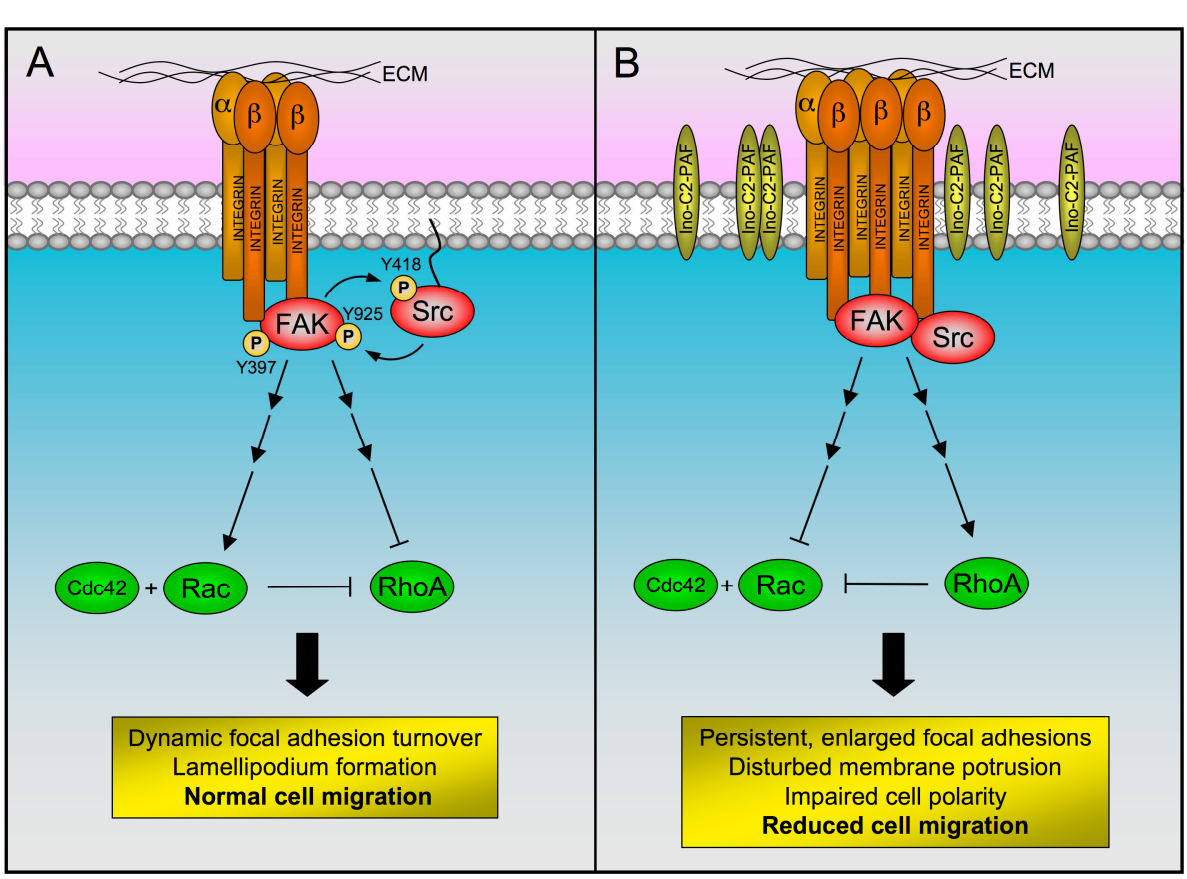

Figure 5.1. Schematic representation of the proposed model for the mechanism of action of Ino-C2-PAF. Haptotactic cell migration in the absence (A) or presence of Ino-C2-PAF (B). Arrows disposed in series indicate a signalling pathway. (A) Normal cell migration initiates at the plasma membrane through the interaction between extracellular matrix (ECM) and integrin, which leads to the activation of FAK/Src complex by phosphorylation. Afterwards, activation of other signalling pathway components induce the activation of Rac and Cdc42, and the inhibition of RhoA. (B) Accumulation of Ino-C2-PAF into the plasma membrane decreases FAK/Src complex phosphorylation and, consequently, it might be responsible for the inhibition of Rac and Cdc42 and the activation of RhoA.

5.9 Outlook

APLs exhibit an impact on gene expression profile of HaCaT cells and modulate genes involved in the processes of cell differentiation and lipid metabolism. In addition, expression of genes related to inflammatory response is inhibited by Ino-C2-PAF. However, these promising data have to be evaluated and confirmed in appropriate models in further studies. The simplest experimental design is represented by the stimulation of keratinocytes with IL-1α and IFN-γ, in order to mimic an immune response and, consequently, the expression profile of autoimmune diseases of the skin (Mee *et al*., 2007). Furthermore, considering chronic skin diseases such as psoriasis, the use of *in vitro* and *in vivo* models in the presence of Ino-C2-PAF would be very helpful. Recently, a novel *in vitro* model of psoriasis produced by tissue engineering has been developed and characterized. In this model, sheets of fibroblasts were superimposed creating a new dermis upon which keratinocytes are

seeded, leading to a complete bilayered skin substitute (Jean *et al.*, 2009). Although there is no naturally occurring disorder in laboratory animals that simulate the phenotype of psoriasis, among the *in vivo* models ((Gudjonsson *et al.*, 2007; Schön, 1999), there are animal models primarily consisting of grafting human psoriatic skin on athymic (Fraki *et al.*, 1983) or on severe combined immunodeficiency (SCID) mice (Raychaudhuri *et al.*, 2001).

Cell movement is governed by many processes. Nonetheless, the cytoplasmic tyrosine kinases FAK and Src regulate only some of them. Therefore, the mechanisms that modulate cell morphology controlled by Ino-C2-PAF have to be further investigated. Moreover, in the context of APLs, this topic is particularly fascinating because it is nearly unexplored.
First of all, the role of Rho GTPases in the presence of Ino-C2-PAF could be clarified by pull-down assays. These experiments might explain whether Ino-C2-PAF-induced reorganization of the F-actin cytoskeleton is dependent on Rho GTPases. Then, since integrins regulate targeting of Rac and Rho GTPases to the plasma membrane via lipids rafts and their coupling to downstream effector molecules (del Pozo *et al.*, 2004), localization of Rac, Rho and Cdc42 at the cell membrane in cells incubated with Ino-C2-PAF can be analyzed by subcellular fractionation. Finally, association of Rho GTPases with cholesterol-enriched membrane microdomains could be detected by isolation of lipid rafts using sucrose gradient centrifugation.

The synthesis of a fluorescently-labeled Ino-C2-PAF could answer many questions about its localization at the plasma membrane and within the cell.

6 SUMMARY

Synthetic alkylphospholipids represent a new class of drugs with antiproliferative properties in tumour cells. These compounds do not interfere with the DNA or mitotic spindle apparatus of the cell. Instead, they are incorporated into cell membranes, where they accumulate and interfere with lipid metabolism and lipid-dependent signalling pathways. Moreover, it has been shown that APLs are able to interfere with a variety of key enzymes implicated in cell growth, motility, invasion and apoptosis.
Recently, a novel group of synthetic alkylphospholipids, the glycosidated phospholipids, has been presented. Members of this subfamily also exhibit antiproliferative capacity and modulate the adhesion, differentiation, and migration of tumour cells. Among this group, Ino-C2-PAF shows the highest efficacy and low cytotoxicity.

To understand the mechanism of action of Ino-C2-PAF, and APLs in general, genome-wide gene expression analyses in skin keratinocyte cell line HaCaT were performed. For the first time, using Agilent cDNA microarray technology, global gene expression profiles of HaCaT cells treated with Ino-C2-PAF, the structurally related glycosidated phospholipids Glc-PAF or the APL prototype edelfosine have been compared with the profile of control cells. It has been found that Ino-C2-PAF has the strongest influence on the gene expression in comparison to edelfosine and Glc-PAF. Gene ontology analysis revealed that differentially expressed transcripts regulated by the three APLs are mainly implicated in lipid metabolism, lipid biosynthesis, cell differentiation, cell development and ion homeostasis. Nevertheless, the most remarkable finding is represented by the ability of Ino-C2-PAF to down-regulate a broad spectrum of genes associated with the regulation of the innate and the acquired immune response and of genes linked to inflammation.

Beside transcriptional regulation, in HaCaT and SCC25 cells, a transformed keratinocyte line derived from a squamous cell carcinoma, Ino-C2-PAF acts as Biological Response Modifier (BRM), and regulates proliferation and migration by controlling important signalling pathways at the post-translational level. Indeed, Ino-C2-PAF influences the activity of Akt/PKB and MAPKs. Moreover, Ino-C2-PAF affects the total tyrosine phosphorylation at focal adhesion sites, which is accompanied by inhibition of the cytoplasmic tyrosine kinases FAK and Src, key regulators of cellular motility. Transient transfection of constitutively active variants of FAK and Src could in part bybass the inhibitory effect of Ino-C2-PAF.
Furthermore, the decrease in motility is accompanied by a redistribution of the F-actin cytoskeleton and increased cell-matrix adhesion. The latter depends mainly on a raised

integrin avidity and valency than a change in affinity of integrins. Nonetheless, the antitumour role of Ino-C2-PAF is also characterized by an increased localization of E-cadherin at cell-cell contacts.

In summary, these results describe Ino-C2-PAF as a promising APL candidate for the development of a therapeutic drug for treatment of auto-inflammatory, hyperproliferative and migration-based skin diseases.

7 ZUSAMMENFASSUNG

Synthetische Alkylphospholipide (APL) repräsentieren eine neue Wirkstoffklasse die antiproliferative Eigenschaften bei Tumorzellen aufweist. Im Gegensatz zu den klassischen Cytostatika, die mit der DNA interferieren und die Ausbildung des mitotischen Spindelapparates und die DNA-Sythese stören, interkalieren APLs mit der zellulären Membran, wo sie akkumulieren und den Lipid-Metabolismus und Lipid-abhängige Signalkaskaden stören. Weiterhin wurde gezeigt, dass APLs eine Vielfalt von Schlüsselenzymen beeinträchtigen, die das Zell-Wachstum, die Zell-Motilität, die Invasion und die Apoptose regulieren.
Kürzlich wurde eine neue Gruppe von APLs, die sogenannten glykosidierten Phospholipide vorgestellt. Mitglieder dieser Familie zeigen antiproliferative Eigenschaften und modulieren die Zelladhesion, die Differenzierung und die Migration von Tumorzellen. Von allen Mitgliedern dieser Gruppe zeigt Ino-C2-PAF die höchste Effizienz und die niedrigste Zytotoxizität.

Um den Wirkungsmechanismus von Ino-C2-PAF und APLs im allgemeinen besser zu verstehen, wurden in der Keratinocyten-Zelllinie HaCaT genomweite Genexpressionsanalysen durchgeführt. Erstmalig wurden mit Hilfe der Agilent cDNA Microarray-Technologie die globalen Genexpressionprofile von HaCaT-Zellen, die mit Ino-C2-PAF, dem strukturell verwandten glycosylierten Phospholipid Glc-PAF oder dem APL Prototypen Edelfosine behandelt wurden mit dem Genexpressionprofil unbehandelter Kontrollzellen verglichen. Dabei stellte sich heraus, dass Ino-C2-PAF im Vergleich zu Edelfosine und Glc-PAF den grössten Einfluss auf die Genexpression besitzt. Die Gene Ontology Analyse zeigte, dass die Transkripte die durch die drei APLs differentiell exprimiert wurden eine Rolle im Lipidstoffwechsel, der Zelldifferenzierung, der Zellentwicklung und der Ionenhomöostase spielen. Bemerkenswert ist die Fähigkeit von Ino-C2-PAF ein breites Spektrum von Genen herunterzuregulieren, die sowohl mit der Kontrolle der angeborenen und erworbenen Immunantwort als auch mit Entzündungsreaktionen assoziiert sind.

Neben der transkriptionellen Regulation in HaCaT- und SCC25-Zellen wirkt Ino-C2-PAF als Biologischer Reaktionsmodifikator (BRM). Als solcher reguliert er die Proliferation und Migration indem er wichtige Signalwege auf der posttranslationalen Ebene kontrolliert. So beeinflusst Ino-C2-PAF die Aktivität von Akt/PKB und MAP Kinasen und beeinträchtigt die gesamte Tyrosinphosphorylierung an fokalen Adhäsionen. Hierzu inhibiert Ino-C2-PAF die Aktivität der zytoplasmatischen Tyrosinkinasen FAK und Src, die Schlüsselenzyme der

Zellbewegung sind. Transiente Transfektion der konstitutiv aktiven Formen von Src und FAK konnten den inhibitorischen Effekt von Ino-C2-PAF nur zum Teil überbrücken.
Die reduzierte Motilität wird von einer Neuverteilung des Aktinzytoskelettes und einer erhöhten Zell-Matrix Adhäsion begleitet. Letztere ist hauptsächlich von der erhöhten Integrin-Avidität und Valenz abhängig, weniger jedoch von einer veränderten Affinität. Die anti-tumorigene Rolle von Ino-C2-PAF ist zudem durch eine erhöhte Lokalisation von E-Cadherin an den Zell-Zell-Kontakten charakterisiert.

Zusammenfassend deuten die Ergebnisse darauf hin, dass Ino-C2-PAF ein vielversprechender APL-Kandidat für die Entwicklung therapeutischer Mittel zur Behandlung von Autoimmunerkrankungen und hyperproliferativen Hautkrankheiten ist.

REFERENCES

Adam AP, Sharenko AL, Pumiglia K, Vincent PA (2009). Src-induced tyrosine phosphorylation of VE-cadherin is not sufficient to decrease barrier function of endothelial monolayers. *J Biol Chem*, **285,** 7045-7055.

Andreesen R, Modolell M, Munder PG (1979). Selective sensitivity of chronic myelogenous leukemia cell populations to alkyl-lysophospholipids. *Blood*, **54,** 519-523.

Andreesen R, Modolell M, Weltzien HU, Eibl H, Common HH, Lohr GW*, et al.* (1978). Selective destruction of human leukemic cells by alkyl-lysophospholipids. *Cancer Res*, **38,** 3894-3899.

Ausili A, Torrecillas A, Aranda FJ, Mollinedo F, Gajate C, Corbalan-Garcia S*, et al.* (2008). Edelfosine is incorporated into rafts and alters their organization. *J Phys Chem B*, **112,** 11643-11654.

Baburina I, Jackowski S (1998). Apoptosis triggered by 1-O-octadecyl-2-O-methyl-rac-glycero-3-phosphocholine is prevented by increased expression of CTP:Phosphocholine cytidylyltransferase. *J Biol Chem*, **273,** 2169-2173.

Bartolmäs T, Heyn T, Mickeleit M, Fischer A, Reutter W, Danker K (2005). Glucosamine-glycerophospholipids that activate cell-matrix adhesion and migration. *J Med Chem*, **48,** 6750-6755.

Berkovic D, Berkovic K, Fleer EA, Eibl H, Unger C (1994). Inhibition of calcium-dependent protein kinase C by hexadecylphosphocholine and 1-O-octadecyl-2-O-methyl-rac-glycero-3-phosphocholine do not correlate with inhibition of proliferation of HL60 and K562 cell lines. *Eur J Cancer*, **30A,** 509-515.

Bershadsky A, Chausovsky A, Becker E, Lyubimova A, Geiger B (1996). Involvement of microtubules in the control of adhesion-dependent signal transduction. *Curr Biol*, **6,** 1279-1289.

Boggs K, Rock CO, Jackowski S (1998). The antiproliferative effect of hexadecylphosphocholine toward HL60 cells is prevented by exogenous lysophosphatidylcholine. *Biochim Biophys Acta*, **1389,** 1-12.

Boggs KP, Rock CO, Jackowski S (1995a). Lysophosphatidylcholine and 1-O-octadecyl-2-O-methyl-rac-glycero-3-phosphocholine inhibit the CDP-choline pathway of phosphatidylcholine synthesis at the CTP:Phosphocholine cytidylyltransferase step. *J Biol Chem*, **270,** 7757-7764.

Boggs KP, Rock CO, Jackowski S (1995b). Lysophosphatidylcholine attenuates the cytotoxic effects of the antineoplastic phospholipid 1-O-octadecyl-2-O-methyl-rac-glycero-3-phosphocholine. *J Biol Chem*, **270,** 11612-11618.

Borst P, Kool M, Evers R (1997). Do cMOAT (MRP2), other MRP homologues, and LRP play a role in MDR? *Semin Cancer Biol*, **8,** 205-213.

Boukamp P, Petrussevska RT, Breitkreutz D, Hornung J, Markham A, Fusenig NE (1988). Normal keratinization in a spontaneously immortalized aneuploid human keratinocyte cell line. *J Cell Biol*, **106,** 761-771.

Bowcock AM, Shannon W, Du F, Duncan J, Cao K, Aftergut K*, et al.* (2001). Insights into psoriasis and other inflammatory diseases from large-scale gene expression studies. *Hum Mol Genet*, **10,** 1793-1805.

Brabek J, Constancio SS, Shin NY, Pozzi A, Weaver AM, Hanks SK (2004). CAS promotes invasiveness of Src-transformed cells. *Oncogene*, **23,** 7406-7415.

Braga VM, Del Maschio A, Machesky L, Dejana E (1999). Regulation of cadherin function by Rho and Rac: Modulation by junction maturation and cellular context. *Mol Biol Cell*, **10,** 9-22.

Bratton DL, Dreyer E, Kailey JM, Fadok VA, Clay KL, Henson PM (1992). The mechanism of internalization of platelet-activating factor in activated human neutrophils. Enhanced transbilayer movement across the plasma membrane. *J Immunol*, **148,** 514-523.

Bretscher MS (1996). Moving membrane up to the front of migrating cells. *Cell*, **85,** 465-467.

Broussard JA, Webb DJ, Kaverina I (2008). Asymmetric focal adhesion disassembly in motile cells. *Curr Opin Cell Biol*, **20,** 85-90.

Bryant DM, Stow JL (2004). The ins and outs of E-cadherin trafficking. *Trends Cell Biol*, **14,** 427-434.

Bryant P, Ploegh H (2004). Class II MHC peptide loading by the professionals. *Curr Opin Immunol*, **16,** 96-102.

Busto JV, Sot J, Goni FM, Mollinedo F, Alonso A (2007). Surface-active properties of the antitumour ether lipid 1-O-octadecyl-2-O-methyl-rac-glycero-3-phosphocholine (edelfosine). *Biochim Biophys Acta*, **1768,** 1855-1860.

Cabaner C, Gajate C, Macho A, Munoz E, Modolell M, Mollinedo F (1999). Induction of apoptosis in human mitogen-activated peripheral blood T-lymphocytes by the ether phospholipid ET-18-OCH3: Involvement of the Fas receptor/ligand system. *Br J Pharmacol*, **127,** 813-825.

Cance WG, Harris JE, Iacocca MV, Roche E, Yang X, Chang J*, et al.* (2000). Immunohistochemical analyses of focal adhesion kinase expression in benign and malignant human breast and colon tissues: Correlation with preinvasive and invasive phenotypes. *Clin Cancer Res*, **6,** 2417-2423.

Cao Z, Xiang J, Li C (2009). Expression of extracellular matrix metalloproteinase inducer and enhancement of the production of matrix metalloproteinase-1 in tongue squamous cell carcinoma. *Int J Oral Maxillofac Surg*, **38,** 880-885.

Carman CV, Springer TA (2003). Integrin avidity regulation: Are changes in affinity and conformation underemphasized? *Curr Opin Cell Biol*, **15,** 547-556.

Carrasco MP, Jimenez-Lopez JM, Rios-Marco P, Segovia JL, Marco C (2010). Disruption of cellular cholesterol transport and homeostasis as a novel mechanism of action of membrane-targeted alkylphospholipid analogues. *Br J Pharmacol*, **160,** 355-366.

Cary LA, Guan JL (1999). Focal adhesion kinase in integrin-mediated signaling. *Front Biosci*, **4,** D102-113.

Castellano F, Le Clainche C, Patin D, Carlier MF, Chavrier P (2001). A WASP-VASP complex regulates actin polymerization at the plasma membrane. *Embo J*, **20,** 5603-5614.

Cavallaro U, Christofori G (2004). Cell adhesion and signalling by cadherins and Ig-CAMs in cancer. *Nat Rev Cancer*, **4,** 118-132.

Chabner BA, Roberts TG, Jr. (2005). Timeline: Chemotherapy and the war on cancer. *Nat Rev Cancer*, **5,** 65-72.

Chambers AF, Matrisian LM (1997). Changing views of the role of matrix metalloproteinases in metastasis. *J Natl Cancer Inst*, **89,** 1260-1270.

Chandler S, Cossins J, Lury J, Wells G (1996). Macrophage metalloelastase degrades matrix and myelin proteins and processes a tumour necrosis factor-alpha fusion protein. *Biochem Biophys Res Commun*, **228,** 421-429.

Chen BH, Tzen JT, Bresnick AR, Chen HC (2002). Roles of Rho-associated kinase and myosin light chain kinase in morphological and migratory defects of focal adhesion kinase-null cells. *J Biol Chem*, **277,** 33857-33863.

Chen HC, Appeddu PA, Isoda H, Guan JL (1996). Phosphorylation of tyrosine 397 in focal adhesion kinase is required for binding phosphatidylinositol 3-kinase. *J Biol Chem*, **271,** 26329-26334.

Chen Z, Gibson TB, Robinson F, Silvestro L, Pearson G, Xu B*, et al.* (2001). MAP kinases. *Chem Rev*, **101,** 2449-2476.

Chignard M, Le Couedic JP, Tence M, Vargaftig BB, Benveniste J (1979). The role of platelet-activating factor in platelet aggregation. *Nature*, **279,** 799-800.

Cho SY, Klemke RL (2002). Purification of pseudopodia from polarized cells reveals redistribution and activation of Rac through assembly of a CAS/Crk scaffold. *J Cell Biol*, **156,** 725-736.

Clive S, Gardiner J, Leonard RC (1999). Miltefosine as a topical treatment for cutaneous metastases in breast carcinoma. *Cancer Chemother Pharmacol*, **44 Suppl,** S29-30.

Daniel LW, Etkin LA, Morrison BT, Parker J, Morris-Natschke S, Surles JR*, et al.* (1987). Ether lipids inhibit the effects of phorbol diester tumor promoters. *Lipids*, **22,** 851-855.

Daniel LW, Waite M, Wykle RL (1986). A novel mechanism of diglyceride formation. 12-O-tetradecanoylphorbol-13-acetate stimulates the cyclic breakdown and resynthesis of phosphatidylcholine. *J Biol Chem*, **261,** 9128-9132.

Danker K, Gabriel B, Heidrich C, Reutter W (1998). Focal adhesion kinase pp125FAK and the beta 1 integrin subunit are constitutively complexed in HaCaT cells. *Exp Cell Res*, **239,** 326-331.

Danker K, Reutter W, Semini G (2010). Glycosidated phospholipids: Uncoupling of signalling pathways at the plasma membrane. *Br J Pharmacol*, **160,** 36-47.

Dasmahapatra GP, Didolkar P, Alley MC, Ghosh S, Sausville EA, Roy KK (2004). *In vitro* combination treatment with perifosine and UCN-01 demonstrates synergism against prostate (PC-3) and lung (A549) epithelial adenocarcinoma cell lines. *Clin Cancer Res*, **10,** 5242-5252.

Day MJ (1996). Expression of major histocompatibility complex class II molecules by dermal inflammatory cells, epidermal Langerhans cells and keratinocytes in canine dermatological disease. *J Comp Pathol*, **115,** 317-326.

De Luca M, Pellegrini G, Zambruno G, Marchisio PC (1994). Role of integrins in cell adhesion and polarity in normal keratinocytes and human skin pathologies. *J Dermatol*, **21,** 821-828.

Debry P, Nash EA, Neklason DW, Metherall JE (1997). Role of multidrug resistance P-glycoproteins in cholesterol esterification. *J Biol Chem*, **272,** 1026-1031.

Defilippi P, Di Stefano P, Cabodi S (2006). p130CAS: A versatile scaffold in signaling networks. *Trends Cell Biol*, **16,** 257-263.

del Pozo MA, Alderson NB, Kiosses WB, Chiang HH, Anderson RG, Schwartz MA (2004). Integrins regulate Rac targeting by internalization of membrane domains. *Science*, **303,** 839-842.

Dennis G, Sherman BT, Hosack DA, Yang J, Gao W, Lane HC*, et al.* (2003). DAVID: Database for Annotation, Visualization, and Integrated Discovery. *Genome Biol*, **4,** P3.

Deussing J, Kouadio M, Rehman S, Werber I, Schwinde A, Peters C (2002). Identification and characterization of a dense cluster of placenta-specific cysteine peptidase genes and related genes on mouse chromosome 13. *Genomics*, **79,** 225-240.

Dhillon AS, Hagan S, Rath O, Kolch W (2007). MAP kinase signalling pathways in cancer. *Oncogene*, **26,** 3279-3290.

Diomede L, Colotta F, Piovani B, Re F, Modest EJ, Salmona M (1993). Induction of apoptosis in human leukemic cells by the ether lipid 1-octadecyl-2-methyl-rac-glycero-3-phosphocholine. A possible basis for its selective action. *Int J Cancer*, **53,** 124-130.

Dummer R, Roger J, Vogt T, Becker J, Hefner H, Sindermann H*, et al.* (1992). Topical application of hexadecylphosphocholine in patients with cutaneous lymphomas. *Prog Exp Tumor Res*, **34,** 160-169.

Dymond M, Attard G, Postle AD (2008). Testing the hypothesis that amphiphilic antineoplastic lipid analogues act through reduction of membrane curvature elastic stress. *J R Soc Interface*, **5,** 1371-1386.

Eddy RJ, Pierini LM, Maxfield FR (2002). Microtubule asymmetry during neutrophil polarization and migration. *Mol Biol Cell*, **13,** 4470-4483.

Edmondson SR, Thumiger SP, Kaur P, Loh B, Koelmeyer R, Li A*, et al.* (2005). Insulin-like growth factor binding protein-3 (IGFBP-3) localizes to and modulates proliferative epidermal keratinocytes in vivo. *Br J Dermatol*, **152,** 225-230.

Edwards LJ, Constantinescu CS (2009). Platelet activating factor/platelet activating factor receptor pathway as a potential therapeutic target in autoimmune diseases. *Inflamm Allergy Drug Targets*, **8,** 182-190.

Eibl H (1996) Phospholipide als funktionelle Bausteine biologischer Membranen. *Angew Chem*, **96**, 247-262

Elrod HA, Lin YD, Yue P, Wang X, Lonial S, Khuri FR*, et al.* (2007). The alkylphospholipid perifosine induces apoptosis of human lung cancer cells requiring inhibition of Akt and activation of the extrinsic apoptotic pathway. *Mol Cancer Ther*, **6,** 2029-2038.

Endicott JA, Ling V (1989). The biochemistry of P-glycoprotein-mediated multidrug resistance. *Annu Rev Biochem*, **58,** 137-171.

Engel JB, Honig A, Schonhals T, Weidler C, Hausler S, Krockenberger M*, et al.* (2008). Perifosine inhibits growth of human experimental endometrial cancers by blockade of Akt phosphorylation. *Eur J Obstet Gynecol Reprod Biol*, **141,** 64-69.

Etienne-Manneville S, Hall A (2001). Integrin-mediated activation of Cdc42 controls cell polarity in migrating astrocytes through PKCzeta. *Cell*, **106,** 489-498.

Etienne-Manneville S, Hall A (2002). Rho GTPases in cell biology. *Nature*, **420,** 629-635.

Evers EE, Zondag GC, Malliri A, Price LS, ten Klooster JP, van der Kammen RA*, et al.* (2000). Rho family proteins in cell adhesion and cell migration. *Eur J Cancer*, **36,** 1269-1274.

Exton JH (1990). Effects of extracellular ATP on phosphatidylcholine phospholipase signaling systems. *Ann N Y Acad Sci*, **603,** 246-254; discussion 254-245.

Fayard B, Bianchi F, Dey J, Moreno E, Djaffer S, Hynes NE*, et al.* (2009). The serine protease inhibitor protease nexin-1 controls mammary cancer metastasis through lrp-1-mediated MMP-9 expression. *Cancer Res*, **69,** 5690-5698.

Fernandez-Figueras MT, Puig L, Musulen E, Gilaberte M, Lerma E, Serrano S*, et al.* (2007). Expression profiles associated with aggressive behavior in Merkel cell carcinoma. *Mod Pathol*, **20,** 90-101.

Fidler IJ, Kim SJ, Langley RR (2007). The role of the organ microenvironment in the biology and therapy of cancer metastasis. *J Cell Biochem*, **101,** 927-936.

Fischer A (2006). Aufklärung der Wirkung eines neuartigen, modifizierten Phospholipidanalogons: Inositol-C2-PAF. *PhD Thesis FU Berlin, Germany*.

Fischer A, Muller D, Zimmermann-Kordmann M, Kleuser B, Mickeleit M, Laabs S*, et al.* (2006). The ether lipid Inositol-C2-PAF is a potent inhibitor of cell proliferation in HaCaT cells. *Chembiochem*, **7,** 441-449.

Fleer EA, Berkovic D, Unger C, Eibl H (1992). Cellular uptake and metabolic fate of hexadecylphosphocholine. *Prog Exp Tumor Res*, **34,** 33-46.

Fleer EA, Kim DJ, Nagel GA, Eibl H, Unger C (1990). Cytotoxic activity of lysophosphatidylcholine analogues on human lymphoma Raji cells. *Onkologie*, **13,** 295-300.

Foller M, Huber SM, Lang F (2008). Erythrocyte programmed cell death. *IUBMB Life*, **60,** 661-668.

Fraki JE, Briggaman RA, Lazarus GS (1983). Transplantation of psoriatic skin onto nude mice. *J Invest Dermatol*, **80 Suppl,** 31s-35s.

Frasca F, Pandini G, Sciacca L, Pezzino V, Squatrito S, Belfiore A*, et al.* (2008). The role of insulin receptors and IGF-1 receptors in cancer and other diseases. *Arch Physiol Biochem*, **114,** 23-37.

Friedrich M, Holzmann R, Sterry W, Wolk K, Truppel A, Piazena H*, et al.* (2003). Ultraviolet B radiation-mediated inhibition of interferon-gamma-induced keratinocyte activation is independent of interleukin-10 and other soluble mediators but associated with enhanced intracellular suppressors of cytokine-signaling expression. *J Invest Dermatol*, **121,** 845-852.

Fukuyama T, Ogita H, Kawakatsu T, Fukuhara T, Yamada T, Sato T*, et al.* (2005). Involvement of the c-Src-Crk-C3G-Rap1 signaling in the nectin-induced activation of Cdc42 and formation of adherens junctions. *J Biol Chem*, **280,** 815-825.

Gajate C, Del Canto-Janez E, Acuna AU, Amat-Guerri F, Geijo E, Santos-Beneit AM*, et al.* (2004). Intracellular triggering of fas aggregation and recruitment of apoptotic molecules into Fas-enriched rafts in selective tumor cell apoptosis. *J Exp Med*, **200,** 353-365.

Gajate C, Fonteriz RI, Cabaner C, Alvarez-Noves G, Alvarez-Rodriguez Y, Modolell M*, et al.* (2000a). Intracellular triggering of Fas, independently of FasL, as a new mechanism of antitumor ether lipid-induced apoptosis. *Int J Cancer*, **85,** 674-682.

Gajate C, Gonzalez-Camacho F, Mollinedo F (2009a). Involvement of raft aggregates enriched in Fas/CD95 death-inducing signaling complex in the antileukemic action of edelfosine in Jurkat cells. *PLoS One*, **4,** e5044.

Gajate C, Gonzalez-Camacho F, Mollinedo F (2009b). Lipid raft connection between extrinsic and intrinsic apoptotic pathways. *Biochem Biophys Res Commun*, **380,** 780-784.

Gajate C, Mollinedo F (2001). The antitumor ether lipid ET-18-OCH(3) induces apoptosis through translocation and capping of Fas/CD95 into membrane rafts in human leukemic cells. *Blood*, **98,** 3860-3863.

Gajate C, Mollinedo F (2002). Biological activities, mechanisms of action and biomedical prospect of the antitumor ether phospholipid ET-18-OCH(3) (edelfosine), a proapoptotic agent in tumor cells. *Curr Drug Metab*, **3,** 491-525.

Gajate C, Mollinedo F (2007). Edelfosine and perifosine induce selective apoptosis in multiple myeloma by recruitment of death receptors and downstream signaling molecules into lipid rafts. *Blood*, **109,** 711-719.

Gajate C, Santos-Beneit A, Modolell M, Mollinedo F (1998). Involvement of c-jun NH-2-terminal kinase activation and c-jun in the induction of apoptosis by the ether phospholipid 1-O-octadecyl-2-O-methyl-rac-glycero-3-phosphocholine. *Mol Pharmacol*, **53,** 602-612.

Gajate C, Santos-Beneit AM, Macho A, Lazaro M, Hernandez-De Rojas A, Modolell M*, et al.* (2000b). Involvement of mitochondria and caspase-3 in ET-18-OCH(3)-induced apoptosis of human leukemic cells. *Int J Cancer*, **86,** 208-218.

Gao S, Krogdahl A, Sorensen JA, Kousted TM, Dabelsteen E, Andreasen PA (2008). Overexpression of protease nexin-1 mRNA and protein in oral squamous cell carcinomas. *Oral Oncol*, **44,** 309-313.

Geilen CC, Haase A, Wieder T, Arndt D, Zeisig R, Reutter W (1994). Phospholipid analogues: Side chain- and polar head group-dependent effects on phosphatidylcholine biosynthesis. *J Lipid Res*, **35,** 625-632.

Geilen CC, Haase R, Buchner K, Wieder T, Hucho F, Reutter W (1991). The phospholipid analogue, hexadecylphosphocholine, inhibits protein kinase C in vitro and antagonises phorbol ester-stimulated cell proliferation. *Eur J Cancer*, **27,** 1650-1653.

Geilen CC, Wieder T, Reutter W (1992). Hexadecylphosphocholine inhibits translocation of CTP:Choline-phosphate cytidylyltransferase in Madin-Darby canine kidney cells. *J Biol Chem*, **267,** 6719-6724.

Gills JJ, Dennis PA (2009). Perifosine: Update on a novel Akt inhibitor. *Curr Oncol Rep*, **11,** 102-110.

Gonzalez-Gay MA, Nabozny GH, Bull MJ, Zanelli E, Douhan J, 3rd, Griffiths MM*, et al.* (1994). Protective role of major histocompatibility complex class II EBD transgene on collagen-induced arthritis. *J Exp Med*, **180,** 1559-1564.

Goodwin M, Yap AS (2004). Classical cadherin adhesion molecules: Coordinating cell adhesion, signaling and the cytoskeleton. *J Mol Histol*, **35,** 839-844.

Gottlieb AB, Lifshitz B, Fu SM, Staiano-Coico L, Wang CY, Carter DM (1986). Expression of HLA-DR molecules by keratinocytes, and presence of Langerhans cells in the dermal infiltrate of active psoriatic plaques. *J Exp Med*, **164,** 1013-1028.

Griner EM, Kazanietz MG (2007). Protein kinase C and other diacylglycerol effectors in cancer. *Nat Rev Cancer*, **7,** 281-294.

Guan G, Jiang G, Koch RL, Shechter I (1995). Molecular cloning and functional analysis of the promoter of the human squalene synthase gene. *J Biol Chem*, **270,** 21958-21965.

Gudjonsson JE, Ding J, Li X, Nair RP, Tejasvi T, Qin ZS*, et al.* (2009). Global gene expression analysis reveals evidence for decreased lipid biosynthesis and increased innate immunity in uninvolved psoriatic skin. *J Invest Dermatol*, **129,** 2795-2804.

Gudjonsson JE, Johnston A, Dyson M, Valdimarsson H, Elder JT (2007). Mouse models of psoriasis. *J Invest Dermatol*, **127,** 1292-1308.

Gupton SL, Waterman-Storer CM (2006). Spatiotemporal feedback between actomyosin and focal-adhesion systems optimizes rapid cell migration. *Cell*, **125,** 1361-1374.

Haase R, Wieder T, Geilen CC, Reutter W (1991). The phospholipid analogue hexadecylphosphocholine inhibits phosphatidylcholine biosynthesis in Madin-Darby canine kidney cells. *FEBS Lett*, **288,** 129-132.

Hac-Wydro K, Dynarowicz-Latka P (2010).Effect of edelfosine on tumor and normal cells model membranes--a comparative study. *Colloids Surf B Biointerfaces*, **76,** 366-369.

Hac-Wydro K, Dynarowicz-Latka P, Zuk R (2009). Langmuir monolayer study toward combined antileishmanian therapy involving amphotericin B and edelfosine. *J Phys Chem B*, **113,** 14239-14246.

Hager G, Formanek M, Gedlicka C, Thurnher D, Knerer B, Kornfehl J (2001). 1,25(OH)2 vitamin D3 induces elevated expression of the cell cycle-regulating genes p21 and p27 in squamous carcinoma cell lines of the head and neck. *Acta Otolaryngol*, **121,** 103-109.

Hall A (2005). Rho GTPases and the control of cell behaviour. *Biochem Soc Trans*, **33,** 891-895.

Hanks SK, Ryzhova L, Shin NY, Brabek J (2003). Focal adhesion kinase signaling activities and their implications in the control of cell survival and motility. *Front Biosci*, **8,** d982-996.

Haskell H, Natarajan M, Hecker TP, Ding Q, Stewart J, Jr., Grammer JR*, et al.* (2003). Focal adhesion kinase is expressed in the angiogenic blood vessels of malignant astrocytic tumors *in vivo* and promotes capillary tube formation of brain microvascular endothelial cells. *Clin Cancer Res*, **9,** 2157-2165.

Hauck CR, Hsia DA, Ilic D, Schlaepfer DD (2002a). v-Src SH3-enhanced interaction with focal adhesion kinase at beta 1 integrin-containing invadopodia promotes cell invasion. *J Biol Chem*, **277,** 12487-12490.

Hauck CR, Hsia DA, Puente XS, Cheresh DA, Schlaepfer DD (2002b). FRNK blocks v-Src-stimulated invasion and experimental metastases without effects on cell motility or growth. *Embo J*, **21,** 6289-6302.

Hauck CR, Sieg DJ, Hsia DA, Loftus JC, Gaarde WA, Monia BP*, et al.* (2001). Inhibition of focal adhesion kinase expression or activity disrupts epidermal growth factor-stimulated signaling promoting the migration of invasive human carcinoma cells. *Cancer Res*, **61,** 7079-7090.

Hauser P, Ma L, Agrawal D, Haura E, Cress WD, Pledger WJ (2004). Efficient down-regulation of cyclin A-associated activity and expression in suspended primary keratinocytes requires p21(Cip1). *Mol Cancer Res*, **2,** 96-104.

Heczkova B, Slotte JP (2006). Effect of anti-tumor ether lipids on ordered domains in model membranes. *FEBS Lett*, **580,** 2471-2476.

Hideshima T, Catley L, Yasui H, Ishitsuka K, Raje N, Mitsiades C*, et al.* (2006). Perifosine, an oral bioactive novel alkylphospholipid, inhibits Akt and induces *in vitro* and *in vivo* cytotoxicity in human multiple myeloma cells. *Blood*, **107,** 4053-4062.

Higgs HN, Pollard TD (1999). Regulation of actin polymerization by Arp2/3 complex and WASp/Scar proteins. *J Biol Chem*, **274,** 32531-32534.

Hochhuth C, Berkovic D, Eibl H, Unger C, Doenecke D (1990). Effects of antineoplastic phospholipids on parameters of cell differentiation in U937 cells. *J Cancer Res Clin Oncol*, **116,** 459-466.

Houlihan WJ, Lohmeyer M, Workman P, Cheon SH (1995). Phospholipid antitumor agents. *Med Res Rev*, **15,** 157-223.

Howard J, Hyman AA (2003). Dynamics and mechanics of the microtubule plus end. *Nature*, **422,** 753-758.

Hsia DA, Mitra SK, Hauck CR, Streblow DN, Nelson JA, Ilic D*, et al.* (2003). Differential regulation of cell motility and invasion by FAK. *J Cell Biol*, **160,** 753-767.

Huang DW, Sherman BT, Lempicki RA (2009). Systematic and integrative analysis of large gene lists using DAVID bioinformatics resources. *Nature Protoc*, **4,** 44-57.

Humphries MJ (1990). The molecular basis and specificity of integrin-ligand interactions. *J Cell Sci*, **97 (Pt 4),** 585-592.

Hunter J, Jepson MA, Tsuruo T, Simmons NL, Hirst BH (1993). Functional expression of P-glycoprotein in apical membranes of human intestinal Caco-2 cells. Kinetics of vinblastine secretion and interaction with modulators. *J Biol Chem*, **268,** 14991-14997.

Hynes RO (2002). Integrins: Bidirectional, allosteric signaling machines. *Cell*, **110,** 673-687.

Ilic D, Furuta Y, Kanazawa S, Takeda N, Sobue K, Nakatsuji N*, et al.* (1995). Reduced cell motility and enhanced focal adhesion contact formation in cells from FAK-deficient mice. *Nature*, **377,** 539-544.

Ilic D, Kovacic B, McDonagh S, Jin F, Baumbusch C, Gardner DG*, et al.* (2003). Focal adhesion kinase is required for blood vessel morphogenesis. *Circ Res*, **92,** 300-307.

Impola U, Uitto VJ, Hietanen J, Hakkinen L, Zhang L, Larjava H*, et al.* (2004). Differential expression of matrilysin-1 (MMP-7), 92 kd gelatinase (MMP-9), and metalloelastase (MMP-12) in oral verrucous and squamous cell cancer. *J Pathol.*, **202,** 14-22.

Inbar M, Goldman R, Inbar L, Bursuker I, Goldman B, Akstein E*, et al.* (1977). Fluidity difference of membrane lipids in human normal and leukemic lymphocytes as controlled by serum components. *Cancer Res*, **37,** 3037-3041.

Irby RB, Yeatman TJ (2002). Increased Src activity disrupts cadherin/catenin-mediated homotypic adhesion in human colon cancer and transformed rodent cells. *Cancer Res*, **62,** 2669-2674.

Itoh RE, Kurokawa K, Ohba Y, Yoshizaki H, Mochizuki N, Matsuda M (2002). Activation of Rac and Cdc42 video imaged by fluorescent resonance energy transfer-based single-molecule probes in the membrane of living cells. *Mol Cell Biol*, **22,** 6582-6591.

Jean J, Lapointe M, Soucy J, Pouliot R (2009). Development of an *in vitro* psoriatic skin model by tissue engineering. *J Dermatol Sci*, **53,** 19-25.

Jeanes A, Gottardi CJ, Yap AS (2008). Cadherins and cancer: How does cadherin dysfunction promote tumor progression? *Oncogene*, **27,** 6920-6929.

Jimenez-Lopez JM, Carrasco MP, Segovia JL, Marco C (2002). Hexadecylphosphocholine inhibits phosphatidylcholine biosynthesis and the proliferation of HEPG2 cells. *Eur J Biochem*, **269,** 4649-4655.

Kahan C, Seuwen K, Meloche S, Pouyssegur J (1992). Coordinate, biphasic activation of p44 mitogen-activated protein kinase and S6 kinase by growth factors in hamster fibroblasts. Evidence for thrombin-induced signals different from phosphoinositide turnover and adenylylcyclase inhibition. *J Biol Chem*, **267,** 13369-13375.

Kamsteeg M, Jansen PA, van Vlijmen-Willems IM, van Erp PE, Rodijk-Olthuis D, van der Valk PG*, et al.* (2009). Molecular diagnostics of psoriasis, atopic dermatitis, allergic contact dermatitis and irritant contact dermatitis. *Br J Dermatol*.

Karayiannakis AJ, Syrigos KN, Efstathiou J, Valizadeh A, Noda M, Playford RJ*, et al.* (1998). Expression of catenins and E-cadherin during epithelial restitution in inflammatory bowel disease. *J Pathol*, **185,** 413-418.

Karayiannakis AJ, Syrigos KN, Savva A, Polychronidis A, Karatzas G, Simopoulos C (2002). Serum E-cadherin concentrations and their response during laparoscopic and open cholecystectomy. *Surg Endosc*, **16,** 1551-1554.

Karelina TV, Goldberg GI, Eisen AZ (1994). Matrilysin (PUMP) correlates with dermal invasion during appendageal development and cutaneous neoplasia. *J Invest Dermatol*, **103,** 482-487.

Kaufmann R, Weber L, Klein CE (1990). [integrins--new receptor molecules: Their significance for the differentiation, regeneration and immune response of the skin]. *Hautarzt*, **41,** 256-261.

Keely PJ, Westwick JK, Whitehead IP, Der CJ, Parise LV (1997). Cdc42 and Rac1 induce integrin-mediated cell motility and invasiveness through PI(3)K. *Nature*, **390,** 632-636.

Kelley EE, Modest EJ, Burns CP (1993). Unidirectional membrane uptake of the ether lipid antineoplastic agent edelfosine by L1210 cells. *Biochem Pharmacol*, **45,** 2435-2439.

Kennedy NJ, Sluss HK, Jones SN, Bar-Sagi D, Flavell RA, Davis RJ (2003). Suppression of Ras-stimulated transformation by the JNK signal transduction pathway. *Genes Dev*, **17,** 629-637.

Kerkelä E, Ala-Aho R, Jeskanen L, Rechardt O, Grénman R, Shapiro SD*, et al.* (2000). Expression of human macrophage metalloelastase (MMP-12) by tumor cells in skin cancer. *J Invest Dermatol.*, **114,** 1113-1119.

Kim BS, Miyagawa F, Cho YH, Bennett CL, Clausen BE, Katz SI (2009). Keratinocytes function as accessory cells for presentation of endogenous antigen expressed in the epidermis. *J Invest Dermatol*, **129,** 2805-2817.

Kim JB, Spiegelman BM (1996). Add1/srebp1 promotes adipocyte differentiation and gene expression linked to fatty acid metabolism. *Genes Dev*, **10,** 1096-1107.

Kinsella AR, Smith D, Pickard M (1997). Resistance to chemotherapeutic antimetabolites: A function of salvage pathway involvement and cellular response to DNA damage. *Br J Cancer*, **75,** 935-945.

Klein A, Olendrowitz C, Schmutzler R, Hampl J, Schlag PM, Maass N*, et al.* (2009). Identification of brain- and bone-specific breast cancer metastasis genes. *Cancer Lett*, **276,** 212-220.

Kloth JN, Gorter A, Fleuren GJ, Oosting J, Uljee S, ter Haar N*, et al.* (2008). Elevated expression of SERPINA1 and SERPINA3 in HLA-positive cervical carcinoma. *J Pathol*, **215,** 222-230.

Kodama A, Takaishi K, Nakano K, Nishioka H, Takai Y (1999). Involvement of Cdc42 small G protein in cell-cell adhesion, migration and morphology of MDCK cells. *Oncogene*, **18,** 3996-4006.

Kojima K (1993). Molecular aspects of the plasma membrane in tumor cells. *Nagoya J Med Sci*, **56,** 1-18.

Kondapaka SB, Singh SS, Dasmahapatra GP, Sausville EA, Roy KK (2003). Perifosine, a novel alkylphospholipid, inhibits protein kinase B activation. *Mol Cancer Ther*, **2,** 1093-1103.

Kool M, de Haas M, Scheffer GL, Scheper RJ, van Eijk MJ, Juijn JA*, et al.* (1997). Analysis of expression of cMOAT (MRP2), MRP3, MRP4, and MRP5, homologues of the multidrug resistance-associated protein gene (MRP1), in human cancer cell lines. *Cancer Res*, **57,** 3537-3547.

Korkaya H, Paulson A, Charafe-Jauffret E, Ginestier C, Brown M, Dutcher J*, et al.* (2009). Regulation of mammary stem/progenitor cells by PTEN/Akt/beta-catenin signaling. *PLoS Biol*, **7,** e1000121.

Kren L, Goncharuk VN, Krenova Z, Stratil D, Hermanova M, Skrickova J*, et al.* (2006). Expression of matrix metalloproteinases 3, 10 and 11 (stromelysins 1, 2 and 3) and matrix metalloproteinase 7 (matrilysin) by cancer cells in non-small cell lung neoplasms. Clinicopathologic studies. *Cesk Patol*, **42,** 16-19.

Krueger JG, Krane JF, Carter DM, Gottlieb AB (1990). Role of growth factors, cytokines, and their receptors in the pathogenesis of psoriasis. *J Invest Dermatol*, **94,** 135S-140S.

Kudo I, Nojima S, Chang HW, Yanoshita R, Hayashi H, Kondo E*, et al.* (1987). Antitumor activity of synthetic alkylphospholipids with or without PAF activity. *Lipids*, **22,** 862-867.

Kuivanen TT, Jeskanen L, Kyllönen L, Impola U, Saarialho-Kere UK (2006). Transformation-specific matrix metalloproteinases, MMP-7 and MMP-13, are present in epithelial cells of keratoacanthomas. *Mod Pathol.*, **19,** 1203-1212.

Kulski JK, Kenworthy W, Bellgard M, Taplin R, Okamoto K, Oka A*, et al.* (2005). Gene expression profiling of japanese psoriatic skin reveals an increased activity in molecular stress and immune response signals. *J Mol Med*, **83,** 964-975.

Kyriakis JM, Avruch J (2001). Mammalian mitogen-activated protein kinase signal transduction pathways activated by stress and inflammation. *Physiol Rev*, **81,** 807-869.

Laemmli UK (1970). Cleavage of structural proteins during the assembly of the head of bacteriophage T4. *Nature*, **227,** 680-685.

Lambert M, Choquet D, Mege RM (2002). Dynamics of ligand-induced, Rac1-dependent anchoring of cadherins to the actin cytoskeleton. *J Cell Biol*, **157,** 469-479.

Lampert IA (1984). Expression of HLA-DR (IA like) antigen on epidermal keratinocytes in human dermatoses. *Clin Exp Immunol*, **57,** 93-100.

Lang PA, Kempe DS, Tanneur V, Eisele K, Klarl BA, Myssina S*, et al.* (2005). Stimulation of erythrocyte ceramide formation by platelet-activating factor. *J Cell Sci*, **118,** 1233-1243.

Lange Y, Steck TL (1994). Cholesterol homeostasis. Modulation by amphiphiles. *J Biol Chem*, **269,** 29371-29374.

Lange Y, Ye J, Rigney M, Steck TL (1999). Regulation of endoplasmic reticulum cholesterol by plasma membrane cholesterol. *J Lipid Res*, **40,** 2264-2270.

Larue L, Ohsugi M, Hirchenhain J, Kemler R (1994). E-cadherin null mutant embryos fail to form a trophectoderm epithelium. *Proc Natl Acad Sci U S A*, **91,** 8263-8267.

Leckband D, Prakasam A (2006). Mechanism and dynamics of cadherin adhesion. *Annu Rev Biomed Eng*, **8,** 259-287.

Leroy A, de Bruyne GK, Oomen LC, Mareel MM (2003). Alkylphospholipids reversibly open epithelial tight junctions. *Anticancer Res*, **23,** 27-32.

Lim Y, Han I, Jeon J, Park H, Bahk YY, Oh ES (2004). Phosphorylation of focal adhesion kinase at tyrosine 861 is crucial For ras transformation of fibroblasts. *J Biol Chem*, **279,** 29060-29065.

Lim Y, Lim ST, Tomar A, Gardel M, Bernard-Trifilo JA, Chen XL*, et al.* (2008). Pyk2 and FAK connections to p190Rho guanine nucleotide exchange factor regulate RhoA activity, focal adhesion formation, and cell motility. *J Cell Biol*, **180,** 187-203.

Ling V (1997). Multidrug resistance: Molecular mechanisms and clinical relevance. *Cancer Chemother Pharmacol*, **40 Suppl,** S3-8.

Liu BP, Chrzanowska-Wodnicka M, Burridge K (1998). Microtubule depolymerization induces stress fibers, focal adhesions, and DNA synthesis via the GTP-binding protein Rho. *Cell Adhes Commun*, **5,** 249-255.

Lobert VH, Brech A, Pedersen NM, Wesche J, Oppelt A, Malerod L*, et al.* (2010) Ubiquitination of alpha 5 beta 1 integrin controls fibroblast migration through lysosomal degradation of fibronectin-integrin complexes. *Dev Cell*, **19,** 148-159.

Lopez JM, Bennett MK, Sanchez HB, Rosenfeld JM, Osborne TF (1996). Sterol regulation of acetyl coenzyme a carboxylase: A mechanism for coordinate control of cellular lipid. *Proc Natl Acad Sci U S A*, **93,** 1049-1053.

Luker GD, Nilsson KR, Covey DF, Piwnica-Worms D (1999). Multidrug resistance (MDR1) P-glycoprotein enhances esterification of plasma membrane cholesterol. *J Biol Chem*, **274,** 6979-6991.

Luo BH, Carman CV, Springer TA (2007). Structural basis of integrin regulation and signaling. *Annu Rev Immunol*, **25,** 619-647.

Machesky LM, Reeves E, Wientjes F, Mattheyse FJ, Grogan A, Totty NF*, et al.* (1997). Mammalian Actin-Related Protein 2/3 complex localizes to regions of lamellipodial protrusion and is composed of evolutionarily conserved proteins. *Biochem J*, **328 (Pt 1),** 105-112.

Magdalena J, Millard TH, Machesky LM (2003). Microtubule involvement in NIH3T3 golgi and MTOC polarity establishment. *J Cell Sci*, **116,** 743-756.

Maillard C, Jost M, Romer MU, Brunner N, Houard X, Lejeune A*, et al.* (2005). Host plasminogen activator inhibitor-1 promotes human skin carcinoma progression in a stage-dependent manner. *Neoplasia*, **7,** 57-66.

Makrilia N, Kollias A, Manolopoulos L, Syrigos K (2009). Cell adhesion molecules: Role and clinical significance in cancer. *Cancer Invest*, **27,** 1023-1037.

Margolis RL, Wilson L (1977). Addition of colchicine-tubulin complex to microtubule ends: The mechanism of substoichiometric colchicine poisoning. *Proc Natl Acad Sci U S A*, **74,** 3466-3470.

Marino-Albernas JR, Bittman R, Peters A, Mayhew E (1996). Synthesis and growth inhibitory properties of glycosides of 1-O-hexadecyl-2-O-methyl-*sn*-glycerol, analogs of the antitumor ether lipid ET-18-OCH3 (edelfosine). *J Med Chem*, **39,** 3241-3247.

Massoner P, Colleselli D, Matscheski A, Pircher H, Geley S, Jansen Durr P*, et al.* (2009). Novel mechanism of IGF-binding protein-3 action on prostate cancer cells: Inhibition of proliferation, adhesion, and motility. *Endocr Relat Cancer*, **16,** 795-808.

Mee JB, Johnson CM, Morar N, Burslem F, Groves RW (2007). The psoriatic transcriptome closely resembles that induced by interleukin-1 in cultured keratinocytes: Dominance of innate immune responses in psoriasis. *Am J Pathol*, **171,** 32-42.

Mege RM, Gavard J, Lambert M (2006). Regulation of cell-cell junctions by the cytoskeleton. *Curr Opin Cell Biol*, **18,** 541-548.

Meloche S (1995). Cell cycle reentry of mammalian fibroblasts is accompanied by the sustained activation of p44MAPK and p42MAPK isoforms in the G1 phase and their inactivation at the G1/S transition. *J Cell Physiol*, **163,** 577-588.

Meloche S, Seuwen K, Pages G, Pouyssegur J (1992). Biphasic and synergistic activation of p44MAPK (ERK1) by growth factors: Correlation between late phase activation and mitogenicity. *Mol Endocrinol*, **6,** 845-854.

Mickeleit M, Wieder T, Arnold M, Geilen CC, Mulzer J, Reutter W (1998). A glucose-containing ether lipid (GLC-PAF) as an antiproliferative analogue of the platelet-activating factor. *Angew. Chem. Int. Ed.*, **37,** 351-353.

Mickeleit M, Wieder T, Buchner K, Geilen CC, Mulzer J, Reutter W (1995). Glc-PC, a new type of glucosidic phospholipid. *Angew. Chem. Int. Ed. Engl.*, **34,** 2667-2669.

Middel P, Lippert U, Hummel KM, Bertsch HP, Artuc M, Schweyer S*, et al.* (2000). Expression of lymphotoxin-alpha by keratinocytes: A further mediator for the lichenoid reaction. *Pathobiology*, **68,** 291-300.

Mitra SK, Hanson DA, Schlaepfer DD (2005). Focal adhesion kinase: In command and control of cell motility. *Nat Rev Mol Cell Biol*, **6,** 56-68.

Miyamoto S, Akiyama SK, Yamada KM (1995). Synergistic roles for receptor occupancy and aggregation in integrin transmembrane function. *Science*, **267,** 883-885.

Modolell M, Andreesen R, Pahlke W, Brugger U, Munder PG (1979). Disturbance of phospholipid metabolism during the selective destruction of tumor cells induced by alkyl-lysophospholipids. *Cancer Res*, **39,** 4681-4686.

Mollinedo F, de la Iglesia-Vicente J, Gajate C, Estella-Hermoso de Mendoza A, Villa-Pulgarin JA, Campanero MA*, et al.* (2010). Lipid raft-targeted therapy in multiple myeloma. *Oncogene*, **29,** 3748-3757.

Mollinedo F, Fernandez-Luna JL, Gajate C, Martin-Martin B, Benito A, Martinez-Dalmau R*, et al.* (1997). Selective induction of apoptosis in cancer cells by the ether lipid ET-18-OCH3 (edelfosine): Molecular structure requirements, cellular uptake, and protection by Bcl-2 and Bcl-x(L). *Cancer Res*, **57,** 1320-1328.

Mollinedo F, Gajate C (2006). Fas/CD95 death receptor and lipid rafts: New targets for apoptosis-directed cancer therapy. *Drug Resist Updat*, **9,** 51-73.

Mollinedo F, Gajate C, Martin-Santamaria S, Gago F (2004). ET-18-OCH3 (edelfosine): A selective antitumour lipid targeting apoptosis through intracellular activation of Fas/CD95 death receptor. *Curr Med Chem*, **11,** 3163-3184.

Mollinedo F, Martinez-Dalmau R, Modolell M (1993). Early and selective induction of apoptosis in human leukemic cells by the alkyl-lysophospholipid ET-18-OCH3. *Biochem Biophys Res Commun*, **192,** 603-609.

Momota H, Nerio E, Holland EC (2005). Perifosine inhibits multiple signaling pathways in glial progenitors and cooperates with temozolomide to arrest cell proliferation in gliomas in vivo. *Cancer Res*, **65,** 7429-7435.

Mould AP, Askari JA, Barton S, Kline AD, McEwan PA, Craig SE*, et al.* (2002). Integrin activation involves a conformational change in the alpha 1 helix of the beta subunit A-domain. *J Biol Chem*, **277,** 19800-19805.

Mulder E, van Deenen LL (1965). Metabolism of red-cell lipids. 3. Pathways for phospholipid renewal. *Biochim Biophys Acta*, **106,** 348-356.

Munder PG (1982). Antitumor activity of alkyllysophospholipids. *Human Cancer Immunol*, **3,** 17-29.

Munder PG, Ferber E, Modolell M, Fischer H (1969). The influence of various adjuvants on the metabolism of phospholipids in macrophages. *Int Arch Allergy Appl Immunol*, **36,** 117-128.

Munder PG, Modolell M (1973). Adjuvant induced formation of lysophosphatides and their role in the immune response. *Int Arch Allergy Appl Immunol*, **45,** 133-135.

Munder PG, Modolell M, Andreesen R, Weltzien HU, Westphal O (1979). Lysophosphatidylcholine (lysolecithin) and its synthetic analogues. Immune modulating and other biologic effects. *Immunopathology*, **2,** 187-203.

Munder PG, Westphal O (1990). Antitumoral and other biomedical activities of synthetic ether lysophospholipids. *Chem Immunol*, **49,** 206-235.

Na HK, Surh YJ (2008). The antitumor ether lipid edelfosine (ET-18-OCH3) induces apoptosis in H-ras transformed human breast epithelial cells: By blocking ERK1/2 and p38 mitogen-activated protein kinases as potential targets. *Asia Pac J Clin Nutr*, **17 Suppl 1,** 204-207.

Nelson AR, Fingleton B, Rothenberg ML, Matrisian LM (2000). Matrix metalloproteinases: Biologic activity and clinical implications. *J Clin Oncol*, **18,** 1135-1149.

Nickoloff BJ, Turka LA (1994). Immunological functions of non-professional antigen-presenting cells: New insights from studies of T-cell interactions with keratinocytes. *Immunol Today*, **15,** 464-469.

Nieto-Miguel T, Gajate C, Mollinedo F (2006). Differential targets and subcellular localization of antitumor alkyl-lysophospholipid in leukemic versus solid tumor cells. *J Biol Chem*, **281,** 14833-14840.

Nobes CD, Hall A (1995). Rho, Rac, and Cdc42 gtpases regulate the assembly of multimolecular focal complexes associated with actin stress fibers, lamellipodia, and filopodia. *Cell*, **81,** 53-62.

Nomura I, Gao B, Boguniewicz M, Darst MA, Travers JB, Leung DY (2003). Distinct patterns of gene expression in the skin lesions of atopic dermatitis and psoriasis: A gene microarray analysis. *J Allergy Clin Immunol*, **112,** 1195-1202.

Noseda A, White JG, Godwin PL, Jerome WG, Modest EJ (1989). Membrane damage in leukemic cells induced by ether and ester lipids: An electron microscopic study. *Exp Mol Pathol*, **50,** 69-83.

Nyakern M, Cappellini A, Mantovani I, Martelli AM (2006). Synergistic induction of apoptosis in human leukemia T cells by the akt inhibitor perifosine and etoposide through activation of intrinsic and Fas-mediated extrinsic cell death pathways. *Mol Cancer Ther*, **5,** 1559-1570.

Oestreicher JL, Walters IB, Kikuchi T, Gilleaudeau P, Surette J, Schwertschlag U*, et al.* (2001). Molecular classification of psoriasis disease-associated genes through pharmacogenomic expression profiling. *Pharmacogenomics J*, **1,** 272-287.

Omelchenko T, Vasiliev JM, Gelfand IM, Feder HH, Bonder EM (2002). Mechanisms of polarization of the shape of fibroblasts and epitheliocytes: Separation of the roles of microtubules and Rho-dependent actin-myosin contractility. *Proc Natl Acad Sci U S A*, **99,** 10452-10457.

Palazzo AF, Eng CH, Schlaepfer DD, Marcantonio EE, Gundersen GG (2004). Localized stabilization of microtubules by integrin- and FAK-facilitated Rho signaling. *Science*, **303,** 836-839.

Palazzo AF, Gundersen GG (2002). Microtubule-actin cross-talk at focal adhesions. *Sci STKE*, **2002,** pe31.

Palazzo AF, Joseph HL, Chen YJ, Dujardin DL, Alberts AS, Pfister KK*, et al.* (2001). Cdc42, dynein, and dynactin regulate MTOC reorientation independent of Rho-regulated microtubule stabilization. *Curr Biol*, **11,** 1536-1541.

Papa V, Tazzari PL, Chiarini F, Cappellini A, Ricci F, Billi AM*, et al.* (2008). Proapoptotic activity and chemosensitizing effect of the novel Akt inhibitor perifosine in acute myelogenous leukemia cells. *Leukemia*, **22,** 147-160.

Parsons JT (2003). Focal adhesion kinase: The first ten years. *J Cell Sci*, **116,** 1409-1416.

Pearson G, Robinson F, Beers Gibson T, Xu BE, Karandikar M, Berman K*, et al.* (2001). Mitogen-activated protein (MAP) kinase pathways: Regulation and physiological functions. *Endocr Rev*, **22,** 153-183.

Pfundt R, van Vlijmen-Willems I, Bergers M, Wingens M, Cloin W, Schalkwijk J (2001). In situ demonstration of phosphorylated c-jun and p38 MAP kinase in epidermal keratinocytes following ultraviolet B irradiation of human skin. *J Pathol*, **193,** 248-255.

Pilcher BK, Dumin JA, Sudbeck BD, Krane SM, Welgus HG, Parks WC (1997). The activity of collagenase-1 is required for keratinocyte migration on a type I collagen matrix. *J Cell Biol*, **137,** 1445-1457.

Prescott SM, Zimmerman GA, McIntyre TM (1990). Platelet-activating factor. *J Biol Chem*, **265,** 17381-17384.

Providence KM, Higgins PJ (2004). PAI-1 expression is required for epithelial cell migration in two distinct phases of in vitro wound repair. *J Cell Physiol*, **200,** 297-308.

Quekenborn-Trinquet V, Fogel P, Aldana-Jammayrac O, Ancian P, Demarchez M, Rossio P*, et al.* (2005). Gene expression profiles in psoriasis: Analysis of impact of body site location and clinical severity. *Br J Dermatol*, **152,** 489-504.

Raghavan S, Vaezi A, Fuchs E (2003). A role for alphabeta1 integrins in focal adhesion function and polarized cytoskeletal dynamics. *Dev Cell*, **5,** 415-427.

Rahmani M, Reese E, Dai Y, Bauer C, Payne SG, Dent P*, et al.* (2005). Coadministration of histone deacetylase inhibitors and perifosine synergistically induces apoptosis in human leukemia cells through Akt and ERK1/2 inactivation and the generation of ceramide and reactive oxygen species. *Cancer Res*, **65,** 2422-2432.

Raychaudhuri SP, Dutt S, Raychaudhuri SK, Sanyal M, Farber EM (2001). Severe combined immunodeficiency mouse-human skin chimeras: A unique animal model for the study of psoriasis and cutaneous inflammation. *Br J Dermatol*, **144,** 931-939.

Reinhard M, Halbrugge M, Scheer U, Wiegand C, Jockusch BM, Walter U (1992). The 46/50 kDa phosphoprotein VASp purified from human platelets is a novel protein associated with actin filaments and focal contacts. *Embo J*, **11,** 2063-2070.

Ren XD, Kiosses WB, Sieg DJ, Otey CA, Schlaepfer DD, Schwartz MA (2000). Focal adhesion kinase suppresses Rho activity to promote focal adhesion turnover. *J Cell Sci*, **113 (Pt 20),** 3673-3678.

Ridley AJ, Schwartz MA, Burridge K, Firtel RA, Ginsberg MH, Borisy G, *et al.* (2003). Cell migration: Integrating signals from front to back. *Science*, **302,** 1704-1709.

Roos G, Berdel WE (1986). Sensitivity of human hematopoietic cell lines to an alkyl-lysophospholipid-derivative. *Leuk Res*, **10,** 195-202.

Rottner K, Krause M, Gimona M, Small JV, Wehland J (2001). Zyxin is not colocalized with vasodilator-stimulated phosphoprotein (VASp) at lamellipodial tips and exhibits different dynamics to vinculin, paxillin, and VASp in focal adhesions. *Mol Biol Cell*, **12,** 3103-3113.

Ruiter GA, Verheij M, Zerp SF, Moolenaar WH, Van Blitterswijk WJ (2002). Submicromolar doses of alkyl-lysophospholipids induce rapid internalization, but not activation, of epidermal growth factor receptor and concomitant MAPK/ERK activation in A431 cells. *Int J Cancer*, **102,** 343-350.

Ruiter GA, Zerp SF, Bartelink H, van Blitterswijk WJ, Verheij M (1999). Alkyl-lysophospholipids activate the SAPK/JNK pathway and enhance radiation-induced apoptosis. *Cancer Res*, **59,** 2457-2463.

Ruiter GA, Zerp SF, Bartelink H, van Blitterswijk WJ, Verheij M (2003). Anti-cancer alkyl-lysophospholipids inhibit the phosphatidylinositol 3-kinase-Akt/PKB survival pathway. *Anticancer Drugs*, **14,** 167-173.

Samadder P, Arthur G (1999). Decreased sensitivity to 1-O-octadecyl-2-O-methyl-glycerophosphocholine in MCF-7 cells adapted for serum-free growth correlates with constitutive association of Raf-1 with cellular membranes. *Cancer Res*, **59,** 4808-4815.

Samadder P, Byun HS, Bittman R, Arthur G (1998). Glycosylated antitumor ether lipids are more effective against oncogene-transformed fibroblasts than alkyllysophospholipids. *Anticancer Res*, **18,** 465-470.

Samadder P, Richards C, Bittman R, Bhullar RP, Arthur G (2003). The antitumor ether lipid 1-O-octadecyl-2-O-methyl-rac-glycerophosphocholine (ET-18-OCH3) inhibits the association between Ras and Raf-1. *Anticancer Res*, **23,** 2291-2295.

Sauter A, Stern-Straeter J, Sodha S, Hormann K, Naim R (2008). Regulation of matrix metalloproteinases (MMP)-2/-9 expression in eosinophilic chronic rhinosinusitis--cell culture by interleukin-5 and -13? *In Vivo*, **22,** 415-421.

Schalkwijk J, van Vlijmen IM, Alkemade JA, de Jongh GJ (1993). Immunohistochemical localization of SKALP/elafin in psoriatic epidermis. *J Invest Dermatol*, **100,** 390-393.

Schaller MD, Otey CA, Hildebrand JD, Parsons JT (1995). Focal adhesion kinase and paxillin bind to peptides mimicking beta integrin cytoplasmic domains. *J Cell Biol*, **130,** 1181-1187.

Schallier DC, Bruyneel EA, Storme GA, Hilgard P, Mareel MM (1991). Antiinvasive activity of hexadecylphosphocholine in vitro. *Anticancer Res*, **11,** 1285-1292.

Schlaepfer DD, Jones KC, Hunter T (1998). Multiple GRB2-mediated integrin-stimulated signaling pathways to ERK2/mitogen-activated protein kinase: Summation of both c-Src- and focal adhesion kinase-initiated tyrosine phosphorylation events. *Mol Cell Biol*, **18,** 2571-2585.

Schlaepfer DD, Mitra SK, Ilic D (2004). Control of motile and invasive cell phenotypes by focal adhesion kinase. *Biochim Biophys Acta*, **1692,** 77-102.

Schober M, Raghavan S, Nikolova M, Polak L, Pasolli HA, Beggs HE*, et al.* (2007). Focal adhesion kinase modulates tension signaling to control actin and focal adhesion dynamics. *J Cell Biol*, **176,** 667-680.

Schneider GB, Kurago Z, Zaharias R, Gruman LM, Schaller MD, Hendrix MJ (2002). Elevated focal adhesion kinase expression facilitates oral tumor cell invasion. *Cancer*, **95,** 2508-2515.

Schön MP (1999). Animal models of psoriasis - what can we learn from them? *J Invest Dermatol*, **112,** 405-410.

Schön M, Schön MP, Geilen CC, Hoffmann M, Hakyi N, Orfanos CE*, et al.* (1996). Cell-matrix interactions of normal and transformed human keratinocytes *in vitro* are modulated by the synthetic phospholipid analogue hexadecylphosphocholine. *Br J Dermatol*, **135,** 696-703.

Schwarz G, Boehncke WH, Braun M, Schroter CJ, Burster T, Flad T*, et al.* (2002). Cathepsin s activity is detectable in human keratinocytes and is selectively upregulated upon stimulation with interferon-gamma. *J Invest Dermatol*, **119,** 44-49.

Selzer-Plon J, Bornholdt J, Friis S, Bisgaard HC, Lothe IM, Tveit KM*, et al.* (2009). Expression of prostasin and its inhibitors during colorectal cancer carcinogenesis. *BMC Cancer*, **9,** 201.

Shafer SH, Williams CL (2003). Non-small and small cell lung carcinoma cell lines exhibit cell type-specific sensitivity to edelfosine-induced cell death and different cell line-specific responses to edelfosine treatment. *Int J Oncol*, **23,** 389-400.

Sieg DJ, Hauck CR, Schlaepfer DD (1999). Required role of focal adhesion kinase (FAK) for integrin-stimulated cell migration. *J Cell Sci*, **112 (Pt 16),** 2677-2691.

Slaton JW, Hampton JA, Selman SH (1994). Exposure to alkyllysophospholipids inhibits *in vitro* invasion of transitional cell carcinoma. *J Urol*, **152,** 1594-1598.

Snyder F (1995). Platelet-activating factor: The biosynthetic and catabolic enzymes. *Biochem J*, **305 (Pt 3),** 689-705.

Srinivasan S, Wang F, Glavas S, Ott A, Hofmann F, Aktories K*, et al.* (2003). Rac and Cdc42 play distinct roles in regulating PI(3,4,5)P3 and polarity during neutrophil chemotaxis. *J Cell Biol*, **160,** 375-385.

Steelant WF, Goeman JL, Philippe J, Oomen LC, Hilkens J, Krzewinski-Recchi MA*, et al.* (2001). Alkyl-lysophospholipid 1-O-octadecyl-2-O-methyl-glycerophosphocholine induces invasion through episialin-mediated neutralization of E-cadherin in human mammary MCF-7 cells *in vitro*. *Int J Cancer*, **92,** 527-536.

Steelant WF, Recchi MA, Noe VT, Boilly-Marer Y, Bruyneel EA, Verbert A*, et al.* (1999). Sialylation of E-cadherin does not change the spontaneous or et-18-ome-mediated aggregation of MCF-7 human breast cancer cells. *Clin Exp Metastasis*, **17,** 245-253.

Stoffler HE, Honnert U, Bauer CA, Hofer D, Schwarz H, Muller RT*, et al.* (1998). Targeting of the myosin-I myr 3 to intercellular adherens type junctions induced by dominant active Cdc42 in hela cells. *J Cell Sci*, **111 (Pt 18),** 2779-2788.

Storme GA, Berdel WE, van Blitterswijk WJ, Bruyneel EA, De Bruyne GK, Mareel MM (1985). Antiinvasive effect of racemic 1-O-octadecyl-2-O-methylglycero-3-phosphocholine on MO4 mouse fibrosarcoma cells *in vitro*. *Cancer Res*, **45,** 351-357.

Strassheim D, Shafer SH, Phelps SH, Williams CL (2000). Small cell lung carcinoma exhibits greater phospholipase C-beta1 expression and edelfosine resistance compared with non-small cell lung carcinoma. *Cancer Res*, **60,** 2730-2736.

Takagi A, Nishiyama C, Kanada S, Niwa Y, Fukuyama K, Ikeda S*, et al.* (2006). Prolonged MHC class II expression and CIITA transcription in human keratinocytes. *Biochem Biophys Res Commun*, **347,** 388-393.

Takaishi K, Sasaki T, Kotani H, Nishioka H, Takai Y (1997). Regulation of cell-cell adhesion by Rac and Rho small G proteins in MDCK cells. *J Cell Biol*, **139,** 1047-1059.

Tarnowski GS, Mountain IM, Stock CC, Munder PG, Weltzien HU, Westphal O (1978). Effect of lysolecithin and analogs on mouse ascites tumors. *Cancer Res*, **38,** 339-344.

Tazzari PL, Tabellini G, Ricci F, Papa V, Bortul R, Chiarini F*, et al.* (2008). Synergistic proapoptotic activity of recombinant trail plus the Akt inhibitor perifosine in acute myelogenous leukemia cells. *Cancer Res*, **68,** 9394-9403.

Tertoolen LG, Kempenaar J, Boonstra J, de Laat SW, Ponec M (1988). Lateral mobility of plasma membrane lipids in normal and transformed keratinocytes. *Biochem Biophys Res Commun*, **152,** 491-496.

Tomar A, Lim ST, Lim Y, Schlaepfer DD (2009). A FAK-p120RasGAP-p190RhoGAP complex regulates polarity in migrating cells. *J Cell Sci*, **122,** 1852-1862.

Torrecillas A, Aroca-Aguilar JD, Aranda FJ, Gajate C, Mollinedo F, Corbalan-Garcia S*, et al.* (2006). Effects of the anti-neoplastic agent ET-18-OCH3 and some analogs on the biophysical properties of model membranes. *Int J Pharm*, **318,** 28-40.

Tseng MY, Liu SY, Chen HR, Wu YJ, Chiu CC, Chan PT*, et al.* (2009). Serine protease inhibitor (SERPIN) B1 promotes oral cancer cell motility and is over-expressed in invasive oral squamous cell carcinoma. *Oral Oncol*, **45,** 771-776.

Turk B, Turk D, Turk V (2000). Lysosomal cysteine proteases: More than scavengers. *Biochim Biophys Acta*, **1477,** 98-111.

Unger C, Eibl H (1988). Hexadecylphosphocholine (D 18506) in the topical treatment of skin metastases: A phase-i trial. *Onkologie*, **11,** 295-296.

Unger C, Fleer EA, Kotting J, Neumuller W, Eibl H (1992). Antitumoral activity of alkylphosphocholines and analogues in human leukemia cell lines. *Prog Exp Tumor Res*, **34,** 25-32.

Unger C, Peukert M, Sindermann H, Hilgard P, Nagel G, Eibl H (1990). Hexadecylphosphocholine in the topical treatment of skin metastases in breast cancer patients. *Cancer Treat Rev*, **17,** 243-246.

van Blitterswijk WJ, van der Bend RL, Kramer IM, Verhoeven AJ, Hilkmann H, de Widt J (1987). A metabolite of an antineoplastic ether phospholipid may inhibit transmembrane signalling via protein kinase c. *Lipids*, **22,** 842-846.

van der Luit AH, Budde M, Ruurs P, Verheij M, van Blitterswijk WJ (2002). Alkyl-lysophospholipid accumulates in lipid rafts and induces apoptosis via raft-dependent endocytosis and inhibition of phosphatidylcholine synthesis. *J Biol Chem*, **277,** 39541-39547.

Van der Luit AH, Budde M, Zerp S, Caan W, Klarenbeek JB, Verheij M*, et al.* (2007). Resistance to alkyl-lysophospholipid-induced apoptosis due to downregulated sphingomyelin synthase 1 expression with consequent sphingomyelin- and cholesterol-deficiency in lipid rafts. *Biochem J*, **401,** 541-549.

Van der Veer E, Van der Weide D, Heijmans HS, Hoekstra D (1993). Translocation of fluorescent ether phospholipid, but not its diacyl counterpart, after insertion in plasma membranes of control and plasmalogen-deficient fibroblasts. *Biochim Biophys Acta*, **1146,** 294-300.

Van Slambrouck S, Grijelmo C, De Wever O, Bruyneel E, Emami S, Gespach C*, et al.* (2007). Activation of the FAK-Src molecular scaffolds and p130CAS-JNK signaling cascades by alpha1-integrins during colon cancer cell invasion. *Int J Oncol*, **31,** 1501-1508.

Van Slambrouck S, Hilkens J, Steelant WF (2008). Ether lipid 1-O-octadecyl-2-O-methyl-3-glycero-phosphocholine inhibits cell-cell adhesion through translocation and clustering of E-cadherin and episialin in membrane microdomains. *Oncol Rep*, **19,** 123-128.

Vasioukhin V, Bauer C, Yin M, Fuchs E (2000). Directed actin polymerization is the driving force for epithelial cell-cell adhesion. *Cell*, **100,** 209-219.

Vicente-Manzanares M, Webb DJ, Horwitz AR (2005). Cell migration at a glance. *J Cell Sci*, **118,** 4917-4919.

Vink SR, van der Luit AH, Klarenbeek JB, Verheij M, van Blitterswijk WJ (2007). Lipid rafts and metabolic energy differentially determine uptake of anti-cancer alkylphospholipids in lymphoma versus carcinoma cells. *Biochem Pharmacol*, **74,** 1456-1465.

Vrablic AS, Albright CD, Craciunescu CN, Salganik RI, Zeisel SH (2001). Altered mitochondrial function and overgeneration of reactive oxygen species precede the induction of apoptosis by 1-O-octadecyl-2-methyl-rac-glycero-3-phosphocholine in p53-defective hepatocytes. *Faseb J*, **15,** 1739-1744.

Wadhawan A, Smith C, Nicholson RI, Barrett-Lee P, Hiscox S (2010). Src-mediated regulation of homotypic cell adhesion: Implications for cancer progression and opportunities for therapeutic intervention. *Cancer Treat Rev*.

Webb DJ, Donais K, Whitmore LA, Thomas SM, Turner CE, Parsons JT*, et al.* (2004). FAK-Src signalling through paxillin, ERK and MLCK regulates adhesion disassembly. *Nat Cell Biol*, **6,** 154-161.

Weber A, Hengge UR, Stricker I, Tischoff I, Markwart A, Anhalt K*, et al.* (2007). Protein microarrays for the detection of biomarkers in head and neck squamous cell carcinomas. *Hum Pathol*, **38,** 228-238.

Weinberg A, Krisanaprakornkit S, Dale BA (1998). Epithelial antimicrobial peptides: Review and significance for oral applications. *Crit Rev Oral Biol Med*, **9,** 399-414.

Welch HC, Coadwell WJ, Stephens LR, Hawkins PT (2003). Phosphoinositide 3-kinase-dependent activation of Rac. *FEBS Lett*, **546,** 93-97.

Wells A (2000). Tumor invasion: Role of growth factor-induced cell motility. *Adv Cancer Res*, **78,** 31-101.

Wessel R, Foos V, Aspelmeier A, Jurgens M, Graessmann A, Klein A (2006). CorrXpression--identification of significant groups of genes and experiments by means of correspondence analysis and ratio analysis. *In Silico Biol*, **6,** 61-70.

Wieder T, Haase A, Geilen CC, Orfanos CE (1995a). The effect of two synthetic phospholipids on cell proliferation and phosphatidylcholine biosynthesis in Madin-Darby canine kidney cells. *Lipids*, **30,** 389-393.

Wieder T, Haase A, Geilen CC, Orfanos CE (1995b). The effect of two synthetic phospholipids on cell proliferation and phosphatidylcholine biosynthesis in Madin-Darby canine kidney cells. *Lipids*, **30,** 389-393.

Wieder T, Orfanos CE, Geilen CC (1998). Induction of ceramide-mediated apoptosis by the anticancer phospholipid analog, hexadecylphosphocholine. *J Biol Chem*, **273,** 11025-11031.

Wiedow O, Schroder JM, Gregory H, Young JA, Christophers E (1990). Elafin: An elastase-specific inhibitor of human skin. Purification, characterization, and complete amino acid sequence. *J Biol Chem*, **265,** 14791-14795.

Wiese A, Wieder T, Mickeleit M, Reinohl S, Geilen CC, Seydel U*, et al.* (2000). Structure-dependent effects of glucose-containing analogs of platelet activating factor (PAF) on membrane integrity. *Biol Chem*, **381,** 135-144.

Wirtz KW (1991). Phospholipid transfer proteins. *Annu Rev Biochem*, **60,** 73-99.

Wittmann T, Waterman-Storer CM (2001). Cell motility: Can Rho GTPases and microtubules point the way? *J Cell Sci*, **114,** 3795-3803.

Wolf P, Nghiem DX, Walterscheid JP, Byrne S, Matsumura Y, Matsumura Y*, et al.* (2006). Platelet-activating factor is crucial in psoralen and ultraviolet A-induced immune suppression, inflammation, and apoptosis. *Am J Pathol*, **169,** 795-805.

Wolk K, Witte E, Wallace E, Docke WD, Kunz S, Asadullah K*, et al.* (2006). IL-22 regulates the expression of genes responsible for antimicrobial defense, cellular differentiation, and mobility in keratinocytes: A potential role in psoriasis. *Eur J Immunol*, **36,** 1309-1323.

Wong ST, Goodin S (2009). Overcoming drug resistance in patients with metastatic breast cancer. *Pharmacotherapy*, **29,** 954-965.

Worthylake RA, Burridge K (2003). RhoA and ROCK promote migration by limiting membrane protrusions. *J Biol Chem*, **278,** 13578-13584.

Xu J, Wang F, Van Keymeulen A, Herzmark P, Straight A, Kelly K*, et al.* (2003). Divergent signals and cytoskeletal assemblies regulate self-organizing polarity in neutrophils. *Cell*, **114,** 201-214.

Yap AS, Kovacs EM (2003). Direct cadherin-activated cell signaling: A view from the plasma membrane. *J Cell Biol*, **160,** 11-16.

Zaidel-Bar R, Ballestrem C, Kam Z, Geiger B (2003). Early molecular events in the assembly of matrix adhesions at the leading edge of migrating cells. *J Cell Sci*, **116,** 4605-4613.

Zaremberg V, Gajate C, Cacharro LM, Mollinedo F, McMaster CR (2005). Cytotoxicity of an anti-cancer lysophospholipid through selective modification of lipid raft composition. *J Biol Chem*, **280,** 38047-38058.

Zhang W, Liu W, Poradosu E, Ratain MJ (2008). Genome-wide identification of genetic determinants for the cytotoxicity of perifosine. *Hum Genomics*, **3,** 53-70.

Zhou X, Lu X, Richard C, Xiong W, Litchfield DW, Bittman R*, et al.* (1996). 1-O-octadecyl-2-O-methyl-glycerophosphocholine inhibits the transduction of growth signals via the MAPK cascade in cultured MCF-7 cells. *J Clin Invest*, **98,** 937-944.

PUBLICATIONS

Original articles

Semini G, Klein A, Danker K. Impact of alkylphospholipids on the gene expression profile of HaCaT cells. (in press)

Semini G*, Hildmann A*, Reissig H-U, Reutter W, Danker K. The novel synthethic ether lipid Ino-C2-PAF uncouples integrin-mediated attachment from integrin-dependent signalling in transformedskin cells. (in press)

(*) These authors contributed equally to this work

Review

Danker K, Reutter W, Semini G. (2010) Glycosidated phospholipids: uncoupling of signalling pathways at the plasma membrane. *Br J Pharmacol*; **160**:36-47.

Poster presentations

Semini G, Hildmann A, Reutter W, Danker K. The ether lipid Inositol-C2-PAF inhibits cell migration by affecting signal transduction pathways in the keratinocyte cell line HaCaT. Invasion and Metastasis, Max Delbrück Center for Molecular Medicine (MDC), Berlin-Buch, Germany, March 26-29, 2008

Semini G, Hildmann A, Reutter W, Danker K. The ether lipid Inositol-C2-PAF inhibits cell migration of keratinocyte cell lines HaCaT and SCC25. 31th Annual Meeting of the German Society for Cell Biology, Marburg, Germany, March 12-15, 2008

Semini G, Reutter W, Danker K. The alkyl-lysophospholipid Inositol-C2-PAF affects signalling cascades in HaCaT cells. 11th Joint Meeting – Signal Transduction, Weimar, Germany, November 01-03, 2007

Semini G, Fischer A, Reutter W, Danker K. The alkylphospholipid Inositol-C2-PAF affects signal transduction pathways in HaCaT cells. 98th AOCS Annual Meeting & Expo, Québec City, Canada, May 13 – 16, 2007.

CURRICULUM VITAE

For reasons of data protection, the curriculum vitae is not included in the online version.

APPENDIX

A) Differentially expressed transcripts by APLs

Table A1: Differentially expressed transcripts by Ino-C2-PAF

Probe_ID	Gene_ID	Definition	FC	Up/Down
A_23_P414654	*RAB37*	RAB37, member RAS oncogene family	41,38	up
A_23_P1833	*B3GAT1*	beta-1,3-glucuronyltransferase 1 (glucuronosyltransferase P)	40,94	up
A_23_P372946	*TM4SF19*	transmembrane 4 L six family member 19	35,59	up
A_23_P119196	*KLF2*	Kruppel-like factor 2 (lung)	34,85	up
A_23_P52714	*FGF19*	fibroblast growth factor 19	23,27	up
A_24_P532232	*CREB5*	cAMP responsive element binding protein 5	22,38	up
A_23_P9836	*ETV5*	ets variant gene 5 (ets-related molecule)	21,86	up
A_32_P187571	*SCN2B*	sodium channel, voltage-gated, type II, beta	21,36	up
A_24_P62783	*FABP3*	fatty acid binding protein 3, muscle and heart (mammary-derived growth inhibitor)	20,38	up
A_32_P200144	*IGH@*	immunoglobulin heavy locus	18,85	up
A_32_P30649	*ETV5*	ets variant gene 5 (ets-related molecule)	17,9	up
A_23_P406025	*KIAA0367*	KIAA0367	14,9	up
A_23_P427587	*FGF19*	fibroblast growth factor 19	14,37	up
A_23_P157117	*CREB5*	cAMP responsive element binding protein 5	13,33	up
A_23_P87982	*ATP12A*	ATPase, H+/K+ transporting, nongastric, alpha polypeptide	12,68	up
A_24_P227927	*IL21R*	interleukin 21 receptor	12,43	up
A_23_P161190	*VIM*	vimentin	12,38	up
A_23_P125233	*CNN1*	calponin 1, basic, smooth muscle	12,26	up
A_32_P33802			12,12	up
A_24_P115096	*MGC45491*	hypothetical protein MGC45491	11,34	up
A_24_P633825			10,88	up
A_23_P161194	*VIM*	vimentin	10,29	up
A_23_P316012	*RHOJ*	ras homolog gene family, member J	10,28	up
A_24_P328524	*KALRN*	kalirin, RhoGEF kinase	9,7	up
A_23_P131074	*THEG*	Theg homolog (mouse)	9,02	up
A_32_P219135	*LOC401317*	hypothetical LOC401317	8,94	up
A_32_P189781			8,82	up
A_23_P348183	*MGC45491*	hypothetical protein MGC45491	8,76	up
A_24_P226008	*MGLL*	monoglyceride lipase	8,47	up
A_32_P20613			8,23	up
A_23_P435477	*TMPRSS13*	transmembrane protease, serine 13	7,25	up
A_23_P66739	*SLC13A5*	solute carrier family 13 (sodium-dependent citrate transporter), member 5	7,07	up
A_23_P125972	*PRDM16*	PR domain containing 16	7,01	up
A_24_P933828	*LOC401317*	hypothetical LOC401317	6,93	up
A_24_P10137	*C13orf15*	chromosome 13 open reading frame 15	6,88	up
A_23_P101054	*KRT34*	keratin 34	6,71	up
A_23_P204937	*C13orf15*	chromosome 13 open reading frame 15	6,6	up
A_23_P207911	*TRPV2*	transient receptor potential cation channel, subfamily V, member 2	6,54	up
A_32_P45615			6,25	up
A_23_P431776	*ETV4*	ets variant gene 4 (E1A enhancer binding protein, E1AF)	5,85	up
A_24_P156295	*ACSS2*	acyl-CoA synthetase short-chain family member 2	5,6	up
A_24_P416346	*ETV4*	ets variant gene 4 (E1A enhancer binding protein, E1AF)	5,42	up
A_23_P5536	*SLC9A2*	solute carrier family 9 (sodium/hydrogen exchanger), member 2	5,34	up
A_23_P96271	*MYOM1*	myomesin 1, 185kDa	5,3	up
A_24_P686965	*SH2D5*	SH2 domain containing 5	5,29	up
A_32_P47754	*SLC2A14*	solute carrier family 2 (facilitated glucose transporter), member 14	5,26	up
A_24_P24371			5,22	up
A_23_P210900	*ACSS2*	acyl-CoA synthetase short-chain family member 2	5,21	up
A_23_P119362	*EMP3*	epithelial membrane protein 3	5,19	up
A_24_P305541	*TRIB3*	tribbles homolog 3 (Drosophila)	5,06	up
A_24_P81900	*SLC2A3*	solute carrier family 2 (facilitated glucose transporter), member 3	5,05	up
A_24_P156490	*KCNMA1*	potassium large conductance calcium-activated channel, subfamily M, alpha member 1	4,99	up
A_23_P30634	*BACH2*	BTB and CNC homology 1, basic leucine zipper transcription factor 2	4,89	up

Probe_ID	Gene_ID	Definition	FC	Up/Down
A_23_P87013	*TAGLN*	transgelin	4,8	up
A_23_P46039	*FCRLA*	Fc receptor-like A	4,69	up
A_23_P103361	*LCK*	lymphocyte-specific protein tyrosine kinase	4,67	up
A_24_P912048	*MGC50722*	hypothetical MGC50722	4,63	up
A_23_P87011	*TAGLN*	transgelin	4,63	up
A_32_P14721	*DNHD2*	dynein heavy chain domain 2	4,62	up
A_24_P103004	*SLC20A1*	solute carrier family 20 (phosphate transporter), member 1	4,57	up
A_23_P203150	*TMPRSS13*	transmembrane protease, serine 13	4,48	up
A_23_P341938	*NOG*	noggin	4,48	up
A_23_P28927			4,33	up
A_23_P93938	*NACAD*	NAC alpha domain containing	4,32	up
A_23_P66787	*ACLY*	ATP citrate lyase	4,21	up
A_23_P51136	*RHOB*	ras homolog gene family, member B	4,16	up
A_24_P393065			4,16	up
A_23_P74012	*SPRR1A*	small proline-rich protein 1A	4,1	up
A_23_P22422	*PNMA3*	paraneoplastic antigen MA3	4,09	up
A_24_P200420	*SLC7A11*	solute carrier family 7, (cationic amino acid transporter, y+ system) member 11	4,04	up
A_24_P395415			4,01	up
A_23_P404045	*MTHFR*	5,10-methylenetetrahydrofolate reductase (NADPH)	4	up
A_23_P311875	*CD6*	CD6 molecule	3,94	up
A_23_P400078	*MTHFR*	5,10-methylenetetrahydrofolate reductase (NADPH)	3,86	up
A_23_P406227	*MGC23284*	hypothetical protein MGC23284	3,81	up
A_32_P29200			3,78	up
A_32_P83845	*HEY1*	hairy/enhancer-of-split related with YRPW motif 1	3,73	up
A_23_P400081	*MTHFR*	5,10-methylenetetrahydrofolate reductase (NADPH)	3,71	up
A_24_P396753	*TRIB2*	tribbles homolog 2 (Drosophila)	3,7	up
A_24_P63522	*HMGCS1*	3-hydroxy-3-methylglutaryl-Coenzyme A synthase 1 (soluble)	3,69	up
A_23_P210690	*TRIB3*	tribbles homolog 3 (Drosophila)	3,67	up
A_23_P59388	*DST*	dystonin	3,65	up
A_23_P8640	*GPR30*	G protein-coupled receptor 30	3,62	up
A_32_P208078	*MTHFR*	5,10-methylenetetrahydrofolate reductase (NADPH)	3,6	up
A_32_P2050			3,59	up
A_23_P165657	*SLC20A1*	solute carrier family 20 (phosphate transporter), member 1	3,59	up
A_23_P83634	*ALOX12B*	arachidonate 12-lipoxygenase, 12R type	3,56	up
A_23_P148753	*PLEKHA6*	pleckstrin homology domain containing, family A member 6	3,52	up
A_24_P923251	*TGM2*	transglutaminase 2 (C polypeptide, protein-glutamine-gamma-glutamyltransferase)	3,52	up
A_23_P136724	*LOC344887*	similar to NmrA-like family domain containing 1	3,51	up
A_23_P63618	*SCD*	stearoyl-CoA desaturase (delta-9-desaturase)	3,51	up
A_23_P152125	*MVD*	mevalonate (diphospho) decarboxylase	3,48	up
A_23_P158817	*IGH@*	immunoglobulin heavy locus	3,48	up
A_23_P105963	*AK7*	adenylate kinase 7	3,46	up
A_32_P223140	*RASGEF1A*	RasGEF domain family, member 1A	3,44	up
A_24_P68908	*LOC344887*	similar to NmrA-like family domain containing 1	3,44	up
A_23_P83007	*C9orf150*	chromosome 9 open reading frame 150	3,44	up
A_23_P302568	*SLC30A3*	solute carrier family 30 (zinc transporter), member 3	3,44	up
A_24_P341538	*USP51*	ubiquitin specific peptidase 51	3,44	up
A_24_P335759	*MYO15A*	myosin XVA	3,42	up
A_24_P167668	*LTBP2*	latent transforming growth factor beta binding protein 2	3,42	up
A_23_P118158	*HS3ST2*	heparan sulfate (glucosamine) 3-O-sulfotransferase 2	3,4	up
A_24_P252739	*KLF6*	Kruppel-like factor 6	3,39	up
A_23_P27229	*MYO15A*	myosin XVA	3,38	up
A_24_P933908	*GPNMB*	glycoprotein (transmembrane) nmb	3,37	up
A_23_P256158	*ADRA2C*	adrenergic, alpha-2C-, receptor	3,35	up
A_23_P110184	*SC4MOL*	sterol-C4-methyl oxidase-like	3,33	up
A_23_P158976	*ABCC2*	ATP-binding cassette, sub-family C (CFTR/MRP), member 2	3,33	up
A_23_P405129	*LTBP2*	latent transforming growth factor beta binding protein 2	3,3	up
A_24_P879740			3,3	up
A_23_P122863	*GRB10*	growth factor receptor-bound protein 10	3,29	up
A_23_P305759	*ABHD3*	abhydrolase domain containing 3	3,28	up
A_23_P431268	*PLEKHA6*	pleckstrin homology domain containing, family A member 6	3,26	up
A_24_P357914			3,26	up
A_32_P80245			3,25	up
A_23_P81529	*ISL1*	ISL1 transcription factor, LIM/homeodomain, (islet-1)	3,22	up
A_23_P430818	*HSPC159*	galectin-related protein	3,22	up
A_24_P67268	*FDPSL4*	farnesyl diphosphate synthase-like 4 (farnesyl pyrophosphate synthetase-like 4)	3,2	up
A_32_P26144			3,2	up
A_24_P123408	*ABLIM3*	actin binding LIM protein family, member 3	3,16	up
A_23_P211252	*LSS*	lanosterol synthase (2,3-oxidosqualene-lanosterol cyclase)	3,14	up
A_23_P134935	*DUSP4*	dual specificity phosphatase 4	3,14	up

Probe_ID	Gene_ID	Definition	FC	Up/Down
A_23_P31135	*ACAT2*	acetyl-Coenzyme A acetyltransferase 2 (acetoacetyl Coenzyme A thiolase)	3,13	up
A_32_P113971	*RP5-1054A22.3*	KIAA1755 protein	3,13	up
A_24_P162211	*LSS*	lanosterol synthase (2,3-oxidosqualene-lanosterol cyclase)	3,11	up
A_23_P128728	*ARG2*	arginase, type II	3,08	up
A_23_P22735	*BEX2*	brain expressed X-linked 2	3,07	up
A_23_P76743	*LOC374569*	Similar to Lysophospholipase	3,05	up
A_23_P44569	*ABCC2*	ATP-binding cassette, sub-family C (CFTR/MRP), member 2	3,03	up
A_23_P204847	*LCP1*	lymphocyte cytosolic protein 1 (L-plastin)	3,02	up
A_23_P383835	*ACAT2*	acetyl-Coenzyme A acetyltransferase 2 (acetoacetyl Coenzyme A thiolase)	3,01	up
A_24_P266131	*FSTL4*	follistatin-like 4	3	up
A_23_P129856	*HIC1*	hypermethylated in cancer 1	3	up
A_32_P95223	*FDPSL2A*	MGC44478	3	up
A_23_P161218	*ANKRD1*	ankyrin repeat domain 1 (cardiac muscle)	2,99	up
A_23_P397376	*MAF*	v-maf musculoaponeurotic fibrosarcoma oncogene homolog (avian)	2,98	up
A_24_P201171	*STXBP1*	syntaxin binding protein 1	2,93	up
A_23_P218144	*LTBP2*	latent transforming growth factor beta binding protein 2	2,93	up
A_23_P17814	*PLA2G3*	phospholipase A2, group III	2,93	up
A_24_P406480	*LONRF1*	LON peptidase N-terminal domain and ring finger 1	2,93	up
A_23_P8196	*ME1*	malic enzyme 1, NADP(+)-dependent, cytosolic	2,93	up
A_24_P195240			2,92	up
A_32_P165477	*SLC7A11*	solute carrier family 7, (cationic amino acid transporter, y+ system) member 11	2,91	up
A_23_P361584	*TMEM154*	transmembrane protein 154	2,91	up
A_23_P372888	*SC5DL*	sterol-C5-desaturase (ERG3 delta-5-desaturase homolog, S. cerevisiae)-like	2,87	up
A_23_P131754	*C20orf195*	chromosome 20 open reading frame 195	2,86	up
A_23_P257716	*CYP51A1*	cytochrome P450, family 51, subfamily A, polypeptide 1	2,86	up
A_23_P77415	*OSGIN1*	oxidative stress induced growth inhibitor 1	2,84	up
A_24_P69654	*KLF6*	Kruppel-like factor 6	2,84	up
A_24_P592560			2,81	up
A_32_P44349			2,81	up
A_23_P135310	*STXBP1*	syntaxin binding protein 1	2,8	up
A_23_P88580	*ARID3B*	AT rich interactive domain 3B (BRIGHT-like)	2,79	up
A_23_P122508	*DPCR1*	diffuse panbronchiolitis critical region 1	2,75	up
A_24_P123385	*MAP1B*	microtubule-associated protein 1B	2,74	up
A_23_P11859	*HSD17B7*	hydroxysteroid (17-beta) dehydrogenase 7	2,74	up
A_24_P114183	*FDPS*	farnesyl diphosphate synthase	2,72	up
A_23_P257993	*DNASE1L3*	deoxyribonuclease I-like 3	2,72	up
A_23_P89550	*NLRP1*	NLR family, pyrin domain containing 1	2,7	up
A_32_P50223			2,7	up
A_23_P136573	*ST3GAL5*	ST3 beta-galactoside alpha-2,3-sialyltransferase 5	2,69	up
A_32_P104334			2,69	up
A_24_P103886	*IDI1*	isopentenyl-diphosphate delta isomerase 1	2,68	up
A_23_P259071	*AREG*	amphiregulin (schwannoma-derived growth factor)	2,65	up
A_24_P130041	*CYP51A1*	cytochrome P450, family 51, subfamily A, polypeptide 1	2,65	up
A_23_P78053	*FAM117A*	family with sequence similarity 117, member A	2,65	up
A_23_P63798	*KLF6*	Kruppel-like factor 6	2,64	up
A_23_P161624	*FOSL1*	FOS-like antigen 1	2,64	up
A_32_P52282	*HSD17B7*	hydroxysteroid (17-beta) dehydrogenase 7	2,63	up
A_23_P156826	*C6orf105*	chromosome 6 open reading frame 105	2,62	up
A_32_P15070			2,61	up
A_23_P147404			2,61	up
A_23_P374862	*CD55*	CD55 molecule, decay accelerating factor for complement (Cromer blood group)	2,6	up
A_32_P122492			2,59	up
A_23_P72096	*IL1A*	interleukin 1, alpha	2,59	up
A_23_P110941	*GSTA4*	glutathione S-transferase A4	2,58	up
A_23_P161647	*PC*	pyruvate carboxylase	2,58	up
A_23_P257542	*MYO1G*	myosin IG	2,58	up
A_23_P141600			2,58	up
A_32_P104432			2,58	up
A_23_P74887	*SDC3*	syndecan 3	2,57	up
A_24_P270728	*NUPR1*	nuclear protein 1	2,57	up
A_23_P52676	*CATSPER1*	cation channel, sperm associated 1	2,57	up
A_23_P370027	*GGTL3*	gamma-glutamyltransferase-like 3	2,56	up
A_23_P145786	*MLXIPL*	MLX interacting protein-like	2,56	up
A_24_P169634	*MBL1P1*	mannose-binding lectin (protein A) 1, pseudogene 1	2,55	up
A_23_P72001	*PHYHD1*	phytanoyl-CoA dioxygenase domain containing 1	2,53	up
A_32_P53183	*HSD17B7P2*	hydroxysteroid (17-beta) dehydrogenase 7 pseudogene 2	2,53	up
A_23_P138495	*PTPRE*	protein tyrosine phosphatase, receptor type, E	2,53	up

Probe_ID	Gene_ID	Definition	FC	Up/Down
A_23_P422026	*ME1*	malic enzyme 1, NADP(+)-dependent, cytosolic	2,52	up
A_23_P111995	*LOXL2*	lysyl oxidase-like 2	2,51	up
A_23_P30495	*HMGCR*	3-hydroxy-3-methylglutaryl-Coenzyme A reductase	2,51	up
A_32_P39944			2,48	up
A_23_P118722	*ASGR1*	asialoglycoprotein receptor 1	2,47	up
A_23_P11644	*SPRR2D*	small proline-rich protein 2D	2,47	up
A_24_P418250			2,47	up
A_23_P217564	*ACSL4*	acyl-CoA synthetase long-chain family member 4	2,46	up
A_32_P52609	*LPIN1*	lipin 1	2,46	up
A_23_P103601	*MAN1C1*	mannosidase, alpha, class 1C, member 1	2,45	up
A_23_P413641	*PREX1*	phosphatidylinositol 3,4,5-trisphosphate-dependent RAC exchanger 1	2,45	up
A_32_P360193	*CCDC35*	coiled-coil domain containing 35	2,44	up
A_23_P322519	*FOSL1*	FOS-like antigen 1	2,43	up
A_23_P46351	*TDRKH*	tudor and KH domain containing	2,42	up
A_23_P380298	*ProSAPiP1*	ProSAPiP1 protein	2,41	up
A_23_P73096			2,41	up
A_23_P431404	*TANC2*	tetratricopeptide repeat, ankyrin repeat and coiled-coil containing 2	2,4	up
A_23_P213319	*ADAMTS6*	ADAM metallopeptidase with thrombospondin type 1 motif, 6	2,4	up
A_23_P10614	*PDK1*	pyruvate dehydrogenase kinase, isozyme 1	2,39	up
A_23_P210330	*HSPC159*	galectin-related protein	2,37	up
A_24_P179400	*VEGFA*	vascular endothelial growth factor A	2,35	up
A_24_P376287	*LRRC8A*	leucine rich repeat containing 8 family, member A	2,34	up
A_23_P117782	*LARP6*	La ribonucleoprotein domain family, member 6	2,34	up
A_24_P235266	*GRB10*	growth factor receptor-bound protein 10	2,34	up
A_23_P134744	*RNF122*	ring finger protein 122	2,33	up
A_24_P176173	*LTBP2*	latent transforming growth factor beta binding protein 2	2,33	up
A_24_P37441	*PDK1*	pyruvate dehydrogenase kinase, isozyme 1	2,33	up
A_23_P44132	*FASN*	fatty acid synthase	2,33	up
A_23_P257497			2,33	up
A_23_P405878	*C12orf54*	chromosome 12 open reading frame 54	2,33	up
A_23_P502142	*FYN*	FYN oncogene related to SRC, FGR, YES	2,32	up
A_23_P156732	*PHF1*	PHD finger protein 1	2,31	up
A_23_P108823	*OSBPL6*	oxysterol binding protein-like 6	2,31	up
A_23_P390528	*DUSP8*	dual specificity phosphatase 8	2,31	up
A_32_P7721	*LOC283666*	hypothetical protein LOC283666	2,3	up
A_32_P93584			2,29	up
A_23_P44505	*KLF11*	Kruppel-like factor 11	2,28	up
A_23_P409417	*VPS37D*	vacuolar protein sorting 37 homolog D (S. cerevisiae)	2,27	up
A_23_P146284	*SQLE*	squalene epoxidase	2,27	up
A_23_P70398	*VEGFA*	vascular endothelial growth factor A	2,27	up
A_23_P12113	*FLVCR1*	feline leukemia virus subgroup C cellular receptor 1	2,27	up
A_24_P220947	*AKR1C1*	aldo-keto reductase family 1, member C1	2,27	up
A_23_P110212	*ACSL1*	acyl-CoA synthetase long-chain family member 1	2,27	up
A_32_P196142			2,27	up
A_24_P626920	*SCD*	stearoyl-CoA desaturase (delta-9-desaturase)	2,26	up
A_24_P107859	*SPRED1*	sprouty-related, EVH1 domain containing 1	2,26	up
A_23_P47614	*PHLDA2*	pleckstrin homology-like domain, family A, member 2	2,26	up
A_23_P254522	*COL4A4*	collagen, type IV, alpha 4	2,25	up
A_23_P336554	*IL1RAP*	interleukin 1 receptor accessory protein	2,25	up
A_24_P41975	*TDRKH*	tudor and KH domain containing	2,25	up
A_23_P24275	*C10orf110*	chromosome 10 open reading frame 110	2,24	up
A_23_P26847	*SOX9*	SRY (sex determining region Y)-box 9 (campomelic dysplasia, autosomal sex-reversal)	2,24	up
A_23_P121533	*SPON2*	spondin 2, extracellular matrix protein	2,23	up
A_32_P332320			2,23	up
A_32_P153195			2,23	up
A_23_P1331	*COL13A1*	collagen, type XIII, alpha 1	2,21	up
A_24_P99639	*NEK8*	NIMA (never in mitosis gene a)- related kinase 8	2,21	up
A_23_P131502	*TTL*	tubulin tyrosine ligase	2,21	up
A_23_P171077	*EBP*	emopamil binding protein (sterol isomerase)	2,2	up
A_23_P405761	*RRAS2*	related RAS viral (r-ras) oncogene homolog 2	2,2	up
A_23_P257971	*AKR1C1*	aldo-keto reductase family 1, member C1	2,2	up
A_32_P40288	*KIAA1913*	KIAA1913	2,2	up
A_23_P99906	*HOMER2*	homer homolog 2 (Drosophila)	2,2	up
A_23_P250274	*LRRC8A*	leucine rich repeat containing 8 family, member A	2,2	up
A_23_P22027	*INSIG1*	insulin induced gene 1	2,19	up
A_23_P24444	*DHCR7*	7-dehydrocholesterol reductase	2,19	up
A_24_P394533	*NEU1*	sialidase 1 (lysosomal sialidase)	2,19	up
A_24_P154037	*IRS2*	insulin receptor substrate 2	2,18	up
A_23_P157865	*TNC*	tenascin C (hexabrachion)	2,18	up

Probe_ID	Gene_ID	Definition	FC	Up/Down
A_23_P98786	*MYO7A*	myosin VIIA	2,18	up
A_23_P345887			2,17	up
A_23_P393034	*HAS3*	hyaluronan synthase 3	2,17	up
A_23_P103951			2,17	up
A_32_P139894			2,16	up
A_23_P34597	*CDA*	cytidine deaminase	2,16	up
A_23_P131202	*HES6*	hairy and enhancer of split 6 (Drosophila)	2,16	up
A_23_P213102	*PALLD*	palladin, cytoskeletal associated protein	2,16	up
A_23_P82503	*PEG10*	paternally expressed 10	2,16	up
A_23_P159237	*GPR20*	G protein-coupled receptor 20	2,15	up
A_24_P90005	*COL13A1*	collagen, type XIII, alpha 1	2,15	up
A_24_P943597	*PHLDA1*	pleckstrin homology-like domain, family A, member 1	2,15	up
A_23_P89780	*LAMA3*	laminin, alpha 3	2,15	up
A_32_P213103			2,15	up
A_23_P40975	*EDEM1*	ER degradation enhancer, mannosidase alpha-like 1	2,15	up
A_23_P106389	*SEMA7A*	semaphorin 7A, GPI membrane anchor (John Milton Hagen blood group)	2,14	up
A_23_P341860			2,14	up
A_24_P42693	*CYP4F11*	cytochrome P450, family 4, subfamily F, polypeptide 11	2,14	up
A_23_P54918	*LDHD*	lactate dehydrogenase D	2,13	up
A_32_P106553			2,13	up
A_32_P52519	*OTOA*	otoancorin	2,13	up
A_23_P338912	*PHLDA1*	pleckstrin homology-like domain, family A, member 1	2,13	up
A_23_P103996	*GCLM*	glutamate-cysteine ligase, modifier subunit	2,13	up
A_23_P368909			2,13	up
A_23_P387471	*MICB*	MHC class I polypeptide-related sequence B	2,12	up
A_23_P43820	*MFSD2*	major facilitator superfamily domain containing 2	2,11	up
A_23_P126103	*CTH*	cystathionase (cystathionine gamma-lyase)	2,11	up
A_32_P74983			2,11	up
A_23_P257457	*RDHE2*	epidermal retinal dehydrogenase 2	2,11	up
A_23_P201636	*LAMC2*	laminin, gamma 2	2,11	up
A_23_P404108	*KIAA1128*	KIAA1128	2,11	up
A_23_P14083	*AMIGO2*	adhesion molecule with Ig-like domain 2	2,1	up
A_24_P207503	*MEIS3*	Meis homeobox 3	2,1	up
A_23_P88767	*PLA2G10*	phospholipase A2, group X	2,1	up
A_23_P416112	*RNF168*	ring finger protein 168	2,09	up
A_23_P257516	*MICA*	MHC class I polypeptide-related sequence A	2,09	up
A_24_P302374	*CLCN6*	chloride channel 6	2,09	up
A_23_P127868	*SLC22A18*	solute carrier family 22 (organic cation transporter), member 18	2,08	up
A_32_P154911	*PRR15*	proline rich 15	2,08	up
A_24_P100368	*DYNLT3*	dynein, light chain, Tctex-type 3	2,08	up
A_23_P94216	*LONRF1*	LON peptidase N-terminal domain and ring finger 1	2,08	up
A_23_P397293	*LY6K*	lymphocyte antigen 6 complex, locus K	2,07	up
A_32_P107876	*FRAS1*	Fraser syndrome 1	2,06	up
A_23_P314760	*PRKAG2*	protein kinase, AMP-activated, gamma 2 non-catalytic subunit	2,06	up
A_32_P137382			2,06	up
A_23_P138541	*AKR1C3*	aldo-keto reductase family 1, member C3 (3-alpha hydroxysteroid dehydrogenase, type II)	2,06	up
A_23_P78795	*MEIS3*	Meis homeobox 3	2,05	up
A_32_P138260			2,05	up
A_23_P391906	*KIAA1913*	KIAA1913	2,05	up
A_32_P225854	*SPRED2*	sprouty-related, EVH1 domain containing 2	2,05	up
A_23_P59210	*CDKN1A*	cyclin-dependent kinase inhibitor 1A (p21, Cip1)	2,05	up
A_24_P115183	*CLDN4*	claudin 4	2,05	up
A_32_P201958	*FLVCR1*	feline leukemia virus subgroup C cellular receptor 1	2,04	up
A_24_P110983	*AKT3*	v-akt murine thymoma viral oncogene homolog 3 (protein kinase B, gamma)	2,04	up
A_32_P41026	*SC5DL*	sterol-C5-desaturase (ERG3 delta-5-desaturase homolog, S. cerevisiae)-like	2,04	up
A_23_P81993	*C6orf1*	chromosome 6 open reading frame 1	2,04	up
A_24_P110799	*LSS*	lanosterol synthase (2,3-oxidosqualene-lanosterol cyclase)	2,04	up
A_23_P169039	*SNAI2*	snail homolog 2 (Drosophila)	2,04	up
A_23_P107295	*LRRC37B*	leucine rich repeat containing 37B	2,04	up
A_32_P138348	*LY6K*	lymphocyte antigen 6 complex, locus K	2,04	up
A_23_P322562	*NEURL*	neuralized homolog (Drosophila)	2,04	up
A_24_P291044			2,03	up
A_23_P352879	*GCLC*	glutamate-cysteine ligase, catalytic subunit	2,03	up
A_24_P943156	*MIB1*	mindbomb homolog 1 (Drosophila)	2,03	up
A_23_P112187	*FIBCD1*	fibrinogen C domain containing 1	2,03	up
A_32_P226525			2,03	up
A_23_P417363	*CLIP4*	CAP-GLY domain containing linker protein family, member 4	2,02	up

Probe_ID	Gene_ID	Definition	FC	Up/Down
A_23_P51646	*PLK3*	polo-like kinase 3 (Drosophila)	2,02	up
A_23_P68006	*IL1R1*	interleukin 1 receptor, type I	2,02	up
A_24_P283341	*MICAL1*	microtubule associated monoxygenase, calponin and LIM domain containing 1	2,02	up
A_23_P413051	*NOXO1*	NADPH oxidase organizer 1	2,01	up
A_24_P384839	*LSS*	lanosterol synthase (2,3-oxidosqualene-lanosterol cyclase)	2,01	up
A_23_P411379	*C6orf1*	chromosome 6 open reading frame 1	2,01	up
A_23_P258410	*WNT7A*	wingless-type MMTV integration site family, member 7A	2	up
A_23_P8582	*FAM126A*	family with sequence similarity 126, member A	2	up
A_23_P210109	*CYP26B1*	cytochrome P450, family 26, subfamily B, polypeptide 1	2	up
A_24_P313678	*MED31*	mediator of RNA polymerase II transcription, subunit 31 homolog (S. cerevisiae)	2	up
A_24_P98555	*FAM45B*	family with sequence similarity 45, member B	2	up
A_32_P181077	*DOCK8*	dedicator of cytokinesis 8	12,96	down
A_23_P2674	*KRT4*	keratin 4	9,12	down
A_23_P81898	*UBD*	ubiquitin D	9,07	down
A_23_P112026	*INDO*	indoleamine-pyrrole 2,3 dioxygenase	7,37	down
A_23_P312150	*EDN2*	endothelin 2	7,26	down
A_23_P23279	*RCSD1*	RCSD domain containing 1	7,14	down
A_23_P22232	*KLRC2*	killer cell lectin-like receptor subfamily C, member 2	6,84	down
A_23_P99063	*LUM*	lumican	6,38	down
A_24_P181254	*OLFM4*	olfactomedin 4	6,12	down
A_23_P362694	*C4orf7*	chromosome 4 open reading frame 7	5,88	down
A_24_P286951	*C10orf81*	chromosome 10 open reading frame 81	5,87	down
A_23_P215634	*IGFBP3*	insulin-like growth factor binding protein 3	5,67	down
A_23_P64873	*DCN*	decorin	5,53	down
A_24_P859859			5,48	down
A_32_P145502			5,38	down
A_23_P340698	*MMP12*	matrix metallopeptidase 12 (macrophage elastase)	5,31	down
A_23_P87238	*SAA4*	serum amyloid A4, constitutive	5,18	down
A_24_P844984	*PIGR*	polymeric immunoglobulin receptor	5,17	down
A_23_P68183	*ALPPL2*	alkaline phosphatase, placental-like 2	5,16	down
A_23_P45133	*CSF1*	colony stimulating factor 1 (macrophage)	5,07	down
A_32_P351968	*HLA-DMB*	major histocompatibility complex, class II, DM beta	5,07	down
A_23_P59452	*ABP1*	amiloride binding protein 1 (amine oxidase (copper-containing))	4,87	down
A_24_P320699	*IGFBP3*	insulin-like growth factor binding protein 3	4,86	down
A_24_P52697	*H19*	H19, imprinted maternally expressed untranslated mRNA	4,8	down
A_23_P214935	*VNN3*	vanin 3	4,78	down
A_32_P234405			4,71	down
A_23_P310094	*SYNPO2*	synaptopodin 2	4,7	down
A_23_P79587	*ALPP*	alkaline phosphatase, placental (Regan isozyme)	4,69	down
A_23_P160920	*PDZK1IP1*	PDZK1 interacting protein 1	4,65	down
A_23_P421423	*TNFAIP2*	tumor necrosis factor, alpha-induced protein 2	4,56	down
A_32_P31123			4,56	down
A_23_P105939	*C14orf73*	chromosome 14 open reading frame 73	4,53	down
A_23_P394304	*PDZK1IP1*	PDZK1 interacting protein 1	4,5	down
A_23_P320054	*WNT7B*	wingless-type MMTV integration site family, member 7B	4,48	down
A_23_P103496	*GBP4*	guanylate binding protein 4	4,38	down
A_23_P306203	*SAA2*	serum amyloid A2	4,37	down
A_24_P920715			4,36	down
A_24_P923854			4,36	down
A_23_P52888	*MPPED2*	metallophosphoesterase domain containing 2	4,32	down
A_23_P138655	*CYP26A1*	cytochrome P450, family 26, subfamily A, polypeptide 1	4,3	down
A_24_P183544			4,3	down
A_23_P213020			4,29	down
A_24_P242646	*CTSS*	cathepsin S	4,29	down
A_24_P131580	*ALPPL2*	alkaline phosphatase, placental-like 2	4,25	down
A_23_P210465	*PI3*	peptidase inhibitor 3, skin-derived (SKALP)	4,24	down
A_24_P666035	*KRT77*	keratin 77	4,2	down
A_24_P53778	*ITLN2*	intelectin 2	4,2	down
A_23_P104188	*ELF3*	E74-like factor 3 (ets domain transcription factor, epithelial-specific)	4,16	down
A_23_P98622	*SAA2*	serum amyloid A2	4,15	down
A_23_P413693	*C21orf129*	chromosome 21 open reading frame 129	4,13	down
A_32_P56249			4,12	down
A_24_P911607	*WNT7B*	wingless-type MMTV integration site family, member 7B	4,07	down
A_23_P6909	*CCRL1*	chemokine (C-C motif) receptor-like 1	4,01	down
A_23_P118894	*ATAD4*	ATPase family, AAA domain containing 4	3,99	down
A_24_P923271			3,95	down
A_23_P36531	*TSPAN8*	tetraspanin 8	3,88	down
A_23_P33384	*CIITA*	class II, major histocompatibility complex, transactivator	3,82	down
A_24_P326084	*HLA-DQA1*	major histocompatibility complex, class II, DQ alpha 1	3,79	down

Probe_ID	Gene_ID	Definition	FC	Up/Down
A_23_P142815	*ATP6V1B1*	ATPase, H+ transporting, lysosomal 56/58kDa, V1 subunit B1 (Renal tubular acidosis with deafness)	3,76	down
A_23_P151046	*KLRC1*	killer cell lectin-like receptor subfamily C, member 1	3,75	down
A_23_P258769	*HLA-DPB1*	major histocompatibility complex, class II, DP beta 1	3,74	down
A_23_P71170	*TRPV6*	transient receptor potential cation channel, subfamily V, member 6	3,73	down
A_32_P105825	*MPPED2*	metallophosphoesterase domain containing 2	3,72	down
A_24_P45446	*GBP4*	guanylate binding protein 4	3,63	down
A_32_P69368	*ID2*	inhibitor of DNA binding 2, dominant negative helix-loop-helix protein	3,58	down
A_32_P75141			3,54	down
A_23_P259561			3,54	down
A_24_P335092	*SAA1*	serum amyloid A1	3,53	down
A_24_P337700	*VNN1*	vanin 1	3,5	down
A_23_P353478	*CIITA*	class II, major histocompatibility complex, transactivator	3,45	down
A_23_P503072	*CCL28*	chemokine (C-C motif) ligand 28	3,44	down
A_24_P228149	*KRT13*	keratin 13	3,41	down
A_24_P339514	*CYP2B6*	cytochrome P450, family 2, subfamily B, polypeptide 6	3,41	down
A_23_P216108	*ANK1*	ankyrin 1, erythrocytic	3,4	down
A_32_P87697	*HLA-DRA*	major histocompatibility complex, class II, DR alpha	3,37	down
A_23_P252306	*ID1*	inhibitor of DNA binding 1, dominant negative helix-loop-helix protein	3,34	down
A_32_P149011			3,28	down
A_23_P45871	*IFI44L*	interferon-induced protein 44-like	3,27	down
A_23_P137381	*ID3*	inhibitor of DNA binding 3, dominant negative helix-loop-helix protein	3,26	down
A_23_P71480	*DEFB1*	defensin, beta 1	3,26	down
A_23_P45099	*HLA-DRB5*	major histocompatibility complex, class II, DR beta 5	3,22	down
A_23_P31006	*HLA-DRB5*	major histocompatibility complex, class II, DR beta 5	3,2	down
A_24_P403417	*PTGES*	prostaglandin E synthase	3,17	down
A_24_P845223			3,17	down
A_23_P52761	*MMP7*	matrix metallopeptidase 7 (matrilysin, uterine)	3,15	down
A_23_P145336	*HLA-DRB3*	major histocompatibility complex, class II, DR beta 3	3,15	down
A_24_P602320			3,11	down
A_23_P98350	*BIRC3*	baculoviral IAP repeat-containing 3	3,1	down
A_24_P246626			3,08	down
A_24_P595567			3,05	down
A_23_P145874	*SAMD9L*	sterile alpha motif domain containing 9-like	3,04	down
A_23_P424561	*RHOV*	ras homolog gene family, member V	3,03	down
A_23_P117912	*RHOV*	ras homolog gene family, member V	3,02	down
A_23_P70095	*CD74*	CD74 molecule, major histocompatibility complex, class II invariant chain	3,02	down
A_23_P1691	*MMP1*	matrix metallopeptidase 1 (interstitial collagenase)	3	down
A_23_P211267	*RIPK4*	receptor-interacting serine-threonine kinase 4	3	down
A_23_P80162	*TMPRSS3*	transmembrane protease, serine 3	2,99	down
A_23_P315364	*CXCL2*	chemokine (C-X-C motif) ligand 2	2,99	down
A_23_P29237	*APOL3*	apolipoprotein L, 3	2,99	down
A_24_P252155	*GPR110*	G protein-coupled receptor 110	2,98	down
A_23_P1962	*RARRES3*	retinoic acid receptor responder (tazarotene induced) 3	2,95	down
A_24_P257579	*EPB41L4A*	erythrocyte membrane protein band 4.1 like 4A	2,93	down
A_23_P30913	*HLA-DPA1*	major histocompatibility complex, class II, DP alpha 1	2,93	down
A_23_P135948			2,93	down
A_24_P125871	*RIPK4*	receptor-interacting serine-threonine kinase 4	2,9	down
A_32_P164971			2,89	down
A_24_P196827	*HLA-DQA1*	major histocompatibility complex, class II, DQ alpha 1	2,89	down
A_23_P53176	*FOLR1*	folate receptor 1 (adult)	2,84	down
A_32_P162862			2,83	down
A_24_P370472	*HLA-DRB4*	major histocompatibility complex, class II, DR beta 4	2,83	down
A_23_P122127	*FYB*	FYN binding protein (FYB-120/130)	2,82	down
A_23_P216023	*ANGPT1*	angiopoietin 1	2,82	down
A_24_P393740	*FYB*	FYN binding protein (FYB-120/130)	2,8	down
A_23_P42353	*ETV7*	ets variant gene 7 (TEL2 oncogene)	2,79	down
A_23_P424734	*EXOC3L*	exocyst complex component 3-like	2,79	down
A_24_P343233	*HLA-DRB1*	major histocompatibility complex, class II, DR beta 1	2,79	down
A_23_P84118	*CDH18*	cadherin 18, type 2	2,78	down
A_23_P29773	*LAMP3*	lysosomal-associated membrane protein 3	2,78	down
A_23_P43276	*GPR124*	G protein-coupled receptor 124	2,77	down
A_23_P502520	*IL4I1*	interleukin 4 induced 1	2,77	down
A_23_P252981	*ACE2*	angiotensin I converting enzyme (peptidyl-dipeptidase A) 2	2,77	down
A_24_P397928	*CTSB*	cathepsin B	2,76	down
A_23_P157628	*DEFB4*	defensin, beta 4	2,76	down
A_23_P104464	*ALOX5*	arachidonate 5-lipoxygenase	2,76	down
A_23_P114713	*CYP4B1*	cytochrome P450, family 4, subfamily B, polypeptide 1	2,75	down

Probe_ID	Gene_ID	Definition	FC	Up/Down
A_24_P402222	*HLA-DRB3*	major histocompatibility complex, class II, DR beta 3	2,74	down
A_24_P416997	*APOL3*	apolipoprotein L, 3	2,74	down
A_23_P65779	*STRA6*	stimulated by retinoic acid gene 6 homolog (mouse)	2,74	down
A_23_P257111	*FBP1*	fructose-1,6-bisphosphatase 1	2,74	down
A_23_P121253	*TNFSF10*	tumor necrosis factor (ligand) superfamily, member 10	2,72	down
A_23_P93973	*TRPV5*	transient receptor potential cation channel, subfamily V, member 5	2,71	down
A_23_P6263	*MX2*	myxovirus (influenza virus) resistance 2 (mouse)	2,71	down
A_23_P126613	*AQP10*	aquaporin 10	2,7	down
A_23_P122393	*EGFL9*	EGF-like-domain, multiple 9	2,7	down
A_24_P127641			2,69	down
A_32_P48279			2,69	down
A_23_P162918	*SERPINA3*	serpin peptidase inhibitor, clade A (alpha-1 antiproteinase, antitrypsin), member 3	2,67	down
A_24_P557479	*XAF1*	XIAP associated factor-1	2,67	down
A_23_P33759	*DHRS3*	dehydrogenase/reductase (SDR family) member 3	2,65	down
A_23_P108157	*TJP3*	tight junction protein 3 (zona occludens 3)	2,64	down
A_24_P344961	*AMOT*	angiomotin	2,64	down
A_23_P2920	*SERPINA3*	serpin peptidase inhibitor, clade A (alpha-1 antiproteinase, antitrypsin), member 3	2,63	down
A_24_P257416	*CXCL2*	chemokine (C-X-C motif) ligand 2	2,63	down
A_24_P478940			2,62	down
A_23_P17837	*APOL1*	apolipoprotein L, 1	2,61	down
A_23_P24077	*C10orf54*	chromosome 10 open reading frame 54	2,57	down
A_24_P286114	*SLC1A3*	solute carrier family 1 (glial high affinity glutamate transporter), member 3	2,57	down
A_23_P86021	*SELENBP1*	selenium binding protein 1	2,56	down
A_23_P334955	*C8orf13*	chromosome 8 open reading frame 13	2,55	down
A_23_P93348	*LTB*	lymphotoxin beta (TNF superfamily, member 3)	2,54	down
A_23_P207905	*SECTM1*	secreted and transmembrane 1	2,54	down
A_23_P156687	*CFB*	complement factor B	2,54	down
A_24_P829156	*LOC441108*	hypothetical gene supported by AK128882	2,53	down
A_32_P92355			2,52	down
A_23_P85903	*TLR5*	toll-like receptor 5	2,51	down
A_23_P36831	*GPRC5A*	G protein-coupled receptor, family C, group 5, member A	2,5	down
A_23_P389897	*NGFR*	nerve growth factor receptor (TNFR superfamily, member 16)	2,5	down
A_24_P269315	*SERPINB1*	serpin peptidase inhibitor, clade B (ovalbumin), member 1	2,46	down
A_23_P203498	*TRIM22*	tripartite motif-containing 22	2,46	down
A_24_P918147			2,45	down
A_23_P214267	*GPR110*	G protein-coupled receptor 110	2,44	down
A_23_P140821	*PARD6A*	par-6 partitioning defective 6 homolog alpha (C. elegans)	2,43	down
A_32_P54628			2,43	down
A_32_P123589			2,41	down
A_23_P41765	*IRF1*	interferon regulatory factor 1	2,4	down
A_23_P207213	*ALDH3A1*	aldehyde dehydrogenase 3 family, memberA1	2,39	down
A_24_P813520			2,39	down
A_23_P11980			2,38	down
A_23_P46141	*CTSS*	cathepsin S	2,38	down
A_32_P87074			2,38	down
A_23_P344531	*SYNPO*	synaptopodin	2,38	down
A_24_P218688	*ALDH3B1*	aldehyde dehydrogenase 3 family, member B1	2,36	down
A_23_P379864	*ASRGL1*	asparaginase like 1	2,36	down
A_24_P48204	*SECTM1*	secreted and transmembrane 1	2,35	down
A_24_P166443	*HLA-DPB1*	major histocompatibility complex, class II, DP beta 1	2,35	down
A_23_P8363	*MGC16075*	hypothetical protein MGC16075	2,34	down
A_24_P172481	*TRIM22*	tripartite motif-containing 22	2,33	down
A_24_P66027	*APOBEC3B*	apolipoprotein B mRNA editing enzyme, catalytic polypeptide-like 3B	2,32	down
A_23_P6535			2,32	down
A_32_P171793			2,31	down
A_23_P218058	*KLRC4*	killer cell lectin-like receptor subfamily C, member 4	2,31	down
A_24_P311917	*BTN3A3*	butyrophilin, subfamily 3, member A3	2,3	down
A_24_P117294	*MX2*	myxovirus (influenza virus) resistance 2 (mouse)	2,3	down
A_23_P303978			2,3	down
A_23_P64828	*OAS1*	2',5'-oligoadenylate synthetase 1, 40/46kDa	2,29	down
A_32_P214860			2,29	down
A_23_P408955	*E2F2*	E2F transcription factor 2	2,29	down
A_23_P161439	*C10orf116*	chromosome 10 open reading frame 116	2,29	down
A_23_P369966	*APOBEC3D*	apolipoprotein B mRNA editing enzyme, catalytic polypeptide-like 3D (putative)	2,28	down
A_23_P13094	*MMP10*	matrix metallopeptidase 10 (stromelysin 2)	2,28	down
A_23_P58082	*CCDC80*	coiled-coil domain containing 80	2,27	down

Probe_ID	Gene_ID	Definition	FC	Up/Down
A_32_P4199	*RNF152*	ring finger protein 152	2,27	down
A_23_P384816	*SLC45A4*	solute carrier family 45, member 4	2,26	down
A_23_P107350	*SLC2A4*	solute carrier family 2 (facilitated glucose transporter), member 4	2,26	down
A_32_P49035			2,26	down
A_23_P28834	*PHACTR3*	phosphatase and actin regulator 3	2,25	down
A_24_P50245	*HLA-DMA*	major histocompatibility complex, class II, DM alpha	2,25	down
A_24_P303770	*CTSB*	cathepsin B	2,25	down
A_24_P14464	*WFDC2*	WAP four-disulfide core domain 2	2,24	down
A_24_P179225	*MATN2*	matrilin 2	2,23	down
A_23_P155786	*SULT1E1*	sulfotransferase family 1E, estrogen-preferring, member 1	2,23	down
A_23_P218675	*WFDC2*	WAP four-disulfide core domain 2	2,23	down
A_23_P111000	*PSMB9*	proteasome (prosome, macropain) subunit, beta type, 9 (large multifunctional peptidase 2)	2,23	down
A_23_P50638	*LRG1*	leucine-rich alpha-2-glycoprotein 1	2,23	down
A_23_P422144	*FAM43A*	family with sequence similarity 43, member A	2,22	down
A_24_P48898	*APOL2*	apolipoprotein L, 2	2,22	down
A_23_P42306	*HLA-DMA*	major histocompatibility complex, class II, DM alpha	2,22	down
A_32_P153361			2,22	down
A_23_P140807	*PSMB10*	proteasome (prosome, macropain) subunit, beta type, 10	2,21	down
A_23_P65618	*TGM1*	transglutaminase 1 (K polypeptide epidermal type I, protein-glutamine-gamma-glutamyltransferase)	2,2	down
A_24_P335656	*SECTM1*	secreted and transmembrane 1	2,2	down
A_23_P14986	*HSD11B2*	hydroxysteroid (11-beta) dehydrogenase 2	2,2	down
A_23_P214330	*SERPINB1*	serpin peptidase inhibitor, clade B (ovalbumin), member 1	2,2	down
A_24_P43810	*FAM83A*	family with sequence similarity 83, member A	2,2	down
A_23_P54709	*RAB26*	RAB26, member RAS oncogene family	2,19	down
A_23_P146855	*MPPED1*	metallophosphoesterase domain containing 1	2,18	down
A_32_P227059			2,18	down
A_32_P214925	*FLJ40722*	hypothetical protein FLJ40722	2,18	down
A_24_P8116	*CCDC80*	coiled-coil domain containing 80	2,18	down
A_32_P93841			2,17	down
A_23_P5211	*MUC16*	mucin 16, cell surface associated	2,17	down
A_23_P15146	*IL32*	interleukin 32	2,16	down
A_23_P384355			2,16	down
A_23_P500741	*CBFA2T3*	core-binding factor, runt domain, alpha subunit 2; translocated to, 3	2,15	down
A_24_P354800	*HLA-DOA*	major histocompatibility complex, class II, DO alpha	2,13	down
A_24_P333077			2,12	down
A_23_P214499	*BTN3A1*	butyrophilin, subfamily 3, member A1	2,12	down
A_23_P204087	*OAS2*	2'-5'-oligoadenylate synthetase 2, 69/71kDa	2,1	down
A_23_P115064	*CRABP2*	cellular retinoic acid binding protein 2	2,1	down
A_23_P39465	*BST2*	bone marrow stromal cell antigen 2	2,1	down
A_23_P27133	*KRT15*	keratin 15	2,1	down
A_23_P310	*MARCKSL1*	MARCKS-like 1	2,09	down
A_23_P43283	*GPR124*	G protein-coupled receptor 124	2,09	down
A_23_P29975	*C4orf19*	chromosome 4 open reading frame 19	2,09	down
A_23_P166508			2,07	down
A_23_P887	*IKBKE*	inhibitor of kappa light polypeptide gene enhancer in B-cells, kinase epsilon	2,06	down
A_23_P127948	*ADM*	adrenomedullin	2,06	down
A_24_P398210	*ZNF488*	zinc finger protein 488	2,06	down
A_23_P106002	*NFKBIA*	nuclear factor of kappa light polypeptide gene enhancer in B-cells inhibitor, alpha	2,06	down
A_23_P144916	*GFPT2*	glutamine-fructose-6-phosphate transaminase 2	2,05	down
A_23_P158880	*STARD5*	START domain containing 5	2,05	down
A_23_P201459	*IFI6*	interferon, alpha-inducible protein 6	2,05	down
A_23_P8812			2,05	down
A_23_P36700	*TAPBPL*	TAP binding protein-like	2,04	down
A_23_P202978	*CASP1*	caspase 1, apoptosis-related cysteine peptidase (interleukin 1, beta, convertase)	2,04	down
A_23_P102950	*TSGA2*	testis specific A2 homolog (mouse)	2,03	down
A_23_P131676	*CXCR7*	chemokine (C-X-C motif) receptor 7	2,02	down
A_32_P27097			2,02	down
A_24_P261259	*PFKFB3*	6-phosphofructo-2-kinase/fructose-2,6-biphosphatase 3	2,02	down
A_24_P101651			2,02	down
A_23_P31921	*ASS1*	argininosuccinate synthetase 1	2,02	down
A_23_P112921	*STARD5*	START domain containing 5	2,02	down
A_24_P393449	*DAPK1*	death-associated protein kinase 1	2,01	down
A_24_P33055			2	down
A_23_P152782	*IFI35*	interferon-induced protein 35	2	down
A_32_P228886			2	Down

Table A2: Differentially expressed transcripts by Glc-PAF

Probe_ID	Gene_ID	Definition	FC	Up/Down
A_23_P119196	*KLF2*	Kruppel-like factor 2 (lung)	19,42	up
A_23_P414654	*RAB37*	RAB37, member RAS oncogene family	16,56	up
A_23_P372946	*TM4SF19*	transmembrane 4 L six family member 19	13,17	up
A_23_P1833	*B3GAT1*	beta-1,3-glucuronyltransferase 1 (glucuronosyltransferase P)	12,11	up
A_23_P9836	*ETV5*	ets variant gene 5 (ets-related molecule)	12,09	up
A_23_P52714	*FGF19*	fibroblast growth factor 19	10,51	up
A_23_P406025	*KIAA0367*	KIAA0367	10,27	up
A_24_P532232	*CREB5*	cAMP responsive element binding protein 5	9,53	up
A_24_P227927	*IL21R*	interleukin 21 receptor	9,5	up
A_24_P633825			8,84	up
A_32_P200144	*IGH@*	immunoglobulin heavy locus	8,38	up
A_23_P348183	*MGC45491*	hypothetical protein MGC45491	7,33	up
A_23_P316012	*RHOJ*	ras homolog gene family, member J	6,94	up
A_23_P157117	*CREB5*	cAMP responsive element binding protein 5	6,36	up
A_32_P219135	*LOC401317*	hypothetical LOC401317	5,8	up
A_23_P161194	*VIM*	vimentin	4,75	up
A_23_P125972	*PRDM16*	PR domain containing 16	4,69	up
A_24_P933828	*LOC401317*	hypothetical LOC401317	4,53	up
A_23_P204937	*C13orf15*	chromosome 13 open reading frame 15	4,16	up
A_23_P207911	*TRPV2*	transient receptor potential cation channel, subfamily V, member 2	3,97	up
A_23_P119362	*EMP3*	epithelial membrane protein 3	3,89	up
A_24_P396753	*TRIB2*	tribbles homolog 2 (Drosophila)	3,77	up
A_23_P431776	*ETV4*	ets variant gene 4 (E1A enhancer binding protein, E1AF)	3,77	up
A_23_P210900	*ACSS2*	acyl-CoA synthetase short-chain family member 2	3,73	up
A_24_P156295	*ACSS2*	acyl-CoA synthetase short-chain family member 2	3,71	up
A_23_P256158	*ADRA2C*	adrenergic, alpha-2C-, receptor	3,55	up
A_32_P29200			3,48	up
A_23_P435477	*TMPRSS13*	transmembrane protease, serine 13	3,46	up
A_32_P47754	*SLC2A14*	solute carrier family 2 (facilitated glucose transporter), member 14	3,42	up
A_24_P266131	*FSTL4*	follistatin-like 4	3,33	up
A_23_P66787	*ACLY*	ATP citrate lyase	3,19	up
A_23_P210690	*TRIB3*	tribbles homolog 3 (Drosophila)	3,07	up
A_23_P101054	*KRT34*	keratin 34	2,95	up
A_23_P148753	*PLEKHA6*	pleckstrin homology domain containing, family A member 6	2,95	up
A_32_P83845	*HEY1*	hairy/enhancer-of-split related with YRPW motif 1	2,92	up
A_24_P200420	*SLC7A11*	solute carrier family 7, (cationic amino acid transporter, y+ system) member 11	2,89	up
A_23_P404045	*MTHFR*	5,10-methylenetetrahydrofolate reductase (NADPH)	2,87	up
A_23_P158976	*ABCC2*	ATP-binding cassette, sub-family C (CFTR/MRP), member 2	2,82	up
A_23_P400081	*MTHFR*	5,10-methylenetetrahydrofolate reductase (NADPH)	2,82	up
A_23_P400078	*MTHFR*	5,10-methylenetetrahydrofolate reductase (NADPH)	2,81	up
A_24_P162211	*LSS*	lanosterol synthase (2,3-oxidosqualene-lanosterol cyclase)	2,8	up
A_23_P397376	*MAF*	v-maf musculoaponeurotic fibrosarcoma oncogene homolog (avian)	2,8	up
A_23_P51136	*RHOB*	ras homolog gene family, member B	2,78	up
A_23_P105963	*AK7*	adenylate kinase 7	2,78	up
A_23_P211252	*LSS*	lanosterol synthase (2,3-oxidosqualene-lanosterol cyclase)	2,73	up
A_23_P431268	*PLEKHA6*	pleckstrin homology domain containing, family A member 6	2,7	up
A_23_P17814	*PLA2G3*	phospholipase A2, group III	2,69	up
A_23_P8640	*GPR30*	G protein-coupled receptor 30	2,66	up
A_24_P220947	*AKR1C1*	aldo-keto reductase family 1, member C1	2,63	up
A_23_P31124	*COL21A1*	collagen, type XXI, alpha 1	2,62	up
A_23_P257971	*AKR1C1*	aldo-keto reductase family 1, member C1	2,6	up
A_23_P77415	*OSGIN1*	oxidative stress induced growth inhibitor 1	2,59	up
A_23_P63618	*SCD*	stearoyl-CoA desaturase (delta-9-desaturase)	2,58	up
A_32_P208078	*MTHFR*	5,10-methylenetetrahydrofolate reductase (NADPH)	2,53	up
A_23_P302568	*SLC30A3*	solute carrier family 30 (zinc transporter), member 3	2,53	up
A_24_P67268	*FDPSL4*	farnesyl diphosphate synthase-like 4 (farnesyl pyrophosphate synthetase-like 4)	2,52	up
A_23_P44569	*ABCC2*	ATP-binding cassette, sub-family C (CFTR/MRP), member 2	2,5	up
A_24_P887615			2,41	up
A_23_P141600			2,4	up
A_32_P95223	*FDPSL2A*	MGC44478	2,39	up
A_23_P257716	*CYP51A1*	cytochrome P450, family 51, subfamily A, polypeptide 1	2,39	up
A_23_P134935	*DUSP4*	dual specificity phosphatase 4	2,36	up
A_23_P203150	*TMPRSS13*	transmembrane protease, serine 13	2,31	up
A_32_P138260			2,3	up

Probe_ID	Gene_ID	Definition	FC	Up/Down
A_24_P357914			2,3	up
A_24_P114183	*FDPS*	farnesyl diphosphate synthase	2,3	up
A_23_P131754	*C20orf195*	chromosome 20 open reading frame 195	2,28	up
A_23_P135310	*STXBP1*	syntaxin binding protein 1	2,28	up
A_23_P74012	*SPRR1A*	small proline-rich protein 1A	2,27	up
A_23_P145786	*MLXIPL*	MLX interacting protein-like	2,26	up
A_23_P22735	*BEX2*	brain expressed X-linked 2	2,25	up
A_32_P210168	*LOC388135*	similar to RIKEN cDNA 6030419C18 gene	2,24	up
A_23_P87013	*TAGLN*	transgelin	2,23	up
A_23_P422026	*ME1*	malic enzyme 1, NADP(+)-dependent, cytosolic	2,22	up
A_24_P201171	*STXBP1*	syntaxin binding protein 1	2,18	up
A_23_P52676	*CATSPER1*	cation channel, sperm associated 1	2,17	up
A_23_P122655	*FLJ13744*	hypothetical protein FLJ13744	2,17	up
A_24_P200831	*MLXIPL*	MLX interacting protein-like	2,16	up
A_23_P11859	*HSD17B7*	hydroxysteroid (17-beta) dehydrogenase 7	2,16	up
A_23_P38876	*LIPE*	lipase, hormone-sensitive	2,16	up
A_32_P104334			2,14	up
A_23_P352879	*GCLC*	glutamate-cysteine ligase, catalytic subunit	2,09	up
A_23_P72001	*PHYHD1*	phytanoyl-CoA dioxygenase domain containing 1	2,09	up
A_23_P54918	*LDHD*	lactate dehydrogenase D	2,08	up
A_23_P413641	*PREX1*	phosphatidylinositol 3,4,5-trisphosphate-dependent RAC exchanger 1	2,07	up
A_32_P52282	*HSD17B7*	hydroxysteroid (17-beta) dehydrogenase 7	2,07	up
A_23_P82503	*PEG10*	paternally expressed 10	2,06	up
A_32_P53183	*HSD17B7P2*	hydroxysteroid (17-beta) dehydrogenase 7 pseudogene 2	2,05	up
A_32_P52609	*LPIN1*	lipin 1	2,05	up
A_23_P161647	*PC*	pyruvate carboxylase	2,05	up
A_23_P382775	*BBC3*	BCL2 binding component 3	2,04	up
A_23_P341860			2,02	up
A_23_P146284	*SQLE*	squalene epoxidase	2,02	up
A_23_P214432			2,01	up
A_23_P78053	*FAM117A*	family with sequence similarity 117, member A	2	up
A_23_P312150	*EDN2*	endothelin 2	6,28	down
A_23_P81898	*UBD*	ubiquitin D	4,5	down
A_24_P920715			4,23	down
A_23_P64873	*DCN*	decorin	4,2	down
A_24_P181254	*OLFM4*	olfactomedin 4	3,57	down
A_32_P145502			3,29	down
A_23_P215634	*IGFBP3*	insulin-like growth factor binding protein 3	3,28	down
A_24_P320699	*IGFBP3*	insulin-like growth factor binding protein 3	3,13	down
A_23_P18751	*TMPRSS11E*	transmembrane protease, serine 11E	2,83	down
A_23_P87238	*SAA4*	serum amyloid A4, constitutive	2,81	down
A_23_P79587	*ALPP*	alkaline phosphatase, placental (Regan isozyme)	2,78	down
A_23_P413693	*C21orf129*	chromosome 21 open reading frame 129	2,73	down
A_23_P213020			2,72	down
A_32_P149011			2,63	down
A_32_P31123			2,56	down
A_23_P98622	*SAA2*	serum amyloid A2	2,55	down
A_32_P56249			2,49	down
A_23_P408363			2,46	down
A_23_P6909	*CCRL1*	chemokine (C-C motif) receptor-like 1	2,44	down
A_23_P310094	*SYNPO2*	synaptopodin 2	2,33	down
A_24_P252155	*GPR110*	G protein-coupled receptor 110	2,29	down
A_23_P117912	*RHOV*	ras homolog gene family, member V	2,26	down
A_23_P211267	*RIPK4*	receptor-interacting serine-threonine kinase 4	2,25	down
A_23_P43276	*GPR124*	G protein-coupled receptor 124	2,24	down
A_24_P335092	*SAA1*	serum amyloid A1	2,23	down
A_23_P93973	*TRPV5*	transient receptor potential cation channel, subfamily V, member 5	2,23	down
A_24_P397928	*CTSB*	cathepsin B	2,21	down
A_23_P36831	*GPRC5A*	G protein-coupled receptor, family C, group 5, member A	2,2	down
A_23_P1691	*MMP1*	matrix metallopeptidase 1 (interstitial collagenase)	2,19	down
A_24_P829156	*LOC441108*	hypothetical gene supported by AK128882	2,17	down
A_23_P122393	*EGFL9*	EGF-like-domain, multiple 9	2,14	down
A_23_P53176	*FOLR1*	folate receptor 1 (adult)	2,13	down
A_32_P162862			2,11	down
A_24_P125871	*RIPK4*	receptor-interacting serine-threonine kinase 4	2,08	down
A_23_P29237	*APOL3*	apolipoprotein L, 3	2,07	down
A_24_P179225	*MATN2*	matrilin 2	2,05	down
A_23_P503072	*CCL28*	chemokine (C-C motif) ligand 28	2,04	down

Table A3: Differentially expressed transcripts by edelfosine

Probe_ID	Gene_ID	Definition	FC	Up/Down
A_23_P372946	*TM4SF19*	transmembrane 4 L six family member 19	21,84	up
A_23_P119196	*KLF2*	Kruppel-like factor 2 (lung)	20,65	up
A_32_P189781			18,69	up
A_23_P9836	*ETV5*	ets variant gene 5 (ets-related molecule)	15,82	up
A_24_P532232	*CREB5*	cAMP responsive element binding protein 5	14,87	up
A_23_P414654	*RAB37*	RAB37, member RAS oncogene family	13,68	up
A_32_P200144	*IGH@*	immunoglobulin heavy locus	12,93	up
A_32_P208350	*TDRD9*	tudor domain containing 9	11,46	up
A_23_P157117	*CREB5*	cAMP responsive element binding protein 5	11,26	up
A_23_P1833	*B3GAT1*	beta-1,3-glucuronyltransferase 1 (glucuronosyltransferase P)	10,37	up
A_32_P33802			10,31	up
A_23_P52714	*FGF19*	fibroblast growth factor 19	10,12	up
A_24_P226008	*MGLL*	monoglyceride lipase	9,68	up
A_32_P20613			8,92	up
A_32_P219135	*LOC401317*	hypothetical LOC401317	8,27	up
A_23_P161624	*FOSL1*	FOS-like antigen 1	8,26	up
A_23_P101054	*KRT34*	keratin 34	7,72	up
A_23_P322519	*FOSL1*	FOS-like antigen 1	7,72	up
A_32_P187571	*SCN2B*	sodium channel, voltage-gated, type II, beta	7,47	up
A_23_P103361	*LCK*	lymphocyte-specific protein tyrosine kinase	6,92	up
A_23_P161218	*ANKRD1*	ankyrin repeat domain 1 (cardiac muscle)	6,71	up
A_24_P933828	*LOC401317*	hypothetical LOC401317	6,68	up
A_23_P161190	*VIM*	vimentin	6,4	up
A_23_P427587	*FGF19*	fibroblast growth factor 19	6,38	up
A_23_P133408	*CSF2*	colony stimulating factor 2 (granulocyte-macrophage)	6,37	up
A_24_P328524	*KALRN*	kalirin, RhoGEF kinase	6,28	up
A_23_P161194	*VIM*	vimentin	6,14	up
A_24_P10137	*C13orf15*	chromosome 13 open reading frame 15	5,97	up
A_23_P204937	*C13orf15*	chromosome 13 open reading frame 15	5,67	up
A_23_P66739	*SLC13A5*	solute carrier family 13 (sodium-dependent citrate transporter), member 5	5,6	up
A_23_P87013	*TAGLN*	transgelin	5,56	up
A_23_P431776	*ETV4*	ets variant gene 4 (E1A enhancer binding protein, E1AF)	5,51	up
A_23_P259071	*AREG*	amphiregulin (schwannoma-derived growth factor)	5,46	up
A_23_P87011	*TAGLN*	transgelin	5,43	up
A_24_P416346	*ETV4*	ets variant gene 4 (E1A enhancer binding protein, E1AF)	5,25	up
A_23_P30634	*BACH2*	BTB and CNC homology 1, basic leucine zipper transcription factor 2	5,21	up
A_23_P146146	*ATP6V0D2*	ATPase, H+ transporting, lysosomal 38kDa, V0 subunit d2	5,19	up
A_24_P227927	*IL21R*	interleukin 21 receptor	5	up
A_23_P341938	*NOG*	noggin	4,92	up
A_23_P41344	*EREG*	epiregulin	4,83	up
A_23_P96271	*MYOM1*	myomesin 1, 185kDa	4,79	up
A_23_P204847	*LCP1*	lymphocyte cytosolic protein 1 (L-plastin)	4,76	up
A_32_P44349			4,74	up
A_23_P50919	*SERPINE2*	serpin peptidase inhibitor, clade E (nexin, plasminogen activator inhibitor type 1), member 2	4,71	up
A_23_P213319	*ADAMTS6*	ADAM metallopeptidase with thrombospondin type 1 motif, 6	4,64	up
A_32_P47754	*SLC2A14*	solute carrier family 2 (facilitated glucose transporter), member 14	4,63	up
A_23_P348183	*MGC45491*	hypothetical protein MGC45491	4,63	up
A_23_P435477	*TMPRSS13*	transmembrane protease, serine 13	4,61	up
A_23_P393034	*HAS3*	hyaluronan synthase 3	4,59	up
A_23_P128728	*ARG2*	arginase, type II	4,57	up
A_23_P74012	*SPRR1A*	small proline-rich protein 1A	4,35	up
A_23_P27013	*HOXB9*	homeobox B9	4,28	up
A_23_P159325	*ANGPTL4*	angiopoietin-like 4	4,23	up
A_23_P406025	*KIAA0367*	KIAA0367	4,16	up
A_24_P28977	*TRPC1*	transient receptor potential cation channel, subfamily C, member 1	4,11	up
A_23_P134935	*DUSP4*	dual specificity phosphatase 4	4,07	up
A_23_P170719			4,05	up
A_32_P83845	*HEY1*	hairy/enhancer-of-split related with YRPW motif 1	4,05	up
A_24_P934008			4,04	up
A_23_P203150	*TMPRSS13*	transmembrane protease, serine 13	3,93	up
A_24_P943597	*PHLDA1*	pleckstrin homology-like domain, family A, member 1	3,82	up
A_32_P235358			3,79	up
A_23_P102364	*NGEF*	neuronal guanine nucleotide exchange factor	3,7	up

Probe_ID	Gene_ID	Definition	FC	Up/Down
A_23_P17826	*SLC5A1*	solute carrier family 5 (sodium/glucose cotransporter), member 1	3,69	up
A_23_P86599	*DMBT1*	deleted in malignant brain tumors 1	3,67	up
A_24_P158089	*SERPINE1*	serpin peptidase inhibitor, clade E (nexin, plasminogen activator inhibitor type 1), member 1	3,65	up
A_24_P103004	*SLC20A1*	solute carrier family 20 (phosphate transporter), member 1	3,64	up
A_23_P310972	*PCDHGB1*	protocadherin gamma subfamily B, 1	3,61	up
A_23_P138495	*PTPRE*	protein tyrosine phosphatase, receptor type, E	3,55	up
A_23_P123234			3,54	up
A_23_P79518	*IL1B*	interleukin 1, beta	3,53	up
A_23_P40174	*MMP9*	matrix metallopeptidase 9 (gelatinase B, 92kDa gelatinase, 92kDa type IV collagenase)	3,46	up
A_23_P129856	*HIC1*	hypermethylated in cancer 1	3,42	up
A_24_P123408	*ABLIM3*	actin binding LIM protein family, member 3	3,37	up
A_23_P122924	*INHBA*	inhibin, beta A (activin A, activin AB alpha polypeptide)	3,37	up
A_23_P256581	*PRDM13*	PR domain containing 13	3,31	up
A_23_P122863	*GRB10*	growth factor receptor-bound protein 10	3,26	up
A_32_P159706			3,24	up
A_23_P76450	*PHLDA1*	pleckstrin homology-like domain, family A, member 1	3,22	up
A_23_P51136	*RHOB*	ras homolog gene family, member B	3,21	up
A_23_P211428	*SMTN*	smoothelin	3,19	up
A_23_P218646	*TNFRSF6B*	tumor necrosis factor receptor superfamily, member 6b, decoy	3,15	up
A_23_P207911	*TRPV2*	transient receptor potential cation channel, subfamily V, member 2	3,13	up
A_23_P502142	*FYN*	FYN oncogene related to SRC, FGR, YES	3,12	up
A_24_P305541	*TRIB3*	tribbles homolog 3 (Drosophila)	3,11	up
A_23_P156826	*C6orf105*	chromosome 6 open reading frame 105	3,09	up
A_23_P28999	*CDH4*	cadherin 4, type 1, R-cadherin (retinal)	3,08	up
A_24_P535256			3,05	up
A_23_P21092	*CALB2*	calbindin 2, 29kDa (calretinin)	3,01	up
A_23_P123503	*TRIB1*	tribbles homolog 1 (Drosophila)	3	up
A_24_P931690			2,98	up
A_23_P108823	*OSBPL6*	oxysterol binding protein-like 6	2,96	up
A_23_P361584	*TMEM154*	transmembrane protein 154	2,94	up
A_24_P944991	*P18SRP*	P18SRP protein	2,94	up
A_32_P218707			2,9	up
A_32_P10403			2,89	up
A_23_P83007	*C9orf150*	chromosome 9 open reading frame 150	2,88	up
A_23_P102551	*MALL*	mal, T-cell differentiation protein-like	2,88	up
A_24_P80204	*MALL*	mal, T-cell differentiation protein-like	2,86	up
A_23_P258612	*ATP8A2*	ATPase, aminophospholipid transporter-like, Class I, type 8A, member 2	2,82	up
A_23_P52676	*CATSPER1*	cation channel, sperm associated 1	2,81	up
A_32_P161855	*KIAA1199*	KIAA1199	2,79	up
A_32_P122492			2,76	up
A_23_P103951			2,74	up
A_23_P315571	*RFTN1*	raftlin, lipid raft linker 1	2,74	up
A_23_P119362	*EMP3*	epithelial membrane protein 3	2,72	up
A_24_P156295	*ACSS2*	acyl-CoA synthetase short-chain family member 2	2,71	up
A_23_P431404	*TANC2*	tetratricopeptide repeat, ankyrin repeat and coiled-coil containing 2	2,7	up
A_32_P39944			2,7	up
A_23_P1331	*COL13A1*	collagen, type XIII, alpha 1	2,69	up
A_23_P158817	*IGH@*	immunoglobulin heavy locus	2,69	up
A_23_P126888	*KIF21B*	kinesin family member 21B	2,68	up
A_23_P165657	*SLC20A1*	solute carrier family 20 (phosphate transporter), member 1	2,68	up
A_23_P338912	*PHLDA1*	pleckstrin homology-like domain, family A, member 1	2,67	up
A_23_P210690	*TRIB3*	tribbles homolog 3 (Drosophila)	2,62	up
A_24_P130959	*KIAA1804*	mixed lineage kinase 4	2,62	up
A_23_P322562	*NEURL*	neuralized homolog (Drosophila)	2,54	up
A_24_P179400	*VEGFA*	vascular endothelial growth factor A	2,51	up
A_23_P69810	*MAG1*	lung cancer metastasis-associated protein	2,51	up
A_23_P210900	*ACSS2*	acyl-CoA synthetase short-chain family member 2	2,5	up
A_23_P88580	*ARID3B*	AT rich interactive domain 3B (BRIGHT-like)	2,47	up
A_23_P138492	*NEURL*	neuralized homolog (Drosophila)	2,46	up
A_23_P56703			2,46	up
A_24_P154037	*IRS2*	insulin receptor substrate 2	2,45	up
A_23_P157865	*TNC*	tenascin C (hexabrachion)	2,44	up
A_23_P430818	*HSPC159*	galectin-related protein	2,43	up
A_32_P139894			2,43	up
A_24_P90005	*COL13A1*	collagen, type XIII, alpha 1	2,42	up
A_24_P37409	*DUSP2*	dual specificity phosphatase 2	2,42	up

Probe_ID	Gene_ID	Definition	FC	Up/Down
A_24_P109921			2,41	up
A_23_P106389	*SEMA7A*	semaphorin 7A, GPI membrane anchor (John Milton Hagen blood group)	2,4	up
A_23_P431388	*SPOCD1*	SPOC domain containing 1	2,38	up
A_23_P88347	*PLEKHC1*	pleckstrin homology domain containing, family C (with FERM domain) member 1	2,38	up
A_24_P376391	*PLXND1*	plexin D1	2,38	up
A_23_P70398	*VEGFA*	vascular endothelial growth factor A	2,38	up
A_24_P114255	*MBOAT2*	membrane bound O-acyltransferase domain containing 2	2,37	up
A_24_P376287	*LRRC8A*	leucine rich repeat containing 8 family, member A	2,36	up
A_24_P167668	*LTBP2*	latent transforming growth factor beta binding protein 2	2,35	up
A_23_P53838	*IRS2*	insulin receptor substrate 2	2,33	up
A_32_P76720	*NT5DC3*	5'-nucleotidase domain containing 3	2,32	up
A_23_P67980	*KLF7*	Kruppel-like factor 7 (ubiquitous)	2,3	up
A_23_P118722	*ASGR1*	asialoglycoprotein receptor 1	2,3	up
A_23_P391906	*KIAA1913*	KIAA1913	2,29	up
A_24_P213503	*PTPRE*	protein tyrosine phosphatase, receptor type, E	2,29	up
A_24_P337796	*STK17A*	serine/threonine kinase 17a	2,27	up
A_23_P121657	*HS3ST1*	heparan sulfate (glucosamine) 3-O-sulfotransferase 1	2,25	up
A_23_P44132	*FASN*	fatty acid synthase	2,25	up
A_23_P49338	*TNFRSF12A*	tumor necrosis factor receptor superfamily, member 12A	2,24	up
A_32_P7721	*LOC283666*	hypothetical protein LOC283666	2,23	up
A_32_P3783			2,23	up
A_23_P81805	*VEGFA*	vascular endothelial growth factor A	2,21	up
A_23_P356581	*ROBO3*	roundabout, axon guidance receptor, homolog 3 (Drosophila)	2,2	up
A_24_P406480	*LONRF1*	LON peptidase N-terminal domain and ring finger 1	2,2	up
A_23_P207850	*TNS4*	tensin 4	2,19	up
A_23_P256205	*ABLIM3*	actin binding LIM protein family, member 3	2,18	up
A_23_P418031			2,18	up
A_23_P15394	*CD68*	CD68 molecule	2,17	up
A_32_P21993	*TPM4*	tropomyosin 4	2,14	up
A_32_P196142			2,14	up
A_23_P59388	*DST*	dystonin	2,14	up
A_23_P138099	*ABL2*	v-abl Abelson murine leukemia viral oncogene homolog 2 (arg, Abelson-related gene)	2,12	up
A_23_P8640	*GPR30*	G protein-coupled receptor 30	2,11	up
A_23_P368779	*ZNF114*	zinc finger protein 114	2,11	up
A_24_P100368	*DYNLT3*	dynein, light chain, Tctex-type 3	2,1	up
A_32_P34920	*FOXD1*	forkhead box D1	2,09	up
A_24_P82880	*TPM4*	tropomyosin 4	2,09	up
A_24_P368575	*SLC4A7*	solute carrier family 4, sodium bicarbonate cotransporter, member 7	2,09	up
A_23_P256334	*ITGA1*	integrin, alpha 1	2,08	up
A_23_P47614	*PHLDA2*	pleckstrin homology-like domain, family A, member 2	2,08	up
A_23_P22735	*BEX2*	brain expressed X-linked 2	2,08	up
A_24_P144773	*RNF145*	ring finger protein 145	2,07	up
A_23_P67847	*GALNT14*	UDP-N-acetyl-alpha-D-galactosamine:polypeptide N-acetylgalactosaminyltransferase 14 (GalNAc-T14)	2,07	up
A_23_P136724	*LOC344887*	similar to NmrA-like family domain containing 1	2,07	up
A_23_P141974	*TPM4*	tropomyosin 4	2,06	up
A_23_P115478	*PADI1*	peptidyl arginine deiminase, type I	2,06	up
A_32_P332320			2,06	up
A_23_P16469	*PLAUR*	plasminogen activator, urokinase receptor	2,06	up
A_23_P247			2,04	up
A_23_P154367	*STK17B*	serine/threonine kinase 17b	2,02	up
A_23_P81529	*ISL1*	ISL1 transcription factor, LIM/homeodomain, (islet-1)	2,02	up
A_23_P257457	*RDHE2*	epidermal retinal dehydrogenase 2	2,01	up
A_23_P99906	*HOMER2*	homer homolog 2 (Drosophila)	2,01	up
A_23_P34325	*LRP8*	low density lipoprotein receptor-related protein 8, apolipoprotein e receptor	2	up
A_24_P68908	*LOC344887*	similar to NmrA-like family domain containing 1	2	up
A_32_P181077	*DOCK8*	dedicator of cytokinesis 8	8,19	down
A_23_P99063	*LUM*	lumican	7,45	down
A_23_P23279	*RCSD1*	RCSD domain containing 1	7,09	down
A_24_P286951	*C10orf81*	chromosome 10 open reading frame 81	6,49	down
A_23_P64873	*DCN*	decorin	6,09	down
A_23_P420442	*SEMA6D*	sema domain, transmembrane domain (TM), and cytoplasmic domain, (semaphorin) 6D	5,64	down
A_23_P36531	*TSPAN8*	tetraspanin 8	4,95	down
A_23_P68183	*ALPPL2*	alkaline phosphatase, placental-like 2	4,53	down
A_23_P79587	*ALPP*	alkaline phosphatase, placental (Regan isozyme)	4,41	down
A_32_P125832			4,01	down

Probe_ID	Gene_ID	Definition	FC	Up/Down
A_23_P413693	*C21orf129*	chromosome 21 open reading frame 129	4	down
A_23_P92730	*HSPB3*	heat shock 27kDa protein 3	3,86	down
A_32_P211301			3,31	down
A_24_P131580	*ALPPL2*	alkaline phosphatase, placental-like 2	3,31	down
A_23_P213020			3,26	down
A_32_P48279			3,26	down
A_23_P35564	*SEC31B*	SEC31 homolog B (S. cerevisiae)	3,15	down
A_23_P81898	*UBD*	ubiquitin D	3,13	down
A_23_P127948	*ADM*	adrenomedullin	3,09	down
A_23_P53176	*FOLR1*	folate receptor 1 (adult)	3,07	down
A_23_P91910	*PLSCR4*	phospholipid scramblase 4	2,89	down
A_23_P216023	*ANGPT1*	angiopoietin 1	2,77	down
A_23_P54709	*RAB26*	RAB26, member RAS oncogene family	2,76	down
A_32_P93841			2,68	down
A_32_P54628			2,61	down
A_23_P422144	*FAM43A*	family with sequence similarity 43, member A	2,55	down
A_23_P18751	*TMPRSS11E*	transmembrane protease, serine 11E	2,54	down
A_23_P58082	*CCDC80*	coiled-coil domain containing 80	2,53	down
A_23_P131676	*CXCR7*	chemokine (C-X-C motif) receptor 7	2,52	down
A_32_P145502			2,49	down
A_24_P268993	*LEAP2*	liver expressed antimicrobial peptide 2	2,47	down
A_32_P196287			2,46	down
A_32_P75141			2,42	down
A_23_P215634	*IGFBP3*	insulin-like growth factor binding protein 3	2,4	down
A_23_P421423	*TNFAIP2*	tumor necrosis factor, alpha-induced protein 2	2,39	down
A_32_P56249			2,36	down
A_23_P118571	*SOST*	sclerosteosis	2,36	down
A_23_P1962	*RARRES3*	retinoic acid receptor responder (tazarotene induced) 3	2,34	down
A_23_P337262	*APCDD1*	adenomatosis polyposis coli down-regulated 1	2,34	down
A_23_P344531	*SYNPO*	synaptopodin	2,28	down
A_23_P211267	*RIPK4*	receptor-interacting serine-threonine kinase 4	2,28	down
A_24_P125871	*RIPK4*	receptor-interacting serine-threonine kinase 4	2,27	down
A_24_P182947	*GCET2*	germinal center expressed transcript 2	2,2	down
A_23_P116743	*LOC338799*	hypothetical locus LOC338799	2,2	down
A_32_P226678			2,19	down
A_23_P11980			2,19	down
A_24_P8116	*CCDC80*	coiled-coil domain containing 80	2,19	down
A_23_P415021	*METTL7A*	methyltransferase like 7A	2,18	down
A_24_P286114	*SLC1A3*	solute carrier family 1 (glial high affinity glutamate transporter), member 3	2,18	down
A_32_P154223			2,17	down
A_23_P29237	*APOL3*	apolipoprotein L, 3	2,16	down
A_23_P93973	*TRPV5*	transient receptor potential cation channel, subfamily V, member 5	2,15	down
A_32_P54128			2,15	down
A_23_P86021	*SELENBP1*	selenium binding protein 1	2,12	down
A_23_P64808	*HOXC13*	homeobox C13	2,12	down
A_24_P320699	*IGFBP3*	insulin-like growth factor binding protein 3	2,11	down
A_23_P41765	*IRF1*	interferon regulatory factor 1	2,11	down
A_23_P16225	*BEST2*	bestrophin 2	2,1	down
A_23_P116173	*LOC120376*	hypothetical protein LOC120376	2,1	down
A_32_P100258	*FLJ37453*	hypothetical protein LOC645580	2,09	down
A_23_P24077	*C10orf54*	chromosome 10 open reading frame 54	2,04	down
A_23_P29922	*TLR3*	toll-like receptor 3	2,03	down
A_32_P330000			2,01	down
A_24_P760945			2	down
A_23_P121665	*SORCS2*	sortilin-related VPS10 domain containing receptor 2	2	down
A_32_P163472			2	down

Complete list of differentially expressed transcripts by Ino-C2-PAF (A1), Glc-PAF (A2) and edelfosine (A3). Empty text in Gene_ID and Definition columns indicates no availability of associated gene information for Agilent ID. FC: Fold Change; Up/Down: Up- or down-regulated transcript.

B) Differentially expressed genes by APLs represented in Venn diagrams

Table B1: UP-regulated genes

Ino-C2-PAF	Glc-PAF	Edelfosine	Ino-C2-PAF & Glc-PAF	Glc-PAF & edelfosine	Ino-C2-PAF & edelfosine	All APLs
ABHD3	*BBC3*	*ABL2*	*ABCC2*		*ABLIM3*	*ACSS2*
ACAT2	*COL21A1*	*ANGPTL4*	*ACLY*		*ADAMTS6*	*B3GAT1*
ACSL1	*FLJ13744*	*ATP6V0D2*	*ADRA2C*		*ANKRD1*	*BEX2*
ACSL4	*LIPE*	*ATP8A2*	*AK7*		*AREG*	*C13orf15*
AKR1C3	*LOC388135*	*CALB2*	*AKR1C1*		*ARG2*	*CATSPER1*
AKT3		*CD68*	*C20orf195*		*ARID3B*	*CREB5*
ALOX12B		*CDH4*	*CYP51A1*		*ASGR1*	*DUSP4*
AMIGO2		*CSF2*	*FAM117A*		*BACH2*	*EMP3*
ATP12A		*DMBT1*	*FDPS*		*C6orf105*	*ETV4*
C10orf110		*DUSP2*	*FDPSL2A*		*C9orf150*	*ETV5*
C12orf54		*EREG*	*FDPSL4*		*COL13A1*	*FGF19*
C6orf1		*FOXD1*	*FSTL4*		*DST*	*GPR30*
CCDC35		*GALNT14*	*GCLC*		*DYNLT3*	*HEY1*
CD55		*HOXB9*	*HSD17B7*		*FASN*	*IGH@*
CD6		*HS3ST1*	*HSD17B7P2*		*FOSL1*	*IL21R*
CDA		*IL1B*	*LDHD*		*FYN*	*KIAA0367*
CDKN1A		*INHBA*	*LPIN1*		*GRB10*	*KLF2*
CLCN6		*ITGA1*	*LSS*		*HAS3*	*KRT34*
CLDN4		*KIAA1199*	*MAF*		*HIC1*	*LOC401317*
CLIP4		*KIAA1804*	*ME1*		*HOMER2*	*MGC45491*
CNN1		*KIF21B*	*MLXIPL*		*HSPC159*	*RAB37*
COL4A4		*KLF7*	*MTHFR*		*IRS2*	*RHOB*
CTH		*LRP8*	*OSGIN1*		*ISL1*	*SLC2A14*
CYP26B1		*MAG1*	*PC*		*KALRN*	*SPRR1A*
CYP4F11		*MALL*	*PEG10*		*KIAA1913*	*TAGLN*
DHCR7		*MBOAT2*	*PHYHD1*		*LCK*	*TM4SF19*
DNASE1L3		*MMP9*	*PLA2G3*		*LCP1*	*TMPRSS13*
DNHD2		*NGEF*	*PLEKHA6*		*LOC283666*	*TRIB3*
DPCR1		*NT5DC3*	*PRDM16*		*LOC344887*	*TRPV2*
DUSP8		*P18SRP*	*PREX1*		*LONRF1*	*VIM*
EBP		*PADI1*	*RHOJ*		*LRRC8A*	
EDEM1		*PCDHGB1*	*SCD*		*LTBP2*	
FABP3		*PLAUR*	*SLC30A3*		*MGLL*	
FAM126A		*PLEKHC1*	*SLC7A11*		*MYOM1*	
FAM45B		*PLXND1*	*SQLE*		*NEURL*	
FCRLA		*PRDM13*	*STXBP1*		*NOG*	
FIBCD1		*RFTN1*	*TRIB2*		*OSBPL6*	
FLVCR1		*RNF145*			*PHLDA1*	
FRAS1		*ROBO3*			*PHLDA2*	
GCLM		*SERPINE1*			*PTPRE*	
GGTL3		*SERPINE2*			*RDHE2*	
GPNMB		*SLC4A7*			*SCN2B*	
GPR20		*SLC5A1*			*SEMA7A*	
GSTA4		*SMTN*			*SLC13A5*	
HES6		*SPOCD1*			*SLC20A1*	
HMGCR		*STK17A*			*TANC2*	
HMGCS1		*STK17B*			*TMEM154*	
HS3ST2		*TDRD9*			*TNC*	
IDI1		*TNFRSF12A*			*VEGFA*	
IL1A		*TNFRSF6B*				
IL1R1		*TNS4*				
IL1RAP		*TPM4*				

Ino-C2-PAF	Glc-PAF	Edelfosine	Ino-C2-PAF & Glc-PAF	Glc-PAF & edelfosine	Ino-C2-PAF & edelfosine	All APLs
INSIG1 *KCNMA1* *KIAA1128* *KLF11* *KLF6* *LAMA3* *LAMC2* *LARP6* *LOC374569* *LOXL2* *LRRC37B* *LY6K* *MAN1C1* *MAP1B* *MBL1P1* *MED31* *MEIS3* *MFSD2* *MGC23284* *MGC50722* *MIB1* *MICA* *MICAL1* *MICB* *MVD* *MYO15A* *MYO1G* *MYO7A* *NACAD* *NEK8* *NEU1* *NLRP1* *NOXO1* *NUPR1* *OTOA* *PALLD* *PDK1* *PHF1* *PLA2G10* *PLK3* *PNMA3* *PRKAG2* *PRR15* *ProSAPiP1* *RASGEF1A* *RNF122* *RNF168* *RP5-1054A22.3* *RRAS2* *SC4MOL* *SC5DL* *SDC3* *SH2D5* *SLC22A18* *SLC2A3* *SLC9A2*		*TRIB1* *TRPC1* *ZNF114*				

Ino-C2-PAF	Glc-PAF	Edelfosine	Ino-C2-PAF & Glc-PAF	Glc-PAF & edelfosine	Ino-C2-PAF & edelfosine	All APLs
SNAI2 *SOX9* *SPON2* *SPRED1* *SPRED2* *SPRR2D* *ST3GAL5* *TDRKH* *TGM2* *THEG* *TTL* *USP51* *VPS37D* *WNT7A*						

Table B2: DOWN-regulated genes

Ino-C2-PAF	Glc-PAF	Edelfosine	Ino-C2-PAF & Glc-PAF	Glc-PAF & edelfosine	Ino-C2-PAF & edelfosine	All APLs
ABP1 *ACE2* *ALDH3A1* *ALDH3B1* *ALOX5* *AMOT* *ANK1* *APOBEC3B* *APOBEC3D* *APOL1* *APOL2* *AQP10* *ASRGL1* *ASS1* *ATAD4* *ATP6V1B1* *BIRC3* *BST2* *BTN3A1* *BTN3A3* *C10orf116* *C14orf73* *C4orf19* *C4orf7* *C8orf13* *CASP1* *CBFA2T3* *CD74* *CDH18* *CFB* *CIITA* *CRABP2* *CSF1* *CTSS* *CXCL2*		*APCDD1* *BEST2* *FLJ37453* *GCET2* *HOXC13* *HSPB3* *LEAP2* *LOC120376* *LOC338799* *METTL7A* *PLSCR4* *SEC31B* *SEMA6D* *SORCS2* *SOST* *TLR3*	*CCL28* *CCRL1* *CTSB* *EDN2* *EGFL9* *GPR110* *GPR124* *GPRC5A* *LOC441108* *MATN2* *MMP1* *OLFM4* *RHOV* *SAA1* *SAA2* *SAA4* *SYNPO2*	*TMPRSS11E*	*ADM* *ALPPL2* *ANGPT1* *C10orf54* *C10orf81* *CCDC80* *CXCR7* *DOCK8* *FAM43A* *IRF1* *LUM* *RAB26* *RARRES3* *RCSD1* *SELENBP1* *SLC1A3* *SYNPO* *TNFAIP2* *TSPAN8*	*ALPP* *APOL3* *C21orf129* *DCN* *FOLR1* *IGFBP3* *RIPK4* *TRPV5* *UBD*

Ino-C2-PAF	Glc-PAF	Edelfosine	Ino-C2-PAF & Glc-PAF	Glc-PAF & edelfosine	Ino-C2-PAF & edelfosine	All APLs
CYP26A1 *CYP2B6* *CYP4B1* *DAPK1* *DEFB1* *DEFB4* *DHRS3* *E2F2* *ELF3* *EPB41L4A* *ETV7* *EXOC3L* *FAM83A* *FBP1* *FLJ40722* *FYB* *GBP4* *GFPT2* *H19* *HLA-DMA* *HLA-DMB* *HLA-DOA* *HLA-DPA1* *HLA-DPB1* *HLA-DQA1* *HLA-DRA* *HLA-DRB1* *HLA-DRB3* *HLA-DRB4* *HLA-DRB5* *HSD11B2* *ID1* *ID2* *ID3* *IFI35* *IFI44L* *IFI6* *IKBKE* *IL32* *IL4I1* *INDO* *ITLN2* *KLRC1* *KLRC2* *KLRC4* *KRT13* *KRT15* *KRT4* *KRT77* *LAMP3* *LRG1* *LTB* *MARCKSL1* *MGC16075* *MMP10* *MMP12* *MMP7*						

Ino-C2-PAF	Glc-PAF	Edelfosine	Ino-C2-PAF & Glc-PAF	Glc-PAF & edelfosine	Ino-C2-PAF & edelfosine	All APLs
MPPED1						
MPPED2						
MUC16						
MX2						
NFKBIA						
NGFR						
OAS1						
OAS2						
PARD6A						
PDZK1IP1						
PFKFB3						
PHACTR3						
PI3						
PIGR						
PSMB10						
PSMB9						
PTGES						
RNF152						
SAMD9L						
SECTM1						
SERPINA3						
SERPINB1						
SLC2A4						
SLC45A4						
STARD5						
STRA6						
SULT1E1						
TAPBPL						
TGM1						
TJP3						
TLR5						
TMPRSS3						
TNFSF10						
TRIM22						
TRPV6						
TSGA2						
VNN1						
VNN3						
WFDC2						
WNT7B						
XAF1						
ZNF488						

List of (B1) up- and (B2) down-regulated transcripts represented in Venn diagrams. Each column, which contains transcripts with an official gene name (Gene_ID), indicates a group or intersection of the Venn diagrams.

ACKNOWLEDGMENT

“Where´s my punk spirit? When I need it”

(“Punk Spirit” by Wave Machines)

Professional

Private